

**Synthese, Reaktivität und Charakterisierung von
Platinkomplexen mit bioaktiven schwefelhaltigen Heterocyclen,
Thionucleobasen und Thioglycosiden**

Dissertation

zur Erlangung des akademischen Grades
doctor rerum naturalium (Dr. rer. nat.)

vorgelegt der

Naturwissenschaftlichen Fakultät II – Chemie und Physik
der Martin-Luther-Universität Halle-Wittenberg

von Frau Dipl. Chem. Cornelia Vetter
geb. am 03.12.1981 in Lutherstadt Wittenberg

Gutachter:

1. Prof. Dr. Dirk Steinborn (Martin-Luther-Universität Halle-Wittenberg)
2. Prof. Dr. Bernhard Lippert (Technische Universität Dortmund)

Tag der Verteidigung: 22.04.2010

INHALTSVERZEICHNIS

Abkürzungsverzeichnis

Nummerierung

1. Einleitung	6
2. Ergebnisse und Diskussion	12
2.1. Mononukleare Platin(IV)-Komplexe mit Thionucleobaseliganden [C,D]	12
2.1.1. Synthese und Charakterisierung	12
2.1.2. Strukturelle Aspekte	14
2.1.3. Zur Tautomerie und zum Koordinationsverhalten der Thionucleobasen	16
2.2. Oligonukleare Platin(IV)-Komplexe mit <i>N,S</i>- und <i>S,S</i>-heterocyclischen und Thionucleobaseliganden [A,B,D,H]	19
2.2.1. Synthese und Charakterisierung	19
2.2.2. Strukturelle Aspekte	20
2.2.3. Koordinationsmodi der <i>N,S</i> - und <i>S,S</i> -heterocyclischen Liganden	23
2.2.4. Cytotoxische Eigenschaften von Platin(IV)-Komplexen mit <i>N,S</i> -heterocyclischen und Thionucleobaseliganden [B,C,D]	25
2.3. Platinkomplexe mit Thioglycosidliganden [E,F,G]	27
2.3.1. Synthese und Charakterisierung von Thioglycosidplatin(II)-Komplexen	27
2.3.2. Synthese und Charakterisierung von Thioglycosidplatin(IV)-Komplexen	29
2.3.3. Zur Reaktivität der Thioglycosidplatin(IV)-Komplexe	32
2.3.4. Thioglycosidplatin(IV)-Komplexe in stereoselektiven Glycosylierungsreaktionen	34
3. Zusammenfassung	38
4. Literaturverzeichnis	44
Anhang	49

ABKÜRZUNGSVERZEICHNIS

Allgemeine Abkürzungen

1-MeSCy	1-Methyl-2-thiocytosin	pymtH	Pyrimidin-2-thion
Ac	Acetyl	pytH	Pyridin-2-thion
Bn	Benzyl	tztH	Thiazolin-2-thion
Bz	Benzoyl	tptH	Thiophen-2-thiol
bpy	2,2'-Bipyridin	s ² Ura	2-Thiouracil
ch	Kohlenhydratrest	s ⁴ Ura	4-Thiouracil
CIS	koordinationsinduzierter Shift	s ² s ⁴ Ura	2,4-Dithiouracil
Et	Ethyl	SCy	2-Thiocytosin
OAc	Acetation	S [⌢] D	N,S- bzw. S,S-Heterocyclus
[M]	Metallfragmentkomplex	solv	Solvens
nb	Thionucleobase	Taz	Thiazolin-2-yl
Me	Methyl	∠	Winkel
Pic	2-Picolin-2-yl		
PT	4-(Pyridin-2-yl)-thiazol-2-yl		

Abkürzungen in der NMR-Spektroskopie

s	Singulett
d	Dublett
tr	Triplett
m	Multiplett
br	breit

Abkürzungen in der IR-Spektroskopie

w	schwach
m	mittel
s	stark

Nummerierung

Die Bezeichnung aller Liganden und Komplexe wird wie in den Publikationen verwendet. Zusätzlich erfolgt unter Angabe der Großbuchstaben **A–I** der Verweis auf die entsprechende Publikation (Anhang 1).

Nummerierung der Liganden

Einige der Liganden kommen in mehreren Veröffentlichungen vor und besitzen auf Grund dessen eine Doppelnummerierung die im Folgenden wiedergegeben ist:

1-MeSCy: **3C/3H**

OAc-SPT: **2E/6aF**

OBz-Sbpy: **6E/7bF**

OBz-SPT: **3E/6bF**

OBn-SEt: **4dF/1aG**

OBn-SPT: **4E/6cF**

OBn-STaz: **5bF/2aG**

OAc-Sbpy: **5E/7aF**

6bpy-OBn-STaz: **5hF/9aG**

Nummerierung der Komplexe

Die Ausgangsstoffe zur Erzeugung der Platin(IV)-Precursorkomplexe sowie die Precursorkomplexe selber werden ohne Angabe eines Großbuchstaben nummeriert. In eckigen Klammern erfolgt einmalig die Angabe der Nummerierung in den Veröffentlichungen. Doppelnummerierungen einzelner Komplexe sind ebenfalls aufgelistet.

- (1) [PtMe₃I(bpy)] [**2A**]
- (2) [(PtMe₃I)₄] [**2B**]
- (3a) [PtMe₃(Me₂CO)(bpy)][BF₄] [**1D, 1aG**]
- (3b) [PtMe₃(Me₂CO)(^tBu₂bpy)][BF₄] [**1bG**]
- (3c) [PtMe₃(MeOH)(bpy)][BF₄] [**1C**]
- (4) [PtMe₃(OAc)(bpy)] [**4A, I**]
- (5) [PtMe₃(OAc-κ²O,O')(Me₂CO)] [**3A, 1B, 2F, 6D**]
- (6) [PtMe₃(Me₂CO)₃][BF₄] [**3F, 1H**]
- (5A) [PtMe₃(bpy)(pymt-κS)]
- (6A) [PtMe₃(bpy)(pyt-κS)]
- (7A) [PtMe₃(bpy)(tzt-κS)]

- (8A) $[\text{PtMe}_3(\text{bpy})(\text{tpt}-\kappa\text{S})]$
- (9A/4B) $[(\text{PtMe}_3)_2(\mu\text{-pymt}-1\kappa\text{N}, 1:2\kappa^2\text{S})_2]$
- (10A/3B) $[(\text{PtMe}_3)_2(\mu\text{-pyt}-1\kappa\text{N}, 1:2\kappa^2\text{S})_2]$
- (11A/5B) $[(\text{PtMe}_3)_2(\mu\text{-tzt}-1\kappa\text{N}, 1:2\kappa^2\text{S})_2]$
- (12A/6B) $[(\text{PtMe}_3)_4(\mu_3\text{-tpt}-\kappa\text{S})_4]$
- (4C) $[\text{PtMe}_3(\text{bpy})(\text{SCy}-\kappa\text{S})][\text{BF}_4]$
- (5C) $[\text{PtMe}_3(\text{bpy})(1\text{-MeSCy}-\kappa\text{S})][\text{BF}_4]$
- (3D) $[\text{PtMe}_3(\text{bpy})(\text{s}^2\text{Ura}-\kappa\text{S}^2)][\text{BF}_4]$
- (4D) $[\text{PtMe}_3(\text{bpy})(\text{s}^4\text{Ura}-\kappa\text{S}^4)][\text{BF}_4]$
- (5D) $[\text{PtMe}_3(\text{bpy})(\text{s}^2\text{s}^4\text{Ura}-\kappa\text{S}^4)][\text{BF}_4]$
- (7D) $[(\text{PtMe}_3)_2(\mu\text{-s}^4\text{Ura}_{\text{-H}})_2]$
- (7aD) $[\{(\text{PtMe}_3)(\mu\text{-s}^4\text{Ura}_{\text{-2H}})\}_2\{(\text{PtMe}_2(\mu\text{-S}^4\text{Ura}_{\text{-H}})\}_2\{(\text{PtMe}_3(\text{H}_2\text{O}))(\mu\text{-S}^4\text{Ura}_{\text{-H}})\}_2]$
- (1E) $[\text{Pt}(\text{COMe})_2(\text{NH}_2\text{Bn})_2]$
- (7E) $[\text{Pt}(\text{COMe})_2(\text{OAc-SPT})]$
- (8E) $[\text{Pt}(\text{COMe})_2(\text{OBz-SPT})]$
- (9E) $[\text{Pt}(\text{COMe})_2(\text{OBn-SPT})]$
- (10E) $[\text{Pt}(\text{COMe})_2(\text{OAc-Sbpy})]$
- (11E) $[\text{Pt}(\text{COMe})_2(\text{OBz-Sbpy})]$
- (8F) $[\text{PtMe}_3(\text{bpy})(\mathbf{4aF}-\kappa\text{S})][\text{BF}_4]$
- (9F) $[\text{PtMe}_3(\text{bpy})(\mathbf{4bF}-\kappa\text{S})][\text{BF}_4]$
- (10F) $[\text{PtMe}_3(\text{bpy})(\mathbf{4cF}-\kappa\text{S})][\text{BF}_4]$
- (11F/1cG) $[\text{PtMe}_3(\text{bpy})(\mathbf{4dF}-\kappa\text{S})][\text{BF}_4]$
- (12F) $[\text{PtMe}_3(\text{bpy})(\mathbf{4eF}-\kappa\text{S})][\text{BF}_4]$
- (13F) $[\text{PtMe}_3(\textit{t}\text{Bu}_2\text{bpy})(\mathbf{4aF}-\kappa\text{S})][\text{BF}_4]$
- (14F) $[\text{PtMe}_3(\textit{t}\text{Bu}_2\text{bpy})(\mathbf{4cF}-\kappa\text{S})][\text{BF}_4]$
- (15F) $[\text{PtMe}_3(\textit{t}\text{Bu}_2\text{bpy})(\mathbf{5cF}-\kappa\text{N})][\text{BF}_4]$
- (16F) $[\text{PtMe}_3(\textit{t}\text{Bu}_2\text{bpy})(\mathbf{5gF}-\kappa\text{N})][\text{BF}_4]$
- (17F) $[\text{PtMe}_3(\text{bpy})(\mathbf{5aF}-\kappa\text{N})][\text{BF}_4]$
- (18F) $[\text{PtMe}_3(\text{bpy})(\mathbf{5bF}-\kappa\text{N})][\text{BF}_4]$
- (19F) $[\text{PtMe}_3(\text{bpy})(\mathbf{5cF}-\kappa\text{N})][\text{BF}_4]$
- (20F/2cG) $[\text{PtMe}_3(\text{bpy})(\mathbf{5dF}-\kappa\text{N})][\text{BF}_4]$
- (21F) $[\text{PtMe}_3(\text{bpy})(\mathbf{5eF}-\kappa\text{N})][\text{BF}_4]$

- (21aF) [PtMe₃(bpy)(STazH-κS)]
- (22F) [PtMe₃(bpy)(5fF-κN)][BF₄]
- (23F) [PtMe₃(bpy)(5gF-κN)][BF₄]
- (23aF) 1,6-Anhydro-2,3,4-*O*-tribenzoyl-β-D-glucopyranose
- (24F) [PtMe₃(OAc-κ²*O, O'*)(4aF-κS)]
- (25F) [PtMe₃(OAc-κ²*O, O'*)(4bF-κS)]
- (26F) [PtMe₃(OAc-κ²*O, O'*)(4cF-κS)]
- (27F/1dG) [PtMe₃(OAc-κ²*O, O'*)(4dF-κS)]
- (28F) [PtMe₃(OAc-κ²*O, O'*)(4eF-κN)]
- (29F) [PtMe₃(OAc-κ²*O, O'*)(5aF-κN)]
- (30F) [PtMe₃(OAc-κ²*O, O'*)(5bF-κN)]
- (31F) [PtMe₃(OAc-κ²*O, O'*)(5cF-κN)]
- (32F/2dG) [PtMe₃(OAc-κ²*O, O'*)(5dF-κN)]
- (33F) [PtMe₃(OAc-κ²*O, O'*)(5eF-κN)]
- (34F) [PtMe₃(OAc-κ²*O, O'*)(5fF-κN)]
- (35F) [PtMe₃(OAc-κ²*O, O'*)(5gF-κN)]
- (36F) [PtMe₃(4aF)][BF₄]
- (37F) [PtMe₃(4cF)][BF₄]
- (38F/1bG) [PtMe₃(4dF)][BF₄]
- (39F) [PtMe₃(4eF)][BF₄]
- (40F) [PtMe₃(4fF)][BF₄]
- (41F/9bG) [PtMe₃(5hF)][BF₄]
- (42F) [PtMe₃(6aF)][BF₄]
- (43F) [PtMe₃(6bF)][BF₄]
- (44F) [PtMe₃(6cF)][BF₄]
- (45F) [PtMe₃(7aF)][BF₄]
- (46F) [PtMe₃(7bF)][BF₄]
- (2bG) [PtMe₃(OAc-κ²*O, O'*)(2aG)]
- (5bG) [PtMe₃(5aG)][BF₄]
- (6bG) [PtMe₃(6aG)][BF₄]
- (8bG) [PtMe₃(8aG)][BF₄]
- (3H) [(PtMe₃)₂(μ-1-MeSCy)₂][BF₄]

1. Einleitung und Problemstellung

Die Erkenntnis, dass Metalle in biologischen Verbindungen und Prozessen eine zentrale Rolle spielen, führte zur Entwicklung der Bioanorganischen Chemie als ein junges eigenständiges Wissenschaftsgebiet [1]. Im Fokus dabei steht die Aufklärung der Wirkungsweise und Funktion von Metalloproteinen, Vitaminen und Naturstoffen. Zu den bekanntesten Vertretern gehören dabei das Hämoglobin, Vitamin B₁₂ und auch Chlorophyll (Abb. 1), also Porphyrin-/Corrin-Komplexe vom Fe, Co und Mg, die für einige der wichtigsten Funktionen wie Sauerstofffixierung und -transport, Speicherung von Spurenelementen oder auch Photosynthese verantwortlich sind. Die Bioanorganik stellt dabei eine interdisziplinäre Wissenschaft dar, die nicht nur die anorganische und organische Chemie sowie Biochemie miteinander verbindet, sondern mit weiteren grundlegenden Wissenschaften ein enges Netzwerk bildet (Abb. 2).

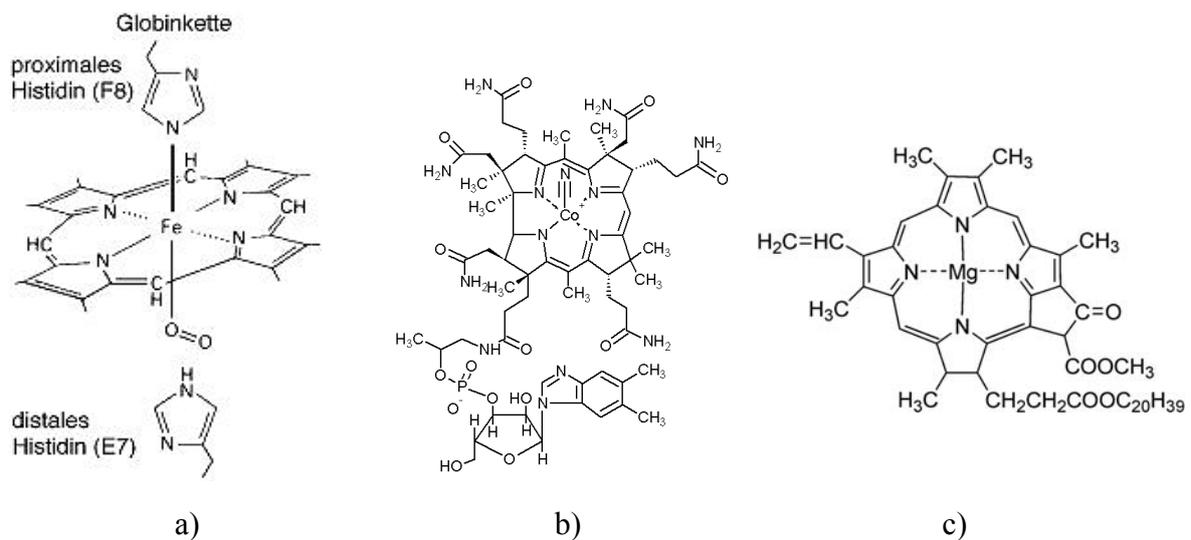


Abbildung 1. a) Hämoglobin, b) Vitamin B₁₂, c) Chlorophyll a.

Zu den bedeutendsten bioanorganischen Pharmaka zählt Cisplatin (Abbildung 3), das seit seiner Entdeckung im Jahr 1965 von ROSENBERG [2] und der Einführung in die Chemotherapie 1978, bis heute eines der meist verwendeten Cancerostatica ist. Die cytotoxische Wirkung des Platin(II)-Komplexes beruht zunächst auf der Hydrolyse der Chloroliganden und der daraus folgenden Generierung eines hochreaktiven Diammindiaquakomplexes [3]. Die anschließende Koordination an die DNA erfolgt hauptsächlich über N7-Atome von zwei Guanin-Nucleobasen, was vorwiegend zu Intrastrangvernetzungen (intrastrand cross-linking) führt, aber auch Interstrangvernetzungen (interstrand cross-linking) der DNA-Doppelhelix zur Folge haben kann. Des Weiteren kommt es zu einer Aktivierung zahlreicher Signal-Transduk-

Einleitung

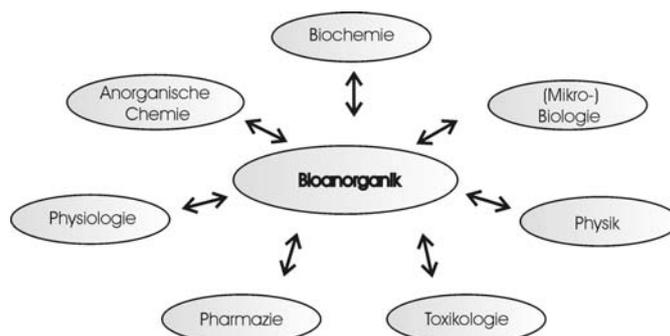


Abbildung 2. Bioanorganische Chemie als interdisziplinäres Wissenschaftsgebiet (nach [1]).

tionswege und im Endeffekt zur Unterbindung der DNA-Replikation und dem anschließenden Zelltod [3,4]. Auf Grund von Resistenzen einiger Tumorarten gegenüber Cisplatin sowie erheblicher Nebenwirkungen wurden bis heute zahlreiche weitere Platinkomplexe auf ihre cytotoxische Aktivität untersucht. Allerdings ist die Anzahl der Komplexe, die eine vergleichbare Aktivität zeigen und in klinischen Studien getestet wurden, minimal und beschränkt sich auf rund 30 Komplexe [3,5]. Davon wurden allein vier als Cancerostatica eingeführt. Abbildung 3 zeigt die zweite Generation der Platin(II)-Cancerostatica: Carboplatin, Oxaplatin und Oxaliplatin. Der letztere Komplex ist der einzige, der auch bei Cisplatin-resistenten Tumorarten angewendet werden kann [3]. Die cytotoxische Aktivität von Platin(IV)-Komplexen ist ebenfalls von hohem Interesse und Gegenstand zahlreicher Untersuchungen [6]. Platin(IV)-Komplexe sind kinetisch inert gegenüber Ligandensubstitutionen, was die toxischen Nebenwirkungen erheblich minimieren kann. Man geht derzeit davon aus, dass Platin(IV)-Komplexe als Pro-Pharmaka agieren und im Organismus zu Platin(II)-Verbindungen reduziert werden [6]. Jedoch existieren auch Studien die zeigen, dass Platin(IV)-Verbindungen ebenfalls mit der DNA interagieren können und *in vitro* cytotoxische Aktivität besitzen [7]. Von den Platin(IV)-Verbindungen die in klinischen Studien getestet wurden (Abb. 3) werden diese allerdings nur für Satraplatin weitergeführt [6,8].

Einleitung

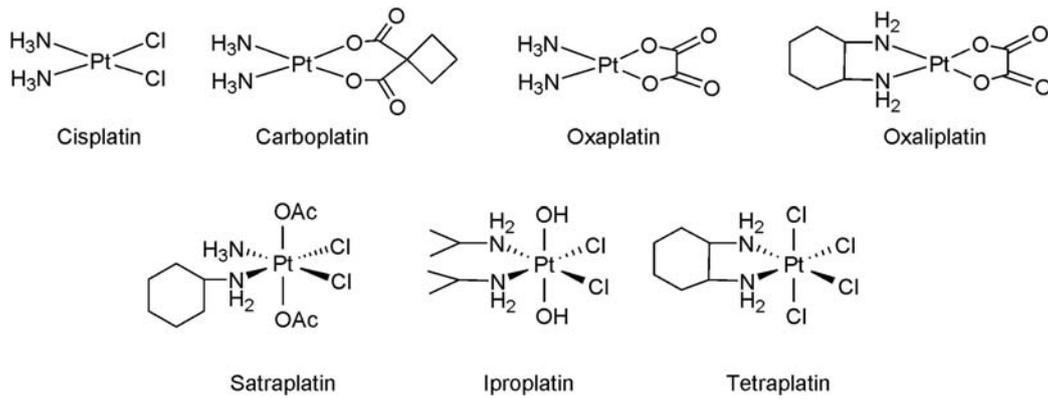


Abbildung 3. Platin(II)- und potente Platin(IV)-Cancerostatica.

Die bioanorganischen Pharmaka sind jedoch nicht nur auf Platinkomplexe beschränkt. Seit langer Zeit ist die therapeutische Aktivität von Gold(I)-Verbindungen bekannt, die vor allem Anwendung in der Rheuma- und Arthritistherapie finden (Abb. 4). Dabei handelt es sich um Gold(I)-Komplexe mit Thioglucoseliganden, wobei heutzutage hauptsächlich das „Auranofin“ als Nachfolger des „Solganols“ eingesetzt wird. Die therapeutische Wirkung des „Auranofins“ beruht dabei auf der hohen Affinität von Gold(I)-Verbindungen zu Schwefel. „Auranofin“ bindet an die Mercaptogruppe eines Cysteinrestes der Cathepsinproteasen und agiert somit als Enzyminhibitor. Die Cathepsinproteasen zählen zu den Lysozymenzymen, die als Ursache für Gewebsentzündungen angesehen werden [9].

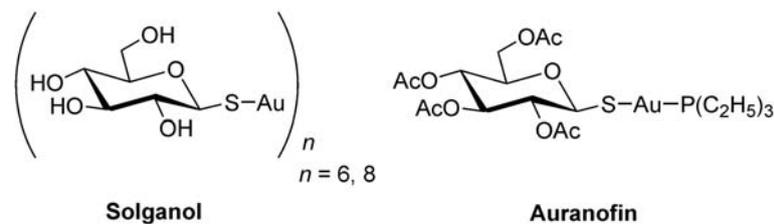


Abbildung 4. Gold(I)-Kohlenhydratkomplexe in der Rheuma- und Arthritistherapie.

Thioanaloga von Biomolekülen, wie Kohlenhydraten oder Nucleobasen, sind bezüglich ihrer Bioaktivität von großem Interesse. In Abbildung 5 sind die Grundtypen beider Verbindungsklassen zusammengefasst. Thionucleobasen leiten sich formal von Nucleobasen durch die sukzessive Substitution eines Sauerstoffatoms durch Schwefel ab. Gemäß der Einteilung der Nucleobasen unterscheidet man auch hier Pyrimidin- und Purinbasen, die sich von den Grundgerüsten der entsprechenden Heterocyclen ableiten lassen. 1965 gelang CARBON erstmals die Isolierung von 2-Thiouracil aus der tRNA von *E.coli* Bakterien [10].

Einleitung

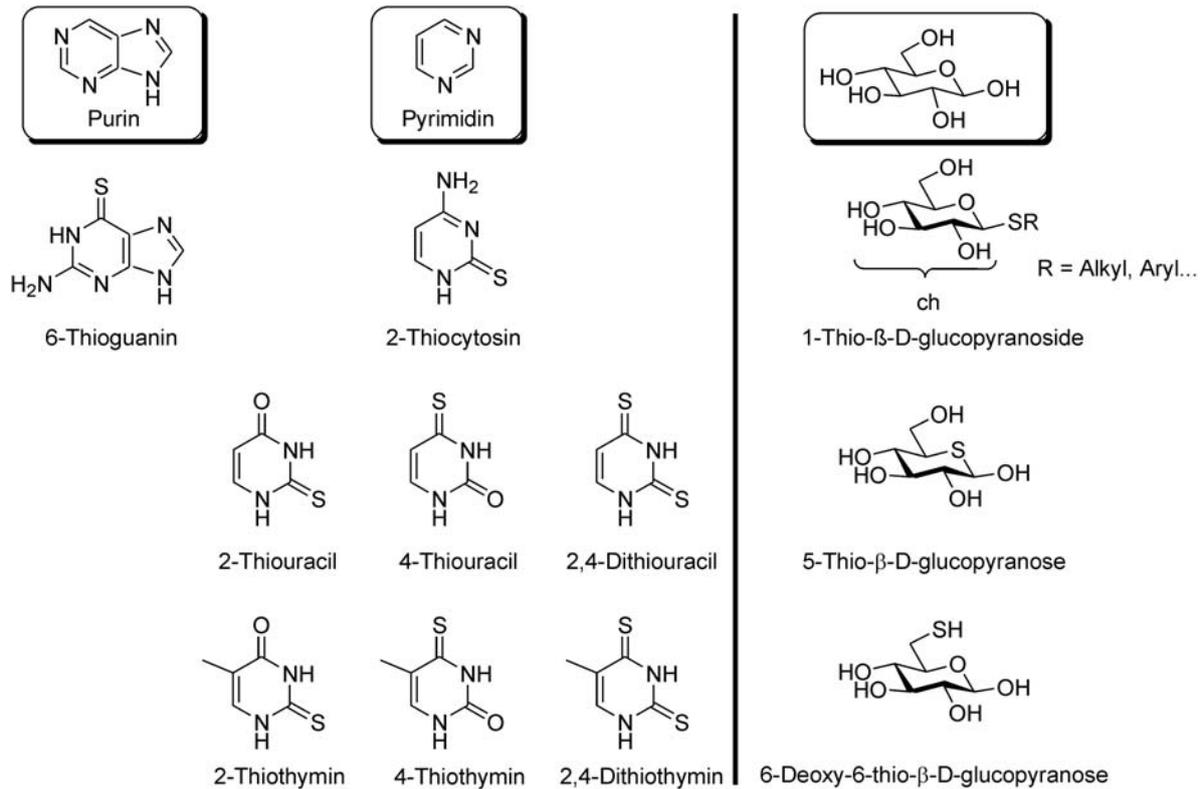


Abbildung 5. Thionucleobasen und schwefelfunktionalisierte Kohlenhydrate.

Auch 4-Thiouracil und 2-Thiocytosin konnten als Bestandteile der tRNA in verschiedenen Quellen nachgewiesen werden [11]. Von großem Interesse sind die biologischen Aktivitäten der Thionucleobasen und deren Derivate, insbesondere die cancerostatischen und antiviralen Eigenschaften [12]. Dies macht sie zu potentiellen Pharmaka und mit entsprechender Isotopenmarkierung auch zu Radiopharmaka [13,14]. Das Schwefelatom ist für die Bioaktivität essentiell und löst hauptsächlich enzyminhibitorische Effekte aus. Auf Grund der hohen Ähnlichkeit zu den Sauerstoffanaloga werden diese Verbindungen in Stoffwechselprozessen nicht erkannt und als sogenannte Antimetabolite in die RNA und DNA mit eingebaut, was zur Unterdrückung von Protein- und Glycoproteinsynthesen führt [15]. Weiterhin finden Thionucleobasen Anwendung in der Photochemie zur räumlichen Strukturaufklärung von Nucleinsäuren sowie zur Identifizierung von Nucleobasen-Protein-Kontakten in Nucleoprotein-komplexen [16]. Die Absorption der C=S-Bindung erfolgt im Vergleich zur C=O-Bindung der Sauerstoffanaloga in längerwelligen Bereichen ($\lambda > 320 \text{ nm}$) und kann so selektiv mit Hilfe von UV-Licht angeregt werden kann.

Einleitung

Unter Thioglycosiden versteht man im strengen Sinne Kohlenhydrate (Abb. 5), die über die glycosidische Bindung mit einem Thioalkohol (R–SH) verbunden sind, gemäß der allgemeinen Struktur ch-S-R^1 . Darüber hinaus gibt es schwefelfunktionalisierte Kohlenhydrate, bei denen der Ringsauerstoff durch Schwefel substituiert wurde, oder aber auch anstelle einer Hydroxylgruppe die entsprechende Mercaptogruppe eingeführt wurde (Abb. 5). 5-Thio-kohlenhydrate mit Ringschwefelatom besitzen cancerostatische und fertilitätshemmende Eigenschaften [17]. Weiterhin wurde gezeigt, dass sie ebenfalls als Enzyminhibitoren agieren [18]. In Diabetesstudien lösten sie in Tierversuchen bei Ratten eine erhebliche Störung des Glucosestoffwechsels aus, was zu kurzzeitiger Hyperglycämie führte [19]. Neuere Untersuchungen zeigen, dass auch Thioglycoside und Kohlenhydrate mit Mercaptogruppen Enzyminhibitoren sind und auf Grund dessen cancerostatische oder auch entzündungshemmende Eigenschaften besitzen [20]. Auch Metallkomplexe mit Thionucleobase- und Thioglycosidliganden besitzen potentielle Bioaktivität. Silber(I)-Komplexe mit Thioglycosidliganden wirken antibakteriell und als Fungizid [21]. WHITEHOUSE synthetisierte 1998 Auranofin-analoga Gold(I)-Verbindungen mit Thionucleobaseliganden, die bei verminderter Toxizität eine vergleichbare oder sogar höhere Aktivität als „Auranofin“ aufweisen (Abbildung 6) [22]. Darüber hinaus konnte gezeigt werden, dass diese Verbindungen auch antitumorale Eigenschaften besitzen, wobei die cytotoxische Aktivität zum Teil deutlich höher im Vergleich zu Cisplatin ist [23].

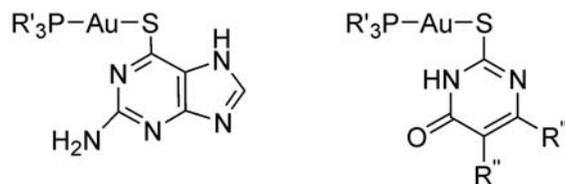


Abbildung 6. Auranofin analoge Thionucleobasegold(I)-Komplexe.

Dies macht deutlich, dass die Synthese von Metallkomplexen, insbesondere von Platinkomplexen, mit Thionucleobase- und Thioglycosidliganden von besonderem Interesse ist. Die Koordination eines bioaktiven Liganden an Platin kann zu Komplexen führen, die eine höhere Bioaktivität (insbesondere Cytotoxizität) besitzen als vergleichbare Komplexe mit „abiotischen“ Liganden.

¹ ch = Kohlenhydratrest

Zielstellung der Arbeit

Das Ziel der vorliegenden Arbeit kann in drei Themengebiete unterteilt werden:

Zunächst sollten in Weiterführung der Diplomarbeit [24] Platin(IV)-Komplexe mit Thionucleobase-analogen *N,S*-heterocyclischen- sowie Thionucleobaseliganden synthetisiert und charakterisiert und darüber hinaus Untersuchungen zur cytotoxischen Aktivität dieser Verbindungen durchgeführt werden. Die Synthese und Charakterisierung von Platin(II)- und Platin(IV)-Komplexen mit Thioglycosidliganden, stellt den zweiten Schwerpunkt der Arbeit dar. Dabei stand die Ermittlung des Koordinationsverhaltens der Kohlenhydrate im Mittelpunkt. Die Kohlenhydratplatin(IV)-Komplexe sollten darüber hinaus auf ihre Eignung als Glycosyldonoren in Glycosylierungsreaktionen getestet werden. Dabei stand im Fokus zu untersuchen, ob es durch die Koordination des Kohlenhydrates an das Platin(IV)-Atom zu einer Beeinflussung des anomeren α/β -Gemisches zu Gunsten des α -Anomeren kommt.

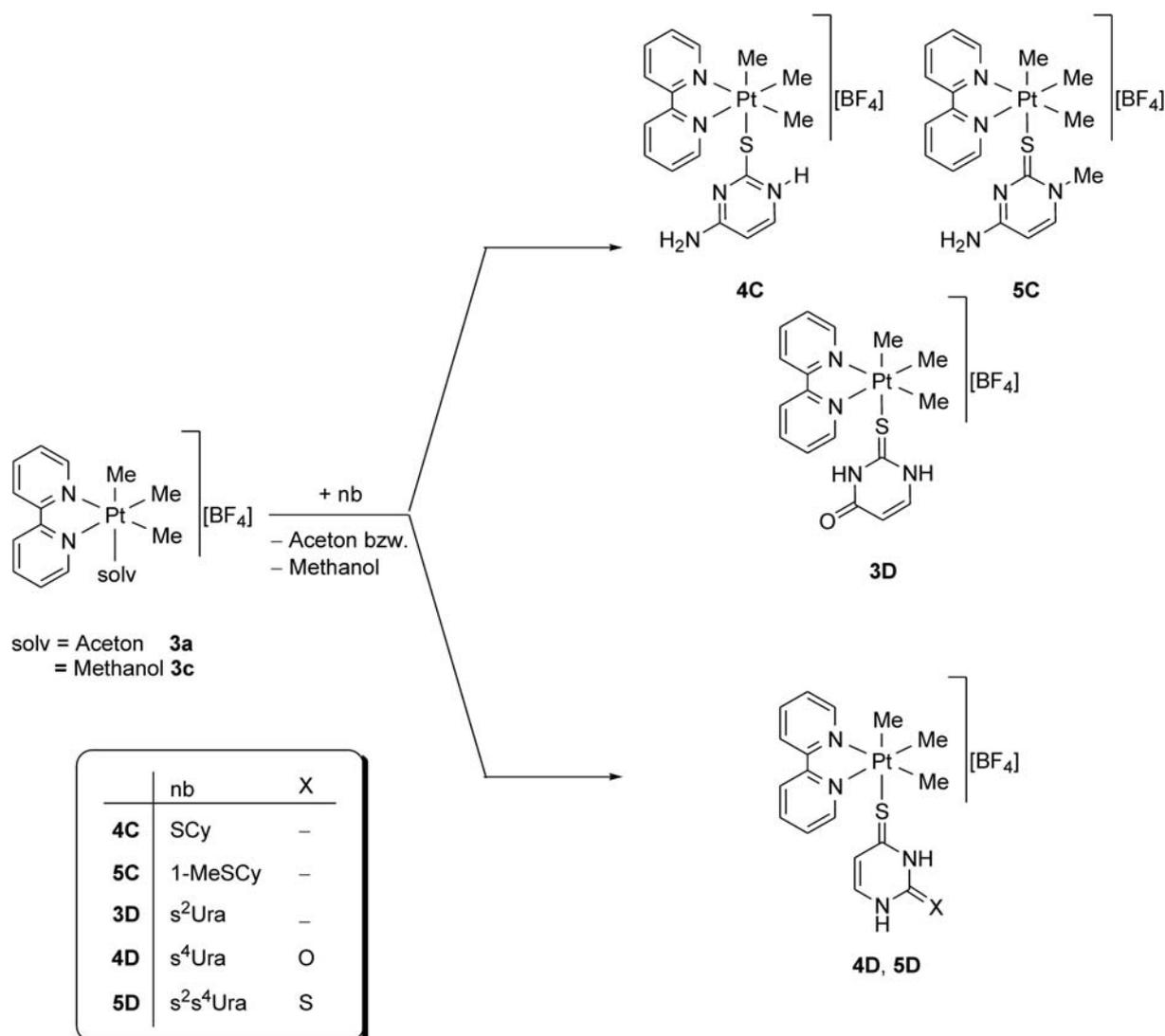
2. Ergebnisse und Diskussion

2.1. Mononukleare Platin(IV)-Komplexe mit Thionucleobaseliganden [C,D]

2.1.1. Synthese und Charakterisierung

In Anlehnung an die in [A,24] beschriebenen Arbeiten, in denen das Koordinationsverhalten der *N,S*- und *S,S*- heterocyclischen Modellliganden Pyridin-2-thion (pytH), Pyrimidin-2-thion (pymtH), Thiazolin-2-thion (tztH) und Thiophen-2-thiol (tptH) untersucht wurde, wurden nun die Thionucleobasen 2-Thiocytosin (SCy, **2C**), 1-Methyl-2-thiocytosin (1-MeSCy, **3C/1H**), 2-Thiouracil (s^2 Ura), 4-Thiouracil (s^4 Ura) und 2,4-Dithiouracil (s^2s^4 Ura) in die Untersuchungen einbezogen, die auf Grund ihrer höheren Anzahl an potentiellen Donoratomen ein komplexeres Koordinationsvermögen besitzen. Um das bevorzugte Koordinationsverhalten der Thionucleobasen gegenüber Platin(IV)-Komplexen zu ermitteln, wurden zunächst die Komplexe $[\text{PtMe}_3(\text{solv})(\text{bpy})][\text{BF}_4]$ (solv = Aceton, **3a**; Methanol, **3c**) als Precursorkomplexe verwendet, die nur über eine substitutionslabile Koordinationsstelle verfügen. Die Umsetzung von **3a** mit den Thionucleobasen SCy (**2C**) und 1-MeSCy (**3C/1H**) bzw. von **3c** mit s^2 Ura, s^4 Ura und s^2s^4 Ura führt gemäß Schema 1 zur Bildung der mononuklearen Komplexe des allgemeinen Typs $[\text{PtMe}_3(\text{nb-}\kappa\text{S})][\text{BF}_4]$. Die Komplexe $[\text{PtMe}_3(\text{nb-}\kappa\text{S})][\text{BF}_4]$ (nb = SCy, **4C**; 1-MeSCy, **5C**; s^2 Ura, **3D**; s^4 Ura, **4D**; s^2s^4 Ura, **5D**) wurden in Ausbeuten von 41–68% isoliert und vollständig durch ^1H -, ^{13}C - und ^{195}Pt -NMR Spektroskopie, Elementaranalyse sowie IR-Spektroskopie charakterisiert.

In allen Fällen erfolgt die Koordination über das exocyclische Schwefelatom. Dies belegen die Röntgeneinkristallstrukturanalysen von **4C**·MeOH und **5C** sowie die NMR-spektroskopischen Daten aller Komplexe und quantenchemische Rechnungen von **4D** und **5D**. Dabei ist die Koordination über C4=S für **4D** und **5D** um 5.8 bzw. 3.3 kcal/mol stabiler als über C2=O (**4D**) bzw. C2=S (**5D**). Im Fall von $[\text{PtMe}_3(\text{bpy})(s^2\text{Ura})][\text{BF}_4]$ (**3D**) zeigen die quantenchemischen Rechnungen, dass die Donorstärke der C2=S-Gruppe deutlich geringer ist und mit der der C4=O-Gruppe vergleichbar ist. Das kann auf die zwei elektronegativen Stickstoffatome in direkter Nachbarschaft der C2=S-Gruppe zurückgeführt werden.



Schema 1. Darstellung von mononuklearen Thionucleobaseplatin(IV)-Komplexen.

In Trimethylplatin(IV)-Komplexen lässt sich der *trans*-Einfluss der Liganden anhand der $^1J_{\text{Pt,C}}$ -Kopplungskonstante des Methylgruppen in *trans* Position zum jeweiligen Liganden abschätzen, die sich umgekehrt proportional zueinander verhalten [25,26]. Auf dieser Grundlage (Tabelle 1) ergibt sich folgende Abstufung:

$$\text{SCy} > 1\text{-MeSCy} \approx \text{s}^4\text{Ura} \approx \text{s}^2\text{s}^4\text{Ura} > \text{s}^2\text{Ura}.$$

Der relativ geringe *trans*-Einfluss des 2-Thiouracilliganden, der sich in der bis zu 31.6 Hz größeren Kopplungskonstante widerspiegelt, steht im Einklang mit dem bereits erwähnten Ergebnis der quantenchemischen Rechnungen, das eine geringe Donorstärke der C2=S-Gruppe ergab.

Tabelle 1. Vergleich der $^1J_{\text{Pt,C}}$ -Kopplungskonstanten (in Hz) der Methylgruppen in *trans*-Position zu Thionucleobase- bzw. $\widehat{\text{S}}\text{N}^-$ -Liganden in Komplexen der Typen $[\text{PtMe}_3(\text{bpy})(\text{nb-}\kappa\text{S})][\text{BF}_4]$ und $[\text{PtMe}_3(\text{bpy})(\widehat{\text{S}}\text{N-}\kappa\text{S})]$.

	$[\text{PtMe}_3(\text{bpy})(\text{nb-}\kappa\text{S})][\text{BF}_4]$		$[\text{PtMe}_3(\text{bpy})(\widehat{\text{S}}\text{N-}\kappa\text{S})]^{\text{a)}$	
	nb	$^1J_{\text{Pt,C}}^{\text{b)}$	$\widehat{\text{S}}\text{N}^-$	$^1J_{\text{Pt,C}}$
4C	SCy	642.1	pyt ⁻	622.8
5C	1-MeSCy	649.5	pymt ⁻	622.7
3D	s ² Ura	673.7	tzt ⁻	622.9
4D	s ⁴ Ura	651.5	tpt ⁻	608.6
5D	s ² s ⁴ Ura	649.5		

^{a)} Daten entnommen aus [A]. ^{b)} *Trans* zu S. ^{c)} $\widehat{\text{S}}\text{N}^-$ = Pyridin-2-thiolat, pyt⁻; Pyrimidin-2-thiolat, pymt⁻, Thiazolin-2-thiolat, tzt⁻; Thiophen-2-thiolat, tpt⁻).

Erwartungsgemäß zeigt der Vergleich der $^1J_{\text{Pt,C}}$ -Kopplungskonstanten der Neutralliganden in **4C**, **5C**, **3D–5D** mit anionischen Thiolatoliganden der analogen Komplexe $[\text{PtMe}_3(\text{bpy})(\widehat{\text{S}}\text{N-}\kappa\text{S})]$ ($\widehat{\text{S}}\text{N}^-$ = Pyridin-2-thiolat, Pyrimidin-2-thiolat, Thiazolin-2-thiolat, Thiophen-2-thiolat) [A,24] eine deutlich höhere Donorstärke der Thiolatoliganden gegenüber den Neutralliganden (Tabelle 1).

2.1.2. Strukturelle Aspekte

In den Komplexen **4C** und **5C** finden sich charakteristische Unterschiede in den Bindungsmodi der SCy- κS - (**2C**) und 1-MeSCy- κS -Liganden (**3C/1H**). In den Kristallen von **4C**·MeOH ist der Ligand nahezu parallel zur zentralen $[\text{PtC}_2\text{N}_2]$ -Ebene angeordnet (Abb. 7). Zwischen dem SCy-Liganden und dem Bipyridinliganden kommt es zur Ausbildung intramolekularer attraktiver Wechselwirkungen durch π - π -Stapelung. Darüber hinaus findet man in Kristallen von **4C**·MeOH intermolekulare π - π -Wechselwirkungen und Wasserstoffbrückenbindungen. Im Unterschied dazu ist der 1-MeSCy-Ligand (**3C/1H**) in einem Winkel von 71.1° zur $[\text{PtC}_2\text{N}_2]$ -Ebene angeordnet, was nur zur Ausbildung intermolekularer C–H \cdots π -Wechselwirkungen und Wasserstoffbrückenbindungen führt. Damit ist das Schwefelatom in **4C** als sp³- und in **5C** als sp²-hybridisiert zu beschreiben. In Übereinstimmung damit stehen sowohl die ungewöhnlich lange C–S-Bindung von 1.745(7) Å

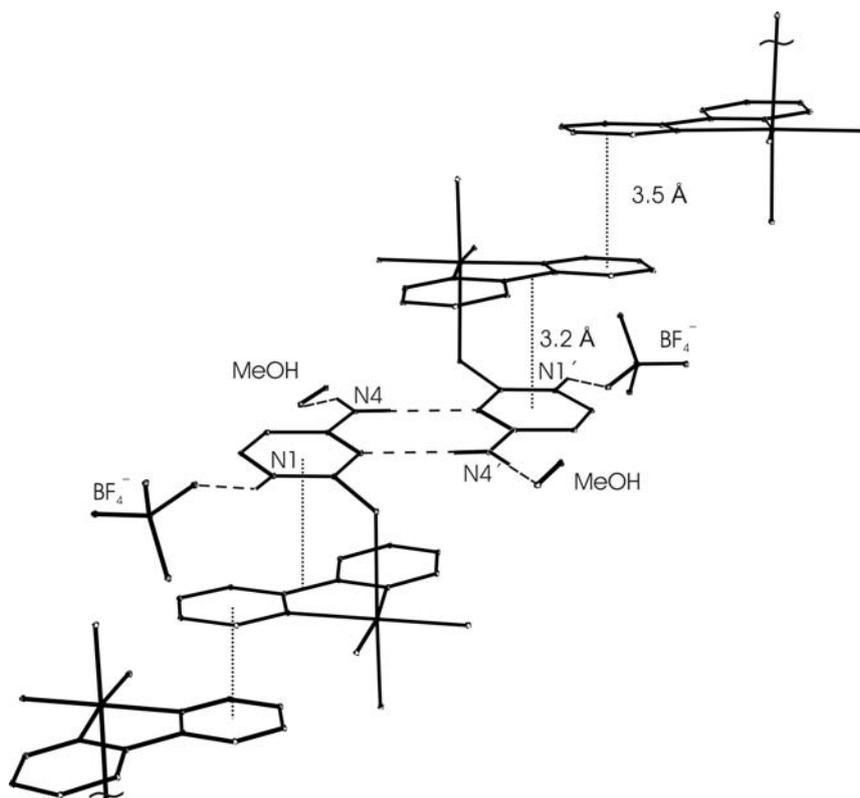


Abbildung 7. Packung der $[\text{PtMe}_3(\text{bpy})(\text{SCy})]^+$ -Kationen und BF_4^- -Anionen in $4\text{C}\cdot\text{MeOH}$ unter Einbeziehung der π - π -Wechselwirkungen (\cdots) und der Wasserstoffbrückenbindungen (---).

in $4\text{C}\cdot\text{MeOH}$ als auch der C2-S-Pt-Winkel ($103.0(2)^\circ$) sowie der Winkel von 78.2° , den die Thiocytosinebene und der Pt-S-Vektor einschließen. Die entsprechenden Werte in 5C (C-S $1.702(6)$ Å; C2-S-Pt 113.8° , $\angle_{(1-\text{MeSCy}, \text{Pt-S})}$ 19.3°) belegen andererseits eine sp^2 -Hybridisierung des Schwefelatoms.

Quantenchemische Rechnungen¹

Quantenchemische Rechnungen zeigen für die kationischen Thionucleobaseplatin(IV)-Komplexe $[\text{PtMe}_3(\text{bpy})(\text{nb-}\kappa\text{S})]^+$ (nb = s^2Ura , **3D**; s^4Ura , **4D**; $\text{s}^2\text{s}^4\text{Ura}$, **5D**_{calc.}) bzw. $[\{\text{PtMe}_3(\text{bpy})(\text{SCy-}\kappa\text{S})\}_2]^{2+}$ (**6C**_{calc.}) eine nahezu senkrechte Anordnung (88.8 – 90.0°) der Thionucleobaseliganden gegenüber der $[\text{PtC}_2\text{N}_2]$ -Ebene. Dabei kann der Ligand eine der fünf ausgezeichneten Konformationen (**a**–**e**) über der $[\text{PtC}_2\text{N}_2]$ -Ebene einnehmen (Abb. 8), wobei in allen Fällen Gleichgewichtsstrukturen lokalisiert werden konnten, die der Konformation **a** entsprechen. Im Unterschied dazu sind im Neutralkomplex $[\text{PtMe}_3(\text{bpy})(\text{pymt})]$ zwei nahezu

¹ Die quantenchemischen Rechnungen wurden von Herrn Prof. Dr. Steinborn und Herr Dr. G. N. Kaluderović angefertigt.

energiegleiche Gleichgewichtsstrukturen mit den Konformationen **c** und **d** lokalisiert worden. Des Weiteren wurde ein Übergangszustand (**e**) gefunden, der eine sehr niedrige Rotationsbarriere von nur 2.9 kcal/mol besitzt [A]. Die Konformation (**a**, Abb. 8) des SCy-Liganden in $[\{\text{PtMe}_3(\text{bpy})(\text{SCy-}\kappa\text{S})\}_2]^{2+}$ (**6C_{calc.}**) entspricht nicht der in Kristallen von **4C**·MeOH (Abb. 7) experimentell gefundenen. Zum einen nimmt der Ligand in **4C**·MeOH die Konformation **c** ein und zum anderen ist der Heterocyclus annähernd parallel zur $[\text{PtC}_2\text{N}_2]$ -Ebene angeordnet und steht nicht nahezu senkrecht auf ihr wie in **6C_{calc.}**.

Weiterführende quantenchemischen Rechnungen belegen, dass unter Einbeziehung der Tetrafluoroborat-Anionen eine Verringerung des SCy/bpy-Winkels zu beobachten ist. Daraus kann geschlussfolgert werden, dass die ungewöhnliche Konformation des SCy-Liganden in **4C**·MeOH ein Resultat der Kombination aus sp^2 -Hybridisierung des Schwefelatoms und der attraktiven Wechselwirkungen (π - π -Stapelung/Wasserstoffbrückenbindungen) ist.

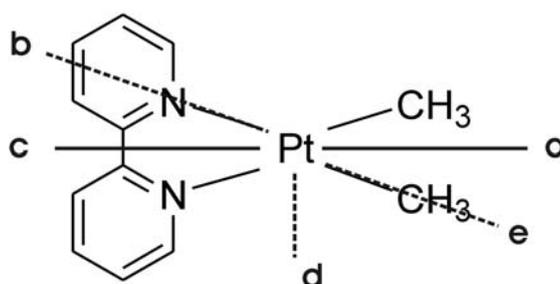


Abbildung 8. Konformationen der Thionucleobaseliganden (nb) in Bezug auf die $[\text{PtC}_2\text{N}_2]$ -Ebene mit Blickrichtung entlang der $\text{S}_{\text{nb}}\text{-Pt-CH}_3$ -Achse.

2.1.3. Zur Tautomerie und zum Koordinationsverhalten der Thionucleobasen

Die möglichen tautomeren Formeln der Thiocytosin- bzw. Thiouracilliganden sind in Abbildung 9 in der Reihenfolge Ihrer Stabilität wiedergegeben [27]. Demzufolge liegen die Thionucleobaseliganden in den Komplexen $[\text{PtMe}_3(\text{bpy})(\text{nb-}\kappa\text{S})][\text{BF}_4]$ (nb = 1-MeSCy, **5C**; s^2Ura , **3D**; s^4Ura , **4D**; $\text{s}^2\text{s}^4\text{Ura}$, **5D**) in der stabilsten Form als Amino-Thion- (1-MeSCy), Oxo-Thion- (s^2Ura , S^4Ura) bzw. Thion-Thion-Tautomer ($\text{s}^2\text{s}^4\text{Ura}$) vor. Dahingegen ist der 2-Thiocytosinligand in $[\text{PtMe}_3(\text{bpy})(\text{SCy-}\kappa\text{S})][\text{BF}_4]\cdot\text{MeOH}$ (**4C**·MeOH) in einer ungewöhnlichen tautomeren Form koordiniert, die als eine an N1 protonierte Amino-Thiolat-Form beschrieben werden kann (Abb. 9).

Ergebnisse und Diskussion

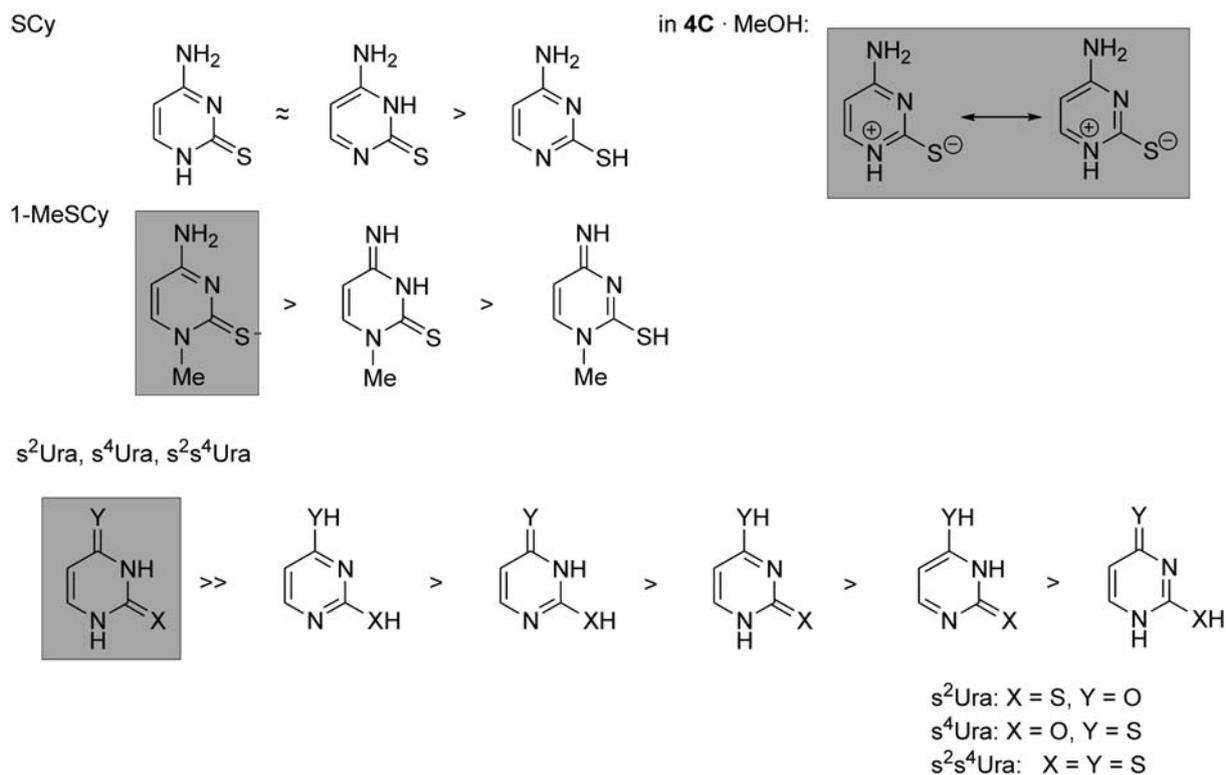


Abbildung 9. Tautomere von Thionucleobasen (nb) geordnet nach ihrer Stabilität [27]. Die grau unterlegten Formeln beziehen sich auf die tautomeren Formen der Thionucleobasen in den Komplexen $[\text{PtMe}_3(\text{bpy})(\text{nb}-\kappa\text{S})][\text{BF}_4]$ (nb = SCy, **4C**; 1-MeSCy, **5C**; $s^2\text{Ura}$, **3D**; $s^4\text{Ura}$, **4D**; $s^2s^4\text{Ura}$, **5D**).

Neben einer sehr großen Anzahl von Übergangsmetallkomplexen mit anionischen Thionucleobaseliganden findet man in der Literatur auch zahlreiche Komplexe mit neutralen Thionucleobaseliganden. Wie erwartet weisen neutrale Thionucleobaseliganden ein flexibles Koordinationsverhalten auf, welches in Abbildung 10 dargestellt ist [28]. Am besten untersucht sind Komplexe mit 2-Thiouracilliganden, die überwiegend κS^2 -koordiniert sind (**a**). Der 2-Thiocytosinligand ist mehrheitlich $\kappa\text{N}^3, \kappa\text{S}$ -koordiniert (**a**). Für 4-Thiouracil ist bisher nur die κS^4 -Koordinationsart beschrieben. Strukturell charakterisiert [29,30] wurden bislang nur zwei Komplexe mit einem monodentat gebundenen $s^2\text{Ura}-\kappa\text{S}^2$ - (**a**) und $s^2s^4\text{Ura}-\kappa\text{S}^4$ -Liganden (**a**). Im Rahmen dieser Arbeit konnten durch die Strukturen von **4C**·MeOH und **5C** zwei weitere Koordinationsmodi strukturell gesichert werden. Dabei ist der Platin(IV)-Komplex (**5C**) der erste Komplex mit 1-Methyl-2-thiocytosinliganden.

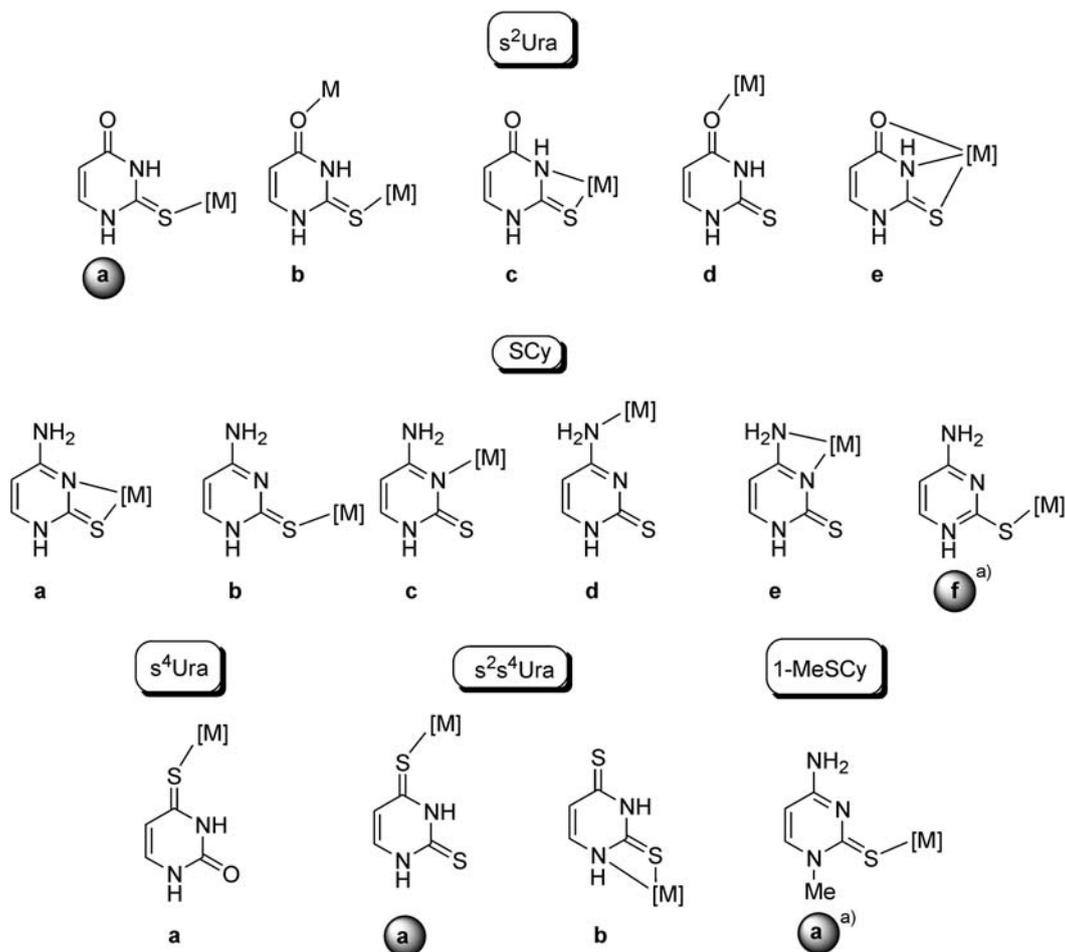


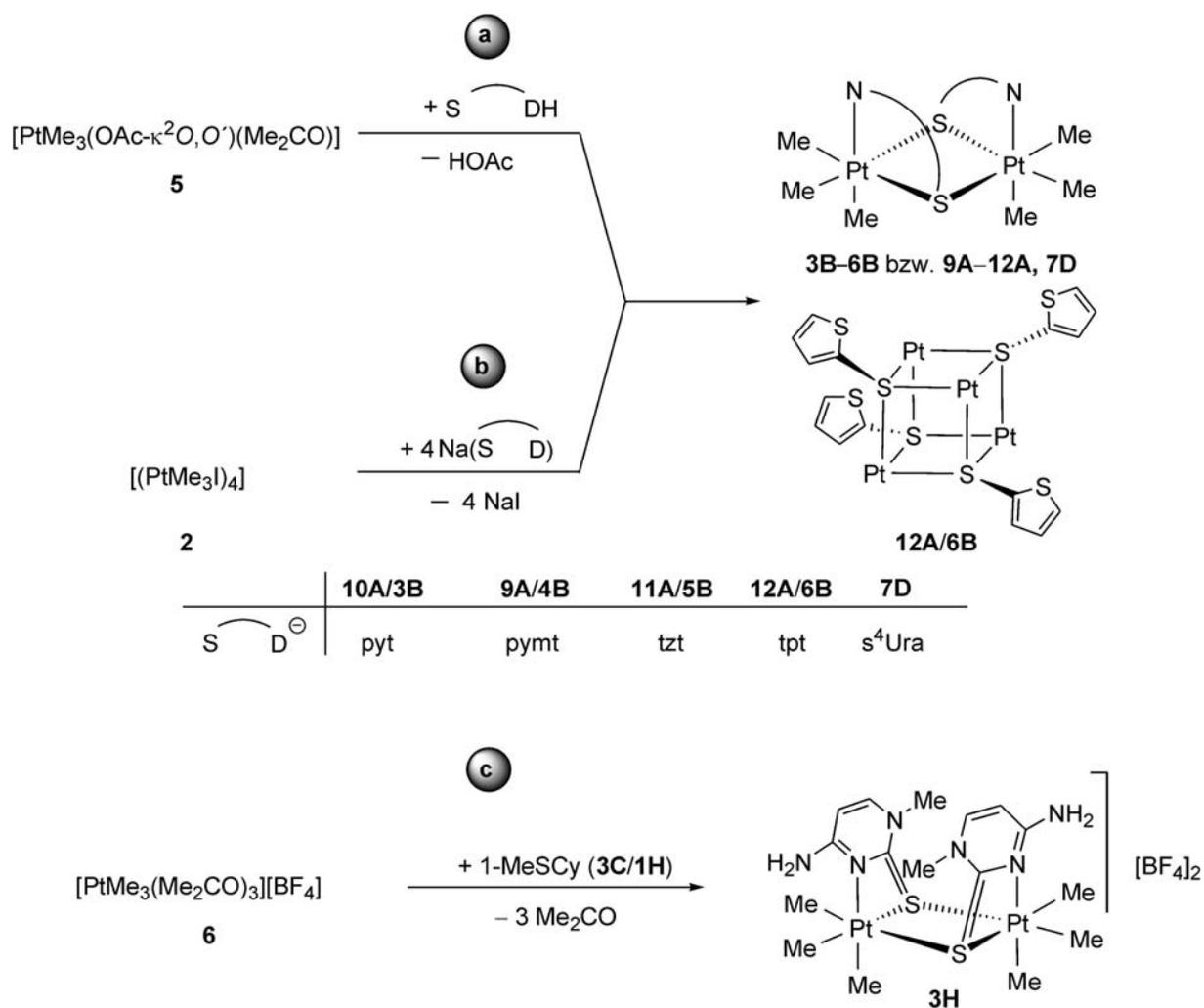
Abbildung 10. Experimentell ermittelte Koordinationsmodi neutraler Thionucleobaseliganden. Die grau unterlegten Buchstaben weisen auf Komplexe hin, deren Konstitution durch Röntgeneinkristallstrukturanalysen bewiesen wurde. ^{a)} Diese Arbeit. [M] = Metallfragmentkomplex.

Bisher wurden nur Platin(II)-Komplexe mit neutralen SCy- und s²Ura-Liganden beschrieben, in denen der SCy-Ligand mono- (c) bzw. bidentat (a) koordiniert vorliegt und der s²Ura Ligand eine Chelatkoordination (c) besitzt [28]. In der vorliegenden Arbeit konnte gezeigt werden, dass in Thionucleobaseplatin(IV)-Komplexen des Typs [PtMe₃(bpy)(nb-κS)][BF₄] (nb = SCy, 4C; 1-MeSCy, 5C; s²Ura, 3D; s⁴Ura, 4D; s²s⁴Ura, 5D), in dem durch fest gebundene Coliganden eine monodentate Koordination der Thionucleobasen erzwungen wird, diese immer über das exocyclische Schwefelatom erfolgt. Im Falle von 2,4-Dithiouracil (Komplex 5D) ist dies die C=S₄-Gruppe, die nur ein elektronegatives N-Atom in unmittelbarer Nachbarschaft besitzt.

2.2. Oligonukleare Platin(IV)-Komplexe mit *N,S*- und *S,S*-heterocyclischen und Thionucleobaseliganden [A, B, H]

2.2.1. Synthese und Charakterisierung

Im vorhergehenden Teil dieser Arbeit konnte gezeigt werden, dass Thionucleobaseliganden in Platin(IV)-Komplexen, die nur über eine substitutionslabile Koordinationsstelle verfügen, bevorzugt über das exocyclische Schwefelatom koordinieren. Im Folgenden stand das Koordinationsverhalten gegenüber Platin(IV)-Komplexen im Fokus, die bis zu drei substitutionslabile Koordinationsstellen besitzen. Als Precusorkomplexe wurden die Platin(IV)-Komplexe $[\text{PtMe}_3(\text{OAc}-\kappa^2\text{O},\text{O}')(\text{Me}_2\text{CO})]$ (**5**) und $[\text{PtMe}_3(\text{Me}_2\text{CO})_3][\text{BF}_4]$ (**6**) gewählt. Da Thionucleobasen, wie eingangs erwähnt, auf Grund ihrer Vielzahl an Donoratomen ein flexibles Koordinationsverhalten besitzen, wurden zunächst die *N,S*- und *S,S*-Heterocyclen Pyridin-2-thion (pytH), Pyrimidin-2-thion (pymtH), Thiazolin-2-thion (tztH) sowie Thiophen-2-thiol (tptH) als Modellliganden verwendet. Diese besitzen nur zwei mögliche Donorzentren (*N*- und *S*-Donoren). Die Reaktion von $[\text{PtMe}_3(\text{OAc}-\kappa^2\text{O},\text{O}')(\text{Me}_2\text{CO})]$ (**5**) mit den *N,S*- und *S,S*-Heterocyclen sowie 4-Thiouracil ($s^4\text{Ura}$), führt unter Deprotonierung der Liganden zur Ausbildung der di- bzw. tetranuklearen Neutralkomplexe $[(\text{PtMe}_3)_2(\mu\text{-S}\widehat{\text{D}})_2]$ ($\text{S}\widehat{\text{D}}$ = pymt, **9A/4B**; pyt, **10A/3B**; tzt, **11A/5B**; $s^4\text{Ura}$, **7D**) und $[(\text{PtMe}_3)_4(\mu_3\text{-tpt})_4]$ (**12A/6B**, Schema 2a) [**A**]. Darüber hinaus konnte gezeigt werden, dass die Reaktion der Natriumsalze $\text{Na}(\text{S}\widehat{\text{D}})$ ($\text{S}\widehat{\text{D}}$ = pymt, pyt, tzt, tpt) mit $[(\text{PtMe}_3\text{I})_4]$ (**2**) ebenfalls zu den di- (**9A–11A/3B–5B**) und tetranuklearen (**12A/6B**) Komplexen führt und keine anaeroben Bedingungen erfordert (Schema 2b) [**B**]. Währenddessen konnte der ionische dinukleare Komplex $[(\text{PtMe}_3)_2(\mu\text{-1-MeSCy})_2][\text{BF}_4]_2$ (**3H**) in der Umsetzung von $[\text{PtMe}_3(\text{Me}_2\text{CO})_3][\text{BF}_4]$ (**6**) mit 1-Methyl-2-thiocytosin (1-MeSCy, **3C/1H**; Schema 2c) isoliert werden. Die Komplexe wurden in Ausbeuten von 16–93% isoliert und sowohl durch Elementaranalyse und IR-Spektroskopie als auch ^1H -, ^{13}C - und ^{195}Pt -NMR-Spektroskopie, hochauflösender ESI-Massenspektrometrie und Röntgen-einkristallstrukturanalyse charakterisiert.



Schema 2. Synthesewege von di- und tetranuklearen Platin(IV)-Komplexen mit *N,S*- und *S,S*-Heterocyclen und Thionucleobaseliganden.

2.2.2. Strukturelle Aspekte

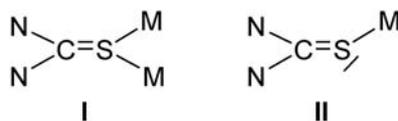
Die Molekülstrukturen der dinuklearen Komplexe $[(\text{PtMe}_3)_2(\text{S} \widehat{\text{N}})_2]$ mit deprotonierten $\text{S} \widehat{\text{N}}$ -Liganden ($\text{S} \widehat{\text{N}} = \text{pyt}$, **10A/3B**, pymt , **9A/4B**) und des dinuklearen Komplexkations $[(\text{PtMe}_3)_2(\mu\text{-1-MeSCy})_2]^{2+}$ in Kristallen von **3H**·1.5 C₆H₆ weisen eine hohe Ähnlichkeit zueinander auf. Alle Komplexe besitzen eine zentrale Pt₂(μ-S)₂-Einheit, die leicht abgewinkelt (Pt1–S1…S2–Pt2: 168.2–173.9°) und somit annähernd C₂-symmetrisch ist (vgl. Abb. 11). Darüber hinaus sind sowohl die heterocyclischen *N,S*-Liganden in **10A/3B** und **9A/4B** als auch die 1-Methyl-2-thiocytosinliganden in **3H**·1.5 C₆H₆ *cis*-ständig¹ zueinander angeordnet und verbrücken in den jeweiligen Komplexen beide Platin(IV)-Atome in einer 1κN,1:2κ²S-Koordination. Zentroid-Zentroid-Abstände (*a*, Abb.11) von 3.4–3.5 Å und

¹ Hier und im Folgenden bezieht sich „*cis*“/„*trans*“ auf die Anordnung der Liganden auf der gleichen/ gegenüberliegenden Seite der Pt₂(μ-S₂)-Einheit.

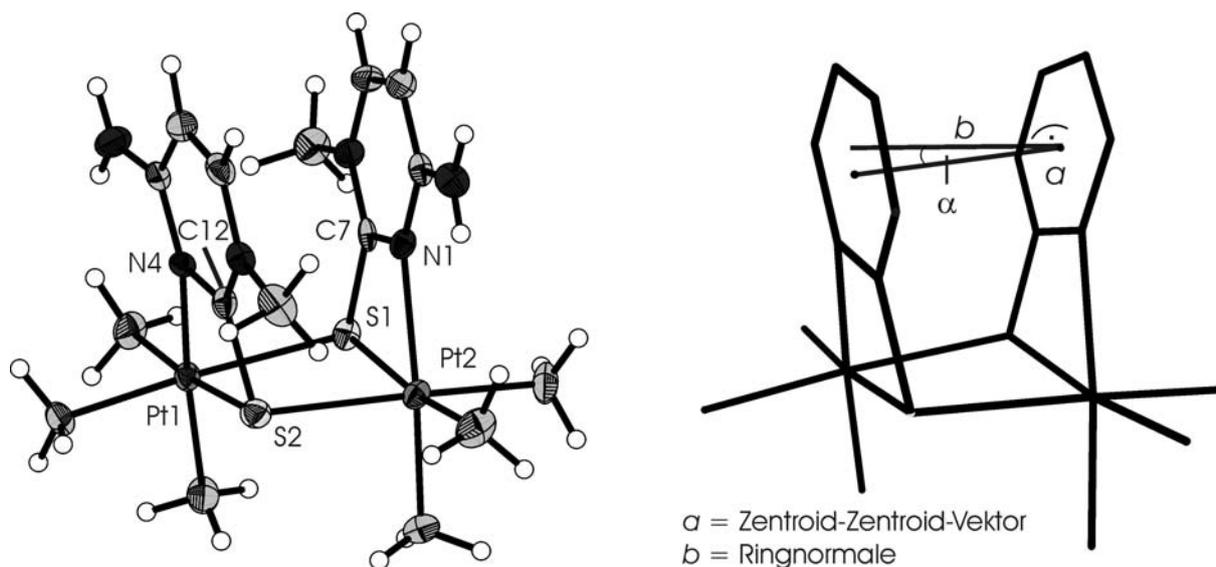
Ergebnisse und Diskussion

Winkel (α) zwischen Zentroid-Zentroid-Vektor und Ringnormalen (b) von $10.4\text{--}16.7^\circ$ lassen auf π - π -Wechselwirkungen schließen [31]. Auf Grund der $1\kappa N^3, 1:2\kappa^2 S$ -Koordination der Liganden und Ausbildung eines Pt–N–C–S-Vierringes kommt es erwartungsgemäß zu erheblichen Abweichungen von der Idealgeometrie innerhalb des Moleküls, was an den sehr kleinen N–Pt–S-Winkeln ($65.4(1)\text{--}66.9(1)^\circ$) deutlich wird.

Interessanterweise ist die C=S-Doppelbindung im Komplexkation $[(PtMe_3)_2(\mu\text{-}1\text{-MeSCy})_2]^{2+}$ in Kristallen von **3H**·1.5 C₆H₆ im Vergleich zu den C–S-Einfachbindungen in **10A/3B** und **9A/4B** fast genauso lang. Offensichtlich beruht die Verlängerung der Doppelbindung hauptsächlich auf der verbrückenden Metallkoordination. Ähnlich lange C=S-Bindungen werden in M₂(μ -S)₂-Metallkomplexen mit verbrückenden μ -CNC=S-Fragmenten (Typ **I**) gefunden (Median: 1.724; unteres/oberes Quartil: 1.710/1.742, $n = 3006$, n -Anzahl der Beobachtungen) [32], während in solchen mit monodentat koordinierten NNC=S Fragmenten (Typ **II**) deutlich kürzere C=S-Bindungslängen beobachtet werden (Median: 1.715; unteres/oberes Quartil: 1.701/1.728, $n = 212$).



Möglicherweise wird die Länge der C=S-Bindung aber auch durch die Ringspannung im Pt–N–C–S-Vierring beeinflusst.



	C–S	Pt–S	Pt1–S1...S2–Pt2	N–Pt–S
3H ·1.5 C ₆ H ₆	1.726(7)/1.737(7)	2.501(2)–2.551(2)	168.2(8)	65.4(1)/66.0(1)
9A/4B, 10A/3B	1.745(7)–1.777(8)	2.465(2)–2.551(3)	169.91(8)–173.91(9)	66.0(2)–66.9(1)

Abbildung 11. Molekülstruktur von $[(\text{PtMe}_3)_2(\mu\text{-1-MeSCy})_2]^{2+}$ in Kristallen von **3H**·1.5 C₆H₆ und charakteristische strukturelle Parameter zur Bestimmung der π – π -Wechselwirkungen. Die Tabelle gibt ausgewählte Strukturdaten (Bindungslängen in Å, Bindungswinkel in °) von **3H**·1.5 C₆H₆, **9A/4B** und **10A/3B** wieder. Die Torsionswinkel sind als Absolutwerte angegeben.

Quantenchemische Rechnungen

Quantenchemische Rechnungen der dinuklearen Komplexe $[(\text{PtMe}_3)_2(\mu\text{-}\widehat{\text{S}}\text{N})_2]$ ($\widehat{\text{S}}\text{N}$ = pyt, **10A/3B**; pymt, **9A/4B**; tzt, **11A/5B**) belegen im Einklang mit den Röntgeneinkristallstrukturanalysen eine leicht höhere Stabilität (1.7–2.9 kcal/mol) der *cis*- gegenüber der *trans*-Konformation (vgl. Fußnote auf Seite 20) [**B**]. Die Bevorzugung der *cis*- gegenüber der *trans*-Anordnung spiegelt sich auch bei anderen Pyridin-2-thiolato- und Pyrimidin-2-thiolato-Metallkomplexen wider. Es werden überwiegend Komplexe mit *cis*-ständig angeordneten Liganden gefunden [33], während es nur relativ wenige Komplexe mit *trans*-ständig angeordneten Liganden gibt [34]. Im Fall des Thiazolin-2-thiolato-Komplexes $[(\text{PtMe}_3)_2(\mu\text{-}\widehat{\text{S}}\text{N})_2]$ (**11A/5B**) wurden vier Gleichgewichtsstrukturen lokalisiert (Abb. 12). Der Komplex mit *S,N*-gebundenen Liganden in *cis*-Stellung ist der stabilste. Interessanterweise konnte keine Gleichgewichtsstruktur mit *S,S'*-gebundenen Liganden

Ergebnisse und Diskussion

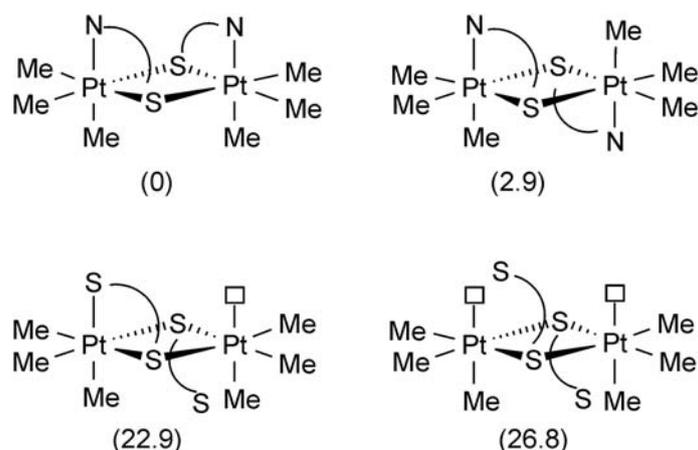


Abbildung 12. Berechnete Gleichgewichtsstrukturen von $[(\text{PtMe}_3)_2(\mu\text{-tzt})_2]$. In Klammern sind die relativen Energien (E_{rel} in kcal/mol) in Bezug auf den stabilsten Komplex angegeben. □ = freie Koordinationsstelle.

lokalisiert werden, wohl aber eine sehr energiereiche in der ein Ligand S,S' -gebunden ist, der andere jedoch nur mononuklear über das exocyclische Schwefelatom, so dass ein Platinatom nur fünffach koordiniert ist. Auch im Fall des Thiophen-2-thiolato-Liganden besitzt das endocyclische Schwefelatom eine geringe Koordinationstendenz, was zur Ausbildung des tetranuklearen Komplexes $[(\text{PtMe}_3)_4(\mu_3\text{-tpt})_4]$ (**12A/6B**) und nicht zum entsprechenden Dimer $[(\text{PtMe}_3)_2(\mu\text{-tpt})_2]$ führt.

2.2.3. Koordinationsmodi der N,S - und S,S -heterocyclischen Liganden

Ein Überblick über die verschiedenartigen Koordinationsmodi in Komplexen mit den im Rahmen dieser Arbeit behandelten N,S -heterocyclischen Liganden ist in Abbildung 13 gegeben. In der überwiegenden Anzahl findet man einfach deprotonierte Liganden, die gemäß **b** bzw. **c** (Abb. 13) vorwiegend κS - [35] und $\kappa S, \kappa N$ -koordiniert sind [36]. Im Falle der Neutralliganden liegt eine κS -Koordinationsart gemäß **a** vor [37]. Am besten untersucht sind Pyridin-2-thiolato-Metallkomplexe. Eine $1\kappa N, 1:2\kappa^2 S$ -Koordinationsart (vgl. **f**, Abb. 13), wie sie in den Pyridin-2-thiolato- und Pyrimidin-2-thiolatoplatin(IV)-Komplexen **10A/3B** und **9A/4B** gefunden wurde, ist für andere Metalle nur relativ selten beschrieben [33,34]. Der Thiazolin-2-thiolatokomplex $[(\text{PtMe}_3)_2(\mu\text{-S} \curvearrowright \text{N})_2]$ (**11A/5B**) ist sogar der erste Komplex mit einer derartigen Koordination.

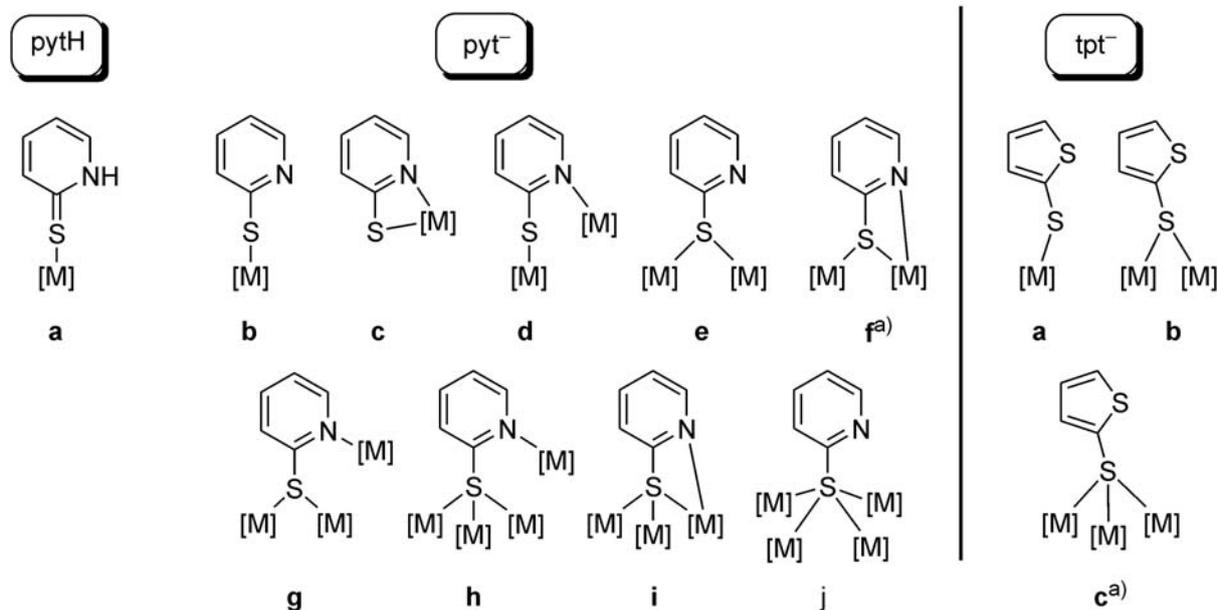


Abbildung 13. Experimentell ermittelte Koordinationsmodi der *N,S*- und *S,S*-Heterocyclen.

^{a)} Diese Arbeit. [M] = Metallfragmentkomplex.

Die verschiedenartigen Koordinationsmodi des *S,S*-heterocyclischen Thiophenthioolato-Liganden sind in Abb. 13 (a-c) aufgeführt. In allen Fällen ist nur das exocyclische Schwefelatom in die Koordination einbezogen. Überwiegend findet sich eine monodentate κS -Koordination (a) [38]. Komplex $[(PtMe_3)_4(\mu_3\text{-tpt-}\kappa S)_4]$ (**12A/6B**) ist der bislang einzige Komplex, in dem eine μ_3 -Koordination gemäß c gefunden wurde.

Lösungen des dinuklearen Komplexes $[(PtMe_3)_2(\mu\text{-s}^4\text{Ura-H})_2]$ (**7D**) mit $1\kappa N,1:2\kappa S$ -koordinierten Thiouracilato-Liganden (Schema 2) erwiesen sich als nicht stabil. Als Zersetzungsprodukt wurde ein hexanuklearer Komplex (**7aD**) gefunden (Abb. 14), der jeweils drei verschiedenartige Platinzentren (Pt1–3) und $s^4\text{Ura}$ -Liganden (**A**, **B**, **C**) aufweist. Die grau unterlegte Struktur zeigt die ursprüngliche $Pt_2(\mu\text{-S})_2$ -Einheit des dinuklearen Komplexes **7D**. Bemerkenswert ist, dass ein $s^4\text{Ura}$ -Ligand doppelt deprotoniert ist und die Bildung von **7aD** unter Abspaltung eines Methyliganden vom Platin abläuft. In der Bildung von **7aD** zeigt sich die Tendenz von 4-Thiouracil zur Ausbildung multinuklearer Komplexe. In der Literatur finden sich analoge Beispiele für die sauerstoffhaltigen Nucleobasen [39].

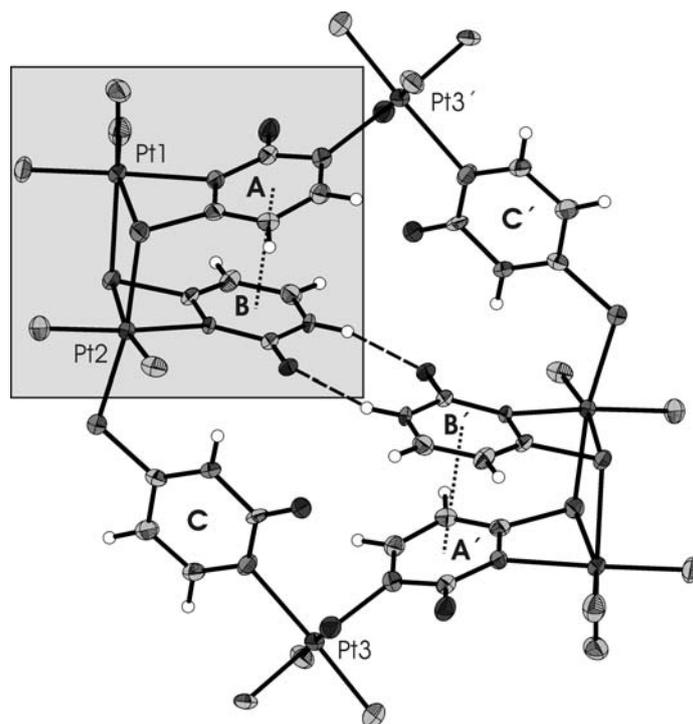


Abbildung 14. Molekülstruktur des hexanuklearen Zersetzungsproduktes **7aD**.

Im Falle von Uracil und dessen Derivaten sind zumeist tetranukleare Platin(II)-Komplexe beschrieben worden [40], aber auch ein hexanuklearer Quecksilber(II)-Komplex ist bekannt [41]. Die *N,S*- und *S,S*-heterocyclischen Modellliganden können ebenfalls oligonukleare (tri-, tetra-, hexanuklear) und polymere Komplexe ausbilden, die auch strukturell charakterisiert wurden [42].

2.2.4. Cytotoxische Eigenschaften von Platin(IV)-Komplexen mit *N,S*-heterocyclischen und Thionucleobaseliganden [**B,C,D**]¹

Cytotoxische Untersuchungen sind mit dem Ziel durchgeführt worden, zu testen ob die Koordination eines bioaktiven Liganden an Platin zu Komplexen führt, die eine höhere cancerostatische Aktivität aufweisen als vergleichbare Komplexe mit „abiotischen“ Liganden. Die mononuklearen Thionucleobaseplatin(IV)-Komplexe [PtMe₃(bpy)(nb-κS)][BF₄] (nb = SCy, **4C**; 1-MeSCy, **5C**; s²Ura, **4D**; s⁴Ura, **5D**; s²s⁴Ura, **6D**) wurden in *In vitro* Studien gegenüber neun Zelllinien untersucht, während die dimeren Komplexe [(PtMe₃)₂(μ-S^κN)₂] (S^κN = pyt, **3B/10A**; pymt = **4B/9A**; tzt = **5B/11A**) gegenüber fünf Zelllinien getestet wurden. Eine Zusammenfassung der Ergebnisse ist in Tabelle 2 gegeben.

¹ Die Untersuchungen der cytotoxischen Eigenschaften wurden von Herrn Dr. G. N. Kaluderović durchgeführt.

Tabelle 2. Zusammenfassung der Ergebnisse der *In vitro* Studien zur Untersuchung der cytotoxischen Aktivitäten von Platin(IV)-Komplexen mit *N,S*-heterocyclischen und Thionucleobaseliganden. Den IC₅₀-Werten sind die entsprechenden Werte von Cisplatin, der freien Liganden sowie von [PtMe₃I(bpy)] zum Vergleich gegenübergestellt.

lfd. Nr.	Verbindung	IC ₅₀ in μM	Bemerkung
1	SCy, 1-MeSCy, s ² Ura, s ⁴ Ura, s ² s ⁴ Ura, S [⌢] NH	>125	keine cancerostatische Aktivität
2	Cisplatin	0.55–5.14	
3	[PtMe ₃ I(bpy)]	7.38–18.36	moderate cancerostatische Aktivität
4	[(PtMe ₃)(bpy)(nb-κS)][BF ₄] (4C , 5C , 3D–5D)	1.74–42.14	3D , 5D : spezifische Aktivität gegenüber A549 bzw. A2780, vergleichbar mit Cisplatin
5	[(PtMe ₃) ₂ (μ-tzt) ₂] 5B/11A	0.53–1.32	aktivster Komplex des Typs [(PtMe ₃) ₂ (μ-S [⌢] N) ₂] vergleichbare (A253) bzw. 4-fach höhere Aktivität (8505C/DLD-1) als Cisplatin
6	[(PtMe ₃) ₂ (μ-S [⌢] N) ₂] (3B/10A ; 4B/9A)	1.10–12.55	3B/10A : spezifische Aktivität gegenüber A2780 und DLD-1; gegenüber DLD-1 2-fach höhere Aktivität als Cisplatin; 4B/9A : spezifische Aktivität gegenüber A2780, vergleichbar mit Cisplatin

Die heterocyclischen Liganden vom Typ S[⌢]NH (S[⌢]NH = pytH, pymtH, tztH) sowie die Thionucleobasen (SCy, **2C**; 1-MeSCy **3C/1H**) zeigen gegenüber allen untersuchten Zelllinien keine Aktivität im untersuchten Konzentrationsbereich (Eintrag 1, Tabelle 2). Sie sind demzufolge zwar prinzipiell bioaktiv [43], wirken aber nicht cancerostatisch. Die Gesamtheit der mononuklearen [PtMe₃(bpy)(nb-κS)][BF₄]-Komplexe sowie die zwei dinuklearen Komplexe [(PtMe₃)₂(μ-S[⌢]N)₂] (S[⌢]N = pyt, **3B/10A**; pymt = **4B/9A**) besitzen überwiegend moderate cytotoxische Eigenschaften (Einträge 4 und 6). Dennoch zeigen sie spezifische Aktivitäten gegenüber einzelnen Zelllinien die in Tabelle 2 aufgeschlüsselt sind. Eine herausragende, bis zu vierfach höhere, Aktivität als Cisplatin wurde für den dinuklearen Komplex [(PtMe₃)₂(μ-tzt)₂] (**5B/11A**) ermittelt (Eintrag 5). Der Vergleich mit Trimethylplatin(IV)-

Komplexen, die nur „abiotische“ Liganden enthalten, zeigt für [PtMe₃I(bpy)] (Eintrag 3) vergleichbare IC₅₀-Werte mit denen der mono- und dinuklearen Komplexe (Einträge 4 und 6). Anhand der Untersuchungen kann man die Aussage treffen, dass die Kombination zweier bioaktiver Spezies nicht generell zu Komplexen mit erhöhten cancerostatischen Aktivitäten führt, sondern von Fall zu Fall unterschiedlich ist.

Komplex **5D** wurde als aktivster Komplex der Untersuchungsreihe **3D–5D** weiteren Untersuchungen zur Ermittlung der Art des eingeleiteten Zelltodes (Apoptose vs. Nekrose) unterzogen. Zellzyklusanalysen als auch ein Trypan-Blau-Ausschlusstest gegenüber der Zelllinie A431 belegen eine Induzierung des apoptotischen Zelltodes. Darüber hinaus zeigen die Zellzyklusanalysen eine Störung während der G1-Phase (postmitotische Phase) des Zellzyklus.

2.3. Platinkomplexe mit Thioglycosidliganden [E,F,G]

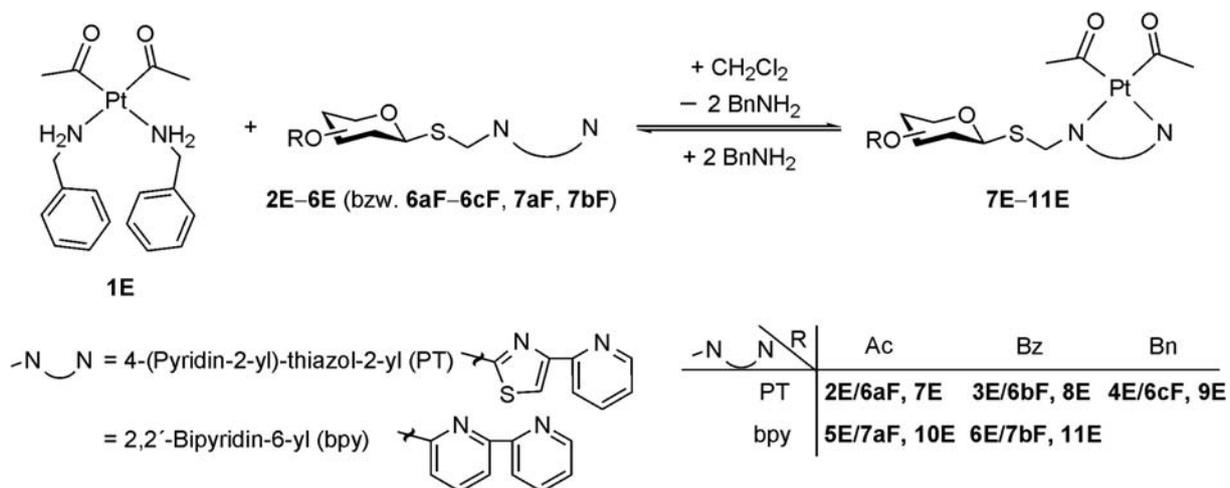
2.3.1. Synthese und Charakterisierung von Thioglycosidplatin(II)-Komplexen

Neben Thionucleobasen sind schwefelhaltige Kohlenhydrate eine weitere wichtige Klasse von schwefelhaltigen Bioliganden. Im Rahmen der vorliegenden Arbeit ist das Koordinationsverhalten von Thioglycosiden gegenüber Platin untersucht worden. Zunächst werden entsprechende Platin(II)-Komplexe besprochen.

In der Reaktion von Diacetylbis(benzylamin)platin(II) (**1E**) mit Thioglycosiden des Typs ch-SPT (**2E–4E** bzw. **6aF–6cF**) die über eine 4-(Pyridin-2-yl)-thiazol-2-yl-Gruppe (PT) in der anomeren Einheit verfügen, bilden sich gemäß Schema 3 in einer Gleichgewichtsreaktion die Thioglycosidplatin(II)-Komplexe [Pt(COMe)₂(ch-SPT)] (**7E–9E**), was zweifelsfrei durch IR- und ¹H-, ¹³C-, ¹⁹⁵Pt-NMR-Spektroskopie sowie hochauflösende ESI-Massenspektrometrie belegt werden konnte. Der Umsetzungsgrad beträgt bis zu 80%. Allerdings konnten die Produkte nicht isoliert werden, da beim Fällern mit Diethylether eine fast vollständige Verschiebung des Gleichgewichtes zu Gunsten der Edukte eintritt. Die Koordination der Thioglycosidliganden an das Platinatom über die anomere SPT-Gruppe (**7E–9E**) kann eindeutig anhand der koordinationsinduzierten Verschiebungen (coordination induced shift's, CIS's) von bis zu 0.32 bzw. 2.8 ppm für die Protonen und Kohlenstoffatome der Chelatliganden in den ¹H-NMR- und ¹³C-NMR-Spektren belegt werden. Daher ist es erstaunlich, dass die Komplexe **7E–9E** trotz chelatgebundener Liganden in Lösung nicht stabil sind. Die analogen Reaktionen von [Pt(COMe)₂(BnNH₂)₂] (**1E**) mit ch-Sbpy-

Thioglycosiden, die in der anomeren Einheit über einen 2,2'-Bipyridin-6-yl-Chelatliganden (bpy) verfügen, liefern widersprüchliche Ergebnisse. Während die Bildung der Komplexe $[\text{Pt}(\text{COMe})_2(\text{ch-Sbpy})]$ (**10E**, **11E**) durch hochauflösende ESI-Massenspektrometrie zweifelsfrei belegt werden kann, zeigen NMR-Versuche nur die Signale der Edukte. Dies deutet darauf hin, dass es sich bei der Bildung der $[\text{Pt}(\text{COMe})_2(\text{ch-Sbpy})]$ (**10E**, **11E**) Komplexe ebenfalls um eine Gleichgewichtsreaktion handelt, die nahezu vollständig auf Seiten der Edukte liegt. Im Gegensatz dazu setzt sich **1E** mit 2,2'-Bipyridin zu $[\text{Pt}(\text{COMe})_2(\text{bpy})]$ um, ohne dass eine Rückreaktion beobachtet wurde [44]. Weitere Untersuchungen zur Synthese und Isolierung der Komplexe, insbesondere im Fall von $[\text{Pt}(\text{COMe})_2(\text{ch-Sbpy})]$ (**10E**, **11E**), sind erforderlich, wobei durch Variation der Lösungsmittel versucht werden muss, nicht den Startkomplex **1E** auszufällen, sondern die Reaktion zu Gunsten der Thioglycosidplatin(II)-Komplexe **7E–11E** zu verschieben.

Im Zusammenhang mit den besprochenen Untersuchungen ist es gelungen, Einkristalle von $[\text{Pt}(\text{COMe})_2(\text{BnNH}_2)_2]$ (**1E**) zu erhalten. Eine Röntgeneinkristallstrukturanalyse zeigt ungewöhnlich lange Pt–N Bindungslängen von 2.164(2) Å (Median: 2.040 Å; unteres/oberes Quartil: 2.027/ 2.053 Å, $n = 2139$; n – Anzahl der Beobachtungen) [32] und belegt damit die experimentell beobachtete hohe Reaktivität von $[\text{Pt}(\text{COMe})_2(\text{BnNH}_2)_2]$ (**1E**) durch Abspaltung der Benzylaminliganden.



Schema 3. Synthese von Platin(II)-Komplexen **7E–11E** mit Thioglycosidliganden.

2.3.2. Synthese und Charakterisierung von Thioglycosidplatin(IV)-Komplexen

Für die Untersuchung des Koordinationsverhaltens von Thioglycosiden in Platin(IV)-Komplexen wurden Platin(IV)-Precursorkomplexe verwendet, die über bis zu drei substitutionslabile Koordinationsstellen verfügen. Dabei besitzen $[\text{PtMe}_3(4,4'\text{-R}_2\text{bpy})(\text{MeCO})][\text{BF}_4]$ ($\text{R} = \text{H}$, **3a**; $\text{R} = \text{'Bu}$, **3b**) und $[\text{PtMe}_3(\text{OAc-}\kappa^2\text{O,O})(\text{Me}_2\text{CO})]$ (**5**) sowie $[\text{PtMe}_3(\text{Me}_2\text{CO})_3][\text{BF}_4]$ (**6**) einen bzw. drei Acetonliganden, die leicht substituierbar sind. Darüber hinaus kann der Acetatokomplex **5** beim Übergang zum η^1 -gebundenen bzw. bei vollständiger Abspaltung des Acetatoliganden eine bzw. zwei weitere Koordinationsstellen generieren. Die Gesamtheit der verwendeten Thioglycoside ist in Abbildung 15 wiedergegeben. Die Umsetzung der Komplexe $[\text{PtMe}_3(4,4'\text{-R}_2\text{bpy})(\text{Me}_2\text{CO})][\text{BF}_4]$ ($\text{R} = \text{H}$, **3a**; $\text{R} = \text{'Bu}$, **3b**) und $[\text{PtMe}_3(\text{OAc-}\kappa^2\text{O,O})(\text{Me}_2\text{CO})]$ (**5**) mit Thioglycosiden der Typen ch-SEt und ch-STaz führt gemäß Schema 4a/b zu den ionischen Komplexen $[\text{PtMe}_3(4,4'\text{-R}_2\text{bpy})(\text{ch}^*)][\text{BF}_4]$ bzw. den Neutralkomplexen $[\text{PtMe}_3(\text{OAc-}\kappa^2\text{O,O})(\text{ch}^*)]$ ($\text{ch}^* = \text{ch-SEt}$, ch-STaz).

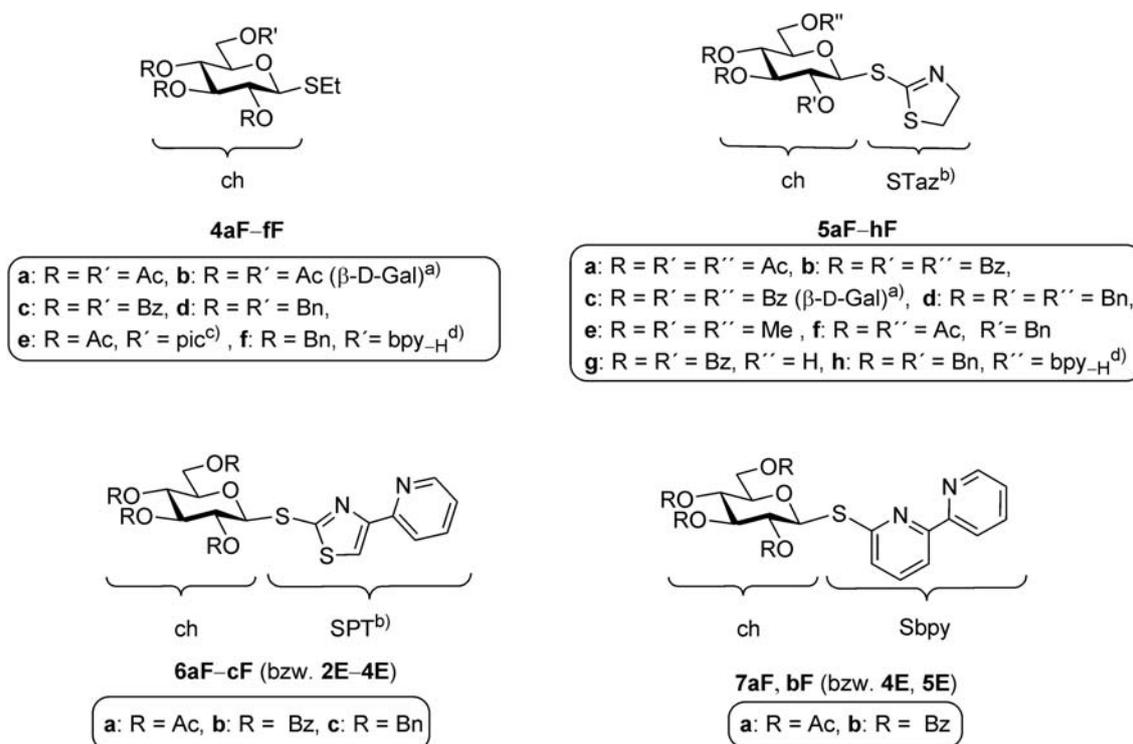
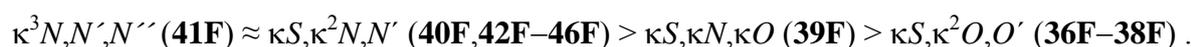


Abbildung 15. Thioglycoside die als Liganden verwendet wurden. ^{a)} $\beta\text{-D-Galactose}$: OR an C4 in axialer Position. ^{b)} Abkürzungen: Taz: Thiazolin-2-yl; PT: 4-(Pyridin-2-yl)-thiazol-2-yl, ^{c)} pic: 2-Picolin-2-yl, ^{d)} bpy-H: 2,2'-Bipyridin-6-yl.

Dahingegen führt die Umsetzung von $[\text{PtMe}_3(\text{Me}_2\text{CO})_3][\text{BF}_4]$ (**6**) mit den Thioglycosiden der Typen ch-SEt, ch-STaz, ch-SPT, und ch-Sbpy zu den Komplexen $[\text{PtMe}_3(\text{ch}^*)][\text{BF}_4]$ ($\text{ch}^* = \text{ch-SEt, ch-STaz, ch-SPT, ch-Sbpy}$) mit tridentat-koordinierten Thioglycosidliganden (Schema 4c). Die Identität aller Komplexe wurde umfassend durch IR- und ^1H -, ^{13}C -, ^{195}Pt -NMR-Spektroskopie, hochauflösende ESI-Massenspektrometrie sowie im Fall von $[\text{PtMe}_3(\text{bpy})(\text{ch-STaz})][\text{BF}_4]$ (**19F**, ch-STaz = **5cF**) auch durch Röntgeneinkristallstrukturanalyse belegt. Die Auswertung der ^1H - und ^{13}C -NMR-Spektren zeigt eine κS -Koordination der ch-SEt-Thioglycosidliganden in den Komplexen. Nur im Falle der Komplexe $[\text{PtMe}_3(\text{bpy})(\text{ch-SEt})][\text{BF}_4]$ (**12F**, ch-SEt = **4eF**) und $[\text{PtMe}_3(\text{OAc-}\kappa^2\text{O},\text{O}')(\text{ch-SEt})][\text{BF}_4]$ (**28F**, ch-SEt = **4eF**) erfolgt die Koordination mit hoher Wahrscheinlichkeit über das Stickstoffatom der Picolin-6-yl-Gruppe. Für die ch-STaz-Thioglycosidliganden wird ausschließlich eine κN -Koordination über das endocyclische Stickstoffatom der anomeren Thiazolin-2-yl-Gruppe beobachtet, was die Röntgeneinkristallstrukturanalyse von $[\text{PtMe}_3(\text{bpy})(\text{ch-STaz-}\kappa\text{N})][\text{BF}_4]$ (**19F**, ch-STaz = **5cF**) zweifelsfrei belegt (vgl. Abb. 16) und auf Grund der analogen ^1H - und ^{13}C -NMR-Spektren ebenfalls für die restlichen Komplexe gleichen Typs abgeleitet werden kann. In den Komplexen $[\text{PtMe}_3(\text{ch}^*)][\text{BF}_4]$ mit tridentat-koordinierten Thioglycosidliganden finden sich vielfältige Koordinationsmodi (vgl. Schema 4c). Dabei ist eine Zunahme der Stabilität der Komplexe in Lösung zu beobachten, je stärker die Donorgruppen des Thioglycosidliganden sind:

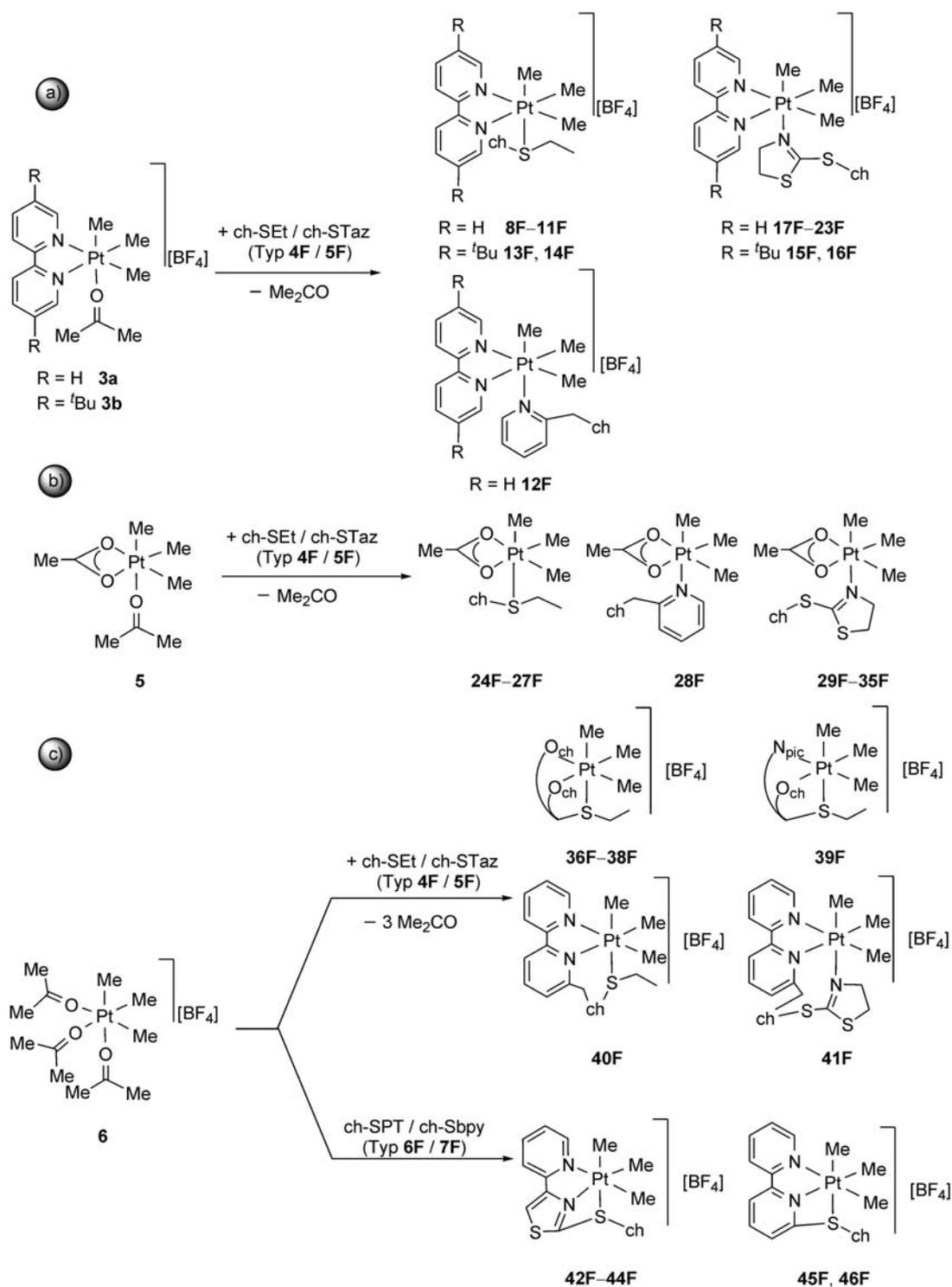


Im Vergleich zu den Trimethylplatin(IV)-Komplexen mit nichtfunktionalisierten Kohlenhydraten [26] besitzen die hier synthetisierten Komplexe mit Thioglycosidliganden eine höhere Stabilität, insbesondere wenn sie über zusätzliche starke *N*-Donoren (pic, bpy, SPT) verfügen. Somit konnte gezeigt werden, dass Substitutionsreaktionen an Platin(IV)-Komplexen – trotz der kinetischen Inertheit (low-spin d^6 -Elektronenkonfiguration) – bereitwillig ablaufen, wenn die Komplexe über schwach koordinierte Liganden wie Aceton verfügen. Darüber hinaus werden die Substitutionsreaktionen durch Coliganden (Me) mit hohem *trans*-Effekt begünstigt.

In der Literatur findet man nur wenige Thioglycosidübergangsmetallkomplexe. Diese können in zwei Typen eingeteilt werden, zum einen in Komplexe mit thioglycosidhaltigen Liganden, wobei die Thioglycoside nicht an der Koordination beteiligt sind. Diese erfolgt in der Regel über die Donorzentren in der anomeren Einheit [45]. Und in Komplexe in denen die

Ergebnisse und Diskussion

Koordination unter Einbezug der Thioglycoside, in der Regel über den Schwefel erfolgt. Zur zweiten Gruppe lässt sich sagen, dass alle Thioglycosidliganden zumeist zusätzliche stabilisierende Donorzentren (*N*-,*P*-,*S*-Donorzentren) enthalten und als Chelatliganden koordinieren. Die Derivatisierung erfolgt dabei überwiegend in der anomeren Einheit [21,46,47].



Schema 4. Synthese von Trimethylplatin(IV)-Komplexen mit Thioglycosidliganden.

Es finden sich aber auch Beispiele, in denen die Hydroxylgruppe an C2 derivatisiert wurde [48]. Es konnte gezeigt werden, dass Komplexe dieser Art in enantioselektiven asymmetrischen Synthesen als Katalysatoren eingesetzt werden können [46,48]. Eine Ausnahme stellen die Zinnkomplexe dar, in denen die Koordination über die Sauerstoffatome der Hydroxylgruppen nichtfunktionalisierter Thioglycoside erfolgt und nicht unter Einbezug des Schwefelatoms [49].

In Bezug auf die hier verwendeten Thioglycoside finden sich in der Literatur Palladium(II)-Komplexe mit ch-STaz- und ch-SPT-Thioglycosidliganden des Typs $[\text{PdBr}_2(\text{ch-STaz-}\kappa\text{N})_2]$ [50] und $[\text{PdBr}_2(\text{ch-SPT-}\kappa^2\text{N,N}')] [51]$, in denen die Thioglycoside ebenfalls monodentat über das endocyclische Stickstoffatom der STaz-Gruppe bzw. bidentat über die Stickstoffatome der SPT-Gruppe koordiniert sind.

2.3.3. Zur Reaktivität von Thioglycosidplatin(IV)-Komplexen

Die Koordination der Thioglycosidliganden an das stark Lewis-saure Platin(IV)-Kation führt zur Aktivierung und leichten Spaltbarkeit der glycosidischen Bindung. Dies belegen zwei Röntgeneinkristallstrukturanalysen von Zersetzungsprodukten, deren Kristalle aus unterschiedlichen Reaktionen in nicht strikt getrockneten Acetonlösungen erhalten wurden (Schema 5, Abb. 17). Durch Hydrolyse bzw. intramolekularen nukleophilen Angriff des Sauerstoffatoms der freien Hydroxylgruppe an C6 des Thioglycosidliganden kommt es zur Spaltung der glycosidischen C–S-Bindung.

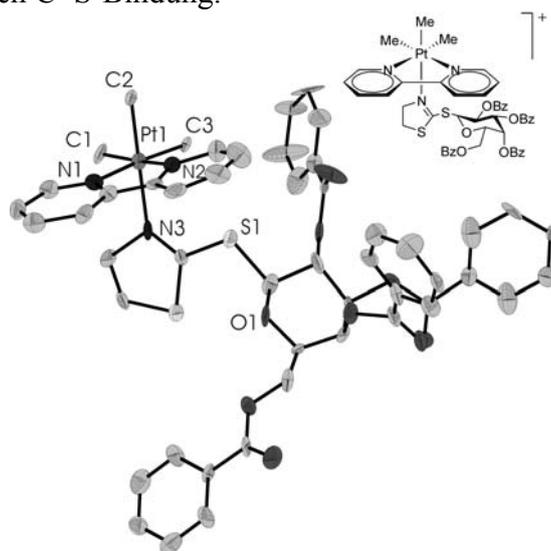


Abbildung 16. Molekülstruktur des Kations in Kristallen von $[\text{PtMe}_3(\text{bpy})(\mathbf{5cF})][\text{BF}_4]$ (**19F**).

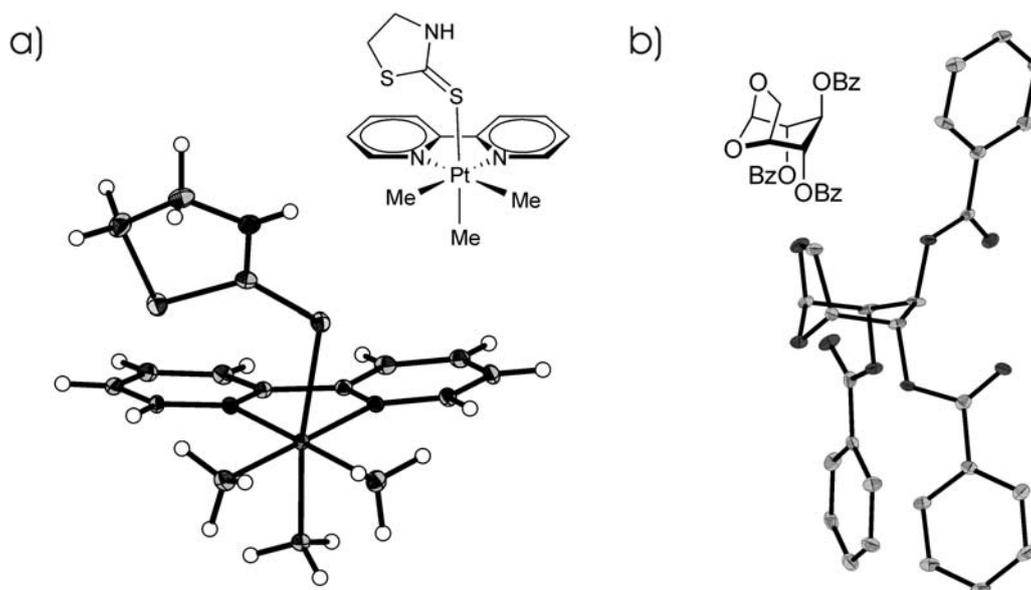
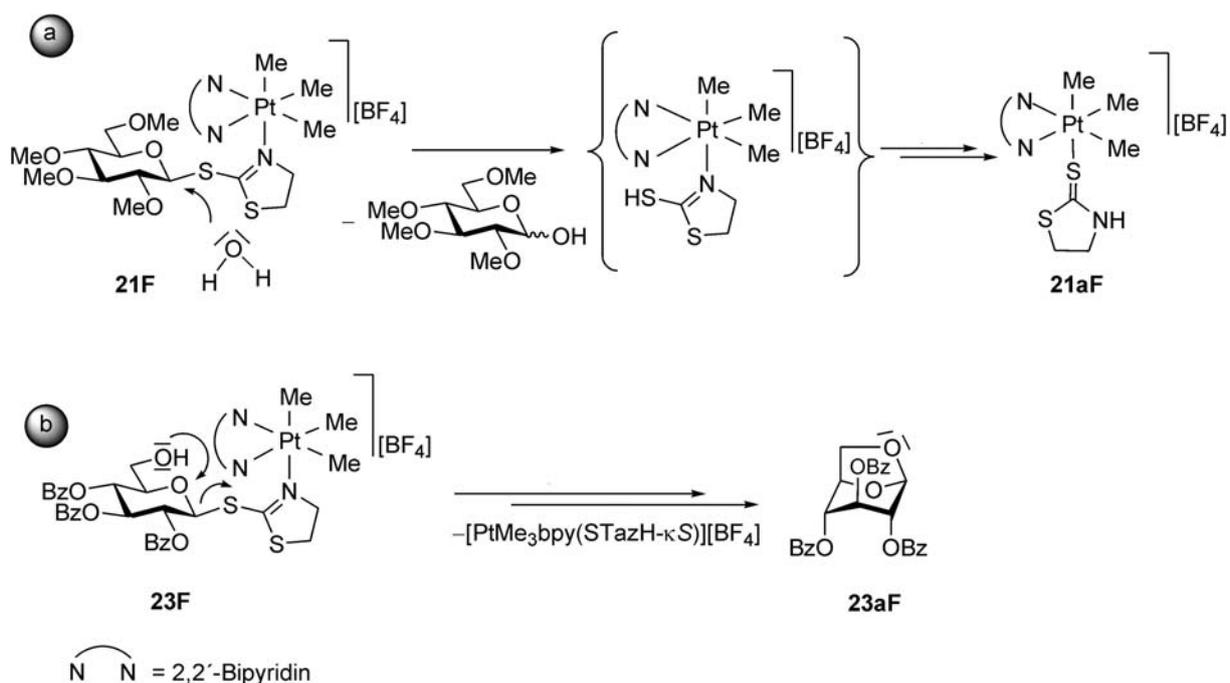


Abbildung 17. a) Molekülstruktur des Kations in Kristallen von $[\text{PtMe}_3(\text{bpy})(\text{STazH})][\text{BF}_4]$ (**21aF**) b) Molekülstruktur von 1,6-Anhydro-2,3,4-*O*-tribenzoyl- β -D-glucopyranose (**23aF**).

Ein weiteres Indiz für die Aktivierung ist die Tatsache, dass es bei der Umsetzung von $[\text{PtMe}_3(\text{Me}_2\text{CO})_3][\text{BF}_4]$ (**6**) mit ch-STaz-Thioglycosiden (außer im Fall des Thioglycosides **5hF**, das über eine stark bindende Bipyridylgruppe verfügt) keine $[\text{PtMe}_3(\text{ch-STaz})][\text{BF}_4]$ -Komplexe isoliert werden konnten, sondern immer nur eine Zersetzung des Thioglycosides unter anderem zum entsprechenden α -Hemiacetal beobachtet wurde.

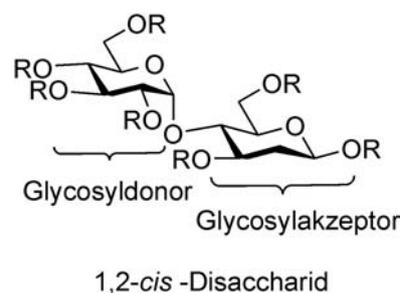
Die Aktivierung der glycosidischen Bindung durch Zugabe und Koordination von Metallsalzen wie AgOTf oder CuOTf ist ein gängiger Schritt bei Glycosylierungsreaktionen, der ebenfalls zur Abspaltung der anomeren Einheit führt [52]. Somit fungiert auch das Trimethylplatin(IV)-Kation in den gesamten Reaktionen als elektrophiler Promotor. Wie beim Methyltriflat [50] erfolgt dabei die Aktivierung in Bezug auf die ch-STaz-Thioglycoside über das endocyclische Stickstoffatom. Im Gegensatz zu den im Rahmen dieser Arbeit synthetisierten Platin(IV)-Komplexen mit κN -gebundenen ch-STaz-Thioglycosidliganden sind die bereits erwähnten Palladium(II)-Komplexe Typs $[\text{PdBr}_2(\text{ch-STaz-}\kappa N)_2]$ [50] und $[\text{PdBr}_2(\text{ch-SPT-}\kappa^2 N, N')]$ [51], deutlich stabiler und deaktivieren die Thioglycoside. Die Abspaltung der Thioglycosidliganden ist nur durch Zugabe von NaCN möglich.



Scheme 5. Mögliche Zersetzungsmechanismen der ch-STaz-Komplexe **21F** und **23F**.

2.3.4. Thioglycosidplatin(IV)-Komplexe in stereoselektiven Glycosylierungsreaktionen¹

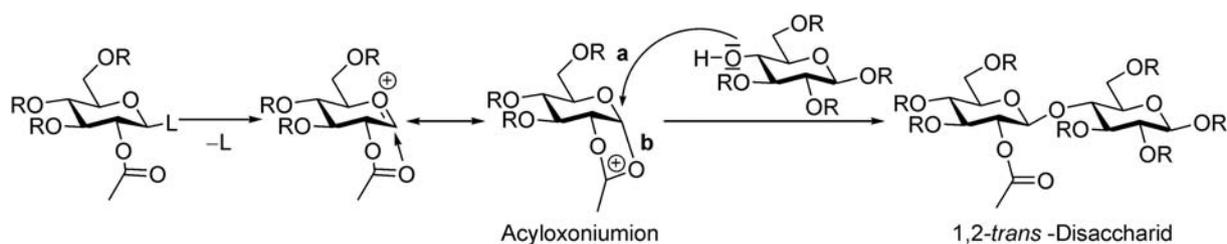
Unter Glycosylierungsreaktionen versteht man die Verlinkung von Monosacchariden unter Ausbildung einer glykosidischen Bindung zu Di-, Oligo- bzw. Polysacchariden. Die stereoselektive Synthese von 1,2-*cis*-Disacchariden² stellt immer noch eine Herausforderung dar. 1,2-*trans*-Disaccharide können dagegen selektiv dargestellt werden. Dazu ist ein Glycosyldonor³ erforderlich, der in Nachbarschaft zum anomeren C-Atom über eine Esterschutzgruppe (OAc, OBz) am C2-Atom verfügt (Schema 6). Nach Abspaltung der Aglyconeinheit (L) erfolgt dann die Ausbildung eines Acyloxoniumions. Das bedingt eine Abschirmung einer Seite (**b**, „bottom face“), so dass der Glykosylakzeptor³ selektiv von der anderen Seite (**a**, „top face“), unter Ausbildung von 1,2-*trans*-Disacchariden, angreift.



¹ Die Glycosylierungsreaktionen wurden von Frau Dr. P. Pornsuriyasak durchgeführt.

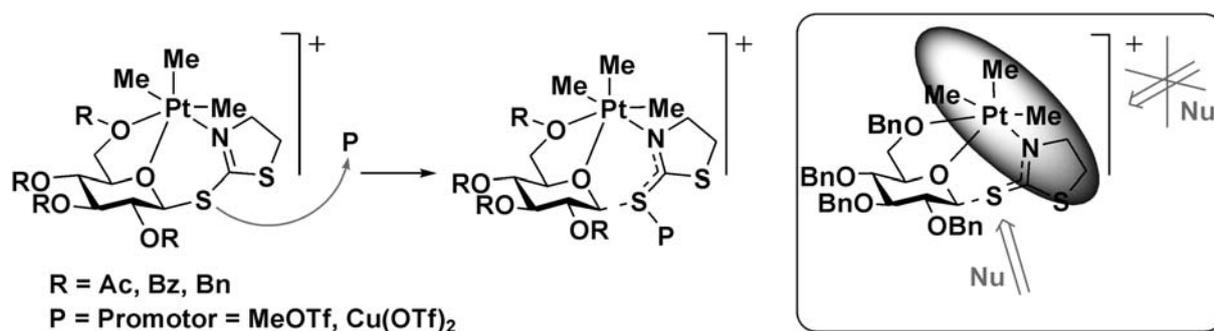
² Die *cis*- bzw. *trans*-Bezeichnung in 1,2-*cis/trans*-Disacchariden bezieht sich auf die relative Position der geknüpften C-C-Bindung zur C1-C2-Bindung im Glycosyldonor.

³ Der Glycosyldonor bzw. -akzeptor stellt den Saccharidbaustein zur Verfügung bzw. akzeptiert diesen.



Schema 6. Allgemeine Synthese von 1,2-*trans*-Disacchariden (für D-Glucopyranoside) am Beispiel einer 1,4'-Disaccharidverknüpfung.

Der Grundgedanke unserer Untersuchungen war nun die Oberseite („top face“) des Glycosyldonors durch Komplexierung an ein Metall abzuschirmen, um so den Angriff des Glycosylakzeptors selektiv von der Unterseite her zu gewährleisten. Die unter Punkt 2.3.2. synthetisierten Platin(IV)-Komplexe waren dafür von besonderem Interesse, da die *facial*-gebundenen Methylgruppen der PtMe₃-Einheit zum Einen abschirmend wirken und die Koordination der Thioglycosidliganden zum Anderen ebenfalls *facial* erfolgen kann (Schema 7). Für die Glycosylierungen wurden ausschließlich Thioglycosidplatin(IV)-Komplexe mit benzylierten Thioglycosidliganden verwendet, die auf Grund des +M-Effektes der Benzylschutzgruppen reaktiver sind, als die entsprechenden Kohlenhydrate mit Esterschutzgruppen (Acetyl, Benzoyl). Im Folgenden wurden die Komplextypen [PtMe₃(bpy)(ch*)][BF₄], [PtMe₃(OAc-κ²O,O')(ch*)] und [PtMe₃(ch*)][BF₄]¹ (ch* = ch-SEt, ch-STaz, ch-SPT) als Glycosyldonoren eingesetzt².



Schema 7. Grundgedanke der platinassistenten stereoselektiven Glycosylierungsreaktion unter Verwendung eines [PtMe₃(ch-STaz)]⁺-Glycosyldonors. Im rechten Bild sind die abschirmenden Methylgruppen grau unterlegt.

¹ Aus Gründen der Übersichtlichkeit wird im Folgenden auf die Nummerierung der einzelnen Komplexe verzichtet. Details siehe [G]

² Die Komplexe wurden *in situ* erzeugt und anschließend mit dem Glycosylakzeptor und Promotor umgesetzt.

Erste Untersuchungen zeigen, dass die beobachtete Aktivierung der glycosidischen Bindung des Glycosyldonors durch die Koordination an das elektrophile Platin(IV)-Atom nicht ausreicht, um als Promotor zu fungieren und die Abspaltung des Aglycons zu initiieren. Demzufolge wurden alle weiteren Glycosylierungsreaktionen unter Zugabe gängiger Promotoren durchgeführt. Die Ergebnisse der Glycosylierungsreaktionen unter Verwendung der $[\text{PtMe}_3(\text{ch}^*)][\text{BF}_4]$ -Komplexe, für die die besten Ergebnisse erzielt wurden, sind in Abbildung 18 zusammengestellt. Die Verwendung der Thioglycosidplatin(IV)-Komplexe mit *ch*-SEt-Liganden führte nicht zur Disaccharidbildung, an Stelle dessen konnte eine partielle Hydrolyse des Glycosyldonors und die Methylierung (bei Einsatz von MeOTf) des Glycosylakzeptors beobachtet werden. In allen anderen Fällen wurde ein α/β -Gemisch erhalten, in dem im Vergleich zu den analogen Reaktion mit unkomplexierten Thioglycosiden eine erhebliche Verbesserung um das 1.5–5.5-fache zu Gunsten des α -Anomers beobachtet werden konnte. Die besten Ergebnisse wurden bei den Thioglycosidplatin(IV)-Komplexen mit *ch*-STaz-Liganden erzielt, die über zusätzliche *N*-Donoren (Picolin-2-yl, 2,2'-Bipyridin-6-yl) in C6-Position des Kohlenhydrates verfügen. Die Verwendung von Komplexen mit stark koordinierenden *N*-Donoren stellt zugleich sicher, dass die Glycosylierungen wirklich

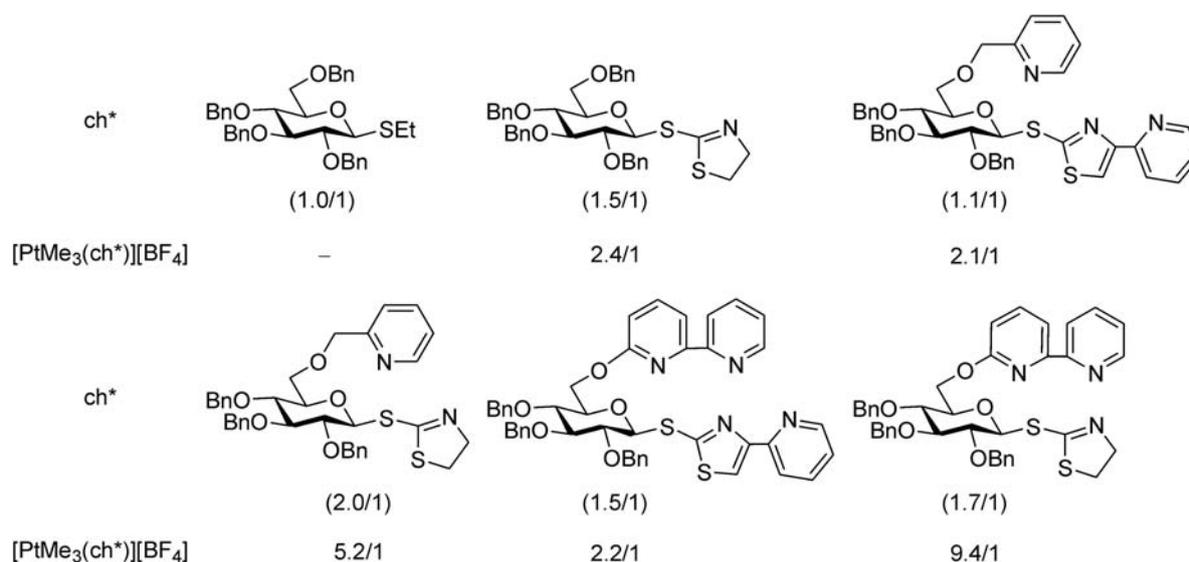


Abbildung 18. α/β -Verhältnis bei Glycosylierungsreaktionen unter Verwendung von Trimethylplatin(IV)-Komplexen als Glycosyldonoren und von MeOTf, NIS/TfOH, DMTST, $\text{Cu}(\text{OTf})_2$, $\text{Ag}(\text{OTf})$ als Promotoren. In Klammern ist das α/β -Verhältnis der analogen Reaktionen unter Verwendung der nichtkomplexierten Thioglycoside angegeben (Weitere Details siehe Publikation [G]).

Ergebnisse und Diskussion

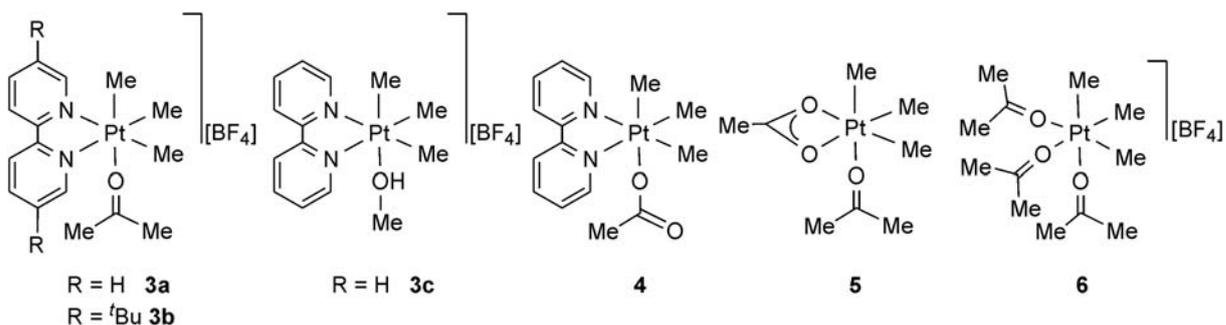
platinassiiert und nicht unter vorzeitiger Zersetzung der Thioglycosidplatin(IV)-Komplexe verlaufen. Diese Ergebnisse belegen das Konzept, dass eine Metallkoordinierung die Stereoselektivität in der Disaccharidbildung beeinflussen kann.

Im Rahmen der vorliegenden Arbeit wurden Platin(II)- und Platin(IV)-Komplexe mit schwefelhaltigen Heterocyclen, Thionucleobasen und Thioglycosiden synthetisiert und umfassend charakterisiert. Dabei konnte gezeigt werden, dass durch die Wahl geeigneter Platin(IV)-Precursorkomplexe, die eine mono-, bi- oder tridentate Koordination der Bioliganden zulassen, gezielt verschiedenartige Koordinationsmodi realisiert werden können. Cytotoxische Untersuchungen der Komplexe ergaben für einige Verbindungen hohe cancerostatische Aktivitäten, zeigten aber auch, dass die Koordination von Bioliganden an Platin – im Vergleich mit analogen Komplexen mit „abiotischen“ Liganden – nicht generell zu Komplexen mit höheren Aktivitäten führen. Darüber hinaus konnte gezeigt werden, dass die Koordination von Thioglycosiden an Platin(IV) zur Aktivierung der glycosidischen Bindung führen kann. Die Verbesserung der Stereoselektivität in Glycosylierungsreaktionen durch Verwendung dieser Komplexe spiegelt das synthetische Potential dieser Verbindungen wider.

3. Zusammenfassung

Die Synthese von Platin(IV)-Komplexen mit schwefelhaltigen Bioliganden wie Thionucleobasen und -glycosiden ist auf Grund der potentiellen Bioaktivität der Komplexe von besonderem Interesse. Ihre Synthese ist eine koordinationschemische Herausforderung, da zum einen die Bioliganden bedingt durch mehrere – unter Umständen sogar gleichartige – Donorzentren ein flexibles Koordinationsverhalten aufweisen und zum anderen Ligandensubstitutionsreaktionen durch die low-spin d^6 -Elektronenkonfiguration von Pt(IV) erschwert sind. Darüber hinaus kann die Koordination von Bioliganden an ein hoch elektrophiles Metallatom wie Pt(IV) entscheidend deren Reaktivität beeinflussen. Im Rahmen dieser Arbeit bestand die Aufgabe darin, Platin(II)- und Platin(IV)-Komplexe mit bioaktiven *N,S*-heterocyclischen sowie mit Thionucleobase- und Thioglycosidliganden zu synthetisieren und zu charakterisieren sowie deren Reaktivität einschließlich der cytotoxischen Aktivität zu untersuchen. Im Einzelnen konnten die folgenden Ergebnisse erzielt werden.

1. Zur Synthese von Trimethylplatin(IV)-Komplexen mit schwefelhaltigen Bioliganden wurde von den literaturbekannten Komplexen **3–6** ausgegangen. Sie verfügen über ein bis drei substitutionslabile Liganden (Me_2CO , MeOH , OAc), deren Abspaltung auch durch den hohen *trans*-Effekt der Methylgruppen gefördert wird. Für Komplex **5** belegen quantenchemische Rechnungen eine $\kappa^2\text{O},\text{O}'$ -Koordination. Die Konstitution des Neutralkomplexes **4** wurde durch eine Röntgeneinkristallstrukturanalyse bewiesen.
2. Die Reaktion der Trimethyl(2,2'-bipyridin)platin-Komplexe **3a** bzw. **3c** mit Thionucleobasen führt zu Platin(IV)-Komplexen des Typs $[\text{PtMe}_3(\text{nb}-\kappa\text{S})][\text{BF}_4]$ ($\text{nb} = \text{SCy}$, **4C**; 1-MeSCy, **5C**; s^2Ura , **3D**; s^4Ura , **4D**, $\text{s}^2\text{s}^4\text{Ura}$, **5D**). ^1H -, ^{13}C - und ^{195}Pt -NMR-spektroskopische Untersuchungen, quantenchemische Rechnungen (**4D**, **5D**) sowie

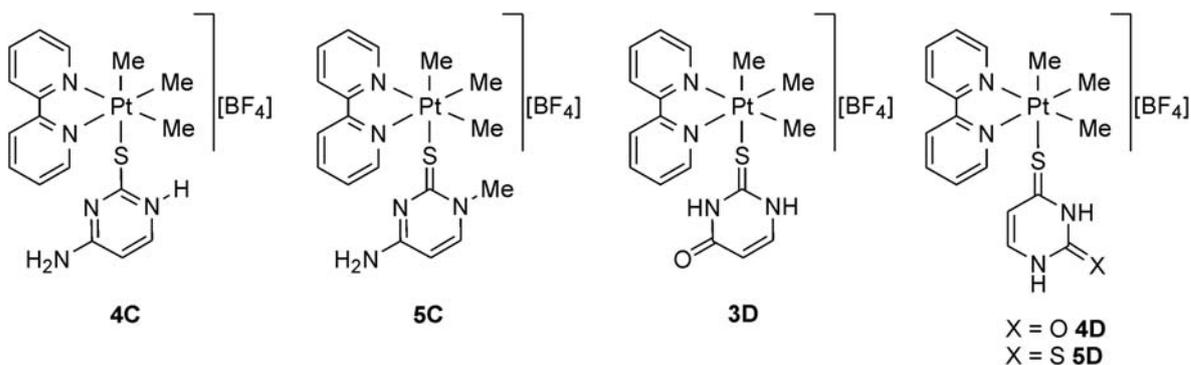


Zusammenfassung

Röntgeneinkristallstrukturanalysen (**4C**·MeOH, **5C**) belegen eine Koordination der Thionucleobase über das exocyclische Schwefelatom (κS^2 : **4C**, **5C**, **3D**; κS^4 : **4D**, **5D**).

3. Röntgeneinkristallstrukturanalysen von **4C**·MeOH und **5C** zeigen, dass π - π -Wechselwirkungen und Wasserstoffbrückenbindungen für die Molekülstruktur als auch für die Stapelung der Moleküle im Kristall von Bedeutung sind. So liegen in Kristallen von **4C**·MeOH dinukleare Komplexkationen $[\{\text{PtMe}_3(\text{bpy})(\text{SCy}-\kappa S)\}_2]^{2+}$ mit N-H \cdots N'-verknüpften Monomereinheiten vor. Strukturelle Parameter zeigen, dass die koordinierten Schwefelatome in **4C**·MeOH und **5C** als sp^3 - bzw. sp^2 -hybridisiert zu beschreiben sind. Diese Befunde sowie ergänzende quantenchemische Rechnungen der Komplexkationen $[\text{PtMe}_3(\text{nb}-\kappa S)]^+$ (nb = $s^2\text{Ura}$, $s^4\text{Ura}$, $s^2s^4\text{Ura}$) und $[\{\text{PtMe}_3(\text{bpy})(\text{SCy}-\kappa S)\}_2]^{2+}$ belegen, dass in diesen Komplexen die Thionucleobaseliganden als Amino-Thion- (**5C**), Oxo-Thion- (**3D**, **4D**) bzw. Thion-Thion-Tautomer (**5D**) vorliegen. Im Unterschied dazu ist der SCy-Ligand in **4C** als eine an N1 protonierte Amino-Thiolat-Form zu beschreiben.

4. $[(\text{PtMe}_3\text{I})_4]$ (**2**) reagiert mit Natriumsalzen von *N,S*-Heterocyclen ($\widehat{\text{S}}\text{N}$)Na ($\widehat{\text{S}}\text{NH}$ = Pyridin-2-thion, pytH; Pyrimidin-2-thion, pymtH; Thiazolin-2-thion, tztH) zu dinuklearen Komplexen (siehe Formelbild auf der folgenden Seite), während die analoge Umsetzung mit dem Natriumsalz eines *S,S*-Heterocyclen (Thiophen-2-thiol, tptH) zu einem tetranuklearen Komplex (**12A/6B**) führt. Damit wurde in Fortführung der Diplomarbeit ein wesentlich verbesserter Syntheseweg gefunden, der keine anaeroben Bedingungen erfordert. Die Komplexe sind vollständig analytisch und spektroskopisch charakterisiert. Röntgeneinkristallstrukturanalysen belegen einen $1\kappa N,1:2\kappa^2 S$ - (**10A/3B**, **9A/4B**) bzw. eine μ_3 - κS -Koordination (**12A/6B**) der heterocyclischen Liganden.

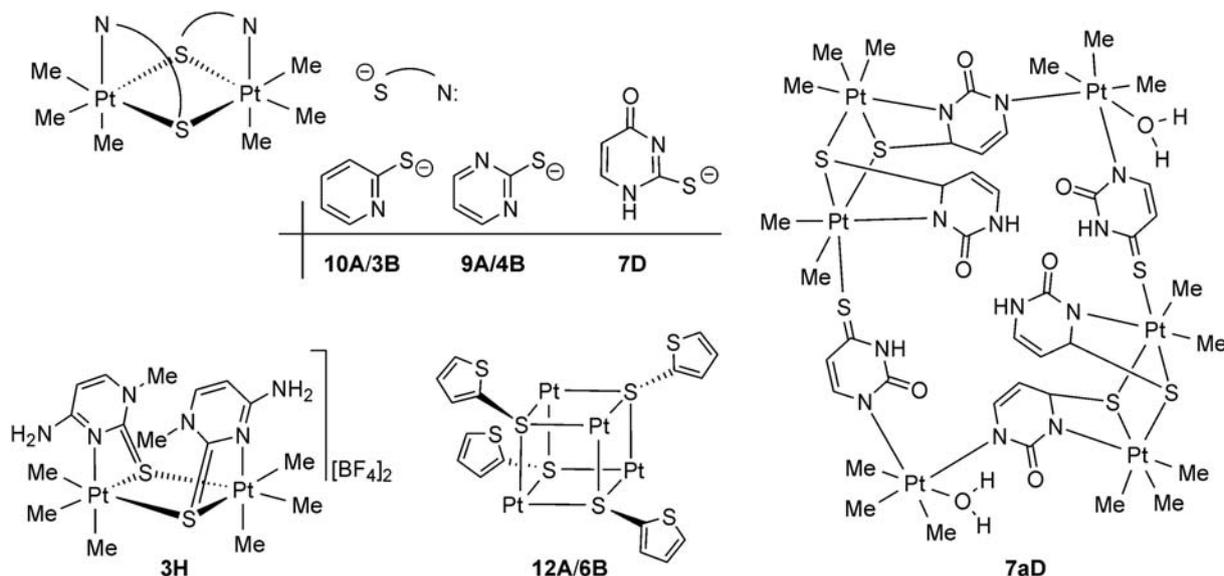


Zusammenfassung

Quantenchemische Rechnungen zeigen, dass bei den dinuklearen Komplexen die experimentell gefundene Struktur auch die stabilste ist und führen die Bildung des tetranuklearen Komplexes auf die geringe Koordinationstendenz des endocyclischen Schwefelatoms im tpt-Liganden zurück.

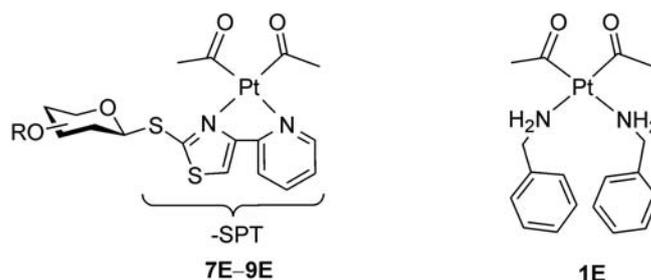
5. Die Umsetzung von $[\text{PtMe}_3(\text{OAc-}\kappa^2\text{O},\text{O})(\text{Me}_2\text{CO})]$ (**5**) mit 4-Thiouracil führt unter Deprotonierung des Liganden zur Ausbildung des dinuklearen Komplexes $[(\text{PtMe}_3)_2(\mu\text{-s}^4\text{Ura-H})_2]$ (**7D**). In analoger Weise bildet sich der ionische Komplex $[(\text{PtMe}_3)_2(\mu\text{-1-MeSCy})_2][\text{BF}_4]_2$ (**3H**) bei der Reaktion von $[\text{PtMe}_3(\text{Me}_2\text{CO})_3][\text{BF}_4]$ (**6**) mit 1-Methylcytosin. Elementaranalyse, IR- und NMR-Spektroskopie (^1H , ^{13}C , ^{195}Pt) sowie ESI-Massenspektrometrie zeigen für beide Komplexe eine $1\kappa\text{N},1:2\kappa^2\text{S}$ -Koordination analog zu der in den dinuklearen $[(\text{PtMe}_3)_2(\mu\text{-S}^{\widehat{\text{N}}})_2]$ -Komplexen. Mittels Röntgeneinkristallstrukturanalyse konnte **3H** charakterisiert werden, sowie ein Zersetzungsprodukt von **7D**, ein hexanuklearer 4-Thiouracilatoplatin(IV)-Komplex (**7aD**).

6. Cytotoxische Untersuchungen der mononuklearen $[\text{PtMe}_3(\text{bpy})(\text{nb-}\kappa\text{S})][\text{BF}_4]$ ($\text{nb} = \text{SCy}$, **4C**; 1-MeSCy, **5C**; s^2Ura , **3D**; s^4Ura , **4D**; $\text{s}^2\text{s}^4\text{Ura}$, **5D**) und dinuklearen Komplexe $[(\text{PtMe}_3)_2(\mu\text{-S}^{\widehat{\text{N}}})_2]$ ($\text{S}^{\widehat{\text{N}}} = \text{pyt}$, **3B/10A**; pymt , **4B/9A**; tzt , **5B/11A**) gegenüber neun bzw. fünf Zelllinien zeigen eine herausragende Aktivität des dinuklearen Komplexes



5B/11A mit bis zu 4-fach höheren cytotoxischen Aktivitäten als Cisplatin, während die restlichen Komplexe überwiegend nur moderate cancerostatische Eigenschaften aufweisen. Die mononuklearen Komplexe **3D** und **5D** besitzen spezifische cytotoxische Aktivitäten gegenüber den Zelllinien A549 (**3D**) bzw. A2780 (**5D**), die vergleichbar mit der Aktivität von Cisplatin sind. Zellzyklusstörungen und ein Trypan-Blau-Ausschlusstest unter Verwendung von $[\text{PtMe}_3(\text{bpy})(\text{s}^2\text{s}^4\text{Ura-}\kappa\text{S}^4)][\text{BF}_4]$ (**5D**) gegenüber der Zelllinie A431 zeigen eine Induzierung des apoptotischen Zelltodes, während der G1-Phase (postmitotische Phase) des Zellzyklus.

- Die Reaktion von $[\text{Pt}(\text{COMe})_2(\text{BnNH}_2)_2]$ (**1E**) mit Thioglycosiden die über 4-(Pyridin-2-yl)-thiazol-2-yl-Chelatliganden (ch-SPT)¹ in der anomeren Einheit verfügen, führt in einer Gleichgewichtsreaktion zur Ausbildung der Komplexe $[\text{Pt}(\text{COMe})_2(\text{ch-SPT})]$ (**7E–9E**). Die Charakterisierung des Reaktionsgemisches zeigt eine $\kappa^2\text{N,N}'$ -Koordination der Thioglycosidliganden an das Platin(II)-Atom. Die Röntgeneinkristallstrukturanalyse von $[\text{Pt}(\text{COMe})_2(\text{BnNH}_2)_2]$ (**1E**) belegt mit einer ungewöhnlich langen Pt–N-Bindungslänge von 2.164(2) Å die experimentell beobachtete hohe Reaktivität von **1E** durch leichte Abspaltung der Benzylaminliganden.
- Die Umsetzung der Trimethylplatin(IV)-Komplexe **3a/3b** bzw. **5** mit den Thioglycosiden der Typen ch-SEt und ch-STaz führt zu den Komplexen $[\text{PtMe}_3(\text{bpy})(\text{ch}^*)][\text{BF}_4]$ (ch* = ch-SEt, **8F–14F**; ch-STaz, **15F–23F**) bzw. $[\text{PtMe}_3(\text{OAc-}\kappa^2\text{O,O})(\text{ch}^*)]$ (ch* = ch-SEt, **24F–28F**; ch-STaz, **29F–35F**; ausgewählte Prototypen s. Formelbilder auf der folgenden Seite). Sie wurden vollständig mittels IR- und NMR-Spektroskopie (¹H, ¹³C, ¹⁹⁵Pt), hochauflösender ESI-Massenspektrometrie und im Falle des Komplexes $[\text{PtMe}_3(\text{bpy})(\text{OBz-Gal-STaz})][\text{BF}_4]$ (**19F**) auch durch Röntgeneinkristallstrukturanalyse charakterisiert.

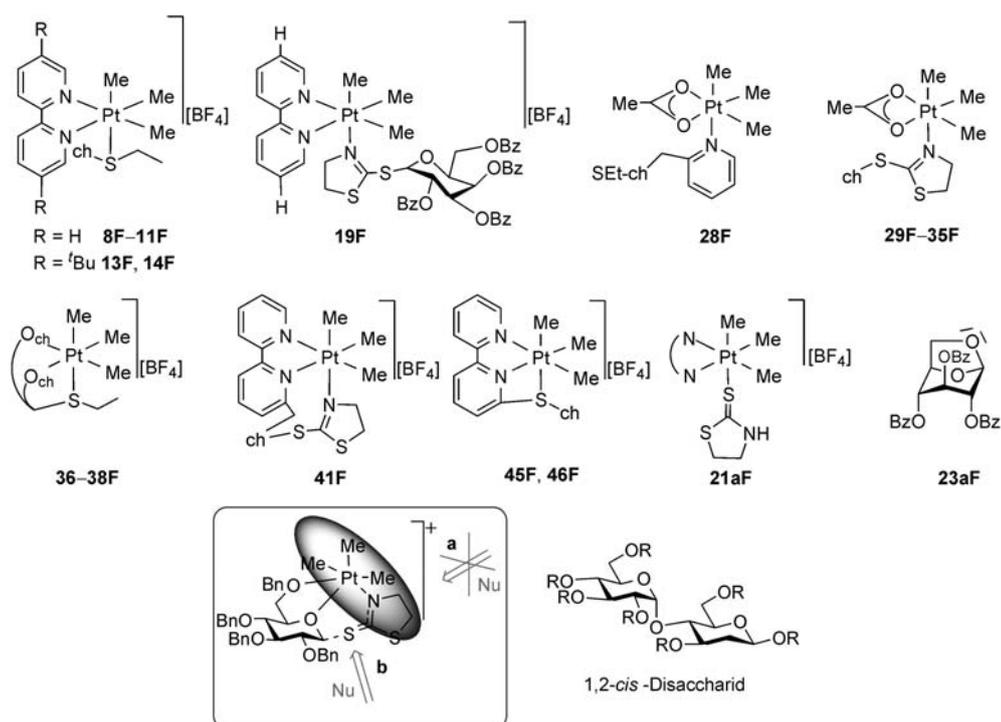


¹ ch = Kohlenhydratrest

Zusammenfassung

Die ch-SEt- und ch-STaz-Liganden sind monodentat κS - bzw. κN -koordiniert. Im Falle der Thioglycoside, die in C6-Position eine Picolylgruppe besitzen, erfolgt die Koordination der Liganden in **12F** und **28F** über das Picolylstickstoffatom.

9. Die Reaktion von $[\text{PtMe}_3(\text{Me}_2\text{CO})_3][\text{BF}_4]$ (**6**) mit Thioglycosiden der Typen ch-SEt, ch-STaz, ch-SPT und ch-Sbpy führt zu Platin(IV)-Komplexen $[\text{PtMe}_3(\text{ch}^*)][\text{BF}_4]$ ($\text{ch}^* = \text{ch-SEt}$, **36–40**; ch-STaz , **41**; ch-SPT , **42–44**, ch-Sbpy , **45**, **46**) in denen die Thioglycosidliganden tridentat $\kappa S, \kappa^2 O, O'$ (**36–38**), $\kappa S, N, O$ (**39**), $\kappa S, \kappa^2 N, N'$ (**40**, **41**) und $\kappa^3 N, N', N''$ -koordiniert (**42–46**) sind. Die Komplexe wurden durch IR- und NMR-Spektroskopie (^1H , ^{13}C , ^{195}Pt) und hochauflösende ESI-Massenspektrometrie charakterisiert.
10. Die Koordination der Thioglycosidliganden an das elektrophile Platin(IV)-Atom führt zu einer Aktivierung der glycosidischen C–S-Bindung, was die Röntgeneinkristallstrukturanalysen der Zersetzungsprodukte **21aF** und **23aF** belegen. Dies kann in Glycosylierungsreaktionen Anwendung finden, in denen die Thioglycosidplatin(IV)-Komplexe als Glycosyldonoren agieren. Durch die zusätzliche Abschirmung der Oberseite (**a**) durch die Methylgruppen der PtMe_3 -Einheit erfolgt der Angriff hauptsächlich von der Unterseite (**b**), was zu einer 1.1–9.4-fachen Erhöhung des α -Anomers (1,2-*cis*-Disaccharid) im α/β -Gemisch führt.



Zusammenfassung

Die Ergebnisse der vorliegenden Arbeit erweitern die Kenntnisse auf dem Gebiet der Koordinationschemie von Bioliganden mit Metallionen in hohen Oxidationsstufen, insbesondere von Thionucleobasen und Thioglycosiden, die bisher weitaus weniger intensiv untersucht wurden als ihre Sauerstoffanaloge. Durch die Wahl geeigneter Platin(IV)-Precursorkomplexe, die eine mono-, bi- oder tridentate Koordination der schwefelhaltigen Bioliganden zulassen ist es gelungen, gezielt verschiedenartige Koordinationsmodi zu realisieren und im Zusammenwirken mit quantenchemischen Rechnungen auch koordinationschemisch zu interpretieren. Insbesondere bei Thioglycosiden konnte gezeigt werden, dass deren Koordination an ein Übergangsmetall in hoher Oxidationsstufe (Pt(IV)) zu einer Aktivierung führen kann, die in einer verbesserten Stereoselektivität bei Glycosylierungsreaktionen auch synthetisches Potential besitzt.

5. Literaturverzeichnis

- [1] W. Kaim, B. Schwederski, *Bioanorganische Chemie*, Teubner, Wiesbaden, **2004**.
- [2] B. Rosenberg, L. Van Camp, T. Krigas, *Nature* **1965**, 205, 698.
- [3] a) M. A. Fuertes, C. Alonso, J. M. Pérez, *Chem. Rev.* **2003**, 103, 645. b) Y. Jung, S. J. Lippard, *Chem Rev.* **2007**, 107, 1387.
- [4] Z. H. Siddik, *Oncogene* **2003**, 22, 7265.
- [5] M. A. Fuertes, J. Castilla, C. Alonso, J. M. Pérez, *Curr. Med. Chem.-Anti Cancer Agents* **2002**, 2, 539.
- [6] a) M. D. Hall, T. W. Hambley, *Coord. Chem. Rev.* **2002**, 232, 49. b) M. D. Hall, H. R. Mellor, R. Callaghan, T. W. Hambley. *J. Med. Chem.* **2007**, 50, 3403.
- [7] a) L. R. Kelland, B. A. Murrer, G. Abel, C. M. Giandomenico, P. Mistry, K. R. Harrap, *Cancer Res.* **1992**, 52, 822. b) O. Nováková, O. Vrána, V. I. Kiseleva, V. Brabec, *Eur. J. Biochem.* **1995**, 228, 616.
- [8] A. Kozubík, A. Vaculová, K. Souček, J. Vondráček, J. Turánek, J. Hofmanová, *Met. Based Drugs* **2008**, 417897.
- [9] A. Chircorian, A. M. Barrios, *Bioorg. Med. Chem. Lett.* **2004**, 14, 5113.
- [10] J. A. Carbon, L. Hung, D. S. Jones, *Proc. Natl. Acad. Sci. U.S.A.* **1965**, 53, 979.
- [11] a) M. N. Lipsett, *J. Biol. Chem.* **1965**, 240, 3975. b) J. Carbon, H. David, M. H. Studier, *Science* **1968**, 161, 1146. c) D.H. Gauss, M. Sprinzl, *Nucleic Acids Res.* **1983**, 11, r1. d) Y. Yamada, S. Saneyoshi, S. Nishimura, H. Ishikura, *FEBS Lett.* **1970**, 7, 207.
- [12] a) W. V. Ruyle, T. Y. Shen, *J. Med. Chem.* **1967**, 10, 331. b) R. K. Ralph, R. E. F. Matthews, A. I. Matus, *Biochim. Biophys. Acta* **1965**, 108, 53. c) M. Bretner, T. Kulikowski, J. M. Dzik, M. Balinska, W. Rode, D. Shugar, *J. Med. Chem* **1993**, 36, 3611. d) M. Bretner, M. Balinska, K. Krawiec, B. Kierdaszuk, D. Shugar, T. Kulikowski, *Nucleosides, Nucleotides Nucleic Acids* **1995**, 14, 657.
- [13] E. B. Astwood, *JAMA, J. Am. Med. Assoc.* **1943**, 122, 78.
- [14] a) A. Napolitano, A. Palumbo, M. d'Ischia, G. Prota, *J. Med. Chem.* **1996**, 39, 5192. b) U. Mårs, V. Tolmachev, A. Sundin *Nucl. Med. Biol.* **2000**, 27, 845.
- [15] L. S. Goodman, A. Gilman (Eds.), *Pharmacological Basis of Therapeutics*, 5th Ed., Macmillian, New York, **1975**, 1248.
- [16] A. Favre, C. Saintomé, J.-L. Fourrey, P. Clivio, P. Laugâa, *J. Photochem. Photobiol., B* **1998**, 42, 109.

-
- [17] a) J. H. Kim, S. H. Kim, E. W. Hahn, C. W. Song, *Science* **1978**, *200*, 206. b) J. R. Zysk, A. A. Bushway, R. L. Whistler, W. W. Carlton, *J. Reprod. Fertil.* **1975**, *45*, 69.
- [18] a) H. Hashimoto, T. Fujimori, H. Yuasa, *J. Carbohydr. Chem.* **1990**, *9*, 683. b) C.-H. Wong, Y. Ichikawa, T. Krach, C. G.-L. Narvor, D. P. Dumas, G. C. Look, *J. Am. Chem. Soc.* **1991**, *113*, 8137. c) B. D. Johnston, B. M. Pinto, *J. Org. Chem.* **1998**, *63*, 5797.
- [19] a) D. J. Hoffman, R. L. Whistler, *Biochemistry* **1968**, *7*, 4479. b) R. L. Whistler, W. C. Lake, *Biochem. J.* **1972**, *130*, 919. c) B. Hellman, Å. Lernmark, J. Sehlin, I.-B. Täljedal, R. L. Whistler, *Biochem. Pharmacol.* **1973**, *22*, 29.
- [20] a) M. Takeuchi, M. Yoshikawa, R. Sasaki, H. Chiba, *Agric. Biol. Chem.* **1982**, *46*, 2741. b) G. Guo, G. Li, D. Liu, Q.-J. Yang, Y. Liu, Y.-K. Jing, L.-X. Zhao, *Molecules* **2008**, *13*, 1487. c) M. Singer, M. Lopez, L. F. Bornaghi, A. Innocenti, D. Vullo, C. T. Supuran, S.-A. Poulsen, *Bioorg. Med. Chem. Lett.* **2009**, *19*, 2273. d) N. Khalifa, M. M. Ramla, A. E.-G. E. Amr, M. M. Abdulla, *Phosphorus, Sulfur Silicon Relat. Elem.* **2008**, *183*, 3046.
- [21] M. Gottschaldt, A. Pfeifer, D. Koth, H. Görls, H.-M. Dahse, U. Möllmann, M. Obata, S. Yano, *Tetrahedron* **2006**, *62*, 11073.
- [22] M. W. Whitehouse, P. D. Cookson, G. Siasios, E. R. T. Tiekink, *Met. Based Drugs* **1998**, *5*, 245.
- [23] a) E. R. T. Tiekink, P. D. Cookson, B. M. Linahan, L. K. Webster, *Met. Based Drugs* **1994**, *5*, 299. b) L. K. Webster, S. Rainone, E. Horn, E. R. T. Tiekink, *Met. Based Drugs* **1996**, *3*, 63.
- [24] C. Vetter *Diplomarbeit*, Martin-Luther-Universität Halle-Wittenberg, Halle, **2005**.
- [25] T. G. Appleton, H. C. Clark, L. E. Manzer, *Coord. Chem. Rev.* **1973**, *10*, 335.
- [26] a) H. Junicke, C. Bruhn, R. Kluge, A. S. Serianni, D. Steinborn, *J. Am. Chem. Soc.* **1999**, *121*, 6232. b) X. Zhu, E. Rusanov, R. Kluge, H. Schmidt, D. Steinborn, *Inorg. Chem.* **2002**, *41*, 2667. c) R. Lindner, C. Wagner, D. Steinborn, *J. Am. Chem. Soc.* **2009**, *131*, 8861.
- [27] a) H. Rostkowska, M. J. Nowak, L. Lapinski, M. Bretner, T. Kulikowski, A. Leś, L. Adamowicz, *Spectrochim. Acta, Part A* **1993**, *49*, 551. b) P. Ü. Cıvırcı, *J. Phys. Org. Chem.* **2001**, *14*, 171. c) A. Les, L. Adamowicz, *J. Am. Chem. Soc.* **1990**, *112*, 1504. d) J. Leszczynski, K. Lammertsma, *J. Phys. Chem.* **1991**, *95*, 3128.
- [28] ausgesuchte Literaturstellen: a) B. Singh, S. A. Khan, U. Bhanu, *Indian J. Chem., Sect. A: Inorg., Bio-inorg., Phys., Theor. Anal. Chem.* **1987**, *26*, 1066. b) B. T Khan, S. R. A. Khan, K. Annapoorna, *Indian J. Chem., Sect. A: Inorg., Bio-inorg., Phys., Theor. Anal.*

-
- Chem.* **1995**, *34*, 878. c) B. T. Khan, K. Annapoorna, *Inorg. Chim. Acta* **1990**, *171*, 157. d) E. Tselepi-Kalouli, N. Katsaros, *J. Inorg. Biochem.* **1988**, *34*, 63. e) H. C. Nelson, J. F. Villa, *Inorg. Chim. Acta* **1979**, *34*, L235. f) B. T. Khan, K. Annapoorna, S. Shamsuddin, K. Najmuddin, *Polyhedron* **1992**, *11*, 2109. g) J. Jolley, W. I. Cross, R. G. Pritchard, C. A. McAuliffe, K. B. Nolan, *Inorg. Chim. Acta* **2001**, *315*, 36. h) E. Meléndez, M. Marrero, C. Rivera, E. Hernández, A. Segal, *Inorg. Chim. Acta* **2000**, *298*, 178. i) D. M. L. Goodgame, G. A. Leach, *Inorg. Chim. Acta* **1979**, *37*, L505. j) Y. Rosopulos, U. Nagel, W. Beck, *Chem. Ber.* **1985**, *118*, 931. k) M. Gupta, M. N. Srivastava, *Synth. React. Inorg., Met.-Org., Nano-Met. Chem.*, **1996**, *26*, 305. l) J. S. Dwivedi, U. Argawala, *Z. Allg. Anorg. Chem.* **1973**, *397*, 74. m) J. R. Lusty, H. S. Chan, J. Peeling, *Trans. Met. Chem.*, **1983**, *8*, 343.
- [29] G. W. Hunt, E. A. H. Griffith, E. L. Amma, *Inorg. Chem.* **1976**, *15*, 2993.
- [30] P. Aslanidis, P. J. Cox, A. Kaltzoglou, A. C. Tsipis, *Eur. J. Inorg. Chem.* **2006**, 334.
- [31] C. Janiak, *J. Chem. Soc., Dalton Trans.* **2000**, 3885.
- [32] Cambridge Structural Database (CSD) Version 5.30 2008, University Chemical Laboratory, Cambridge (England)
- [33] ausgewählte Literaturstellen: a) K.-H. Yih, G.-H. Lee, Y. Wang, *Inorg. Chem. Commun.* **2003**, *6*, 213. b) M. Leeaphon, A. L. Ondracek, R. J. Thomas, P. E. Fanwick, R. A. Walton, *J. Am Chem. Soc.* **1995**, *117*, 9715. c) J. Lee, T. J. Emge, J. G. Brennan, *Inorg. Chem* **1997**, *36*, 5064. d) S. E. Kabir, M. M. Karim, K. Kundu, S. M. B. Ullah, K. I. Hardcastle, *J. Organomet. Chem.* **1996**, *517*, 155. e) M. Schlaf, A. J. Lough, R. H. Morris, *Organometallics* **1996**, *15*, 4423. f) E. Becker, K. Mereiter, R. Schmid, K. Kirchner, *Organometallics* **2004**, *23*, 2876. g) M. Kotera, Y. Sekioka, T. Suzuki, *Inorg. Chem.* **2008**, *47*, 3498. h) W. Su, M. Hong, J. Weng, Y. Liang, Y. Zhao, R. Cao, Z. Zhou, A. S. C. Chan, *Inorg. Chim. Acta* **2002**, *331*, 8. i) M. Sokolov, Y. Sasaki, K. Umakoshi, *Inorg. Chem. Commun.* **2001**, *4*, 142. j) C. Landgrafe, W. S. Sheldrick, *J. Chem. Soc., Dalton Trans.* **1996**, 989.
- [34] a) M. B. Hursthouse, O. F. Z. Khan, M. Mazid, M. Motevalli, P. O'Brien, *Polyhedron* **1990**, *9*, 541. b) J. G. Reynolds, S. C. Sendlinger, A. M. Murray, J. C. Huffman, G. Christou, *Angew. Chem. Int. Ed. Engl.* **1992**, *31*, 1253. c) R. Castro, J. A. García-Vázquez, J. Romero, A. Sousa, A. Castiñeiras, W. Hiller, J. Strähle, *Inorg. Chim. Acta* **1993**, *211*, 47. d) J. A. Castro, J. Romero, J. A. García-Vázquez, A. Sousa, J. Zubieta, Y. Chang, *Polyhedron* **1996**, *15*, 2741. e) Y. Zhao, M. Hong, Y. Liang, R. Cao, W. Li, J. Weng, S. Lu, *Chem. Commun.* **2001**, 1020. f) A. Sousa-Pedrares, J. Romero, J. A.

-
- García-Vázquez, M. L. Durán, I. Casanova, A. Sousa, *Dalton Trans.* **2003**, 1379. g) S. Chadwick, K. Ruhlandt-Senge, *Chem.-Eur. J.* **1998**, *4*, 1768.
- [35] a) G. Ara, S. E. Kabir, K. Kundu, K. M. A. Malik, *J. Chem Crystallogr.* **2003**, *33*, 851. b) T. S. Lobana, P. Kaur, G. Hundal, R. J. Butcher, A. Castineiras, *Z. Allg. Anorg. Chem.* **2008**, 634, 747.
- [36] a) H. Wang, X.-Q. Guo, R. Zhong, Y.-J. Lin, P.-C. Zhang, X.-F. Hou. *J. Organomet. Chem.* **2009**, *694*, 3362. b) S. E. Kabir, J. Alam, S. Ghosh, K. Kundu, G. Hogarth, D. A. sTocher, G. M. G. Hossain, H. W. Roesky, *Dalton Trans.* **2009**, 4458.
- [37] a) C. Schmidt, J. Dalkner, D. Schollmeyer, H. Singer, *Inorg. Chim. Acta* **1997**, 257, 269. b) P. Alanidis, P. J. Cox, P. Tsaliki, *Polyhedron* **2008**, *27*, 3029.
- [38] a) C.-M. Lee, C.-H. Chen, S.-C. Ke, G.-H. Lee, W.-F. Liaw, *J. Am. Chem. Soc.* **2004**, *126*, 8406. b) M. El-Khateeb, M. Al-Noaimi, Z. Al-Amawi, A. Roller, S. Shova, *Inorg. Chim. Acta* **2008**, *361*, 2957. c) W.-F. Liaw, J.-H. Lee, H.-B. Gau, C.-H. Chen, G.-H. Lee, *Inorg. Chim. Acta* **2001**, *322*, 99. d) F.-T. Tsai, S.-J. Chiou, M.-C. Tsai, M.-L. Tsai, H.-W. Huang, M.-H. Chiang, W.-F. Liaw, *Inorg. Chem.* **2005**, *44*, 5872. e) C.-M. Lee, Y.-L. Chuang, C.-Y. Chiang, G.-H. Lee, W.-F. Liaw, *Inorg. Chem.* **2006**, *45*, 10895.
- [39] a) H. Rauter, E. C. Hillgeris, B. Lippert, *J. Chem. Soc., Chem. Commun.* **1992**, 1385. b) B. Lippert, *Inorg Chem.* **1981** *20*, 4326. c) A. Schreiber, H. Rauter, M. Krumm, S. Menzer, E. C. Hillgeris, B. Lippert, *Met.-Based Drugs* **1994** *1*, 241. d) H. Rauter, I. Mutikainen, M. Blomberg, C. J. L. Lock, P. Amo-Ochoa, E. Freisinger, L. Randaccio, E. Zangrando, E. Chiarparin, B. Lippert, *Angew. Chem., Int. Ed.* **1997**, *36*, 1296. e) H. Schöllhorn, R. Beyerle-Pfnür, U. Thewalt, B. Lippert, *J. Am. Chem. Soc.* **1986**, *108*, 3680. f) R. K. O. Sigel, E. Freisinger, S. Metzger, B. Lippert, *J. Am. Chem. Soc.* **1998**, *120*, 12000. g) M. S. Lüth, E. Freisinger, F. Glahé, J. Müller, B. Lippert, *Inorg. Chem.* **1998**, *37*, 3195.
- [40] H. Rauter, E. C. Hillgeris, A. Erxleben, B. Lippert, *J. Am. Chem. Soc.* **1994**, *116*, 616.
- [41] F. Zamora, M. Sabat, M. Janik, C. Siethoff, B. Lippert, *Chem. Commun.* **1997**, 485.
- [42] ausgesuchte Literaturstellen: trinuklear: R. Dilshad, K. M. Hanif, M. B. Hursthouse S. E. Kabir, K. M. A. Malik, E. Rosenberg, *J. Organomet. Chem.* **1999**, 585, 100. tetranuklear: a) L. R. Favello, J. Fornnies, C. Fortuño, M. A. Gómez-Saso, B. Menjón, A. J. Rueda, M. Tomas, *Inorg. Chim. Acta* **1997**, *264*, 219. b) O. Fuhr, L. Fernandez-Recio, D. Fenske, *Can. J. Chem.* **2006**, *84*, 251. c) L. Ballester, E. Coronado, A. Gutierrez, A. Monge, M. F. Perpnan, E. Pinilla, T. Rico, *Inorg. Chem.* **1992**, *31*, 2053. hexanuklear: a) H.-w. Xu, L. Pin, J.-x. Li, Z.-n. Chen, J.-g. Wu, *Trans. Met. Chem.*

-
- 2007, 32, 781. b) L. Han, Z. Chen, J. Luo, M. Hong, R. Cao, *Acta Crystallogr., Sect. E: Struct. Rep. Online* **2002**, 58, m383. Polymer: a) W. Su, M. Hong, J. Weng, R. Cao, S. Lu, *Angew. Chem., Int. Ed.* **2000**, 39, 2911. b) J. Lee, T. J. Emge, J. G. Brennan, *Inorg. Chem.* **1997**, 36, 5064. c) J. Wang, Y.-H. Zhang, H.-X. Li, Z.-J. Lin, M.-L. Tong, *Cryst. Growth Des.* **2007**, 7, 2352. d) W. Su, R. Cao, M. Hong, W.-T. Wong, J. Lu, *Inorg. Chem. Commun.* **1999**, 2, 241. e) L. Han, M. Hong, R. Wang, B. Wu, Y. Xu, B. Lou, Z. Lin, *Chem. Commun.* **2004**, 2578. f) X.-Y. Wei, W. Chu, R.-D. Huang, S.-W. Zhang, H. Li, Q.-L. Zhu, *Inorg. Chem. Commun.* **2006**, 9, 1161.
- [43] a) M. Friedman, F. F. Bautista, *J. Agric. Food. Chem.* **1995**, 43, 69. b) T. Moulard, J. F. Lagorce, J. C. Thomes, C. Raby, *J. Pharm. Pharmacol.* **1993**, 45, 731.
- [44] a) M. Bette, *Diplomarbeit*, Martin-Luther-Universität Halle-Wittenberg, **2008**.
- [45] a) X. Álvarez-Micó, M. J. F. Calvete, M. Hanack, T. Ziegler, *Synthesis* **2007**, 2186. b) M. Gottschaldt, D. Koth, D. Müller, I. Klette, S. Rau, H. Görls, B. Schäfer, R. P. Baum, S. Yano *Chem.-Eur. J.* **2007**, 13, 10273.
- [46] a) M. Tschoerner, G. Trabesinger, A. Albinati, P. S. Pregosin, *Organometallics* **1997**, 16, 3447. b) A. Albinati, P. S. Pregosin, K. Wick, *Organometallics* **1996**, 15, 2419. c) P. Barbaro, A. Currao, J. Herrmann, R. Nesper, P. S. Pregosin, R. Salzmann, *Organometallics* **1996**, 15, 1879. d) N. Khiar, C. S. Araújo, B. Suárez, I. Fernández, *Eur. J. Org. Chem.* **2006**, 1685. e) N. Khiar, C. S. Araújo, B. Suárez, E. Álvarez, I. Fernández, *Chem. Commun.* **2004**, 714. f) K. Boog-Wick, P. S. Pregosin, G. Trabesinger, *Organometallics* **1998**, 17, 3254.
- [47] Y. Sugai, S. Fujii, T. Fujimoto, S. Yano, Y. Mikata, *Dalton Trans.* **2007**, 3705.
- [48] a) N. Khiar, R. Navas, B. Suárez, E. Álvarez, I. Fernández, *Org. Lett.* **2008**, 10, 3697. b) N. Khiar, B. Suárez, V. Valdivia, I. Fernández, *Synlett* **2005**, 2963.
- [49] S. David, S. Hanessian, *Tetrahedron* **1985**, 41, 643.
- [50] P. Pornsuriyasak, U. B. Gangadharmath, N. P. Rath, A. V. Demchenko *Org. Lett.* **2004**, 6, 4515.
- [51] P. Pornsuriyasak, N. P. Rath, A. V. Demchenko, *Chem. Commun.* **2008**, 5633.
- [52] a) T. Lindhorst, *Essentials of Carbohydrate Chemistry*, Wiley-VCH, Weinheim, **2003**. b) A. V. Demchenko, *Lett Org. Chem.* **2005**, 2, 580.

ANHANG

- [A] C. Vetter, C. Wagner, J. Schmidt, D. Steinborn, *Inorg. Chim. Acta* **2006**, 359, 4326.
 “Synthesis and characterization of platinum(IV) complexes with *N,S*- and *S,S*-heterocyclic ligands”
- [B] C. Vetter, G. N. Kaluđerović, R. Paschke, S. Gómez-Ruiz, D. Steinborn, *Polyhedron* **2009**, 28, 3699. “Synthesis, structures and *in vitro* cytotoxicity studies of platinum(IV) complexes with *N,S*- and *S,S*- heterocyclic ligands”
- [C] C. Vetter, C. Wagner, G. N. Kaluđerović, R. Paschke, D. Steinborn *Inorg. Chim. Acta* **2009**, 362, 189. „Synthesis and Characterization of Platinum(IV) Complexes with 2-Thiocytosine and 1-Methyl-2-thiocytosine Ligands“
- [D] C. Vetter, G. N. Kaluđerović, R. Paschke, R. Kluge, J. Schmidt, D. Steinborn, *Inorg. Chim. Acta* **2010**, 363, 2452. „Synthesis, characterization and *in vitro* cytotoxicity studies of platinum(IV) complexes with thiouracile ligands“
- [E] C. Vetter, P. Pornsuriyasak, J. Schmidt, M. Bette, N. P. Rath, A. V. Demchenko, D. Steinborn, **2010**, noch nicht eingereicht. „Synthesis and characterization of platinum(II) carbohydrate complexes with thioglycoside ligands“
- [F] C. Vetter, P. Pornsuriyasak, J. Schmidt, N. P. Rath, T. Ruffer, A. V. Demchenko, D. Steinborn, *Dalton Trans.* **2010**, 6327. „Synthesis, characterization and reactivity of carbohydrate platinum(IV) complexes with thioglycoside ligands“
- [G] P. Pornsuriyasak, C. Vetter, S. Kaeothip, M. Kovermann, J. Balbach, D. Steinborn, A. V. Demchenko, *Chem. Commun.* **2009**, 6379. „Coordination chemistry approach to the long-standing challenge of stereocontrolled chemical glycosylation“
- [H] C. Vetter, C. Wagner, R. Kluge, D. Steinborn, *Z. Naturforsch.* **2010**, 65b, 578.
 „Structural and Computational Studies of 1-Methyl-2-thiocytosine and its Coordination Mode in a Dinuclear Platinum(IV) Complex $[(PtMe_3)_2(\mu-1-MeSCy-1\kappa N^3, 1:2\kappa^2 S)_2][BF_4]_2$ “
- [I] C. Vetter, C. Wagner, D. Steinborn, *Acta Crystallogr., Sect. E: Struct. Rep. Online* **2010**, 66, m286. „(OC-6-33)-(acetato- κO)(2,2'-bipyridine)trimethylplatinum(IV) monohydrate”

Zum Zeitpunkt des Einreichens der Arbeit lagen noch nicht alle Publikationen gedruckt vor und wurden deshalb als Worddokumente im Anhang beigelegt. Die hier vorliegende Version ist diesbezüglich aktualisiert.



Synthesis and characterization of platinum(IV) complexes with *N,S* and *S,S* heterocyclic ligands

Cornelia Vetter^a, Christoph Wagner^a, Jürgen Schmidt^b, Dirk Steinborn^{a,*}

^a Institut für Anorganische Chemie, Martin-Luther-Universität Halle-Wittenberg, D-06120, Halle, Kurt-Mothes Straße 2, Germany

^b Leibniz-Institut für Pflanzenbiochemie, D-06120, Halle, Weinberg 3, Germany

Received 17 May 2006; accepted 4 June 2006

Available online 15 June 2006

Abstract

The reactions of [PtMe₃(OAc)(bpy)] (**4**) with the *N,S* and *S,S* containing heterocycles, pyrimidine-2-thione (pymtH), pyridine-2-thione (pytH), thiazoline-2-thione (tztH) and thiophene-2-thiol (tptH), resulted in the formation of the monomeric complexes [PtMe₃(D[−]S-κS)(bpy)] (D[−]S = pymt, **5**; pyt, **6**; tzt, **7**; tpt, **8**), where the heterocyclic ligand is coordinated via the exocyclic sulfur atom. In contrast, in the reactions of [PtMe₃(OAc)(Me₂CO)_x] (**3**, *x* = 1 or 2) with pymtH, pytH, tztH and tptH dimeric complexes [(PtMe₃(μ-D[−]S))₂] (μ-D[−]S = pymt, **9**; pyt, **10**; tzt, **11**) and the tetrameric complex [(PtMe₃(μ₃-tpt-κS))₄] (**12**), respectively, were formed. The complexes were characterized by microanalyses, ¹H and ¹³C NMR spectroscopy and negative ESI-MS (**12**) measurements. Single-crystal X-ray diffraction analysis of [PtMe₃(pymt-κS)(bpy)] (**5**) exhibited a conformation where the pymt ligand lies nearly perpendicular to the complex plane above the bpy ligand that was also confirmed by quantum chemical calculations on the DFT level of theory.
© 2006 Elsevier B.V. All rights reserved.

Keywords: Platinum(IV) complexes; *N,S* heterocyclic ligands; *S,S* heterocyclic ligands; Sulfur coordination; Single-crystal X-ray diffraction analysis; DFT calculation

1. Introduction

Metal complexes having sulfur and nitrogen containing heterocyclic ligands like pyridine-2-thione or thiazoline-2-thione are of interest in different aspects. On the one hand, such ligands possess several binding modes to metals [1]. They can either act as neutral or anionic ligands and can be bound monodentately via the exocyclic sulfur atom [2,3], the endocyclic nitrogen atom [4] or in a chelating binding fashion [5,6]. Also the formation of a sulfur bridge through the thione group to two metal atoms has been reported [7]. On the other hand, it has been shown that the heterocyclic compounds exhibit bioactive properties. Pyridine-2-thione is able to act as enzyme inhibitor of the polyphenoloxidase, which is responsible for browning in fruits and vegetables [8]. Thiazoline-2-thione is an inhibitor

of the prostaglandine synthetase enzyme complex, which is involved in inflammatory processes causing arthritis, thrombosis or asthma [9]. Also complexes containing heterocyclic *N,S* ligands were shown to have bioactive properties, among them being cytotoxic ones. Since the discovery of the antitumor effect of cisplatin by Rosenberg [10], especially platinum complexes proved to be of interest in this respect. Up to now a number of platinum complexes have been synthesized with ligands like pyridine-2-thione or pyrimidine-2-thione, which showed cytotoxic activities sometimes higher than that of cisplatin and even to cisplatin resistant cell lines [1,11–13]. So complexes of these types are promising potential new cancerostatica. In general, platinum(IV) complexes having *S* bound heterocyclic ligands are much less investigated in this context than the corresponding platinum(II) complexes.

Already in 1907, Pope and Peachey [14] synthesized the tetrameric complex [(PtMe₃I)₄] (**1**) having the *fac*-Pt^{IV}Me₃ unit. In our research group, it was shown that trimethyl-

* Corresponding author. Tel.: +345 5525620; fax: +345 5527028.

E-mail address: dirk.steinborn@chemie.uni-halle.de (D. Steinborn).

platinum(IV) complexes with a broad variety of bioligands can be prepared, even when the ligands are only weak donors and can be easily oxidized, such as carbohydrates [15–17]. Here we report the synthesis and characterization of platinum(IV) complexes with the heterocyclic ligands pyrimidine-2-thione, pyridine-2-thione, thiazoline-2-thione and thiophene-2-thiol. These heterocycles are capable of thione-thiol tautomerism. While pyrimidine-, pyridine- and thiazoline-2-thione exist mainly in the thione form [18], thiophene-2-thiol prefers the thiol form [18,19].

2. Results and discussion

2.1. Synthesis of $[PtMe_3(OAc)(bpy)]$ (**4**)

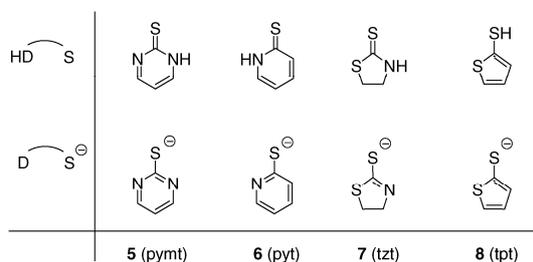
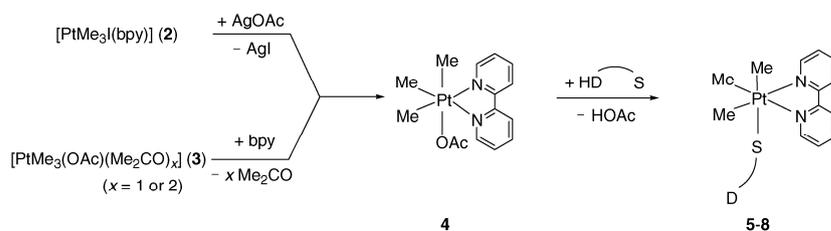
The reaction of $[PtMe_3I(bpy)]$ (**2**) [20] with silver acetate in acetone as well as the reaction of $[PtMe_3(OAc)(Me_2CO)_x]$ ($x = 1, 2$) (**3**) with 2,2'-bipyridine resulted in the formation of $[PtMe_3(OAc)(bpy)]$ (**4**) (Scheme 1). The preparation of this complex starting from **2** and **3** is similar to those previously described by Clegg et al. [20] and by us [16], respectively. Complex **4** was isolated as a white air-stable powder in 70% yield. The identity of **4** was confirmed by microanalysis, 1H and ^{13}C NMR spectroscopy. The 1H and ^{13}C NMR spectra showed the expected pattern for the three methyl ligands *trans* to bpy (δ_H 1.18, $^2J_{Pt,H} = 68.3$ Hz; $\delta_C = 4.9$, $^1J_{Pt,C} = 704.8$ Hz) and that for the methyl ligand *trans* to OAc (δ_H 0.25, $^2J_{Pt,H} = 74.1$ Hz; $\delta_C = 14.9$, $^1J_{Pt,C} = 706.1$ Hz). Here we used complex **4** as the starting material, but for these purposes the complex was prepared in situ.

2.2. Synthesis of mononuclear complexes **5–8**

Complex **4** was found to react in the presence of an excess of AgOAc (4:AgOAc = 1:1.5) with pyrimidine-2-thione (pymtH), pyridine-2-thione (pytH), thiazoline-2-thione (tztH) and thiophene-2-thiol (tptH) in acetone yielding the neutral complexes $[PtMe_3(\eta^3\text{-}\kappa\text{S})(bpy)]$ (**5–8**) (Scheme 1). As shown by 1H NMR measurements of the reaction mixtures, all complexes were formed with a degree of conversion >60%. The surplus AgOAc proved to be decisive. Using equimolar ratio (2:AgOAc = 1:1), much lower degrees of conversion were obtained. The complexes were isolated as yellow powdery (**5**, **6**, **8**) and microcrystalline (**7**) substances in moderate yields. They are stable on air. Complex **6** contained a considerable amount of non-identified platinum complexes. Chromatographic purification failed due to decomposition. The identities of complexes were confirmed by microanalysis (except for **6**), 1H and ^{13}C NMR spectroscopy as well as by single-crystal X-ray diffraction measurements of **5**.

2.3. Structure of $[PtMe_3(pymt\text{-}\kappa\text{S})(bpy)]$ (**5**)

Single crystals of $[PtMe_3(pymt\text{-}\kappa\text{S})(bpy)]$ (**5**) suitable for X-ray diffraction analysis were obtained from acetone/diethyl ether/*n*-pentane solutions. The complex crystallizes in the space group $P2_1/n$ in isolated molecules (shortest intermolecular distance between non-hydrogen atoms: $N2 \cdots S' 5.011(3)$ Å). The molecular structure is shown in Fig. 1. Selected bond lengths and angles are listed in Table 1. The platinum atom is octahedrally coordinated by three methyl ligands in facial configuration, the 2,2'-bipyridine and the *S*-bound pyrimidine-2-thiolato ligand. Due to the



Scheme 1.

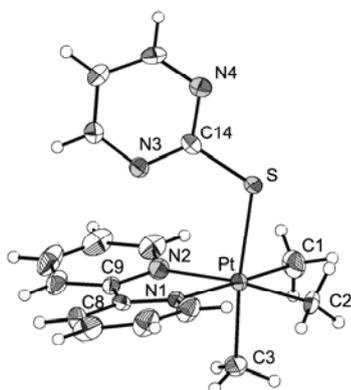


Fig. 1. Molecular structure of $[\text{PtMe}_3(\text{bpy})(\text{pymt})]$ (**5**). The displacement ellipsoids are drawn at the 30% probability level.

restricted bite of the bipyridine ligand (N1-Pt-N2 $76.9(2)^\circ$), the C1-Pt-N2 and C2-Pt-N1 angles of the equatorial plane are distinctly widened ($98.0(3)^\circ$, $98.0(2)^\circ$). The 2,2'-bipyridine ligand is not planar; the two pyridine rings are twisted by $11.1(3)^\circ$. The pyrimidine-2-thiolato ligand coordinates through the exocyclic sulfur atom to the platinum(IV) atom and is directed towards the 2,2'-bipyridine ligand. Notably, the pymt ligand is almost perpendicular to the bpy ligand (interplanar angle $85.4(2)^\circ$). Likely for steric reasons, the Pt-S-C14 angle ($114.79(2)^\circ$) is slightly larger than the tetrahedral one and the S-Pt-C3 , N1-Pt-C1 and N2-Pt-C2 angles are smaller ($172.8(2)$ – $174.8(3)^\circ$) than 180° .

2.4. Quantum chemical calculations

In the crystals of **5**, the pyrimidine-2-thiolato ligand is perpendicular to the PtN_2C_2 plane (interplanar angle 85.4°) and lies above the central C8-C9 bond of the bipyridine ligand (torsional angle $\text{N1-Pt-S-C14/N2-Pt-S-C14}$ $-56.5(2)/20.6(2)^\circ$). Here and in the following, the latter

Table 1
Selected bond lengths (in Å) and bond angles (in $^\circ$) of $[\text{PtMe}_3(\text{pymt-}\kappa\text{S})(\text{bpy})]$ (**5**), compared to the calculated conformers **5a/5b**

	5 (Exp.)	5a	5b
Pt–C1	2.079(6)	2.067	2.066
Pt–C2	2.056(6)	2.068	2.063
Pt–C3	2.067(6)	2.100	2.097
Pt–S	2.427(1)	2.514	2.517
Pt–N1	2.152(4)	2.222	2.227
Pt–N2	2.147(5)	2.232	2.247
C1–Pt–C2	87.0(3)	85.3	86.1
C1–Pt–N2	98.0(3)	100.7	99.6
N1–Pt–N2	76.9(2)	74.7	74.2
C2–Pt–N1	98.0(2)	99.3	100.2
C3–Pt–S	173.9(2)	173.8	175.7
C14–S–Pt	114.8(2)	115.2	113.6

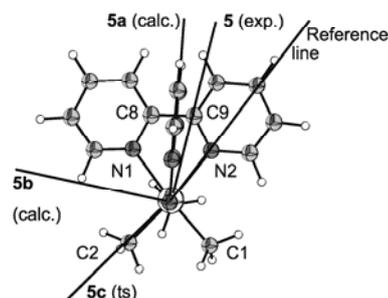


Fig. 2. Conformers of experimental (**5**) and calculated equilibrium (**5a/5b**) and transition state (**5c**) structures. Shown is the calculated structure **5a** in the view along the S-Pt-C3 vector.

torsional angle (N2-Pt-S-C14) is used to describe the conformation of the pyrimidine-2-thiolato ligand with respect to the complex plane (see Fig. 2). To get further insight into the conformation of the complex, quantum chemical calculations on the DFT level of the theory were performed.

Two equilibrium structures were found having, in practice, the same energy ($\Delta E = 0.1$ kcal/mol). In both these structures, the pyrimidine-2-thiolato ligand is perpendicular to the PtN_2C_2 plane (interplanar angles $88.9/89.3^\circ$, **5a/5b**).¹ In **5a**, the pyrimidine-2-thiolato ligand lies above the central C8-C9 bond of the bipyridine ligand approximately bisecting the N1-Pt-N2 angle (torsional angles $\text{N1-Pt-S-C14/N2-Pt-S-C14}$ $-40.7/34.3^\circ$). Thus, the conformation of **5a** is very close to that of the experimental structure **5** (see Fig. 2). In the other equilibrium structure **5b**, the pyrimidine-2-thiolato ligand lies between the bipyridine and the methyl ligand (torsional angle N2-Pt-S-C14 117.8°). Apart from this, the bond lengths and angles in **5a** and **5b** are very similar and agree quite well with the values found in the experimental structure **5** (see Table 1). Notably, the Pt-S and Pt-N bonds were calculated to be longer (up to 0.100 Å) and the strong distortion of the bipyridine ligand in the experimental structure **5** (interplanar angle between the two pyridine rings 11.1°) is not reflected in the calculated structures **5a/5b** ($4.8/5.3^\circ$).

Rotation of the pyrimidine-2-thiolato ligand around the Pt-S vector exhibited that the maximum of the potential energy belongs to a transition state structure **5c** where the pyrimidine-2-thiolato ligand lies above the methyl ligand (N2-Pt-S-C14 -179.6°). Overall, the rotational barrier is very low (2.9 kcal/mol). From all these findings, the conclusion can be drawn that the pyrimidine-2-thiolato ligand can (nearly) freely rotate and that the rotational barrier is mainly caused by steric repulsion between the pyrimidine-2-thiolato ligand and the bpy/Me ligands.

¹ Because the calculated structures are very close to the experimental one, Figs. of **5a/5b** are shown in the Supplemental only. The numbering schemes for **5a/5b** are analogous to that for **5**.

Table 2
 ^1H and ^{13}C NMR spectroscopical data (δ in ppm, J in Hz) of the methyl ligands of complexes **5–8**

$\text{D}^{\ominus}\text{S}^{\ominus}$	pyt (5)	pymt (6)	tzt (7)	tpt (8)
$\delta_{\text{H}}(^2J_{\text{Pt,H}})$				
CH_3 <i>trans</i> to S	0.31 (65.8)	0.29 (66.8)	0.29 (66.2)	0.24 (64.4)
CH_3 <i>trans</i> to N	1.19 (69.5)	1.16 (69.7)	1.14 (69.9)	1.13 (70.5)
$\delta_{\text{C}}(^1J_{\text{Pt,C}})$				
CH_3 <i>trans</i> to S	1.9 (622.8)	1.2 (622.7)	1.5 (622.9)	−0.8 (608.6)
CH_3 <i>trans</i> to N	−5.2 (672.3)	−5.2 (676.8)	−5.4 (673.2)	−5.2 (681.6)

2.5. NMR spectroscopic investigations of complexes **5–8**

^1H and ^{13}C NMR spectroscopic measurements of the complexes $[\text{PtMe}_3(\text{D}^{\ominus}\text{S}^{\ominus}\text{-}\kappa\text{S})(\text{bpy})]$ (**5–8**) gave evidence for their constitution. In the case of complex **5**, the ^1H NMR spectrum shows a symmetrically bound pyrimidine-2-thiolato ligand ($\delta_{\text{H}4} = \delta_{\text{H}6}$ of the pyrimidine ring) giving proof for *S* coordination of the ligand, as verified by its solid-state structure. The chemical shifts and coupling constants of the methyl ligands are given in Table 2. Both the chemical shifts (δ_{H} , δ_{C}) and the coupling constants ($^2J_{\text{Pt,H}}$, $^1J_{\text{Pt,C}}$) of the methyl ligands *trans* to the bipyridine ligand are in a very narrow range, exhibiting that they depend only to a small extent on the nature of the *cis*-bound heterocyclic ligand. The coupling constants $^1J_{\text{Pt,C}}$ of the methyl ligands *trans* to the *S*-bound ligands are smaller by 49.5–73.0 Hz compared with those *trans* to the bipyridine ligands. This indicates a greater *trans* influence of the anionic *S*-bound ligands than the bipyridine ligand. The same holds for the $^2J_{\text{Pt,H}}$ coupling constants ($\Delta J = 2.9$ – 6.1 Hz). On the basis of the $^1J_{\text{Pt,C}}$ coupling constants, the *trans* influence of the tpt $^-$ ligand (608.6 Hz) was found to be slightly larger than those of the other three ligands (tzt $^-$, pymt $^-$, pyt $^-$: 622.7–622.9 Hz).

2.6. Synthesis of di- and tetranuclear complexes **9–12**

The reaction of $[\text{PtMe}_3(\text{OAc})(\text{Me}_2\text{CO})_x]$ (**3**) ($x = 1$ or 2) with $\text{HD}^{\ominus}\text{S}^{\ominus}$ (pymtH, pytH, tztH) in acetone led to the formation of dinuclear platinum complexes **9–11** having bridging $\mu\text{-D}^{\ominus}\text{S}^{\ominus}$ ligands. The reaction of **3** with tptH

resulted in the formation of a tetrameric complex **12** (Scheme 2). As opposed to the synthesis of the monomeric complexes **5–8**, for the syntheses of the di- and tetranuclear complexes **9–12** no excess of AgOAc is necessary. Yellow microcrystals of complex **12** precipitated in 87% yield from the reaction solution within a few minutes. The other complexes were obtained in moderate to good yields (43–93%) as yellow (**9** and **10**) and colorless powdery substances (**11**) after addition of *n*-pentane to the reaction mixtures. Complexes **9–11** are well soluble in acetone, methylene chloride and chloroform, whereas complex **12** is less soluble in these solvents. All complexes were characterized by microanalysis, ^1H and ^{13}C NMR spectroscopy.

2.7. NMR spectroscopic investigations of complexes **9–12**

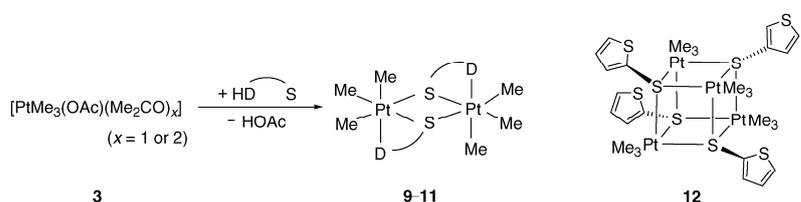
Signal intensities in the ^1H NMR spectra gave evidence for the 1:1 stoichiometry ($\text{PtMe}_3:\text{D}^{\ominus}\text{S}^{\ominus}$) of the complexes. In accordance with the deprotonation of the ligands, no *SH* resonances were found. For complexes **9–11**, the ^1H and ^{13}C NMR spectra are in agreement with a dimeric structure as shown in Scheme 2, see selected NMR parameters in Table 3. As expected all three methyl ligands are chemically non-equivalent both in the ^1H and in the ^{13}C NMR spec-

Table 3
 ^1H and ^{13}C NMR spectroscopical data (δ in ppm, J in Hz) of the methyl ligands of complexes **9–12**

$\mu\text{-D}^{\ominus}\text{S}^{\ominus}$	δ_{H}	\leftrightarrow	$\delta_{\text{C}}^{\text{a}}$	$^1J_{\text{Pt,C}}$	$^2J_{\text{Pt,H}}$
pymt $^-$ (9)	1.19/1.17 ^b	{	1.8	662.7	74.7/73.0
	0.84		−12.3	673.7	73.9
pyt $^-$ (10)	1.08/1.07 ^b	{	2.6	666.6	73.9
	0.84		1.5	670.1	73.0/73.5
tzt $^-$ (11)	1.17	{	−12.2	663.6	72.6
	1.01		2.2	658.6	72.6
	0.85		−0.6	684.6	77.7
tpt $^-$ (12)	1.36	{	0.0	672.4	72.4
			−12.7	672.3	73.2
			7.1	639.5	71.8

^a Correlated signals in ^1H – ^{13}C COSY NMR spectra are given in the same line.

^b Due to the small difference in the chemical shifts no unambiguous assignment in ^1H ^{13}C COSY NMR spectra can be made.



$\text{D}^{\ominus}\text{S}^{\ominus}$	9	10	11	12
	pymt	pyt	tzt	tpt

Scheme 2.

tra. ^1H - ^{13}C COSY experiments revealed the correlation given in Table 3 and exemplified in Fig. 3 for complex **10**. Unexpectedly, the two signals positioned closely together (both in the ^1H and ^{13}C NMR spectra) have not been assigned to the methyl ligands (Me^2/Me^3) *trans* to the $\mu\text{-S}$ -atoms. NOE experiments of complex **10** with irradiation in the resonance of proton H_6 of the pyridine ring (see formula in Fig. 3) gave a strong increase of the intensity for one of the two signals 1.07/1.08 ppm and a weaker one for the signal at 0.84 ppm. This gives further indication

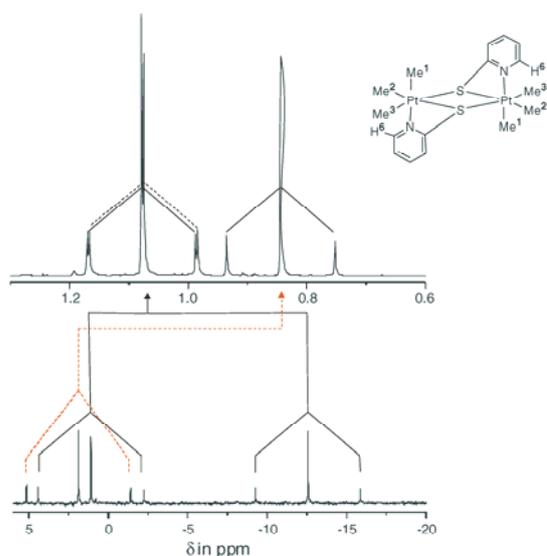


Fig. 3. ^1H - ^{13}C NMR correlation of the chemical shifts for the methyl ligands of $[\{\text{PtMe}_3(\mu\text{-pyt})\}_2]$ (**10**).

for an assignment of these two signals to the methyl protons Me^2/Me^3 . Thus, the methyl protons Me^1 resonate at 1.07 or 1.08 ppm.

Complex **12** exhibited only one resonance in ^1H and ^{13}C NMR spectra for the protons and carbon atoms of the three methyl ligands. Down to -50°C , the signal for the methyl protons remained to be a sharp singlet. This implicates a different constitution than complexes **9–11**. A tetranuclear heterocubane cluster with a $[\text{Pt}_4\text{S}_4]$ core analogously to the Pope cluster $[(\text{PtMe}_3\text{I})_4]$ (**1**) agrees with the ^1H and ^{13}C NMR spectra and could be detected by negative ESI-MS (Fig. 4). The most intensive mass peak is the anion $[(\text{PtMe}_3)_4(\mu_3\text{-tpt-}\kappa\text{S})_3(\mu_3\text{-S})]^-$ at 1338.01 m/z where a thiophene cation is cleaved. The peak shows an isotopic envelope (Fig. 4b) which is characteristic for a monoanion containing four platinum atoms [natural isotopic composition: ^{190}Pt (0.01%), ^{192}Pt (0.79%), ^{194}Pt (32.9%), ^{195}Pt (33.8%), ^{196}Pt (25.3%), ^{198}Pt (7.2%)]. The observed values agree very well with the calculated ones. Furthermore, other signals could be detected which can be assigned to the parent anion $[\{\text{PtMe}_3(\mu_3\text{-tpt-}\kappa\text{S})\}_4]^-_{\text{H}}$ at 1418.97 m/z and to $[\{\text{PtMe}_3(\mu_3\text{-tpt-}\kappa\text{S})\}_4]^-_{\text{CH}_3}$ at 1405.94 m/z (with low intensity). The peak at 1370.51 m/z is formed by the loss of a C_4H_3 unit, probably by the fragmentation of the thiophene ring. This measurement proves unambiguously the tetrameric constitution of complex **12** and, most likely, the tpt^- ligand is monodentately μ_3 -bound through the exocyclic thiolate group as shown in Scheme 2.

2.8. Reactivity of the dimeric complexes

To get insight into the stability of the sulfur bridges in the dinuclear complexes **9–11**, complex **11** was reacted with 2,2'-bipyridine and 4-picoline (pic). NMR spectroscopic investigations revealed the formation of monomeric com-

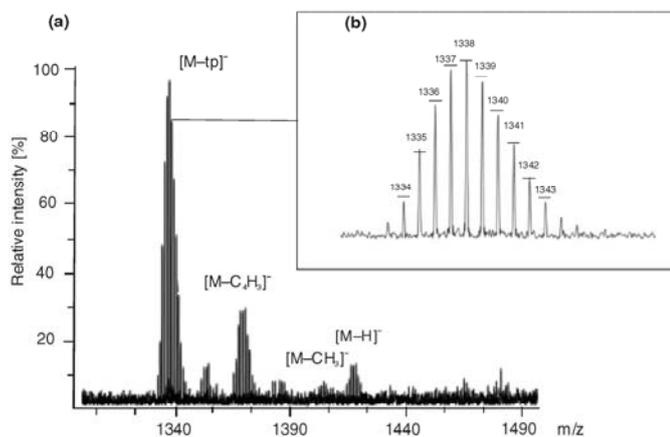
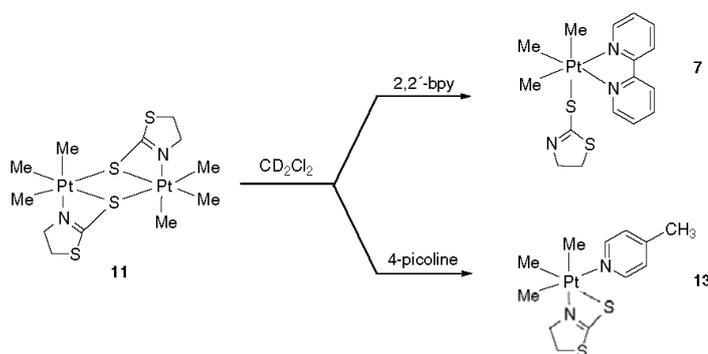


Fig. 4. (a) Negative ESI-mass spectrum of $[(\text{PtMe}_3(\mu_3\text{-tpt-}\kappa\text{S}))_4]$ (**12**). (b) Isotopic pattern of the anion $[(\text{PtMe}_3)_4(\mu_3\text{-tpt-}\kappa\text{S})_3(\mu_3\text{-S})]^-$ at 1338.01 m/z showing the expected intensity due to the isotopic composition (calculated intensities are shown in horizontal bars; $\text{M} = [(\text{PtMe}_3(\mu_3\text{-tpt-}\kappa\text{S}))_4]$, $\text{tp} =$ thiophene).



Scheme 3.

plexes having 1:1:1 stoichiometry of $\text{PtMe}_3\text{:tzt:bpy}$ and $\text{PtMe}_3\text{:tzt:pic}$, respectively (Scheme 3). The complex formed in the reaction with bipyridine contains a monodentately *S*-bound *tzt* ligand and is identical with complex 7, that was obtained from the reaction of $[\text{PtMe}_3(\text{OAc})\text{bpy}]$ (4) with *tztH*. Contrary to that, the reaction with 4-picoline gave rise to the formation of complex 13 containing a bidentately bound *tzt* ligand.

3. Conclusions

The synthesis and characterization of mononuclear (5–8), dinuclear (9–11) and tetranuclear (12) trimethylplatinum(IV) complexes have shown that deprotonated *N,S* and *S,S* heterocycles HD^-S^- ($\text{HD}^-\text{S}^- = \text{pymtH}^-$, pytH^- , tztH^- and tptH^-) are versatile ligands. The strongest coordination site is the exocyclic sulfur atom, thus acting either as a terminal ligand as in the mononuclear complexes 5–8 or as μ_2 - and μ_3 -bridging ligand as in the dinuclear (9–11) and tetranuclear (12) complexes, respectively. As shown in the reactions of dinuclear complex 11 with *bpy* and 4-picoline, a terminal Pt–S bond is formed at the expense of the bridging mode.

The reactions of $[\text{PtMe}_3(\text{OAc})(\text{bpy})]$ (4) with HD^-S^- proceeded only smoothly in excess of OAc^- , indicating that the acetato ligand can only be substituted by the deprotonated species D^-S^- and that the neutral heterocycles HD^-S^- are only weak donors. In contrast, the reactions of $[\text{PtMe}_3(\text{OAc})(\text{Me}_2\text{CO})_x]$ (3, $x = 1$ or 2) with HD^-S^- did not afford excess of OAc^- , indicating that the first step of the reactions is the substitution of a weakly bound acetone ligand from 3 by HD^-S^- followed by its deprotonation by the acetato ligand and formation of the dinuclear and tetranuclear complexes 9–12, respectively. The formation of the tetranuclear complex 12 in the reaction with *tptH* might indicate that its endocyclic sulfur atom is a weaker donor than the endocyclic nitrogen atoms in pymt^- , pyt^- and tzt^- .

Summarizing, in this work it has been shown for the first time that platinum(IV) can be coordinated in different

binding modes to *N,S* and *S,S* heterocyclic ligands, which are of both biological relevance and bioligand models.

4. Experimental

4.1. General considerations

Syntheses were performed under argon using standard Schlenk techniques. Acetone and pentane were dried over phosphorpentoxide followed by 4 Å molecular sieves and LiAlH_4 , respectively. All solvents were distilled prior to use. NMR spectra were obtained with Varian UNITY 500, Gemini 2000, and Gemini 200 spectrometers using solvent signals (^1H and ^{13}C NMR spectroscopy) as internal reference. Microanalyses were performed by the University of Halle microanalytical laboratory using CHNS-932 (LECO). The negative ion high resolution ESI mass spectra were obtained from a Bruker Apex III Fourier transform ion cyclotron resonance (FT-ICR) mass spectrometer (Bruker Daltonics, Billerica, USA) equipped with an Infinity™ cell, a 7.0 Tesla superconducting magnet (Bruker, Karlsruhe, Germany), an RF-only hexapole ion guide and an external electrospray ion source (Agilent, off axis spray, voltages: endplate, 3.700 V; capillary, 4.200 V; capillary exit, –100 V; skimmer 1, –15.0 V; skimmer 2, –6.0 V). Nitrogen was used as drying gas at 150 °C. The sample solutions were introduced continuously via a syringe pump with a flow rate of 120 $\mu\text{l h}^{-1}$. The data were acquired with 512k data points and zero filled to 2048k by averaging 64 scans.

$[(\text{PtMe}_3\text{I})_4]$ (1) [14,21] and $[\text{PtMe}_3\text{I}(\text{bpy})]$ (2) [20] were prepared according to the literature methods. All other materials were purchased commercially. Thiophene-2-thiol was distilled before use and stored under argon.

4.1.1. Synthesis of $[\text{PtMe}_3(\text{OAc})(\text{bpy})]$ (4) [16]

$[(\text{PtMe}_3\text{I})_4]$ (50.0 mg, 0.04 mmol) and AgOAc (23.0 mg, 0.14 mmol) were suspended in acetone (4 ml) and stirred vigorously for 15 h in the absence of light. The precipitate (AgI) was filtered off and 2,2'-bipyridine (42.8 mg,

0.36 mmol) was added to the clear filtrate. After stirring for 30 min the solution was concentrated to ca 1 ml. The white precipitate formed was filtered, washed with pentane (1 ml) and dried in vacuo. Yield: 50 mg (69%). Alternatively [20], [PtMe₃I(bpy)] (70.0 mg, 0.14 mmol) and AgOAc (23.0 mg, 0.14 mmol) were suspended in acetone (4 ml) and stirred vigorously for 15 h in the absence of light. The precipitate (AgI) was filtered off and the clear filtrate was concentrated to ca. 1 ml. The white precipitate formed was filtered, washed with pentane (1 ml) and dried in vacuo. Yield: 52 mg (72%). *Anal.* Calc. for C₁₅H₂₀N₂O₂Pt (455.55): C, 39.56; H, 4.40; N, 6.15. Found: C, 38.20, H, 4.62; N, 5.90%. ¹H NMR (400 MHz, CD₂Cl₂): δ 8.96 (m, 2H, H6/H6' of bpy), 8.22 (d, 2H, H3/H3' of bpy), 8.07 (m, 2H, H4/H4' of bpy), 7.64 (m, 2H, H5/H5' of bpy), 1.54 (s, 3H, CH₃COO), 1.18 (s + d, 6H, ²J_{Pt,H} = 68.3 Hz, PtCH₃ *trans* to N), 0.25 (s + d, 3H, ²J_{Pt,H} = 74.1 Hz, PtCH₃ *trans* to O). ¹³C NMR (125 MHz, CD₂Cl₂): δ 175.6 (s, CH₃COO), 155.5 (s, C2/C2' of bpy), 147.2 (s, C6/C6' of bpy), 138.5 (s, C4/C4' of bpy), 126.1 (s, C5/C5' of bpy), 122.6 (s, C3/C3' of bpy), 24.6 (s, CH₃COO), -4.9 (s + d, ¹J_{Pt,C} = 704.8 Hz, PtCH₃ *trans* to N), -14.9 (s + d, ¹J_{Pt,C} = 706.1 Hz, PtCH₃ *trans* to O).

4.1.2. Synthesis of [PtMe₃(pymt-κS)(bpy)] (5)

A suspension of [PtMe₃I(bpy)] (70.0 mg, 0.14 mmol) in acetone (10 ml) and AgOAc (58.0 mg, 0.34 mmol) was stirred for 15 h in the absence of light. After filtration of AgI, pyrimidine-2-thione (pymtH) (15.0 mg, 0.14 mmol) was added with stirring to the clear filtrate. After 2 h the solution was concentrated up to ca. 3 ml, and pentane (6 ml) was added. The yellow product formed was filtered, washed with pentane (2 ml) and dried in vacuo. Yield: 43 mg (61%). *Anal.* Calc. for C₁₇H₂₀N₄SPt (507.51): C, 40.23; H, 3.97; N, 11.04, S, 6.32. Found: C, 40.16, H, 4.44; N, 10.95, S, 6.54%. ¹H NMR (400 MHz, CD₂Cl₂): δ 8.89 (m, 2H, H6/H6' of bpy), 8.21 (d, 2H, H3/H3' of bpy), 8.01 (m, 2H, H4/H4' of bpy), 7.84 (d, 2H, ³J_{Pt,H} = 4.8 Hz, H4, H6), 7.55 (m, 2H, H5/H5' of bpy), 6.40 (m, 1H, H5), 1.19 (s + d, 6H, ²J_{Pt,H} = 69.5 Hz, PtCH₃ *trans* to N), 0.31 (s + d, 3H, ²J_{Pt,H} = 65.8 Hz, PtCH₃ *trans* to S). ¹³C NMR (100 MHz, CDCl₃): δ 155.6 (s, C6, C4), 147.6 (s, C6/C6' of bpy), 138.5 (s, C4/C4' of bpy), 125.8 (s, C5/C5' of bpy), 122.5 (s, C3/C3' of bpy), 113.1 (s, C5), 1.9 (s + d, ¹J_{Pt,C} = 622.8 Hz, PtCH₃ *trans* to S), -5.2 (s + d, ¹J_{Pt,C} = 672.3 Hz, PtCH₃ *trans* to N).

4.1.3. Reaction of [PtMe₃(OAc)(bpy)] (4) with pyridine-2-thione to 6

To a solution of 4 in acetone (10 ml) prepared from [PtMe₃I(bpy)] (70.0 mg, 0.14 mmol) and AgOAc (58.0 mg, 0.34 mmol) as described above, pyridine-2-thione (pytH) (15.0 mg, 0.14 mmol) was added. After 2 h the solution was concentrated up to ca. 3 ml, and pentane (6 ml) was added. The yellow product formed (containing about 50% 6) was filtered, washed with pentane (1 ml) and dried in vacuo. ¹H NMR (400 MHz, CD₂Cl₂): δ 1.16 (s + d, 6H,

²J_{Pt,H} = 69.7 Hz, PtCH₃ *trans* to N), 0.29 (s + d, 3H, ²J_{Pt,H} = 66.8 Hz, PtCH₃ *trans* to S). ¹³C NMR (100 MHz, CDCl₃): δ 1.2 (s + d, ¹J_{Pt,C} = 622.7 Hz, PtCH₃ *trans* to S), -5.2 (s + d, ¹J_{Pt,C} = 676.8 Hz, PtCH₃ *trans* to N).

4.1.4. Synthesis of [PtMe₃(tzt-κS)(bpy)] (7)

To a solution of 4 in acetone (10 ml) prepared from [PtMe₃I(bpy)] (50.0 mg, 0.09 mmol) and AgOAc (40.0 mg, 0.24 mmol) as described above, thiazoline-2-thione (tztH) (11.0 mg, 0.09 mmol) was added. After 5 h the volume of the reaction mixture was reduced up to ca 1/3 and cooled down to 0 °C for 2 h. The yellow precipitate formed was filtered, washed with tetrahydrofuran and dried in vacuo. Yield: 8 mg (16%). *Anal.* Calc. for C₁₆H₂₁N₃S₂Pt (514.55): C, 37.35; H, 4.11; N, 8.17; S, 12.45. Found: C, 37.49; H, 4.15; N, 7.96; S, 11.8%. ¹H NMR (400 MHz, CD₂Cl₂): δ 8.88 (m, 2H, H6/H6' of bpy), 8.20 (d, 2H, H3/H3' of bpy), 8.05 (m, 2H, H4/H4' of bpy), 7.59 (m, 2H, H5/H5' of bpy), 3.45 (m, 2H, NCH₂), 2.76 (m, 2H, SCH₂) 1.14 (s + d, 6H, ²J_{Pt,H} = 69.9 Hz, PtCH₃ *trans* to N), 0.29 (s + d, 3H, ²J_{Pt,H} = 66.2 Hz, PtCH₃ *trans* to S). ¹³C NMR (100 MHz, CD₂Cl₂) δ 155.6 (s, C2/C2' of bpy), 147.6 (s, C6/C6' of bpy), 138.6 (s, C4/C4' of bpy), 126.1 (s, C5/C5' of bpy), 123.0 (s, C3/C3' of bpy), 65.2 (s, NCH₂), 35.7 (s, SCH₂), 1.5 (s + d, ¹J_{Pt,C} = 622.9 Hz, PtCII₃ *trans* to S), -5.4 (s + d, ¹J_{Pt,C} = 673.2 Hz, PtCII₃ *trans* to N).

4.1.5. Synthesis of [PtMe₃(tpt-κS)(bpy)] (8)

To a solution of 4 in acetone (10 ml) prepared from [PtMe₃I(bpy)] (70.0 mg, 0.14 mmol) and AgOAc (58.0 mg, 0.34 mmol) as described above, thiophene-2-thiol (tptH) (15.0 mg, 0.14 mmol) was added and stirred for 2 h. The volume of the solution was reduced up to about 3 ml, and then pentane (6 ml) was added. The yellow product formed was collected by filtration, washed with pentane (1 ml) and dried in vacuo. Yield: 33 mg (49%). *Anal.* Calc. for C₁₇H₂₀N₂S₂Pt (511.54): C, 39.91; H, 3.94; N, 5.48; S, 12.53. Found: C, 39.79; H, 4.15; N, 5.32; S, 12.28%. ¹H NMR (400 MHz, CD₂Cl₂): δ 8.75 (m, 2H, H6/H6' of bpy), 7.97 (m, 4H, H3/H3', H4/H4' of bpy), 7.54 (m, 2H, H5/H5' of bpy), 6.51 (m, 1H, H3), 6.28 (m, 1H, H5), 5.62 (m, 1H, H4), 1.13 (s + d, 6H, ²J_{Pt,H} = 70.5 Hz, PtCH₃ *trans* to N), 0.24 (s + d, 3H, ²J_{Pt,H} = 64.4 Hz, PtCH₃ *trans* to S). ¹³C NMR (100 MHz, CD₂Cl₂): δ 154.0 (s, C2/C2' of bpy), 146.7 (s, C6/C6' of bpy), 137.9 (s, C4/C4' of bpy), 135.6 (s, C2), 129.3 (s, C5) 127.6 (s, C4), 126.3 (s, C5/C5' of bpy), 123.5 (s, C3), 122.9 (s, C3/C3' of bpy), -0.8 (s + d, ¹J_{Pt,C} = 608.6 Hz, PtCH₃ *trans* to S), -5.2 (s + d, ¹J_{Pt,C} = 681.6 Hz, PtCH₃ *trans* to N).

4.1.6. Synthesis of [PtMe₃(μ-pymt)]₂ (9)

[(PtMe₃I)₄] (50.0 mg, 0.03 mmol) and AgOAc (23.0 mg, 0.14 mmol) were suspended in acetone (5 ml). In the absence of light the reaction mixture was stirred for 15 h. AgI was filtered off and pyrimidine-2-thione (pymtH) (15.3 mg, 0.14 mmol) was added to the clear colorless filtrate with stir-

ring. Pyrimidine-2-thione dissolves within 30 min. After another 30 min the volume of the solution was reduced to about 1/3. The yellow product precipitated by adding pentane (4 ml) and was collected by filtration, washed with pentane (1 ml) and dried in vacuo. Yield: 36 mg (75%). *Anal.* Calc. for $C_{14}H_{24}N_4S_2Pt_2$ (702.64): C, 23.93; H, 3.44; N, 8.02; S, 9.13. Found: C, 24.30; H, 3.72; N, 8.04; S, 9.07%. 1H NMR (500 MHz, CD_2Cl_2): δ 8.46 (m, 2H, *H6/H6'*), 7.94 (m, 2H, *H4/H4'*), 6.90 (m, 2H, *H5/H5'*), 1.19 (s + d, 6H, $^2J_{Pt,H} = 74.7$ Hz, PtCH₃), 1.17 (s + d, 6H, $^2J_{Pt,H} = 73.0$ Hz, PtCH₃), 0.84 (s + d, 6H, $^2J_{Pt,H} = 73.9$ Hz, PtCH₃). ^{13}C NMR (100 MHz, CD_2Cl_2): δ 157.7 (s, C6/C6'), 151.2 (s, C4/C4'), 117.6 (s, C5/C5'), 2.6 (s + d, $^1J_{Pt,C} = 666.6$ Hz, PtCH₃), 1.8 (s + d, $^1J_{Pt,C} = 662.7$ Hz, PtCH₃), -12.3 (s + d, $^1J_{Pt,C} = 673.7$ Hz, PtCH₃).

4.1.7. Synthesis of [$\{PtMe_3(\mu-pyt)\}_2$] (10)

To a solution of **3** in acetone (5 ml) prepared from [(PtMe₃I)₄] (50.0 mg, 0.03 mmol) and AgOAc (23.0 mg, 0.14 mmol) as described above, pyridine-2-thione (pytH) (15.0 mg, 0.14 mmol) was added. The yellow clear solution was stirred for 5 h. Acetone was removed under reduced pressure and the residue was washed with pentane (1 ml) and dried in vacuo. Yield: 34 mg (93%). *Anal.* Calc. for $C_{16}H_{26}N_2S_2Pt_2$ (700.66): C, 27.44; H, 3.74; N, 4.02; S, 9.15. Found: C, 28.05; H, 3.94; N, 4.12; S, 9.44%. 1H NMR (500 MHz, CD_2Cl_2): δ 7.59 (m, 2H, *H6, H6'*), 7.38 (m, 2H, *H4, H4'*), 6.80 (m, 4H, *H3/H3', H5/H5'*), 1.08 (s + d, 6H, $^2J_{Pt,H} = 73.0$ Hz, PtCH₃), 1.07 (s + d, 6H, $^2J_{Pt,H} = 73.5$ Hz, PtCH₃), 0.84 (s + d, 6H, $^2J_{Pt,H} = 72.6$ Hz, PtCH₃). ^{13}C NMR (125 MHz, CD_2Cl_2): δ 168.5 (s, C2/C2'), 143.6 (s, C6/C6'), 136.5 (s, C4/C4'), 131.1 (s, C3/C3'), 120.5 (s, C5/C5'), 2.2 (s + d, $^1J_{Pt,C} = 658.6$ Hz, PtCH₃), 1.5 (s + d, $^1J_{Pt,C} = 670.1$ Hz, PtCH₃), -12.2 (s + d, $^1J_{Pt,C} = 663.6$ Hz, PtCH₃).

4.1.8. Synthesis of [$\{PtMe_3(\mu-tzt)\}_2$] (11)

To a solution of **3** in acetone (5 ml) prepared from [(PtMe₃I)₄] (132.1 mg, 0.09 mmol) and AgOAc (60.0 mg, 0.36 mmol) as described above, thiazoline-2-thione (tztH) (42.8 mg, 0.36 mmol) was added. The clear, colorless solution was stirred for 5 h. The solvent was removed under reduced pressure. The residue was washed with methanol (3 ml) and dried in vacuo. Yield: 110 mg (43%). *Anal.* Calc. for $C_{12}H_{26}N_2S_4Pt_2$ (716.74): C, 20.11; H, 3.63; N, 3.91; S, 17.87. Found: C, 21.28; H, 3.90; N, 4.22; S, 18.29%. 1H NMR (500 MHz, CD_2Cl_2): δ 4.17 (m, 2H, NCH₂), 3.46 (m, 2H, SCH₂), 1.17 (s + d, 3H, $^2J_{Pt,H} = 77.7$ Hz, PtCH₃), 1.01 (s + d, 3H, $^2J_{Pt,H} = 72.4$ Hz, PtCH₃), 0.85 (s + d, 3H, $^2J_{Pt,H} = 73.2$ Hz, PtCH₃). ^{13}C NMR (100 MHz, CD_2Cl_2): δ 57.5 (s, NCH₂), 33.2 (s, SCH₂), 0.0 (s + d, $^1J_{Pt,C} = 672.4$ Hz, PtCH₃), -0.6 (s + d, $^1J_{Pt,C} = 684.6$ Hz, PtCH₃), -12.7 (s + d, $^1J_{Pt,C} = 672.3$ Hz, PtCH₃).

4.1.9. Synthesis of [$\{PtMe_3(\mu-tpt-\kappa S)\}_4$] (12)

To a solution of **3** in acetone (5 ml) prepared from [(PtMe₃I)₄] (50.0 mg, 0.03 mmol) and AgOAc (23.0 mg,

0.14 mmol) as described above, thiophene-2-thiol (tptH) (16.2 mg, 0.14 mmol) was added. After 10 min light yellow microcrystals were formed. To complete the reaction the suspension was stirred for another 2 h. Pentane (15 ml) was added and the formed precipitate was filtrated, washed with pentane and dried in vacuo. Yield: 42 mg (87%). *Anal.* Calc. for $C_{28}H_{48}S_8Pt_4$ (1421.56): C, 23.66; H, 3.40; S, 18.04. Found: C, 23.10; H, 3.45; S, 16.24%. 1H NMR (500 MHz, CD_2Cl_2): δ 7.32 (m, 1H, *H3*), 7.28 (m, 1H, *H5*), 7.05 (m, 1H, *H4*), 1.36 (s + d, 9H, $^2J_{Pt,H} = 71.8$ Hz, PtCH₃). ^{13}C NMR (125 MHz, CD_2Cl_2): δ 134.4 (s, C2), 128.4 (s, C5), 127.0 (s, C4), 119.3 (s, C3), 7.1 (s + d, $^1J_{Pt,C} = 639.5$ Hz, PtCH₃).

4.1.10. Reactions of [$\{PtMe_3(\mu-tzt)\}_2$] (11) with 2,2'-bpy (complex 7) and 4-picoline (complex 13)

In a NMR tube to a solution of **11** (35.5 mg; 0.05 mmol) in CD_2Cl_2 (1 ml), 2,2'-bipyridine and 4-picoline (19 mg, 0.15 mmol), respectively, were added. The reactions were monitored by 1H NMR spectroscopically. Complex **7** (see above). Complex **13**: 1H NMR (500 MHz, CD_2Cl_2) δ 8.50 (m, 2H, *H2, H2'*), 7.23 (d, 2H, *H3, H3'*), 3.90 (m, 2H, NCH₂), 3.27 (m, 2H, SCH₂), 2.40 (s, 3H, CH₃) 1.11 (s + d, 3H, $^2J_{Pt,H} = 72.2$ Hz, PtCH₃), 1.01 (s + d, 3H, $^2J_{Pt,H} = 72.6$ Hz, PtCH₃), 0.90 (s + d, 3H, $^2J_{Pt,H} = 73.5$ Hz, PtCH₃).

4.2. X-ray crystallography

Single crystals of **5** suitable for X-ray diffraction measurements were obtained by recrystallization from chloroform/ether/pentane (1:1:1). Intensity data were collected on a STOE IPDS with Mo K α radiation ($\lambda = 0.71073$ Å, graphite monochromator) at 220(3) K. Absorption correction was carried out numerically ($T_{min}/T_{max} = 0.2291/0.4617$). The structure was solved by direct methods with SHELX-86 [22] and refined using full-matrix least-square routines against F^2 with SHELX-97 [23]. Non-hydrogen atoms were refined with anisotropic displacement parameters and hydrogen atoms with isotropic displacement parameters. Hydrogen atoms were found in the difference Fourier map and refined freely except the aromatic protons, which were refined according to the "riding model" (see Table 4).

4.3. Quantum chemical calculations

All DFT calculations were carried out by the GAUSSIAN98 and GAUSSIAN03 program package, respectively [24], using the hybrid functional B3LYP [25]. For the main group atoms, the basis 6-31G* was employed. The valence shell of platinum has been approximated by a split valence basis set too, for its core orbitals an effective core potential in combination with consideration of relativistic effects has been used [26]. All systems have been fully optimized without any symmetry restrictions. The resulting geometries were characterized as equilibrium structures (**5a/5b**) and

Table 4
Crystal data, data collection and refinement parameters of **5**

Empirical formula	C ₁₇ H ₂₀ N ₄ PtS
Formula weight	507.52
Crystal system/space group	monoclinic/ <i>P</i> 2 ₁ / <i>n</i>
<i>Z</i>	4
<i>a</i> (Å)	9.052(2)
<i>b</i> (Å)	18.696(3)
<i>c</i> (Å)	10.822(2)
β (°)	96.86(2)
<i>V</i> (Å ³)	1818.3(6)
ρ (g cm ⁻³)	1.854
μ (Mo K α) (mm ⁻¹)	7.836
<i>F</i> (000)	976
Scan range (°)	2.18 < θ < 25.91
Reciprocal lattice segments <i>h</i> , <i>k</i> , <i>l</i>	–11 → 11, –22 → 22, –13 → 13
Reflections collected	13970
Reflections independent [<i>R</i> _{int}]	3488 [0.0966]
Observed reflection	2903
Data/restraints/parameters	3488/0/212
Goodness-of-fit on <i>F</i> ²	1.052
<i>R</i> ₁ , <i>wR</i> ₂ [<i>I</i> > 2 σ (<i>I</i>)]	0.0329, 0.0711
<i>R</i> ₁ , <i>wR</i> ₂ (all data)	0.0437, 0.0747
Largest difference in peak and hole (e Å ⁻³)	1.142 and –1.996

transition state (**5c**), respectively, by the analysis of the force constants of normal vibrations.

Acknowledgements

Financial support from the Deutsche Forschungsgemeinschaft and gifts of chemicals by Merck (Darmstadt) is gratefully acknowledged.

Appendix A. Supplementary data

Crystallographic data (excluding structure factors) have been deposited at the Cambridge Crystallographic Data Centre as supplementary publication no. CCDC-610550 (**5**). Copies of the data can be obtained free of charge on application to CCDC, 12 Union Road, Cambridge, CB2, IEZ, UK (fax (internat.): +44 1223 336 033; e-mail: deposit@ccdc.cam.ac.uk). Tables of Cartesian coordinates of atom positions calculated for the equilibrium (**5a/5b**) and transition (**5c**) structures and figures of the molecular structures including the numbering schemes. Supplementary data associated with this article can be found, in the online version, at doi:10.1016/j.ica.2006.06.007.

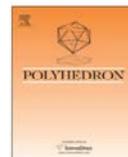
References

- [1] G. Cervantes, S. Marchal, M.J. Prieto, J.M. Pérez, V.M. González, C. Alonso, V. Moreno, *J. Inorg. Chem.* 77 (1999) 197.
- [2] P.D. Cookson, E.R.T. Tiekling, *J. Chem. Soc., Dalton Trans.* (1993) 259.
- [3] A.M. Brodie, H.D. Holden, J. Lewis, M.J. Taylor, *J. Organomet. Chem.* 253 (1983) C1.
- [4] R. Carballo, J.S. Casas, M.S. Garcia-Tasende, A. Sánchez, J. Sordo, E.M. Vázquez-López, *J. Organomet. Chem.* 525 (1996) 49.
- [5] I. Kinoshita, Y. Yasuba, K. Matsumoto, S. Ooi, *Inorg. Chim. Acta* 80 (1983) L13.
- [6] M. Kato, A. Omura, A. Toshikana, S. Kishi, Y. Sugimoto, *Angew. Chem., Int. Ed.* 41 (2002) 3183.
- [7] L. Zhang, H.-X. Zhang, C.-L. Chen, L.-R. Deng, B.-S. Kang, *Inorg. Chim. Acta* 355 (2003) 49.
- [8] M. Friedman, F.F. Bautista, *J. Agric. Food. Chem.* 43 (1995) 69.
- [9] T. Moulard, J.F. Lagorce, J.C. Thomes, C. Raby, *J. Pharm. Pharmacol.* 45 (1993) 731.
- [10] B. Rosenberg, L. Van Camp, T. Krigas, *Nature* 205 (1965) 698.
- [11] M. Carrara, T. Berti, S. D'Ancona, V. Cherchi, L. Sindellari, *Anticancer Res.* 17 (1997) 975.
- [12] G. Cervantes, M.J. Prieto, V. Moreno, *Met.-Based Drugs* 4 (1997) 9.
- [13] J. Dehand, J. Jordanov, *Chem.-Biol. Interact.* 11 (1975) 605.
- [14] W.J. Pope, S.J. Peachey, *Proc. Chem. Soc.* 23 (1907) 86.
- [15] D. Steinborn, H. Junicke, *Chem. Rev.* 100 (2000) 4283.
- [16] X. Zhu, E. Rusanov, R. Kluge, H. Schmidt, D. Steinborn, *Inorg. Chem.* 41 (2002) 2667.
- [17] H. Junicke, D. Steinborn, *Inorg. Chim. Acta* 346 (2003) 129.
- [18] J. Elguero, C. Marzin, A.R. Katritzky, P. Linda, *Tautomerism of Heterocycles*, Academic Press, New York, 1976, pp. 144, 254, 398.
- [19] Y.Yu. Vvendskii, E.D. Shtefan, R.N. Mal'yushenko, E.V. Shilkin, É.N. Deryagina, *Chem. Heterocycl. Compd.* 33 (1997) 1047.
- [20] D.E. Clegg, J.R. Hall, G.A. Swile, *J. Organomet. Chem.* 38 (1972) 403.
- [21] J.C. Baldwin, W.C. Kaska, *Inorg. Chem.* 14 (1975) 2020.
- [22] G.M. Sheldrick, SHELXS-86 Program for Crystal Structure Solution, University of Göttingen, Germany, 1997.
- [23] G.M. Sheldrick, SHELXS-97 Program for the Refinement of Crystal Structures, University of Göttingen, Germany, 1997.
- [24] M.J. Frisch, G.W. Trucks, H.B. Schlegel, G.E. Scuseria, M.A. Robb, J.R. Cheeseman, J.A. Montgomery Jr., T. Vreven, K.N. Kudin, J.C. Burant, J.M. Millam, S.S. Iyengar, J. Tomasi, V. Barone, B. Mennucci, M. Cossi, G. Scalmani, N. Rega, G.A. Petersson, H. Nakatsuji, M. Hada, M. Ehara, K. Toyota, R. Fukuda, J. Hasegawa, M. Ishida, T. Nakajima, Y. Honda, O. Kitao, H. Nakai, M. Klene, X. Li, J.E. Knox, H.P. Hratchian, J.B. Cross, C. Adamo, J. Jaramillo, R. Gomperts, R.E. Stratmann, O. Yazyev, A.J. Austin, R. Cammi, C. Pomelli, J.W. Ochterski, P.Y. Ayala, K. Morokuma, G.A. Voth, P. Salvador, J.J. Dannenberg, V.G. Zakrzewski, S. Dapprich, A.D. Daniels, M.C. Strain, O. Farkas, D.K. Malick, A.D. Rabuck, K. Raghavachari, J.B. Foresman, J.V. Ortiz, Q. Cui, A.G. Baboul, S. Clifford, J. Cioslowski, B.B. Stefanov, G. Liu, A. Liashenko, P. Piskorz, I. Komaromi, R.L. Martin, D.J. Fox, T. Keith, M.A. Al-Laham, C.Y. Peng, A. Nanayakkara, M. Challacombe, P.M.W. Gill, B. Johnson, W. Chen, M.W. Wong, C. Gonzalez, J.A. Pople, GAUSSIAN 03, Revision C.02, Gaussian, Inc., Wallingford, CT, 2004.
- [25] (a) A.D. Becke, *Phys. Rev. A* 38 (1988) 3098;
(b) A.D. Becke, *J. Chem. Phys.* 98 (1993) 5648;
(c) C. Lee, W. Yang, R.G. Parr, *Phys. Rev. B* 37 (1988) 785;
(d) P.J. Stephens, F.J. Devlin, C.F. Chabalowski, M.J. Frisch, *J. Phys. Chem.* 98 (1994) 11623.
- [26] D. Andrae, U. Häußermann, M. Dolg, H. Stoll, H. Preuss, *Theor. Chim. Acta* 77 (1990) 123.



Contents lists available at ScienceDirect

Polyhedron

journal homepage: www.elsevier.com/locate/poly

Synthesis, structures and *in vitro* cytotoxicity studies of platinum(IV) complexes with *N,S* and *S,S* heterocyclic ligands

Cornelia Vetter^a, Goran N. Kaluđerović^{a,b}, Reinhard Paschke^c, Santiago Gómez-Ruiz^d, Dirk Steinborn^{a,*}

^a Institut für Chemie – Anorganische Chemie, Martin-Luther-Universität Halle-Wittenberg, D-06120, Halle, Kurt-Mothes-Straße 2, Germany

^b Department of Chemistry, Institute of Chemistry, Technology and Metallurgy, University of Belgrade, Studentski trg 14, 11000 Belgrade, Serbia

^c Biozentrum, Martin-Luther-Universität Halle-Wittenberg, D-06120, Halle, Weinbergweg 22, Germany

^d Departamento de Química Inorgánica y Analítica, ESCET, Universidad Rey Juan Carlos, 28933 Móstoles, Madrid, Spain

ARTICLE INFO

Article history:

Received 15 May 2009

Accepted 6 August 2009

Available online 13 August 2009

Keywords:

Platinum(IV) complexes

N,S and *S,S* heterocyclic ligands

X-ray diffraction analyses

In vitro cytotoxic studies

DFT calculations

ABSTRACT

Reactions of [(PtMe₃)₄] (2) with the sodium salts of the *N,S* and *S,S* heterocycles *S*-DH (pyridine-2-thione, pytH; pyrimidine-2-thione, pymtH; thiazoline-2-thione, tztH; thiophene-2-thiol, tptH) resulted in the formation of the dinuclear complexes [(PtMe₃)₂(μ-*S*-D)]₂ (*S*-D = pyt, 3; pymt, 4; tzt, 5) and the tetranuclear complex [(PtMe₃)₄(μ₃-tpt)]₄ (6), respectively. Single crystal X-ray diffraction analyses of 3 and 4 exhibited dinuclear complexes having a central [Pt₂(μ-*S*)₂] core. The platinum atoms are octahedrally coordinated by three methyl ligands and the bridging 1κ*N*,1:2κ²*S* heterocyclic ligands. The two heterocyclic rings are face-to-face (*cis*) arranged, indicating stabilization through π-π stacking. The X-ray diffraction analysis of 6 confirmed a tetranuclear [Pt₄S₄] heterocubane structure. Each platinum atom is distorted octahedrally coordinated by three methyl ligands in *facial* arrangement and three μ₃-bridging sulfur atoms. DFT calculations exhibited that the formation of the tetranuclear complex 6 can be mainly attributed to the weak coordination tendency of the thiophene *S* atoms of the tpt ligands to the trimethylplatinum(IV) unit. *In vitro* cytotoxic studies of the complexes 3–5 using five different tumor cell lines (8505C, A253, A549, A2780, DLD-1) revealed moderate to high cytotoxic activities. The most active compound is [(PtMe₃)₂(μ-tzt)]₂ (5) with IC₅₀ values of 0.5–1.2 μM on investigated cell lines, which is comparable to cisplatin or even better.

© 2009 Elsevier Ltd. All rights reserved.

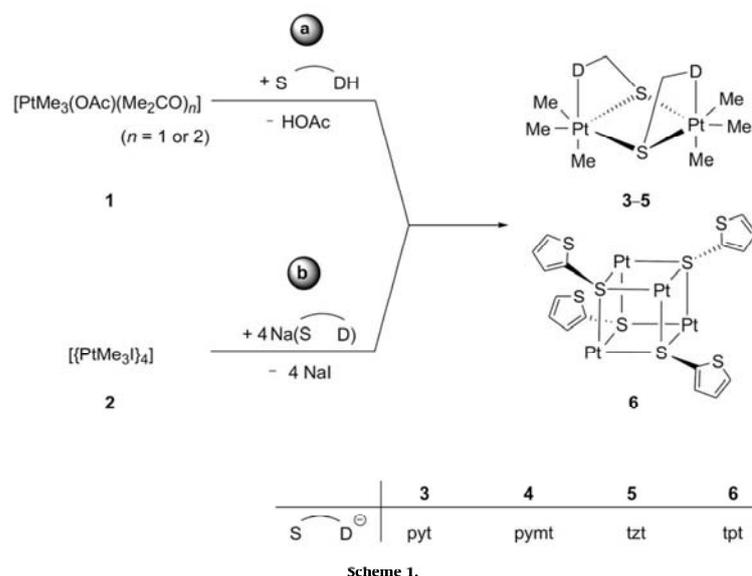
1. Introduction

The biological activity of nitrogen and sulfur containing heterocycles like pyridine-2-thione or thiazoline-2-thione was reported in several cases. It has been shown that such compounds can act as enzyme inhibitors in biological processes [1,2]. This potential bioactivity and also their numerous different binding modes in metal complexes increased the interest in this class of ligands, in particular in transition metal complexes using metals that possess also biological activity [3–8]. The combination of two potentially bioactive building blocks can increase the effect of the respective application. Thus, it was reported that Au(I) complexes with pyrimidine-2-thiolato and pyridine-2-thiolato ligands possess antiarthritic activity [9]. In this context also platinum complexes are of high interest, since Rosenberg discovered in 1965 the cancerostatic activity of cisplatin [10,11]. In the following time numerous Pt(II) complexes were synthesized and tested for their antitumoral activity among them also complexes with pyridine-2-thione ligands [12]. Cervantes synthesized pyridine-2-thiolato

and pyrimidine-2-thiolato platinum(III) complexes that showed significant anticancer activity [13]. Also of interest for this type of studies are Pt(IV) complexes. It is believed that they act mainly as prodrugs, which are reduced to Pt(II) complexes, although it has been shown that Pt(IV) complexes can interact with DNA without reduction leading to cancerostatic effects [14,15]. The kinetic inertness of Pt(IV) complexes may reduce the reactivity including toxic side effects compared to Pt(II) complexes. In this respect the focus of our research work has been on investigations of the synthesis and characterization of trimethylplatinum(IV) complexes with bioactive ligands and their cancerostatic properties. Thus, pyridine-2-thione (pytH), pyrimidine-2-thione (pymtH), thiazoline-2-thione (tztH) and thiophene-2-thiol (tptH) were found to react with [PtMe₃(OAc)(Me₂CO)₂] (1) under deprotonation yielding dinuclear and tetranuclear complexes 3–6, respectively (Scheme 1, route a). NMR and ESI-MS investigations gave proof of their constitution, both of coordination mode of the *N,S* and *S,S* heterocycles and of di- (3–5) and tetranuclear (6) nature of the complexes [16]. Here we report on a more simple way of synthesis for these complexes, on their solid-state structures as well as on DFT calculations to get insight into the formation of dinuclear versus tetranuclear complexes. Furthermore we investigated cytotoxic properties to

* Corresponding author.

E-mail address: dirk.steinborn@chemie.uni-halle.de (D. Steinborn).



testify if the combination of a platinum(IV) complex and a potentially bioactive ligand leads to an increased antitumor activity.

2. Results and discussion

Reaction of the sodium salts Na(S-D) (S-D = pyt; pymt; tzt; tpt) in methanol with a solution of [(PtMe₃)₄] (**2**) in methylene chloride leads to the formation of the dinuclear [(PtMe₃)₂(μ-S-D)₂] (S-D = pyt, **3**; pymt, **4**; tzt, **5**) and tetranuclear [(PtMe₃)₄(μ₃-tpt)₄] (**6**) complexes (Scheme 1, route **b**). ¹H NMR spectroscopic investigations exhibited the identity of complexes **3–6** with those obtained via route **a**. Although the yields of **3–6** via route **b** (16–52%) are lower than those of route **a** (43–93%), the route **b** is superior because the syntheses are faster and do not require anaerobic conditions. Furthermore, via route **b** we were able to yield crystals of complexes **3**, **4** and **6** suitable for X-ray diffraction analyses.

2.1. Structures of [(PtMe₃)₂(μ-pyt)₂] (**3**), [(PtMe₃)₂(μ-pymt)₂] (**4**) and [(PtMe₃)₄(μ₃-tpt)₄] (**6**)

Suitable crystals of **3** and **4** for X-ray diffraction analyses were obtained from solutions in acetone by slow evaporation of the solvent. In crystals of [(PtMe₃)₂(μ-pyt)₂] (**3**) isolated molecules were found without unusual interactions (shortest intermolecular distance between non-hydrogen atoms: C7···C7' 3.65 Å). Complex **3** crystallizes as racemate in the space group *P*₂₁/*c*. The molecular structure of one enantiomer is shown in Fig. 1. Selected bond lengths and angles are given in the figure caption. In crystals of complex **4** were also found isolated dinuclear molecules without unusual interactions (shortest intermolecular distance between non-hydrogen atoms: C20···N4' 3.23 Å). [(PtMe₃)₂(μ-pymt)₂] (**4**) crystallizes in the chiral space group *P*₂, having two structurally very similar symmetry independent molecules in the asymmetric unit. One of them is shown in Fig. 2. The other one is approximately the mirror image. Selected bond lengths and angles are given in the figure caption.

Molecules of the complexes **3** and **4** are dinuclear, the primary donor sets of the octahedrally coordinated platinum atoms

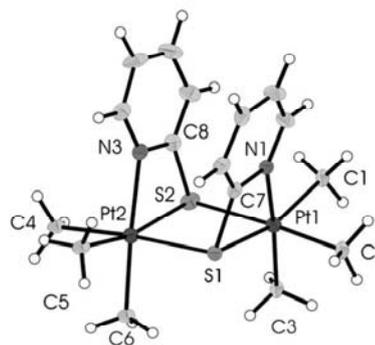


Fig. 1. Molecular structure of one enantiomer of [(PtMe₃)₂(μ-pyt)₂] (**3**). The displacement ellipsoids are drawn at the 30% probability level. Selected bond lengths (in Å) and angles (in °): Pt1–C1 2.267(8), Pt1–C2 2.061(7), Pt1–C3 2.079(7), Pt2–C4 2.196(7), Pt2–C5 2.127(8), Pt2–C6 2.065(7), Pt1–S1 2.530(2), Pt1–S2 2.488(2), Pt2–S1 2.490(2), Pt2–S2 2.551(3), Pt1–N1 2.159(6), Pt2–N3 2.174(6), C7–S1 1.758(8), C8–S2 1.777(8), Pt1–S1–Pt2 94.87(7), Pt1–S2–Pt2 94.39(8), S1–Pt1–S2 85.45(7), S1–Pt2–S2 84.94(7), N1–Pt1–C3 171.6(3), N1–Pt1–S1 66.3(2), N3–Pt2–C6 170.8(3), N3–Pt2–S2 66.0(2).

[PtC₃NS₂] are built up by three methyl ligands in *facial* arrangement and μ-pyridine-2-thiolato-1κ^N,1:2κ²S ligands and μ-pyrimidine-2-thiolato-1N,1:2κ²S ligands, respectively. The central [Pt₂(μ-S)₂] cores are slightly hinged (Pt1–S1···S2–Pt2 torsion angle: 173.91(9)°, **3**; –169.91(8)°/172.20(8)°, **4**). The two *N,S* heterocyclic ligands are face-to-face (*cis*) arranged,¹ thus the dinuclear molecules exhibit C₂ symmetry in rough approximation. The distances between the heterocyclic ligands (3.4 Å, **3**; 3.4/3.5 Å, **4**) and the angles between the centroid-centroid vectors and the ring normals (15.2°, **3**; 16.7/13.9°, **4**) indicate a stabilization through π–π stacking [17].

¹ Here and hereafter “*cis*” and “*trans*” refer to a configuration having the heterocyclic rings on the same and opposite sides, respectively, of the [Pt₂(μ-S)₂] core.

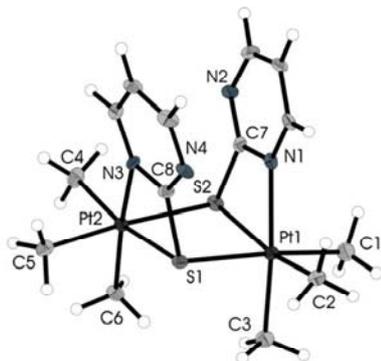


Fig. 2. Molecular structure of one of the two symmetry independent molecules of $[(\text{PtMe}_3)_2(\mu\text{-pymt})_2]$ (**4**). The displacement ellipsoids are drawn at the 30% probability level. Selected bond lengths (in Å) and angles (in $^\circ$) (values for the two symmetric independent molecules are separated by a slash): Pt1–C1 2.060(7)/2.066(6), Pt1–C2 2.032(6)/2.047(7), Pt1–C3 2.049(6)/2.044(6), Pt2–C4 2.047(6)/2.063(7), Pt2–C5 2.048(6)/2.047(6), Pt2–C6 2.027(6)/2.042(7), Pt1–S1 2.465(2)/2.506(2), Pt1–S2 2.515(2)/2.500(2), Pt2–S1 2.496(2)/2.512(2), Pt2–S2 2.506(2)/2.498(2), Pt1–N1 2.164(5)/2.149(5), Pt2–N3 2.150(5)/2.146(5), C7–S2 1.745(7)/1.763(6), C8–S1 1.760(6)/1.748(7), Pt1–S1–Pt2 92.99(5)/92.13(5), Pt1–S2–Pt2 91.58(5)/92.32(6), S1–Pt1–S2 87.48(5)/87.54(6), S1–Pt2–S2 87.02(5)/87.46(6), C3–Pt1–N1 170.6(2)/170.1(2), C6–Pt2–N3 170.1(2)/171.1(3), N1–Pt1–S2 66.3(1)/66.7(2), N3–Pt2–S1 66.9(1)/66.6(2).

Both in **3** and **4** the chelating coordination of the heterocycles leads to the formation of strained Pt–N–C–S four membered rings (S–Pt–N 66.0(2)–66.9(1) $^\circ$) giving rise to greater deviations from the ideal octahedral coordination of the platinum atoms (angles between *cis* arranged ligands: 66.0(2)–105.2(2) $^\circ$). The bridging platinum–sulfur bonds are between 2.465(2) and 2.551(3) Å, whereas some of them belong to the longest ones described for Pt(IV)–(μ -S) bonds so far (median 2.490 Å, lower/higher quartile 2.477/2.513 Å, $n = 41$; n – number of observations) [18]. This is in accord with the high *trans* influence of the methyl ligands [19]. As expected, deprotonation and S coordination of the heterocycles in complexes **3** and **4** give rise to quite long C–S bonds (1.758(8)/1.777(8) Å, **3**; 1.745(7)–1.763(6) Å, **4**) as revealed by the comparison with the C–S bond length in uncoordinated pyridine-2-thione (1.700 Å) [20].

Yellow–green single crystals of $[(\text{PtMe}_3)_4(\mu_3\text{-tpt})_4]$ (**6**) were obtained from acetone solutions. The complex crystallizes in isolated molecules without unusual interactions (shortest intermolecular distances between non-hydrogen atoms: C9...S8' 3.34 Å) in the space group $P2_1/n$. The X-ray diffraction analysis confirms the tetranuclear $[\text{Pt}_4\text{S}_4]$ heterocubane structure of **6** which was already derived from negative ESI measurements [16]. The molecular structure of $[(\text{PtMe}_3)_4(\mu_3\text{-tpt})_4]$ (**6**) is shown in Fig. 3. Selected bond lengths and angles are given in the figure caption. Each platinum atom [PtC₃S₃] is coordinated octahedrally by three methyl ligands in *facial* configuration and three μ_3 -bridging sulfur atoms. The C–Pt–C angles (85.5(4)–90.2(3) $^\circ$) are close to the rectangular angle. However, the S–Pt–S angles (78.40(6)–79.90(6) $^\circ$) are severely deviated from 90 $^\circ$ resulting in the formation of a distorted cubane skeleton. The Pt–S (2.466(2)–2.540(2) Å) and Pt–C bonds (2.045(8)–2.077(9) Å) are as long as those in the structurally analogous thiolato complexes $[(\text{PtMe}_3)_4(\mu_3\text{-SR})_4]$ (R = Me, Ph) [21–23].

2.2. Quantum chemical calculations

DFT calculations using the hybrid functional B3LYP and high-quality 6-311G(d,p) basis sets for all main group atoms as well as a pseudopotential considering relativistic effects and a double

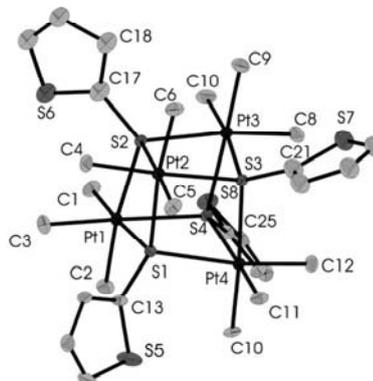


Fig. 3. Molecular structure of $[(\text{PtMe}_3)_4(\mu_3\text{-tpt})_4]$ (**6**). Hydrogen atoms are omitted for clarity. The displacement ellipsoids are drawn at the 30% probability level. Selected bond lengths (in Å) and angles (in $^\circ$): Pt1–S1 2.476(2), Pt1–S2 2.537(2), Pt1–S4 2.501(2), Pt2–S1 2.523(2), Pt2–S2 2.481(2), Pt2–S3 2.507(2), Pt3–S2 2.513(2), Pt3–S3 2.540(2), Pt3–S4 2.476(2), Pt4–S1 2.516(2), Pt4–S3 2.466(2), Pt4–S4 2.533(2), Pt1–C1 2.059(8), Pt1–C2 2.061(8), Pt1–C3 2.071(8), Pt2–C4 2.064(8), Pt2–C5 2.058(8), Pt2–C6 2.052(8), Pt3–C7 2.057(9), Pt3–C8 2.077(9), Pt3–C9 2.057(8), Pt4–C10 2.053(7), Pt4–C11 2.052(8), Pt4–C12 2.045(8), S1–C13 1.741(8), S2–C17 1.76(1), S3–C21 1.77(1), S4–C25 1.763(7), Pt1–S1–Pt2 99.63(6), Pt1–S1–Pt4 100.51(7), Pt1–S4–Pt4 99.37(6), Pt1–S2–Pt2 99.14(7), Pt1–S2–Pt3 99.05(7), Pt1–S4–Pt3 101.06(7), Pt2–S1–Pt4 99.34(6), Pt2–S2–Pt3 100.49(7), Pt2–S3–Pt3 99.05(7), Pt2–S3–Pt4 101.16(7), Pt3–S3–Pt4 99.93(6), Pt3–S4–Pt4 99.84(6), S1–Pt1–S2 79.54(6), S1–Pt1–S4 79.77(6), S1–Pt2–S2 79.72(6), S1–Pt2–S3 78.42(6), S1–Pt4–S3 79.32(6), S1–Pt4–S4 78.40(6), S2–Pt1–S4 78.60(6), S2–Pt2–S3 79.90(6), S2–Pt3–S4 79.53(6), S2–Pt3–S3 78.67(6), S3–Pt3–S4 78.87(6), S3–Pt4–S4 79.18(6).

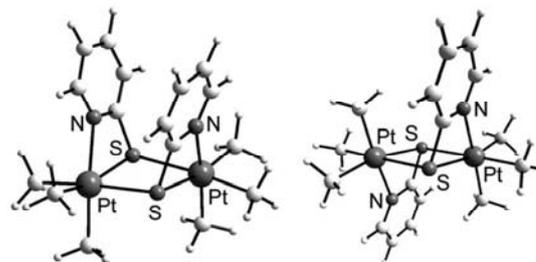


Fig. 4. Calculated equilibrium structures of the dinuclear complexes $[(\text{PtMe}_3)_2(\mu\text{-pymt})_2]$ having face-to-face (*cis*) arranged (**3a***, left) and *trans* arranged heterocyclic rings (**3b***, right).

ζ basis set for Pt (see Experimental) were performed to get insight into the *cis* versus *trans* arrangement of the heterocyclic rings in the dinuclear complexes and into the formation of dinuclear versus tetranuclear complexes.

2.2.1. Dinuclear complexes

At first calculations of dinuclear complexes of the type $[(\text{PtMe}_3)_2(\mu\text{-S-D})_2]$ bearing all the four *N,S* and *S,S* heterocyclic ligands under discussion in this manuscript both with a *cis* (S–D = pyt, **3a***; pymt, **4a***; tzt, **5a***; tpt, **6a***)² and a *trans* arrangement (S–D = pyt, **3b***; pymt, **4b***; tzt, **5b***; tpt, **6b***) of the heterocyclic rings were performed. Selected structures and structural parameters are shown in Figs. 4–6 and in Table 1. The relative energies are given in Table 2. As the comparison of the structural parameters of **3a*** and **4a*** with those in crystals of **3** and **4** reveals there is

² Here and in the following the stars point to calculated structures.

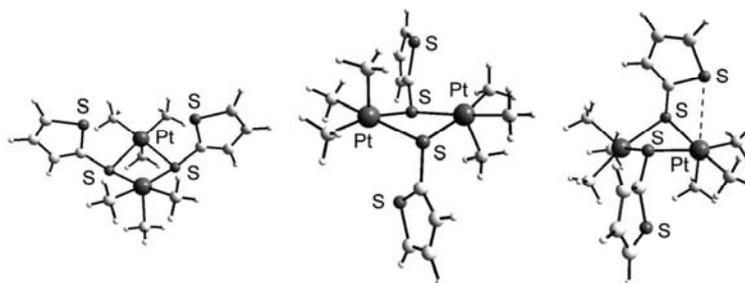


Fig. 5. Calculated equilibrium structures of the dinuclear complexes $[(\text{PtMe}_3)_2(\mu\text{-tpt})_2]$ having *cis* (**6a***, left) and *trans* arranged thiophene rings (**6b***/**6c***, middle/right). In **6c*** the Pt...S distance of 3.22 Å is shown by a dashed line.

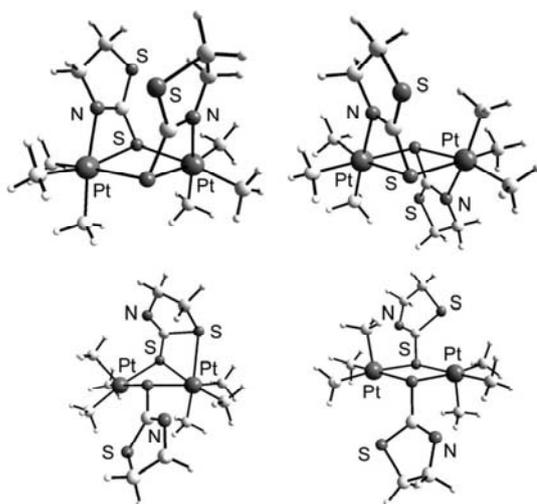


Fig. 6. Calculated equilibrium structures of dinuclear complexes $[(\text{PtMe}_3)_2(\mu\text{-tzt})_2]$ having *S,N* coordinated ligands with *cis* and *trans* arranged heterocyclic rings (**5a***/**5b***, upper row), one *S,S* and one $\mu\text{-S}$ coordinated ligand (**5c***, below left) as well as two $\mu\text{-S}$ coordinated ligands (**5d***, below right).

a good agreement of the calculated structures (representing the structures in the gas phase) and the experimentally found structures in crystals.

The deprotonated *S,N* heterocyclic species (pyt, pymt, tzt) were found to yield dinuclear complexes of the type $[(\text{PtMe}_3)_2(\mu\text{-S-D})_2]$ having $\mu\text{-S-N-1}\kappa\text{N,1:2}\kappa^2\text{S}$ coordinated ligands (Figs. 4 and 6). Those with *cis* arranged heterocyclic rings (**3a***, **4a***, **5a***) proved to be slightly more stable (1.7–2.9 kcal/mol) than those with *trans* arranged ones (**3b***, **4b***, **5b***). This is in accord with the *cis* arrangement of the ring systems in crystals of **3** and **4**. Apart from complex **5a*** the complexes with *cis* and *trans* arranged heterocyclic rings are of C_2 and C_i symmetry, respectively, in very good approximation.³ In the case of complex **5a*** the C_2 symmetry is destroyed by the (distorted) envelope conformation of the non-saturated heterocyclic rings. But the C_2 symmetric structure was found to be only 0.4 kcal/mol less stable.

³ The optimizations were performed without any symmetry restrictions. In the case of complexes **4a*** and **4b***, additionally, complexes having the precise C_2 and C_i symmetry, respectively, were calculated resulting in the same energies.

In principle, the thiophene-2-thiolate anion (tpt^-) could act as a *S,S* chelate forming analogous complexes having $\mu\text{-S-S'-1}\kappa\text{S',1:2}\kappa^2\text{S}$ coordinated ligands. But all calculations failed to localize corresponding local minima on energy hypersurface. Instead of this, complexes **6a*** and **6b*** were obtained in which the thiophene S atoms are not coordinated to platinum (Fig. 5). Thus, complexes were obtained in which the Pt atoms exhibit the coordination number five. As for the other complexes, the complex with *cis* arranged heterocyclic rings is slightly more stable (1.6 kcal/mol) than that with a *trans* arrangement. In these two complexes the two thiophene rings lie in a plane (**6a***) and nearly in a plane (**6b***, interplanar angle between the thiophene planes: 16.8°), respectively. Furthermore, another equilibrium structure (**6c***) could be localized in which one of the *tpt* ligands is rotated (interplanar angle: 85.6°) and bent towards one of the five-coordinated Pt atom (Pt–S–C 92.9°) such that a Pt...S_{thiophene} distance of 3.22 Å results (Fig. 5). This gives rise to a very strong folding of the central $[\text{Pt}_2(\mu\text{-S})_2]$ core along the S...S' vector (Pt–S...S'–Pt' –131.2°) which is already highly hinged in complexes **6a***/**6b*** (150.4/154.6°). But the energy of **6c*** is 4.3 kcal/mol higher than that of **6a***.

Now we come back to complexes $[(\text{PtMe}_3)_2(\mu\text{-tzt})_2]$ (**5a***/**5b***). Trying to localize a complex having *S,S* chelating ligands, we succeeded only for one ligand. In complex **5c*** (Fig. 6) one ligand exhibits the coordination mode $\mu\text{-tzt-1}\kappa\text{S',1:2}\kappa^2\text{S}$ and the other one is only coordinated via the exocyclic S atom ($\mu\text{-tzt-1:2}\kappa^2\text{S}$). Thus, one Pt atom is 6- and the other one 5-coordinated. As for complex **6c*** the $[\text{Pt}_2(\mu\text{-S})_2]$ core in **5c*** is strongly hinged (Pt–S...S'–Pt' –137.1°). Furthermore, an equilibrium structure **5d*** was obtained in which none of the thiazoline S atoms is coordinated to Pt (coordination mode of both ligands: $\mu\text{-tzt-1:2}\kappa^2\text{S}$). **5d*** exhibiting approximately C_i symmetry. As expected from the coordinative unsaturation of the Pt centers, both **5c*** and **5d*** are much higher in energy (22.9/26.8 kcal/mol) than the most stable complex having *S,N* chelating ligands (**5a***).

2.2.2. Tetranuclear complexes

At first the tetranuclear complex $[(\text{PtMe}_3)_4(\mu_3\text{-tpt})_4]$ (**6d***) was calculated, see its structure in Fig. 7. The structural parameters of **6d*** (Table 3) were found in good agreement with those of complex **6**. Greater deviations were found in the relative positions of the thiophene rings. The interplanar angles between them range from 62 to 84° in **6d*** and from 55 to 89° in crystals of **6**. Because it can be assumed that a rotation around the S–C bond does not cost much energy, this difference might be caused by packing effects in crystals of **6**. For comparison, also the tetranuclear complex $[(\text{PtMe}_3)_4(\mu_3\text{-pymt})_4]$ (**4c***) was calculated. As shown in Fig. 7 and Table 3 its structure is very close to that of **6d***/**6**. Even the relative positions of the planes of the pyrimidine rings (interplanar angles: 59–83°) were found to be very close to those of **6d***.

Table 1

Structural parameters (distances in Å, angles in °) of calculated structures in dinuclear complexes $[(\text{PtMe}_3)_2(\mu\text{-S}-\text{D})_2]$. For comparison the corresponding values (without standard deviations) of complexes **3** and **4** are included.

Complex	sym ^a	D/D' ^b	Pt–μ-S	Pt–D/Pt'–D'	μ-S–Pt–μ-S'/μ-S'–Pt'–μ-S	μ-S–Pt–D/μ-S'–Pt'–D'	Pt–μ-S–C/Pt'–μ-S'–C'	Pt–S S'–Pt'
3a*	C ₂	N/N	2.610/2.653	2.256/2.256	85.3/85.3	63.8/63.8	79.0/79.0	168.8
3			2.488–2.551	2.159/2.174	84.9/85.5	66.0/66.3	78.7/78.7	173.9
3b*	C _i	N/N	2.639/2.658	2.241/2.241	84.2/84.2	63.9/63.9	78.2/78.2	180.0
4a*	C ₂	N/N	2.623/2.648	2.250/2.250	85.1/85.1	63.8/63.8	79.3/79.3	168.2
4			2.496–2.515	2.146–2.164	87.0–87.5	66.3–66.9	79.1–79.8	–169.9/172.2
4b*	C _i	N/N	2.644/2.648	2.249/2.249	84.1/84.1	63.9/63.9	79.0/79.0	180.0
5a*	N/N	N/N	2.621–2.731	2.256/2.257	84.8/84.7	62.6/62.6	75.4/75.5	165.6
5b*	C _i	N/N	2.650/2.719	2.260/2.261	83.5/83.5	62.8/62.8	75.1/75.1	179.9
5c*	S/–	S/–	2.572–2.665	2.674/>3.5	79.2/80.9	69.0/–	83.9/121.4	–137.1
5d*	C _i	–/–	2.575/2.590	>3.5	82.1/82.1	–	106.0–111.4	179.8
6a*	C _{2v}	–/–	2.558	>3.5	80.9/80.9	–	109.5	150.4
6b*	–/–	–/–	2.533–2.586	>3.5	80.8/81.0	–	107.0–115.7	154.6
6c*	(S/–)	(S/–)	2.517–2.611	(3.22)/>3.5	80.4/81.6	61.9/–	92.9/108.5–116.8	–131.2

^a Symmetry (approximately).

^b D and D' refers to the donor atoms bound to Pt and Pt', respectively.

Table 2

Coordination modes of ligands, coordination numbers of Pt (CN(Pt)) relative energies (E_{rel} in kcal/mol) and approximate symmetries of calculated dinuclear and tetranuclear complexes with *N,S* and *S,S* heterocyclic ligands.

Complex	Ligand ^a	Coordination mode	CN(Pt)	E_{rel}	Symmetry
3a*	pyt (<i>cis</i>)	2 × μ-S–N	6/6	0	C ₂
3b*	pyt (<i>trans</i>)	2 × μ-S–N	6/6	2.0	C _i
4a*	pymt (<i>cis</i>)	2 × μ-S–N	6/6	0	C ₂
4b*	pymt (<i>trans</i>)	2 × μ-S–N	6/6	1.7	C _i
4c*	pymt	4 × μ ₃ -S	4 × 6	13.8	
5a*	tzt (<i>cis</i>)	2 × μ-S–N	6/6	0	
5b*	tzt (<i>trans</i>)	2 × μ-S–N	6/6	2.9	C _i
5c*	tzt	μ-S–S + μ-S	6/5	22.9	
5d*	tzt	2 × μ-S	5/5	26.8	C _i
6a*	tpt (<i>cis</i>)	2 × μ-S	5/5	0	C _{2v}
6b*	tpt (<i>trans</i>)	2 × μ-S	5/5	1.6	
6c*	tpt (<i>trans</i>)	2 × μ-S	5/5	4.3	
6d*	tpt	4 × μ ₃ -S	4 × 6	–30.9	

^a In parentheses the relative orientation of the heterocyclic rings is given.

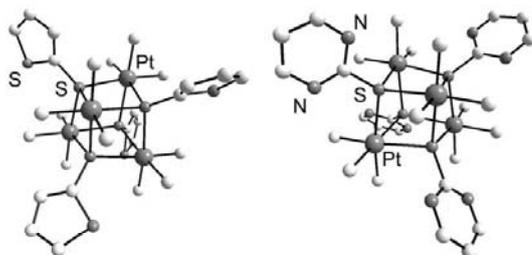


Fig. 7. Calculated equilibrium structures of tetranuclear complexes $[(\text{PtMe}_3)_4(\mu_3\text{-tpt})_4]$ (**6d***, left) and $[(\text{PtMe}_3)_4(\mu_3\text{-pymt})_4]$ (**4c***, right).

Table 3

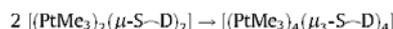
Structural parameters (distances in Å, angles in °) of calculated structures in tetranuclear complexes $[(\text{PtMe}_3)_4(\mu_3\text{-S}-\text{D})_4]$. For comparison the values (without standard deviations) of complex **6** are included.

Complex	Ligand	Pt–S	S–Pt–S'	Pt–S–Pt'	Pt–S–C	\angle_{ip} ^a
6d*^b	tpt	2.600–2.672	77.9–79.1	99.5–101.5	115.2–119.4	62–84
6	tpt	2.466–2.537	78.4–79.9	99.1–101.2	113.8–121.6	55–89
4c*	pymt	2.621–2.664	77.1–78.6	99.9–101.7	113.6–120.6	59–83

^a \angle_{ip} = Interplanar angles between the heterocyclic rings.

^b All values given refer to μ₃-S atoms.

The energies of the reactions



emphasize whether the dinuclear or the tetranuclear complexes are thermodynamically more stable. In the case of the pyrimidine-2-thiolato complexes the energy of +13.8 kcal/mol ($2 \mathbf{4a}^* \rightarrow \mathbf{4c}^*$) clearly indicates that the dinuclear complex **4a*** is thermodynamically more stable than the tetranuclear complex **4c***. In the case of the thiophene-2-thiolato complexes the energy of –30.9 kcal/mol ($2 \mathbf{6a}^* \rightarrow \mathbf{6d}^*$) gives proof that the tetranuclear complex **6d*** is the thermodynamically most stable one. Both these results are in full accord with the experimental findings. Summarizing, the formation of tetranuclear complex **6** can be attributed to the weak coordination tendency of the thiophene sulfur atoms in the thiophene-2-thiolato ligands to the trimethylplatinum(IV) unit.

2.3. In vitro cytotoxic studies

The *in vitro* anticancer activities of the complexes $[(\text{PtMe}_3)_2(\mu\text{-S}-\text{N})_2]$ (S–N = pyt, **3**; pymt, **4**; tzt, **5**) as well as those of the requisite neutral uncoordinated *N,S* heterocycles pytH, pymtH and tztH and the platinum(IV) complex $[\text{PtMe}_3(\text{bpy})]$ (**7**), for comparison, was investigated. The starting complex $[(\text{PtMe}_3)_4]$ (**2**) and $[(\text{PtMe}_3)_4(\mu_3\text{-tpt})_4]$ (**6**) could not be included in the tests due to insufficient solubilities in DMSO requested for SRB assay. The compounds were tested for cytotoxic activities in the human tumor cell lines anaplastic thyroid cancer 8505C, head and neck tumor A253, lung carcinoma A549, ovarian cancer A2780 and colon carcinoma DLD-1, respectively. The IC₅₀ data along with those of cisplatin are collected in Table 4.

The activities of the uncoordinated *N,S* heterocycles exceed the measurement range, while $[\text{PtMe}_3(\text{bpy})]$ (**7**) exhibits moderate activity towards all five cell lines. The corresponding platinum(IV) complexes **3–5** show significant activities. The best results could be observed for complex **5**. The IC₅₀ values are in a range of 0.5–1.3 μM and even lower than those of cisplatin towards all investi-

Table 4

Results of the cytotoxicity assay on the five tumor cell lines 8505C (anaplastic thyroid carcinoma), A253 (head and neck tumor), A549 (lung carcinoma), A2780 (ovarian carcinoma), DLD-1 (colon carcinoma) represented by the IC_{50} [μM]^{a,b}.

compound	IC_{50} [μM]				
	8505C	A253	A549	A2780	DLD-1
pytH	>125	>125	>125	>125	>125
pymtH	>125	>125	>125	>125	>125
tztH	>125	>125	>125	>125	>125
[PtMe ₃](bpy)] (7)	11.56 ± 1.62	7.38 ± 0.71	8.22 ± 1.45	9.43 ± 0.97	18.36 ± 2.26
3	8.42 ± 1.19	7.87 ± 1.21	7.54 ± 2.47	2.12 ± 0.32	2.48 ± 0.35
4	7.98 ± 0.34	7.48 ± 0.13	7.55 ± 0.34	1.10 ± 0.03	12.55 ± 0.95
5	1.31 ± 0.08	1.32 ± 0.20	1.16 ± 0.19	0.53 ± 0.01	1.18 ± 0.04
cisplatin	5.02 ± 0.23	0.81 ± 0.02	1.51 ± 0.02	0.55 ± 0.03	5.14 ± 0.12
[PtMe ₃](pzH)] ^c	35.03 ± 0.86	20.95 ± 0.94	36.22 ± 0.75	4.82 ± 0.31	37.04 ± 0.56
[K(18C6)][(PtMe ₃) ₂ (μ -I)(μ -pz)] ^c	1.96 ± 0.15	1.13 ± 0.03	2.30 ± 0.03	1.49 ± 0.07	2.51 ± 0.14

^a Mean values ± SD (standard deviation) from three experiments.

^b The IC_{50} values of dinuclear complexes are related to the entire complex containing two Pt atoms.

^c Data taken from Ref. [24].

gated cell lines except A253 (**5**: 1.3 μM ; cisplatin: 0.8 μM). For the cisplatin resistant cell lines anaplastic thyroid cancer 8505C and the colon carcinoma DLD-1 the activity of **5** is ca. four times higher than that of cisplatin (Table 4). [(PtMe₃)₂(μ -pyt)]₂ (**3**) and [(PtMe₃)₂(μ -pymt)]₂ (**4**) possess similar anticancer activities, except towards DLD-1. Whereas **3** shows a significant *in vitro* anticancer activity, which is even higher than that of cisplatin (**3**: 2.5 μM ; cisplatin: 5.1 μM), **4** is only moderate active (12.6 μM). Furthermore both complexes possess good activities towards A2780, however the IC_{50} values are lower than that of cisplatin (**4**: 1.1 μM ; **3**: 2.1 μM versus cisplatin: 0.6 μM). Since the other IC_{50} values are significant higher (7.5–12.6 μM) it could be stated that complexes **3** and **4** show selective activity on DLD-1 (**3**) and A2780 (**3**, **4**). Compared to **7** the cytotoxicity of the dinuclear complexes is higher in all cases, except for **3** and **4** towards the cell line A 253 (**3**: 7.9 μM ; **4**: 7.5 μM versus **7**: 7.4 μM). Complex **5** shows the highest increase of the *in vitro* anticancer activity and is about eighteen times more potent than [PtMe₃](bpy)] (**7**) on A2780 (**5**: 0.5 μM ; **7**: 9.4 μM).

3. Conclusions

From the experimental findings and the DFT calculations it can be drawn the conclusion that in reactions of [(PtMe₃)₄] (**2**) with sodium salts Na(S–D) (S–D = N or S) having an *N,S* donor set dinuclear complexes of the type [(PtMe₃)₂(μ -S–N–1 κ N,1:2 κ^2 S)]₂ (S–N–pyt, **3**; pymt, **4**; tzt, **5**) are formed as clearly exhibited by the X-ray structural analyses of complexes **3** and **4** and by the calculations of the tzt complexes where those having *N,S*-coordinated ligands were found at least 20 kcal/mol more stable than those with purely S-coordinated ligands. In full agreement with the solid-state structures of complexes **3** and **4**, the DFT calculations showed, that the face-to-face arrangement of the heterocyclic rings (“*cis*”-configuration) is energetically slightly favored over the *trans* arrangement. On the other hand, [(PtMe₃)₄] (**2**) reacted with Na(tpt) yielding the tetranuclear complex [(PtMe₃)₄(μ_3 -tpt)]₄ (**6**) having monodentately S-bound ligands as exhibited by the X-ray structural analysis and by DFT calculations. Thus, the interplay between the dinuclear (**3–5**) and tetranuclear (**6**) complexes can be understood in terms of the only weak coordination tendency of the thiophene sulfur atoms in the tpt ligands to the trimethylplatinum(IV) unit.

Cytotoxic studies of the dinuclear complexes **3–5** revealed moderate to high activities towards the tested cell lines, whereas [(PtMe₃)₂(μ -tzt)]₂ (**5**) showed the highest antiproliferative activity, which was found to be comparable or in the case of cisplatin resistant cell lines (DLD-1, 8505C) even higher than that of cisplatin. In contrast to it, the non-coordinated heterocycles S–DH (D = N or S) did not show any antitumoral activities in concentrations <125 μM

against the cell lines tested. Interestingly, all dinuclear trimethylplatinum(IV) complexes investigated so far, namely the complexes **3–5** and the ionic complex [K(18C6)][(PtMe₃)₂(μ -I)(μ -pz)]₂ [24] (pzH = pyrazole) proved to have a moderate to high activity that was not found for mononuclear complexes [PtMe₃](bpy)] (**7**) and [PtMe₃](pzH)]₂ [24] (Table 4). Complex **5** seems to be a very promising candidate for further *in vivo* investigations on other cisplatin resistant cell lines and depending on the results, possibly, also for further *in vitro* tests.

4. Experimental

4.1. General considerations

Syntheses were performed at room temperature on air. All solvents were distilled prior to use. ¹H and ¹³C NMR spectra were obtained on Varian Unity 500 and VXR 400 spectrometers using residual protons and solvent signals, respectively, as internal reference. Thiophene-2-thiol was distilled prior to use and stored under argon. [(PtMe₃)₄] (**2**) was prepared according to literature [25,26]. All other chemicals were purchased commercially.

4.2. Synthesis of Na(S–D) (S–D = pymt, pyt, tzt, tpt)

A freshly prepared solution of NaOMe (10 mmol) in methanol (20 ml) was added to a stirred solution of the respective heterocycle (10 mmol) in methanol (20 ml). After stirring for 30 min the solvent was evaporated *in vacuo* and the solid dried *in vacuo*.

Na(tzt): Yield 1.39 g (99%). ¹H NMR (400 MHz, CD₃OD) δ 3.98 (m, 2H, NCH₂), 3.28 (m, 2H, SCH₂). ¹³C NMR (400 MHz, CD₃OD) δ 182.8 (s, C2), 62.3 (s, C4), 35.9 (s, C5).

Na(pymt): Yield 1.27 g (95%). ¹H NMR (400 MHz, CD₃OD) δ 8.13 (d, 2H, H4, H6), 6.71 (t, 1H, H5). ¹³C NMR (400 MHz, CD₃OD) δ 172.4 (s, C2), 147.0 (s, C4, C6), 129.4 (s, C5).

Na(pyt): Yield 1.30 g (98%). ¹H NMR (400 MHz, CD₃OD) δ 8.50 (d, 1H, H6), 7.75 (m, 1H, H4), 7.37 (d, 1H, H3), 6.67 (m, 1H, H5). ¹³C NMR (400 MHz, CD₃OD) δ 147.2 (s, C6), 134.5 (s, C4), 129.5 (s, C3), 115.4 (s, C5).

Na(tpt): Yield 1.35 g (98%). ¹H NMR (400 MHz, CD₃OD) δ 7.39 (m, 1H, H5), 7.15 (m, 1H, H3), 6.93 (m, 1H, H4). ¹³C NMR (400 MHz, CD₃OD) δ 132.6 (s, C5), 129.8 (s, C4), 127.4 (s, C3).

4.3. Syntheses of [(PtMe₃)₂(μ -S–D)]₂ (μ -S–D = pymt, **3**; pyt, **4**; tzt, **5**) and [(PtMe₃)₄(μ_3 -tpt)]₄ (**6**)

To a solution of [(PtMe₃)₄] (50 mg, 0.034 mmol) in methylene chloride (5 ml) a solution of the sodium salt (0.136 mmol) of the

respective heterocycle in methanol (3 ml) was added. After stirring for 30 min the solvent was evaporated *in vacuo*. The residue was extracted with acetone (3 × 3 ml) and the solvent removed *in vacuo*. Afterwards the residue was dried *in vacuo*. The ¹H NMR spectra proved to be identical with those reported in reference [16].

[(PtMe₃)₂(μ-pyt)₂] (3) Yield: 18 mg (49%); [(PtMe₃)₂(μ-pymt)₂] (4) Yield: 25 mg (52%);

[(PtMe₃)₂(μ-tzt)₂] (5) Yield: 40 mg (16%); [(PtMe₃)₄(μ₃-tpt)₄] (6) Yield: 20 mg (21%).

4.4. X-ray crystallography

Single crystals of [(PtMe₃)₂(μ-pyt)₂] (3), [(PtMe₃)₂(μ-pymt)₂] (4) and [(PtMe₃)₄(μ₃-tpt)₄] (6) for X-ray diffraction measurements were obtained from acetone solutions by slow evaporation of the solvent at room temperature. Intensity data were collected on a Oxford Diffraction CCD Xcalibur S diffractometer with Mo K α radiation ($\lambda = 0.71073$ Å, graphite monochromator) at 130(2) K. A summary of the crystallographic data, the data collection parameters and the refinement parameters is given in Table 5. Empirical absorption corrections using spherical harmonics implemented in SCALE3 ABSPACK scaling algorithm were applied (3: T_{\min}/T_{\max} 0.65/1.00; 4: T_{\min}/T_{\max} 0.74/1.00; 6: T_{\min}/T_{\max} 0.61/1.00). The structures were solved by direct methods with SHELXS-97 [27] and refined using full matrix least square routines against F^2 with SHELXL-97 [27]. Non-hydrogen atoms were refined with anisotropic displacement parameters. Hydrogen atoms were positioned geometrically and refined with isotropic displacement parameters according to the "riding model". The large residual electron density in complex 6 is close to C18 due to a non-resolved disorder of the requisite thiophene ring.

4.5. Computational details

DFT calculations of compounds were carried out by the GAUSSIAN03 program package [28] using the hybrid functional B3LYP [29]. The 6-311G(d,p) basis sets as implemented in GAUSSIAN03 were employed for C, H, N, O and S atoms. The valence shell of platinum has been approximated by split valence basis set too; for its core

orbitals an effective core potential in combination with consideration of relativistic effects has been used [30]. The appropriateness of the functional in combination with the basis sets and effective core potential used for reliable interpretation of structural and energetic aspects of related platinum complexes has been demonstrated [16,31]. All systems were fully optimized without any symmetry restrictions if not stated otherwise explicitly. The resulting geometries were characterized as equilibrium structures by the analysis of the force constants of normal vibrations. For that, the tetranuclear complexes 4c* and 6d* proved to be large. Thus, the geometry optimizations and the analyses of the force constants of normal vibrations were performed as described above but using smaller basis sets (6-31G(d)) for the main group atoms. Then, the optimized structures were reoptimized using the better 6-311G(d,p) basis sets. To prove that this procedure is reliable, also the dinuclear complexes 4a* and 6a* were optimized (including the analysis of the force constants) using the smaller 6-31G(d) basis sets for the main group atoms. The energy differences between the dinuclear and tetranuclear complexes obtained in this way (given in the Supporting Information) and using the better 6-311G(d,p) basis sets proved to be very similar.

4.6. In vitro cytotoxic studies

Stock solutions of investigated platinum complexes and reference compound cisplatin were made in dimethyl sulfoxide (DMSO) at concentration of 20 mM and diluted by nutrient medium to various working concentrations. Nutrient medium was RPMI-1640 (PAA Laboratories) supplemented with 10% fetal bovine serum (Biochrom AG) and penicillin/streptomycin (PAA Laboratories).

4.6.1. Cell cultures

The human tumor cell lines anaplastic thyroid cancer 8505C, head and neck tumor A253, lung carcinoma A549, ovarian cancer A2780, colon carcinoma DLD-1 were cultivated in the Biozentrum, Martin-Luther University Halle-Wittenberg. All cells were maintained as monolayers in nutrient medium in a humidified atmosphere with 5% CO₂.

Table 5
Crystal data, data collection and refinement parameters of [(PtMe₃)₂(μ-pyt)₂] (3), [(PtMe₃)₂(μ-pymt)₂] (4) and [(PtMe₃)₄(μ₃-tpt)₄] (6).

	3	4	6
Formula	C ₁₆ H ₂₆ N ₂ Pt ₂ S ₂	C ₁₄ H ₂₄ N ₄ Pt ₂ S ₂	C ₂₈ H ₄₈ Pt ₄ S ₈
Formula weight	700.69	702.67	1421.5
Crystal system	monoclinic	monoclinic	monoclinic
Space group	$P2_1/c$	$P2_1$	$P2_1/n$
<i>a</i> (Å)	14.340(4)	9.0308(3)	14.554(2)
<i>b</i> (Å)	10.428(2)	16.8799(7)	14.4810(4)
<i>c</i> (Å)	14.287(3)	12.9696(4)	18.207(2)
β (°)	111.27(3)	104.785(3)	106.58(1)
<i>V</i> (Å ³)	1990.9(8)	1911.6(1)	3677.5(6)
<i>Z</i>	4	4	4
<i>D</i> _{calc} (g cm ⁻³)	2.338	2.442	2.567
<i>T</i> (K)	130(2)	130(2)	130(2)
μ (mm ⁻¹)	14.246	14.839	15.642
θ (°)	2.61–30.51	2.63–28.28	2.54–30.51
<i>F</i> (0 0 0)	1296	1296	2624
Index ranges	−20 ≤ <i>h</i> ≤ 20 −14 ≤ <i>k</i> ≤ 14 −20 ≤ <i>l</i> ≤ 20	−12 ≤ <i>h</i> ≤ 12 −22 ≤ <i>k</i> ≤ 22 −16 ≤ <i>l</i> ≤ 17	−20 ≤ <i>h</i> ≤ 20 −20 ≤ <i>k</i> ≤ 20 −26 ≤ <i>l</i> ≤ 22
Reflections collected	28 238	42 831	107 372
Reflections observed [<i>I</i> > 2 σ (<i>I</i>)]	3607	7936	7822
Reflections independent	6073 (<i>R</i> _{int} = 0.082)	9478 (<i>R</i> _{int} = 0.061)	11 207 (<i>R</i> _{int} = 0.069)
Data/restraints/parameters	6073/0/181	9478/1/409	11 207/0/325
Goodness-of-fit (GOF) (F^2)	0.866	0.839	0.972
<i>R</i> ₁ , <i>wR</i> ₂ (<i>I</i> > 2 σ)	0.0426/0.0792	0.0277/0.0363	0.0379/0.0904
<i>R</i> ₁ , <i>wR</i> ₂ (all data)	0.0902/0.0863	0.0366/0.0371	0.064/0.0941
Largest differences in peak and hole (e Å ⁻³)	2.458 and −1.53	0.965 and −0.838	7.768 and −2.688

4.6.2. Cytotoxicity assay

The cytotoxic activity of the platinum compounds was measured by the sulforhodamine-B (SRB) assay [32]. In brief, exponentially growing cells were seeded into 96-well plates and 24 h later, after the cell adherence, nine different concentrations of investigated compounds were added to the wells. The final concentrations were in the range from 0.1 to 125 μM . All experiments were done in triplicate. Nutrient medium with corresponding concentrations of compounds, but void of cells was used as blank. Five days after seeding the cells were fixed with 10% trichloroacetic acid and processed according to the published SRB assay protocol. Absorbance was measured at 570 nm using a 96-well plate reader (SpectraFluor Plus Tecan, Germany) and the percentages of surviving cells relative to untreated controls were determined. Concentration IC_{50} was determined as the concentration of a drug that inhibited cell survival by 50%, compared with vehicle-treated control.

Acknowledgement

Financial support from the Deutsche Forschungsgemeinschaft and gifts of chemicals by Merck (Darmstadt) is gratefully acknowledged.

Appendix A. Supplementary data

CCDC 730637, 730638 and 730639 contain the supplementary crystallographic data for **3**, **4** and **6**, respectively. These data can be obtained free of charge via <http://www.ccdc.cam.ac.uk/conts/retrieving.html>, or from the Cambridge Crystallographic Data Centre, 12 Union Road, Cambridge CB2 1EZ, UK; fax: (+44) 1223-336-033; or e-mail: deposit@ccdc.cam.ac.uk. Supplementary data associated with this article can be found, in the online version, at doi:10.1016/j.poly.2009.08.004.

References

- [1] M. Friedman, F.F. Bautista, J. Agric. Food Chem. 43 (1995) 69.
- [2] T. Moulard, J.F. Lagorce, J.C. Thomes, C. Raby, J. Pharm. Pharmacol. 45 (1993) 731.
- [3] P.D. Cookson, E.R.T. Tiekink, J. Chem. Soc., Dalton Trans. 2 (1993) 259.
- [4] A.M. Brodie, H.D. Holden, J. Lewis, M.J. Taylor, J. Organomet. Chem. 253 (1983) C1.
- [5] R. Carballo, J.S. Casas, M.S. Garcia-Tasende, A. Sánchez, J. Sordo, E.M. Vázquez-López, J. Organomet. Chem. 525 (1996) 49.
- [6] I. Kinoshita, Y. Yasuba, K. Matsumoto, S. Ooi, Inorg. Chim. Acta 80 (1983) L13.
- [7] M. Kato, A. Omura, A. Tshikawa, S. Kishi, Y. Sugimoto, Angew. Chem. Int. Ed. 41 (2002) 3183.
- [8] L. Zhang, H.-X. Zhang, C.-L. Chen, L.-R. Deng, B.-S. Kang, Inorg. Chim. Acta 355 (2003) 49.
- [9] M.W. Whitehouse, P.D. Cookson, G. Siasios, E.R.T. Tiekink, Met.-Based Drugs 5 (1998) 245.
- [10] G. Cervantes, S. Marchal, M.J. Prieto, J.M. Pérez, V.M. González, C. Alonso, V. Moreno, J. Inorg. Biochem. 77 (1999) 197.
- [11] B. Rosenberg, L. Van Camp, T. Krigas, Nature 205 (1965) 698.
- [12] M. Carrara, T. Berti, S. D'Ancona, V. Cherchi, L. Sindellari, Anticancer Res. 17 (1997) 975.
- [13] G. Cervantes, M.J. Prieto, V. Moreno, Met.-Based Drugs 4 (1997) 9.
- [14] M.D. Hall, T.W. Hambley, Coord. Chem. Rev. 232 (2002) 49.
- [15] (a) L.R. Kelland, B.A. Murrer, G. Abel, C.M. Giandomenico, P. Mistry, K.R. Harrap, Cancer Res. 52 (1992) 822; (b) O. Nováková, O. Vrána, V.I. Kiseleva, V. Brabec, Eur. J. Biochem. 228 (1995) 616.
- [16] C. Vetter, C. Wagner, J. Schmidt, D. Steinborn, Inorg. Chim. Acta 359 (2006) 4326.
- [17] C. Janiak, J. Chem. Soc., Dalton Trans. (2000) 3885.
- [18] Cambridge Structural Database (CSD), Cambridge Crystallographic Data Centre, University Chemical Laboratory, Cambridge (England), version 5.30, 2008.
- [19] (a) T.G. Appleton, H.C. Clark, L.E. Manzer, Coord. Chem. Rev. 10 (1973) 335; (b) D. Steinborn, Angew. Chem. 104 (1992) 392.
- [20] J.G. Reynolds, S.C. Sendlinger, A.M. Murray, J.C. Huffmann, G. Christou, Inorg. Chem. 34 (1995) 5745.
- [21] G. Smith, C.H.L. Kennard, T.C.W. Mak, J. Organomet. Chem. 290 (1985) C7.
- [22] K.H. Ebert, W. Massa, H. Donath, J. Lorberth, B.-S. Seo, E. Herdtweck, J. Organomet. Chem. 559 (1998) 203.
- [23] D.C. Craig, I.G. Dance, Polyhedron 6 (1987) 1157.
- [24] R. Lindner, G.N. Kaluderović, R. Paschke, C. Wagner, D. Steinborn, Polyhedron 27 (2008) 914.
- [25] W.J. Pope, S.J. Peachey, Proc. Chem. Soc. 23 (1907) 86.
- [26] J.C. Baldwin, W.C. Kaska, Inorg. Chem. 14 (1975) 2020.
- [27] G.M. Sheldrick, Acta Crystallogr. A64 (2008) 112.
- [28] M.J. Frisch, G.W. Trucks, H.B. Schlegel, G.E. Scuseria, M.A. Robb, J.R. Cheeseman, J.A. Montgomery Jr., T. Vreven, K.N. Kudin, J.C. Burant, J.M. Millam, S.S. Iyengar, J. Tomasi, V. Barone, B. Mennucci, M. Cossi, G. Scalmani, N. Rega, G.A. Petersson, H. Nakatsuji, M. Hada, M. Ehara, K. Toyota, R. Fukuda, J. Hasegawa, M. Ishida, T. Nakajima, Y. Honda, O. Kitao, H. Nakai, M. Klene, X. Li, J.E. Knox, H.P. Hratchian, J.B. Cross, V. Bakken, C. Adamo, J. Jaramillo, R. Gomperts, R.E. Stratmann, O. Yazyev, A.J. Austin, R. Cammi, C. Pomelli, J.W. Ochterski, P.Y. Ayala, K. Morokuma, G.A. Voth, P. Salvador, J.J. Dannenberg, V.G. Zakrzewski, S. Dapprich, A.D. Daniels, M.C. Strain, O. Farkas, D.K. Malick, A.D. Rabuck, K. Raghavachari, J.B. Foresman, J.V. Ortiz, Q. Cui, A.G. Baboul, S. Clifford, J. Cioslowski, B.B. Stefanov, G. Liu, A. Liashenko, P. Piskorz, I. Komaromi, R.L. Martin, D.J. Fox, T. Keith, M.A. Al-Laham, C.Y. Peng, A. Nanayakkara, M. Challacombe, P.M.W. Gill, B. Johnson, W. Chen, M.W. Wong, C. Gonzalez, J.A. Pople, GAUSSIAN03, Revision C.02, Gaussian Inc., Wallingford, CT, 2004.
- [29] (a) A.D. Becke, Phys. Rev. A 38 (1988) 3098; (b) A.D. Becke, J. Chem. Phys. 98 (1993) 5648; (c) C. Lee, W. Yang, R.G. Parr, Phys. Rev. B 37 (1988) 785; (d) P.J. Stephens, F.J. Devlin, C.F. Chabalowski, M.J. Frisch, J. Phys. Chem. 98 (1994) 11623.
- [30] D. Andrae, U. Häußermann, M. Dolg, H. Stoll, H. Preuss, Theor. Chim. Acta 77 (1990) 123.
- [31] (a) K. Nordhoff, D. Steinborn, Organometallics 20 (2001) 1408; (b) T. Gosavi, C. Wagner, H. Schmidt, D. Steinborn, J. Organomet. Chem. 690 (2005) 3229; (c) M. Werner, T. Lis, C. Bruhn, R. Lindner, D. Steinborn, Organometallics 25 (2006) 5946; (d) D. Steinborn, S. Schwieger, Chem. Eur. J. 13 (2007) 9668; (e) C. Vetter, C. Wagner, G.N. Kaluderović, R. Paschke, D. Steinborn, Inorg. Chim. Acta 362 (2009) 189.
- [32] P. Skehan, R. Storeng, D. Scudiero, A. Monks, J. McMahon, D. Vistica, J.T. Warren, H. Bokesch, S. Kenney, M.R. Boyd, J. Natl. Cancer Inst. 82 (1990) 1107.



Contents lists available at ScienceDirect

Inorganica Chimica Acta

journal homepage: www.elsevier.com/locate/ica



Synthesis, characterization, and cytotoxicity of trimethylplatinum(IV) complexes with 2-thiocytosine and 1-methyl-2-thiocytosine ligands

Cornelia Vetter^a, Christoph Wagner^a, Goran N. Kaluđerović^{a,b}, Reinhard Paschke^c, Dirk Steinborn^{a,*}

^a Institut für Chemie, Anorganische Chemie, Martin-Luther-Universität Halle-Wittenberg, D-06120 Halle, Kurt-Mothes-Straße 2, Germany

^b Department of Chemistry, Institute of Chemistry, Technology and Metallurgy, Studentski trg 14, 11000 Belgrad, Serbia

^c Biozentrum, Martin-Luther-Universität Halle-Wittenberg, D-06120 Halle, Weinbergweg 22, Germany

ARTICLE INFO

Article history:

Received 7 January 2008

Received in revised form 12 March 2008

Accepted 17 March 2008

Available online 24 March 2008

Keywords:

Platinum complexes

Thionucleobases

Single-crystal X-ray diffraction analysis

In vitro cytotoxic studies

DFT calculations

ABSTRACT

The reaction of [PtMe₃(MeOH)(bpy)][BF₄] (**1**) with the thionucleobases 2-thiocytosine (SCy, **2**) and 1-methyl-2-thiocytosine (1-MeSCy, **3**) resulted in the formation of the complexes [PtMe₃(bpy)(SCy-κS)][BF₄] (**4**) and [PtMe₃(bpy)(1-MeSCy-κS)][BF₄] (**5**), respectively. The complexes were characterized by ¹H and ¹³C NMR spectroscopy as well as by single-crystal X-ray analyses of **4**·MeOH and **5**. In **4**·MeOH two strong hydrogen bonds (N4–H...N3': N4...N3' 2.976(7) Å) between the thiocytosine ligands give rise to base pairing thus forming dinuclear cations [PtMe₃(bpy)(SCy-κS)]₂²⁺. In both complexes the platinum atom is octahedrally coordinated [PtC₃N₂S] by three methyl ligands, the 2,2'-bipyridine ligand and the κS coordinated nucleobase (configuration index: OC-6-33). The structural investigations gave evidence that the sulfur atoms of the nucleobase ligands in **4**·MeOH and **5** have to be regarded as sp³ and sp² hybridized, respectively. Thus, the ligand in **4**·MeOH has to be considered as the deprotonated thiol-amino form of thiocytosine being reprotonated at N1. In complex **5** the 1-MeSCy is coordinated in its thione-amino form. DFT-calculations of the base-paired dinuclear cation in **4** as well as of **4** itself gave proof of the strength of the hydrogen bond (8.5 kcal/mol) and exhibited that cation–anion interactions influence the conformation of the complex. *In vitro* cytotoxicity studies of **4** and **5** using nine different human tumor cell lines revealed moderate cytotoxic activity.

© 2008 Elsevier B.V. All rights reserved.

1. Introduction

Since Carbon discovered in 1965 the presence of 2-thiouracil in tRNA of *Escherichia coli* [1] the role of thiopyrimidine nucleobases and their biological activity was investigated intensively, although they have not been studied as frequently as their oxygen analogues. It was found that also 4-thiouracil [2] and 2-thiocytosine [3–5] are present in tRNA of several sources. These thionucleobases and their derivatives show biological activity. Whereas the thionucleobases possess antiviral properties [6,7], derivatives of their nucleosides are potential antitumor agents [7,8]. Platinum complexes and their applications as cancerostatics were established with the discovery of cisplatin in 1965 by Rosenberg et al. [9]. Since then numerous platinum complexes have been synthesized, especially with platinum in the oxidation state II, among them also complexes with pyrimidine-2-thione ligands, which showed cytotoxic activities sometimes higher than cisplatin and even against cisplatin resistant cell lines [10–12]. Also platinum(IV) complexes proved to be highly promising as anticancer agents. They may have some advantages over platinum(II) complexes due to their greater kinetic inertness that may result in a reduced toxicity and allow

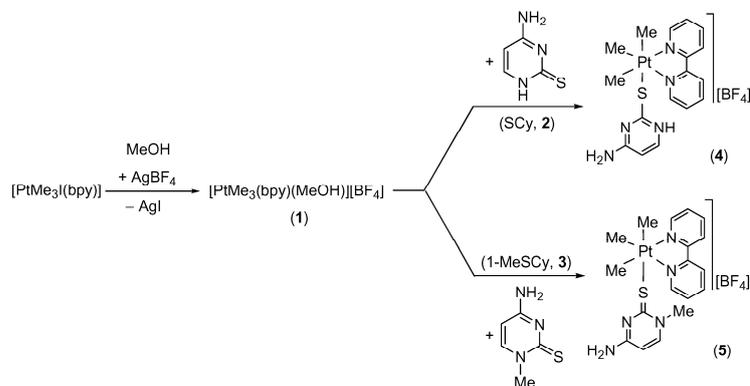
oral application [13–15]. We are interested in the syntheses of platinum(IV) complexes with bioactive nitrogen and sulfur containing ligands, like thio derivatives of pyrimidine nucleobases because of several reasons. The combination of two potentially cancerostatic building blocks in one compound could lead to compounds with increased antitumor activities. From the coordination chemistry point of view these nucleobases exhibit manifold donor sites (N, S) and they can coordinate in a mono or bidentate fashion and also act as bridging ligands. To get control of their binding modes to metal centers is a challenge. In platinum(II) complexes N-bound 2-thiocytosine ligands were found [16]. In continuation of our work on the coordination of sulfur-substituted heterocycles to platinum(IV) [17], we report here the synthesis and characterization of trimethylplatinum(IV) complexes with 2-thiocytosine and 1-methyl-2-thiocytosine ligands.

2. Results and discussion

2.1. Synthesis and characterization of [PtMe₃(bpy)(L)][BF₄] (L = SCy **4**; 1-MeSCy, **5**)

The reaction of [PtMe₃(bpy)] with silver tetrafluoroborate in methanol resulted in the formation of [PtMe₃(bpy)(MeOH)][BF₄]

* Corresponding author. Tel.: +49 345 5525620; fax: +49 345 5527028.
E-mail address: dirk.steinborn@chemie.uni-halle.de (D. Steinborn).



Scheme 1.

(1) (Scheme 1). This complex was prepared in situ and the subsequent reaction with an equimolar amount of the corresponding nucleobase (2-thiocytosine, SCy, **2**; 1-methyl-2-thiocytosine, 1-MeSCy, **3**) yielded the ionic complexes $[\text{PtMe}_3(\text{bpy})(\text{L})][\text{BF}_4]$ (L = SCy- κ S, **4**; 1-MeSCy- κ S, **5**)

The air-stable yellow complexes were isolated in 62% (**4**) and 41% yield (**5**) and identified by ^1H and ^{13}C NMR spectroscopy as well as by X-ray diffraction measurements. Selected ^1H and ^{13}C NMR data are given in Table 1. In accordance with the formula given in Scheme 1, two chemically inequivalent methyl H and C atoms were found, namely one of the methyl ligands in *trans* position to the 2,2'-bipyridine ligand and one for the methyl ligand *trans* to the coordinated thionucleobase. In complexes **4** and **5** the coupling constants ($^2J_{\text{Pt,H}}$, $^1J_{\text{Pt,C}}$) *trans* to the thionucleobase are very similar, showing that 2-thiocytosine (**2**) and its methylated derivative **3** exert virtually the same *trans* influence. In DMSO- d_6 the N11 protons give rise to three (12.4, N11; 8.0/7.4 ppm, NH₂) and two (7.9/7.3 ppm, NH₂) broad signals for complex **4** and **5**, respectively. Due to fast H/D exchange, no NH-resonances were found in methanol- d_4 .

2.2. Structures of $[\text{PtMe}_3(\text{bpy})(\text{L})][\text{BF}_4]$ (L = SCy, **4**; 1-MeSCy, **5**)

Suitable crystals of **4** and **5** for X-ray diffraction analyses were obtained from methanol/diethyl ether/*n*-pentane solutions at 4 °C. Complex **4** · MeOH crystallizes in the centrosymmetric space group $P2_1/n$. The crystal consists of base-paired dinuclear $[\{\text{PtMe}_3(\text{bpy})(\text{SCy-}\kappa\text{S})\}_2]^{2+}$ cations, tetrafluoroborate anions and a solvent molecule. The structure of the cation is shown in Fig. 1. Selected bond lengths and angles are given in Table 2.

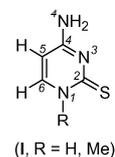
Two hydrogen bonds (N4–H...N3': N4...N3' 2.976(7) Å) between the thiocytosine ligands give rise to base pairing thus forming dinuclear cations that exhibit crystallographically imposed inversion symmetry. In contrast, 2-thiocytosine (**2**) crystallizes in dimers being held together by one N1–H...N3' (N1...N3' 3.022 Å) and one N4'–H'...S (N4'...S 3.345 Å) hydrogen bond [18]. The platinum atom is octahedrally coordinated by three methyl ligands in facial configuration, the 2,2'-bipyridine and the S bound 2-thiocytosine ligand. The pyrimidine ring of the thiocytosine ligand is nearly planar, while the nitrogen atom of the amino group and the sulfur atom are deviated by 0.044 Å and 0.136 Å from this plane, respectively. Coordination of 2-thiocytosine (**2**) in complex **4** · MeOH gives rise to a remarkably lengthening of the C2–S bond (1.745(7) Å versus 1.702 Å [18]). The Pt–S bond (2.524(2) Å) is even longer than those in thioether platinum(IV) complexes (median: 2.405 Å, lower/upper quartile: 2.336/2.452 Å; $n = 67$; n – number

Table 1

Selected ^1H and ^{13}C NMR spectroscopic data (δ in ppm, J in Hz) for $[\text{PtMe}_3(\text{bpy})(\text{L})][\text{BF}_4]$ (L = SCy, **4**; 1-MeSCy, **5**) in CD₃OD

	4 (L = SCy)		5 (L = 1-MeSCy)	
	$\delta_{\text{H}}(^2J_{\text{Pt,H}})$	$\delta_{\text{C}}(^1J_{\text{Pt,C}})$	$\delta_{\text{H}}(^2J_{\text{Pt,H}})$	$\delta_{\text{C}}(^1J_{\text{Pt,C}})$
Me (<i>trans</i> to S)	0.45 (69.72)	2.6 (642.06)	0.47 (69.31)	2.7 (649.50)
Me (<i>trans</i> to N)	1.22 (69.30)	−4.9 (669.91)	1.25 (69.10)	−4.7 (669.26)
H5/C5 ^a	5.97	99.6	6.00	100.3
H6/C6	7.28	143.4	7.58	148.6
N1–Me			3.46	44.3

^a Numbering scheme:



of observations) [19]. This long C2–S bond together with the C2–S–Pt angle (103.0(2)°) and an angle of 78.2° between the Pt–S vector and the thiocytosine plane (distance of Pt from the mean ligand plane: 2.52 Å; see Fig. 1b) indicates that the sulfur atom of the thiocytosine ligand has to be described as sp^3 hybridized. In rough approximation the planes between the thiocytosine and the bipyridine ligand are parallel (interplanar angle: 12.0(2)°). Considering the distance between these two planes of about 3.2 Å, a stabilization by π – π stacking has to be taken into consideration.

The cations $[\{\text{PtMe}_3(\text{bpy})(\text{SCy-}\kappa\text{S})\}_2]^{2+}$ form hydrogen bonds to the tetrafluoroborate anions (N1–H...F4: N1...F4 2.748(9) Å) and to the solvate MeOH molecules (N4–H...O: N4...O 2.935(8) Å). Furthermore, as shown in Fig. 2, the cations are packed like a “staircase” in infinite columns. Neighbored molecules are related by an inversion symmetry. The interplanar distance between the two bpy ligands of 3.5 Å and the displacement¹ of the N10, C11–C15 rings of 26° indicate that there is a stabilization through π – π and σ – π (C–H... π) interactions as thoroughly discussed in Ref. [20].

$[\text{PtMe}_3(\text{bpy})(1\text{-MeSCy-}\kappa\text{S})][\text{BF}_4]$ (**5**) crystallizes in the space group $C2/c$. The crystal consists of $[\text{PtMe}_3(\text{bpy})(1\text{-MeSCy-}\kappa\text{S})]^+$ cations and disordered tetrafluoroborate anions. The structure of the cation of **5** is shown in Fig. 3. Selected bond lengths and angles

¹ The displacement, measured by the angle between the ring normal and the centroid–centroid vector, is a measure for the ring–ring overlap [20].

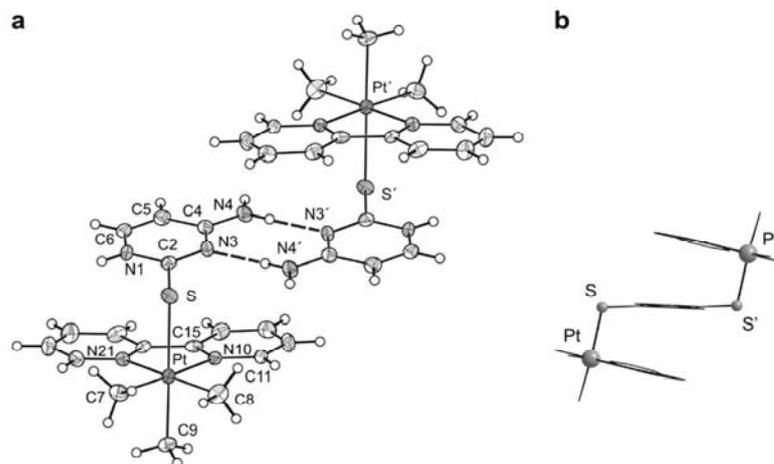


Fig. 1. Structure of the base-paired dinuclear cation $[[PtMe_3(bpy)(SCy-\kappa S)]_2]^{2+}$ in crystals of **4** · MeOH (a) and sketch of the conformation viewed along the plane of the $(SCy)_2$ ligand (b). The displacement ellipsoids are drawn at the 30% probability level.

Table 2
Selected bond lengths (in Å) and angles (in °) of **4** · MeOH and **5**

	4 · MeOH	5	SCy (2) ^a	1-MeSCy (3) ^a
Pt–C9	2.074(6)	2.047(5)		
Pt–C8	2.043(7)	2.052(5)		
Pt–C7	2.067(7)	2.055(5)		
Pt–S	2.524(2)	2.441(1)		
Pt–N21	2.146(5)	2.138(4)		
Pt–N10	2.143(5)	2.150(4)		
C2–S	1.745(7)	1.702(6)	1.702	1.697
C2–N1	1.36(1)	1.378(7)	1.368	1.386
C2–N3	1.310(8)	1.332(7)	1.343	1.344
C4–N3	1.365(8)	1.343(7)	1.345	1.339
C4–N4	1.306(8)	1.324(7)	1.333	1.333
N21–Pt–N10	77.1(2)	77.5(2)		
C8–Pt–N21	174.0(2)	174.6(2)		
C9–Pt–S	176.3(2)	173.5(2)		
C2–S–Pt	103.0(2)	113.8(2)		

For comparison the corresponding values in crystals of 2-thiocytosine (**2**) [18] and 1-methyl-2-thiocytosine (**3**) [21] are given.

^a In crystals of **2** and **3** two symmetry independent molecules were found. The structures are very similar, here the mean values are given.

are given in Table 2. Analogous to complex **4** · MeOH, the platinum atom is coordinated octahedrally by three methyl ligands, the 2,2'-bipyridine ligand and the S bound 1-methyl-2-thiocytosine ligand. The 1-MeSCy ligand is almost planar (greatest deviation from the mean plane: 0.029 Å for C1). The interplanar angle between the 1-MeSCy ligand and the bpy ligand is 71.1(2)°, thus excluding any π interactions. The C2–S bond (1.702(6) Å) is as long as that in the uncoordinated 1-MeSCy (**3**) (1.697 Å, Table 2) [21] indicating that there is no coordination induced lengthening as observed in **4** · MeOH. The C2–S–Pt angle (113.8(2)°) and the position of Pt nearly in the 1-MeSCy plane (distance: 0.78 Å; angle between the Pt–S vector and the mean ligand plane: 19.3°; see Fig. 3b) show that the sulfur atom has to be regarded as sp^2 hybridized. In accordance with that, the Pt–S bond is considerably shorter compared to **4** · MeOH (2.441(1) versus 2.524(2) Å).

In crystals of **5** cation–anion interactions were found through N4–H···F2/N4–H···F3A interactions (N4···F2/N4···F3A 2.93(2)/2.86(2) Å). The hydrogen bonding as well as the packing of complex **5** in crystals are shown in Fig. 4. The cations are packed in infinite strands; neighbored molecules are related by an inversion

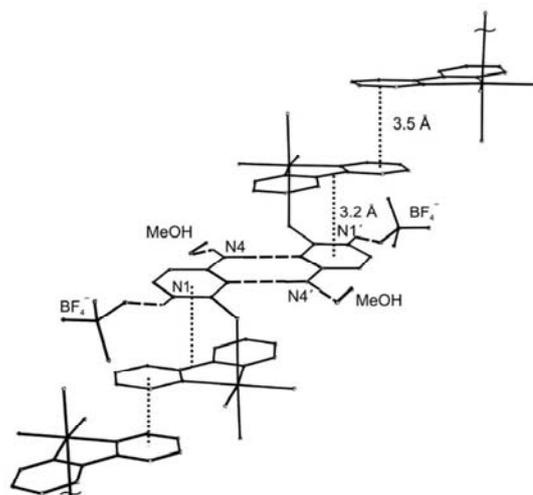


Fig. 2. Solid state structure of $[[PtMe_3(bpy)(SCy-\kappa S)][BF_4]$ (**4** · MeOH) showing the packing of the cations by π - π stacking (···) and the hydrogen bonds (---) between cations and anions and MeOH, respectively. C bound H atoms are omitted for clarity.

symmetry. Accordingly, the bpy ligands of neighboring molecules are arranged parallel to each other as are neighboring 1-MeSCy ligands. Although the distances of heterocyclic rings of 3.5 and 3.3 Å, respectively, might indicate a stabilization by π - π interactions, due to a rather small ring–ring overlap (angle between the ring normal and the centroid–centroid vector: 37° and 43°, respectively) this contribution should be rather small but stabilizing C–H··· π interactions have to be taken into consideration [20].

2-Thiocytosine (**2**) exists in several tautomers, the three most important tautomers (**2a–c**) are shown in Scheme 2. It crystallizes in the 1H-thione-amino form (**2b**) that was also identified by IR spectroscopy of polycrystalline films [22]. On the other hand, IR spectroscopic investigations of matrix isolated species showed

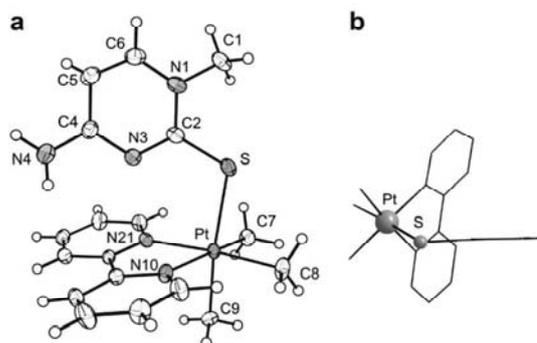


Fig. 3. Structure of the cation $[\text{PtMe}_3(\text{bpy})(1\text{-MeSCy-}\kappa\text{S})]^+$ in crystals of **5** (a) and sketch of the conformation viewed along the plane of the MeSCy ligand (b). The displacement ellipsoids are drawn at the 30% probability level.

the presence of the thiol-amino form (**2a**) [22]. Although lacking explicit consideration of nucleobase–water hydrogen bonding effects, quantum chemical calculations using continuum model (COSMO) indicate that in water the order of stability is $2\text{b} \approx 2\text{c} > 2\text{a}$ [23]. Considering the sp^3 hybridized S atom in complex **4**·MeOH the ligand is best described as the deprotonated thiol-amino form that is reprotonated at N1 (**2d**). Interestingly, the formation of an symmetrical dimer held together by two iden-

tical $\text{N-H}\cdots\text{N}'$ hydrogen bonds can be observed in crystals of 1-MeSCy (**3**) [21], whereas crystals of 2-thiocytosine (**2**) consist of unsymmetrical dimers, linked through $\text{N-H}\cdots\text{N}'$ and $\text{N}'\text{-H}'\cdots\text{S}$ hydrogen bonds [18].

Three tautomers of 1-methyl-2-thiocytosine (**3**) have to be taken into account (**3a–c**, Scheme 2). Quantum chemical calculations gave evidence that both in the gas phase and in aqueous solution the thione-amino form (**3a**) is the most stable one [23]. Exactly that tautomer was found in the solid state structure of **3** as well as in complex **5**.

2.3. Quantum chemical calculations

To get insight into the unusual coordination of the 2-thiocytosine ligand in complex **4**·MeOH, DFT calculations of the base-paired dinuclear cation $[\{\text{PtMe}_3(\text{bpy})(\text{SCy-}\kappa\text{S})\}_2]^{2+}$ (**6**_{calc.}) and the complex **4** itself at the B3LYP/6-31G(d) level using effective core potential with consideration of relativistic effects for platinum have been performed. The calculated structures are shown in Fig. 5, selected structural parameters are given in Table 3. Using the conformation of the cation in **4**·MeOH as the starting point, the calculation ended up with the equilibrium structure **6**_{calc.}. Thus, a severe change in conformation was observed: The planes of the SCy and bpy ligands in **4**·MeOH and in **6**_{calc.} were found to be nearly coplanar and perpendicular (interplanar angles: $12.0(2)^\circ$ versus 89.1°), respectively. This could be reasoned due to the tetrafluoroborate anions in **4**·MeOH that are hydrogen-bonded ($\text{N1-H}\cdots\text{F4}$) to the cations thus preventing a perpendicular

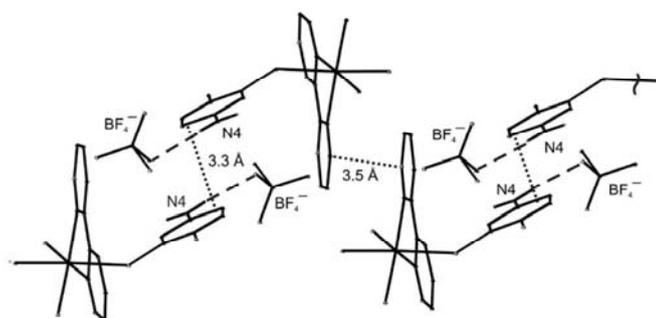
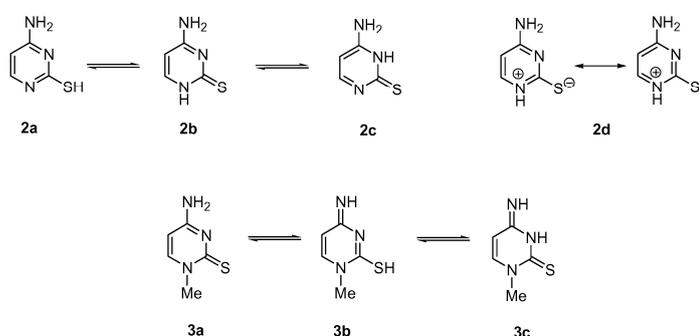


Fig. 4. Solid state structure of $[\text{PtMe}_3(\text{bpy})(1\text{-MeSCy-}\kappa\text{S})][\text{BF}_4]$ (**5**) showing the packing of the cations by π - π stacking (\cdots) and the hydrogen bonds (---) between cations and anions. C bound H atoms are omitted for clarity. Only the major occupied positions of the disordered fluorine atoms are shown.



Scheme 2.

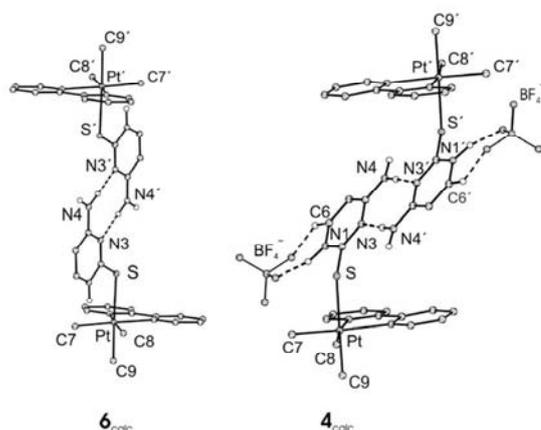


Fig. 5. Calculated structures of $[[\text{PtMe}_3(\text{bpy})(\text{SCy-}\kappa\text{S})]_2]^{2+}$ ($\mathbf{6}_{\text{calc}}$) and $[[\text{PtMe}_3(\text{bpy})(\text{SCy-}\kappa\text{S})]_2][\text{BF}_4]_2$ ($\mathbf{4}_{\text{calc}}$). C bound H atoms are omitted for clarity.

Table 3

Selected structural parameters (distances in Å, angles in °) of the calculated structures of $[[\text{PtMe}_3(\text{bpy})(\text{SCy-}\kappa\text{S})]_2]^{2+}$ ($\mathbf{6}_{\text{calc}}$) and $[[\text{PtMe}_3(\text{bpy})(\text{SCy-}\kappa\text{S})]_2][\text{BF}_4]_2$ ($\mathbf{4}_{\text{calc}}$)

	$\mathbf{6}_{\text{calc}}$	$\mathbf{4}_{\text{calc}}$	$\mathbf{4} \cdot \text{MeOH}^{\text{a}}$	$(\text{SCy})_2^{\text{b}}$
Pt–S	2.615	2.594	2.524(2)	
Pt–C (trans to S)	2.084	2.078	2.074(6)	
Pt–C (trans to N)	2.072/2.073	2.067/2.069	2.043(7)/2.067(7)	
S–Pt–C (trans to S)	176.9	173.0	176.3(2)	
C2–S	1.719	1.733	1.745(7)	1.686
C2–N3	1.337	1.336	1.310(8)	1.348
C2–N1	1.377	1.370	1.36(1)	1.399
N4...N3	3.009	2.984	2.976(7)	2.948
N4–H/N3...H	1.029/1.980	1.029/1.955	0.86/2.12	1.033/1.917
N4–H...N3	179.1	177.3	173	176.1
N1...F		2.692 ^c	2.748(9)	
N1–H/H...F		1.036/1.690	0.86/1.96	
N1–H...F		161.5	152	

For comparison the requisite values of the dimeric ligand (calculated on the same level of theory) and the experimentally determined values in crystals of $\mathbf{4} \cdot \text{MeOH}$ are given.

^a Experimental values.

^b Calculated structure of dimeric 2-thiocytosine having the same hydrogen bond pattern as in $\mathbf{6}_{\text{calc}}$ and $\mathbf{4}_{\text{calc}}$.

^c C6...F 2.920, C6–H 1.085, H...F 2.003, C6–H...F 140.0.

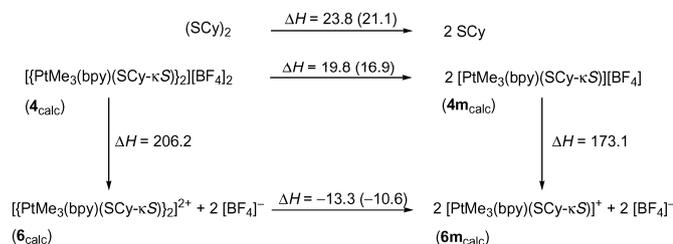
arrangement of the SCy and bpy planes as found in $\mathbf{6}_{\text{calc}}$. Thus, starting once more with the experimentally determined structure in $\mathbf{4} \cdot \text{MeOH}$, the tetrafluoroborate anions were included into the

calculations. The equilibrium structure ($\mathbf{4}_{\text{calc}}$) was found to have an interplanar SCy/bpy angle of 49.0° being in between of that in $\mathbf{4} \cdot \text{MeOH}$ and $\mathbf{6}_{\text{calc}}$. Thus, at least in part, the bulkiness of the $[\text{BF}_4]^-$ anions in close vicinity to the SCy ligand seems to be decisive for the conformation of the complex. It might be that the “intermolecular” π - π stacking between the bpy ligands and the MeOH coordination in $\mathbf{4} \cdot \text{MeOH}$ (see Fig. 2) gives rise to the nearly coplanar arrangement of the SCy and bpy ligands.

The calculated energies of the base-paired dinuclear complexes $\mathbf{4}_{\text{calc}}$ and $\mathbf{6}_{\text{calc}}$, together with those of the requisite mononuclear complexes $\mathbf{4m}_{\text{calc}}$ and $\mathbf{6m}_{\text{calc}}$ (see Supplementary material) gave the basis to estimate the strength of the hydrogen bonds and the cation-anion interactions in $\mathbf{4}_{\text{calc}}$ (Scheme 3). The cleavage of the dimeric 2-thiocytosine having the same hydrogen bond pattern as in $\mathbf{4}_{\text{calc}}$ into monomeric units costs 21.1 kcal/mol (corrected for the basis set superposition error, BSSE) exhibiting a hydrogen bond energy of 10.6 kcal/mol. Thus, the hydrogen bonds in $(\text{SCy})_2$ are of moderate strength [24]. The analogous hydrogen bonds in complex $\mathbf{4}_{\text{calc}}$ proved to be slightly weaker (8.5 kcal/mol, BSSE corrected). As expected, the energy for cation-anion separation in complex $\mathbf{4}_{\text{calc}}$ was found to be much larger (206.2 kcal/mol). The reaction $\mathbf{6}_{\text{calc}} \rightarrow 2 \mathbf{6m}_{\text{calc}}$ is exothermic by -10.6 kcal/mol (BSSE corrected). Most likely, the main contribution to the exothermicity is due to charge separation. Thus, this value must not be interpreted in terms of strength or weakness of hydrogen bonds in $\mathbf{6}_{\text{calc}}$.

2.4. In vitro cytotoxicity studies of $[\text{PtMe}_3(\text{bpy})(\text{L})][\text{BF}_4]$ ($\text{L} = \text{SCy-}\kappa\text{S}$, $\mathbf{4}$; 1-MeSCy- κS , $\mathbf{5}$)

The uncoordinated thionucleobases SCy (**2**) and 1-MeSCy (**3**) as well as the platinum(IV) complexes $[\text{PtMe}_3(\text{bpy})(\text{L})][\text{BF}_4]$ ($\text{L} = \text{SCy-}\kappa\text{S}$, **4**; 1-MeSCy- κS , **5**) were tested for cytotoxic activity in the human tumor cell lines anaplastic thyroid cancer 8505C, head and neck tumor A253 and FaDu, cervical cancer A431, lung carcinoma A549, ovarian cancer A2780 and colon carcinoma DLD-1, HCT-8 and HT-29, respectively. The free thionucleobases **2** and **3** show no activity in the investigated range of concentrations (0.1–125 μM). Complexes **4** and **5** express the dose-dependent antiproliferative action toward investigated target cell lines. The IC_{50} values for **4** and **5** are shown in Table 4. The similarity of these values indicates that the methyl group in 1-MeSCy in **5** has obviously no significant influence on the efficacy in all investigated cell lines except for DLD-1. The highest cytotoxic activity could be observed towards the ovarian cancer cell line A2780 (IC_{50} 6.80 μM (**4**) and 6.10 μM (**5**), respectively). For the cell lines 8505C, A253, A431, A549 and HCT-8 the IC_{50} values are in the range of 8.01–14.05 μM (**4**), revealing a moderate cytotoxic activity. The lowest efficacy was found towards FaDu, DLD-1 and HT-29. Compared to cisplatin the platinum(IV) complexes **4** and **5** are less active.



Scheme 3. Hydrogen bond and cation-anion interaction energies (in kcal/mol: calculated in the gas phase at 0 K) in type **4** and **6** complexes. For comparison the requisite value for 2-thiocytosine having the same hydrogen bond pattern as in the complexes is given (BSSE corrected values in parentheses).

Table 4
IC₅₀ (in μM)^a values for complexes **4**, **5**, and cisplatin^b

	4	5	Cisplatin ^b
8505C	9.45 ± 0.44	8.50 ± 0.34	5.00
A253	8.50 ± 0.34	8.01 ± 0.44	0.80
FaDu	21.99 ± 2.01	22.49 ± 2.00	1.20
A431	14.05 ± 0.59	13.67 ± 0.53	0.65
A549	9.56 ± 0.16	9.25 ± 0.14	1.50
A2780	6.80 ± 0.26	6.10 ± 0.35	0.55
DLD-1	31.39 ± 2.81	23.02 ± 1.66	5.00
HCT-8	12.53 ± 0.34	11.72 ± 0.29	1.50
HT-29	26.92 ± 2.21	26.95 ± 1.71	0.60

^a Mean values ± SD (standard deviation) from three experiments.

^b Values without SD.

2.5. Summary

The present investigations gave proof that platinum(IV) can form highly stable complexes with the thionucleobases 2-thiocytosine (SCy, **2**) and 1-methyl-2-thiocytosine (1-MeSCy, **3**). In both complexes, [PtMe₃(bpy)(L)][BF₄] (L = SCy-*r*-S, **4**; 1-MeSCy-*r*-S, **5**), the nucleobase ligand was found to be monodentately coordinated through the sulfur atom. Both NMR and structural studies gave proof that the complexes exhibit the configuration index OC-6-33. X-ray diffraction analyses revealed severe structural differences in the coordination of the nucleobase ligands such that the sulfur atoms in **4**·MeOH and **5** have to be regarded as sp³ and sp² hybridized, respectively.

3. Experimental

3.1. General considerations

Syntheses were performed under argon using standard Schlenk techniques. Solvents were dried (methanol over NaBH₄/iron(II)-phthalocyanine, diethyl ether and hexane over Na-benzophenone) and distilled prior to use. ¹H and ¹³C NMR spectra were obtained with Varian UNITY 500 and Gemini 2000 spectrometers using solvent signals as internal reference. Microanalyses were performed by the University of Halle microanalytical laboratory using CHNS-932 (LECO) and Vario EL (Elementaranalysensysteme) elemental analysers. 2-thiocytosine was commercially available from Aldrich. [PtMe₃l(bpy)] [25] and 1-methyl-2-thiocytosine [26] were prepared according to literature.

3.2. Synthesis of [PtMe₃(bpy)(L)][BF₄] (L = SCy, **4**; MeSCy, **5**)

A suspension of [PtMe₃l(bpy)] (70.0 mg, 0.13 mmol) in methanol (10 ml) and AgBF₄ (26.0 mg, 0.13 mmol) was stirred for 30 min in the absence of light. After filtration of Agl, 2-thiocytosine (15.0 mg, 0.13 mmol) and 1-methyl-2-thiocytosine (19.7 mg, 0.13 mmol), respectively, was added with stirring to the clear filtrate. After 2 h the solution was concentrated up to ca 1 ml and ether (3 ml) was added. The yellow precipitate formed was filtered, washed with pentane (3 ml) and dried in vacuum.

Complex **4**. Yield: 28 mg (62%). Anal. Calc. for C₁₇H₂₂BF₄N₅Spt (610.13): C, 33.44; H, 3.63. Found: C, 32.82; H, 4.02%. ¹H NMR (400 MHz, CD₃OD): δ 8.96 (m, 2H, H6/H6' of bpy), 8.55 (d, 2H, H3/H3' of bpy), 8.20 (m, 2H, H4/H4' of bpy), 7.75 (m, 2H, H5/H5' of bpy), 7.28 (d, 1H, ³J_{H,H} = 7.06 Hz, H6 of SCy), 5.97 (d, 1H, ³J_{H,H} = 7.06 Hz, H5 of SCy), 1.22 (s + d, 6H, ²J_{Pt,H} = 69.30 Hz, PtCH₃ *trans* to N_{bpy}), 0.45 (s + d, 3H, ²J_{Pt,H} = 69.72 Hz, PtCH₃ *trans* to S). ¹H NMR (400 MHz, DMSO-*d*₆): δ 12.37 (s, br, 1H, NH of SCy), 8.95 (m, 2H, H6/H6' of bpy), 8.67 (d, 2H, H3/H3' of bpy), 8.24 (m, 2H, H4/H4' of bpy), 7.98 (s, br, NH₂ of SCy), 7.77 (m, 2H, H5/H5' of

bpy), 7.40 (s, br, NH₂ of SCy), 7.36 (d, 1H, ³J_{H,H} = 7.06 Hz, H6 of SCy), 5.91 (d, 1H, ³J_{H,H} = 7.06 Hz, H5 of SCy), 1.15 (s + d, 6H, ²J_{Pt,H} = 69.36 Hz, PtCH₃ *trans* to N_{bpy}), 0.35 (s + d, 3H, ²J_{Pt,H} = 68.92 Hz, PtCH₃ *trans* to S). ¹³C NMR (100 MHz, CD₃OD): δ 174.7 (s, C2 of SCy), 164.2 (s, C4 of SCy), 156.0 (s, C2/C2' of bpy), 148.4 (s, ²J_{Pt,C} = 14.6 Hz, C6/C6' of bpy), 143.4 (s, C6 of SCy), 140.6 (s, C4/C4' of bpy), 127.8 (s, ³J_{Pt,C} = 14.2 Hz, C5/C5' of bpy), 124.9 (s, C3/C3' of bpy), 99.6 (s, C5 of SCy), 2.6 (s + d, ¹J_{Pt,C} = 642.06 Hz, PtCH₃ *trans* to S), -4.9 (s + d, ¹J_{Pt,C} = 669.91 Hz, PtCH₃ *trans* to N).

Complex **5**. Yield: 35 mg (41%). Anal. Calc. for C₁₈H₂₄BF₄N₅Spt (624.14): C, 34.61; H, 3.88. Found: C, 35.21; H, 4.46%. ¹H NMR (400 MHz, CD₃OD): δ 9.05 (m, 2H, H6/H6' of bpy), 8.57 (d, 2H, H3/H3' of bpy), 8.21 (m, 2H, H4/H4' of bpy), 7.76 (m, 2H, H5/H5' of bpy), 7.58 (d, 1H, ³J_{H,H} = 7.26 Hz, H6 of 1-MeSCy), 6.00 (d, 1H, ³J_{H,H} = 7.26 Hz, H5 of 1-MeSCy), 3.46 (s, 3H, NCH₃), 1.25 (s + d, 6H, ²J_{Pt,H} = 69.10 Hz, PtCH₃ *trans* to N), 0.47 (s + d, 3H, ²J_{Pt,H} = 69.31 Hz, PtCH₃ *trans* to S). ¹H NMR (400 MHz, DMSO-*d*₆): δ 9.04 (m, 2H, H6/H6' of bpy), 8.67 (d, 2H, H3/H3' of bpy), 8.25 (m, 2H, H4/H4' of bpy), 7.92 (s, br, NH₂ of 1-MeSCy), 7.78 (m, 2H, H5/H5' of bpy), 7.71 (d, 1H, ³J_{H,H} = 7.06 Hz, H6 of 1-MeSCy), 7.31 (s, br, NH₂ of 1-MeSCy), 6.00 (d, 1H, ³J_{H,H} = 7.06 Hz, H5 of 1-MeSCy), 3.34 (s, 3H, NCH₃ of 1-MeSCy), 1.18 (s + d, 6H, ²J_{Pt,H} = 68.89 Hz, PtCH₃ *trans* to N_{bpy}), 0.37 (s + d, 3H, ²J_{Pt,H} = 68.89 Hz, PtCH₃ *trans* to S). ¹³C NMR (50 MHz, CD₃OD): δ 176.7 (s, C2 of 1-MeSCy), 162.7 (s, C4 of 1-MeSCy), 148.9 (s, C6/C6' of bpy), 148.6 (s, C6 of 1-MeSCy), 140.8 (s, C4/C4' of bpy), 127.9 (s, ³J_{Pt,C} = 12.71 Hz C5/C5' of bpy), 125.0 (s, C3/C3' of bpy), 100.3 (s, C5 of 1-MeSCy), 44.3 (s, NCH₃), 2.7 (s + d, ¹J_{Pt,C} = 649.50 Hz, PtCH₃ *trans* to S), -4.7 (s + d, ¹J_{Pt,C} = 669.26 Hz, PtCH₃ *trans* to N).

3.3. X-ray crystallography

Single crystals of **4**·MeOH and **5** suitable for X-ray diffraction measurements were obtained by crystallization from methanol/diethyl ether/*n*-pentane (1/1/1) at 4 °C and were taken directly out of the respective solution. Intensity data were collected on a STOE IPDS diffractometer with Mo K α radiation (λ = 0.71073 Å, graphite monochromator) at 220(2) K. An empirical absorption correction using ψ -scans was applied (**4**·MeOH: $T_{\text{min}}/T_{\text{max}}$ 0.15/0.43; **5**: $T_{\text{min}}/T_{\text{max}}$ 0.07/0.38). Both structures were solved by direct methods with SHELXS-97 [27] and refined using full-matrix least-square routines against F^2 with SHELXL-97 [27]. Non-hydrogen atoms were refined with anisotropic displacement parameters. Hydrogen atoms were included in calculated positions and refined with isotropic displacement parameters according to the "riding model". Three fluorine atoms of the tetrafluoroborate anions in complex **5** are disordered over two positions and each group (F2, F3, F4 and F2A, F3A, F4A) was refined with a concerted occupation factor of 55.9% and 44.1%, respectively. Details of crystal data, data collection and refinement parameters are given in Table 5.

3.4. Quantum chemical calculations

All DFT calculations were carried out by the GAUSSIAN 98/GAUSSIAN 03 program package [28] using the hybrid functional B3LYP [29]. For the main group atoms the basis set 6-31G(d) was employed as implemented in the GAUSSIAN program. The valence shell of platinum has been approximated by split valence basis sets too; for their core orbitals effective core potentials in combination with consideration of relativistic effects have been used [30]. Mono- and dinuclear species have been fully optimized without any symmetry restrictions and in C_v symmetry, respectively. The resulting geometries were characterized as equilibrium structures by the analysis of the force constants of the normal vibrations. Basis set superposition errors (BSSE) were estimated with counterpoise type calculations [31].

Table 5
Crystal data, data collection and refinement parameters of **4** · MeOH and **5**

	4 · MeOH	5
Empirical formula	C ₁₈ H ₂₆ BF ₄ N ₅ O ₂ PtS	C ₁₈ H ₂₄ BF ₄ N ₅ PtS
Formula weight	642.40	624.38
Crystal system/space group	monoclinic/ <i>P</i> 2 ₁ / <i>n</i>	monoclinic/ <i>C</i> 2/ <i>c</i>
Z	4	8
<i>a</i> (Å)	14.097(3)	23.478(2)
<i>b</i> (Å)	9.233 (1)	9.4462(8)
<i>c</i> (Å)	17.791(4)	20.141(2)
β (°)	99.83(3)	100.26(1)
<i>V</i> (Å ³)	2281.6(8)	4395.5(7)
ρ (g cm ⁻³)	1.870	1.887
μ (Mo K α) (mm ⁻¹)	6.293	6.528
<i>F</i> (000)	1248	2416
Scan range (°)	2.2 < θ < 25.9	2.4 < θ < 25.9
Reciprocal lattice segments <i>h</i> , <i>k</i> , <i>l</i>	-17 → 17 -11 → 11 -21 → 20	-28 → 28 -7 → 11, -23 → 21
Reflections collected	17 111	11 172
Reflections independent (<i>R</i> _{int})	4435 (0.1981)	4064 (0.0951)
Data/restraints/parameters	4435/0/285	4064/7/304
Goodness-of-fit on <i>F</i> ²	0.859	1.120
<i>R</i> ₁ , <i>wR</i> ₂ [<i>I</i> > 2 σ (<i>I</i>)]	0.0478, 0.1284	0.0339, 0.0883
<i>R</i> ₁ , <i>wR</i> ₂ (all data)	0.0640, 0.1425	0.0379, 0.0946
Largest difference peak and hole (e Å ⁻³)	1.086 and -3.115	1.493 and -2.016

3.5. *In vitro* studies

Stock solutions of investigated platinum complexes and reference compound cisplatin were made in dimethyl sulfoxide (DMSO) at concentration of 20 mM and diluted by nutrient medium to various working concentrations. Nutrient medium was RPMI-1640 (PAA Laboratories) supplemented with 10% fetal bovine serum (Biochrom AG) and penicillin/streptomycin (PAA Laboratories).

3.5.1. Cell cultures

The human tumor cell lines anaplastic thyroid cancer 8505C, head and neck tumor A253 and FaDu, cervical cancer A431, lung carcinoma A549, ovarian cancer A2780, colon carcinoma DLD-1, HCT-8 and HT-29 were cultivated in the Biozentrum, Martin-Luther-University Halle-Wittenberg. All cells were maintained as monolayers in nutrient medium in a humidified atmosphere with 5% CO₂.

3.5.2. Cytotoxicity assay

The cytotoxic activity of the platinum compounds was measured by the sulforhodamine-B (SRB) assay [32]. In brief, exponentially growing cells were seeded into 96-well plates and 24 h later, after the cell adherence, nine different concentrations of investigated compounds were added to the wells. The final concentrations were in the range from 0.1 to 125 μ M. All experiments were done in triplicate. Nutrient medium with corresponding concentrations of compounds, but void of cells was used as blank. Five days after seeding the cells were fixed with 10% trichloroacetic acid and processed according to the published SRB assay protocol. Absorbance was measured at 570 nm using a 96-well plate reader (SpectraFluor Plus Tecan, Germany) and the percentages of surviving cells relative to untreated controls were determined. Concentration IC₅₀ was determined as the concentration of a drug that inhibited cell survival by 50%, compared with vehicle-treated control.

Acknowledgments

Financial support from the Deutsche Forschungsgemeinschaft and gifts of chemicals by Merck (Darmstadt) is gratefully acknowledged.

Appendix A. Supplementary material

CCDC 671762 and 671763 contain the supplementary crystallographic data for **4** · MeOH and **5**. These data can be obtained free of charge from The Cambridge Crystallographic Data Centre via www.ccdc.cam.ac.uk/data_request/cif. Tables of Cartesian coordinates of atom positions calculated for the equilibrium structures of the base-paired dinuclear complex **4**, the cation $\{[\text{PtMe}_3(\text{bpy})(\text{SCy}-\kappa\text{S})]_2\}^{2+}$ (**6**_{calc.}), the dimeric 2-thiocytosine (SCy)₂ and the requisite monomolecular species. Supplementary data associated with this article can be found, in the online version, at [doi:10.1016/j.ica.2008.03.085](https://doi.org/10.1016/j.ica.2008.03.085).

References

- [1] J. Carbon, L. Hung, D.S. Jones, Proc. Natl. Acad. Sci. USA 53 (1965) 979.
- [2] M.N. Lipsett, J. Biol. Chem. 240 (1965) 3975.
- [3] J. Carbon, H. David, M.H. Studier, Science 161 (1968) 1146.
- [4] D.H. Gauss, M. Sprinzl, Nucleic Acids Res. 11 (1983) r1.
- [5] Y. Yamada, M. Saneyoshi, S. Nishimura, H. Ishikura, FEBS Lett. 7 (1970) 207.
- [6] R.K. Ralph, R.E.F. Matthews, A.I. Matus, Biochim. Biophys. Acta 108 (1965) 53.
- [7] W.V. Ruyle, T.Y. Shen, J. Med. Chem. 10 (1967) 331, and references therein.
- [8] H. Rostkowska, M.J. Nowak, L. Lapinski, M. Bretner, T. Kulikowski, A. Leś, L. Adamowicz, Biochim. Biophys. Acta 1172 (1993) 239, and references therein.
- [9] B. Rosenberg, L. Van Camp, T. Krigas, Nature 205 (1965) 698.
- [10] G. Cervantes, S. Marchal, M.J. Prieto, J.M. Pérez, V.M. González, C. Alonso, V. Moreno, J. Inorg. Biochem. 77 (1999) 197.
- [11] M. Carrara, T. Berti, S. D'Ancona, V. Cherchi, L. Sindellari, Anticancer Res. 17 (1997) 975.
- [12] G. Cervantes, M.J. Prieto, V. Moreno, Met.-Based Drugs 4 (1997) 9.
- [13] M.D. Hall, T.W. Hambley, Coord. Chem. Rev. 232 (2002) 49.
- [14] (a) L. Kelland, Nat. Rev. Cancer 7 (2007) 573;
(b) G. Cavaletti, Nat. Rev. Cancer 8 (2008) 71.
- [15] J. Reedijk, Platinum Metals Rev. 52 (2008) 2.
- [16] (a) B.T. Khan, S.M. Zakeeruddin, Trans. Met. Chem. 16 (1991) 119;
(b) B.T. Khan, K. Annapurna, S. Shamsuddin, K. Najmuddin, Polyhedron 11 (1992) 2109;
(c) J. Jolley, W.I. Cross, R.G. Pritchard, C.A. McAuliffe, K.B. Nolan, Inorg. Chim. Acta 315 (2001) 36.
- [17] C. Vetter, C. Wagner, J. Schmidt, D. Steinborn, Inorg. Chim. Acta 359 (2006) 4326.
- [18] S. Furberg, L.H. Jensen, Acta Crystallogr., Sect. B 26 (1970) 1260.
- [19] Cambridge Structural Database (CSD), Cambridge Crystallographic Data Centre, University Chemical Laboratory, Cambridge (England).
- [20] C. Janiak, Dalton Trans. (2000) 3885.
- [21] C. Vetter, C. Wagner, D. Steinborn, unpublished results.
- [22] H. Rostkowska, M.J. Nowak, L. Lapinski, M. Bretner, T. Kulikowski, A. Leś, L. Adamowicz, Spectrochim. Acta, Part A 49 (1993) 551.
- [23] P.Ú. Cívrcir, J. Phys. Org. Chem. 14 (2001) 171.
- [24] G.A. Jeffrey, An Introduction to Hydrogen Bonding, Oxford University Press, Oxford, 1997.
- [25] D.E. Clegg, J.R. Hall, G.A. Swile, J. Organomet. Chem. 38 (1972) 403.
- [26] D.J. Brown, B.T. England, J. Chem. Soc. C (1971) 2507.
- [27] G.M. Sheldrick, SHELXS-97, SHELXL-97, Programs for Crystal Structure Determination, University of Göttingen, Göttingen, 1990/1997.
- [28] M.J. Frisch, G.W. Trucks, H.B. Schlegel, G.E. Scuseria, M.A. Robb, J.R. Cheeseman, V.G. Zakrzewski, J.A. Montgomery Jr., R.E. Stratmann, J.C. Burant, S. Dapprich, J.M. Millam, A.D. Daniels, K.N. Kudin, M.C. Strain, O. Farkas, J. Tomasi, V. Barone, M. Cossi, R. Cammi, B. Mennucci, C. Pomelli, C. Adamo, S. Clifford, J. Ochterski, G.A. Petersson, P.Y. Ayala, Q. Cui, K. Morokuma, D.K. Malick, A.D. Rabuck, K. Raghavachari, J.B. Foresman, J. Cioslowski, J.V. Ortiz, B.B. Stefanov, G. Liu, A. Liashenko, P. Piskorz, I. Komaromi, R. Gomperts, R.L. Martin, D.J. Fox, T. Keith, M.A. Al-Laham, C.Y. Peng, A. Nanayakkara, C. Gonzalez, M. Challacombe, P.M.W. Gill, B. Johnson, W. Chen, M.W. Wong, J.L. Andres, C. Gonzalez, M. Head-Gordon, E.S. Replogle, J.A. Pople, GAUSSIAN 98 (Revision A.9)/GAUSSIAN 03 (Revision C.02), Gaussian Inc., Pittsburgh, PA, 1998/Wallingford CT, 2004.
- [29] (a) A.D. Becke, Phys. Rev. A 38 (1988) 3098;
(b) A.D. Becke, J. Chem. Phys. 98 (1993) 5648;
(c) C. Lee, W. Yang, R.G. Parr, Phys. Rev. B 37 (1988) 785;
(d) P.J. Stephens, F.J. Devlin, C.F. Chabalowski, M.J. Frisch, J. Phys. Chem. 98 (1994) 11623.
- [30] D. Andrae, U. Häußermann, M. Dolg, H. Stoll, H. Preuss, Theor. Chim. Acta 77 (1990) 123.
- [31] S.F. Boys, F. Bernardi, Mol. Phys. 19 (1970) 553.
- [32] P. Skehan, R. Storeng, D. Scudiero, A. Monks, J. McMahon, D. Vistica, J.T. Warren, H. Bokesch, S. Kenney, M.R. Boyd, J. Natl. Cancer Inst. 82 (1990) 1107.



Contents lists available at ScienceDirect

Inorganica Chimica Acta

journal homepage: www.elsevier.com/locate/ica

Synthesis, characterization and *in vitro* cytotoxicity studies of platinum(IV) complexes with thiouracil ligands

Cornelia Vetter^a, Goran N. Kaluđerović^{a,b}, Reinhard Paschke^c, Ralph Kluge^a, Jürgen Schmidt^d, Dirk Steinborn^{a,*}

^a Institut für Chemie – Anorganische und Organische Chemie, Martin-Luther-Universität Halle-Wittenberg, D-06120, Halle, Kurt-Mothes-Straße 2, Germany

^b Department of Chemistry, Institute of Chemistry, Technology and Metallurgy, University of Belgrade, Studentski trg 14, 11000 Belgrade, Serbia

^c Biozentrum, Martin-Luther-Universität Halle-Wittenberg, D-06120, Halle, Weinbergweg 22, Germany

^d Leibniz-Institut für Pflanzenbiochemie, D-06120, Halle, Weinberg 3, Germany

ARTICLE INFO

Article history:

Received 25 January 2010

Received in revised form 23 March 2010

Accepted 31 March 2010

Available online 9 April 2010

Keywords:

Platinum(IV) complexes

Thionucleobases

Thionucleobase complexes

In vitro cytotoxic studies

DFT calculations

ABSTRACT

Reactions of $[\text{PtMe}_3(\text{bpy})(\text{Me}_2\text{CO})][\text{BF}_4]$ (**2**) with the thionucleobases 2-thiouracil ($s^2\text{Ura}$), 4-thiouracil ($s^4\text{Ura}$) and 2,4-dithiouracil ($s^2s^4\text{Ura}$) resulted in the formation of complexes of the type $[\text{PtMe}_3(\text{bpy})(\text{L}-\kappa\text{S})][\text{BF}_4]$ ($\text{L} = s^2\text{Ura}$, **3**; $s^4\text{Ura}$, **4**; $s^2s^4\text{Ura}$, **5**). The complexes were characterized by NMR spectroscopy (^1H , ^{13}C , ^{195}Pt), IR spectroscopy as well as microanalyses. The coordination through the C4=S groups (**4**, **5**) was additionally confirmed by DFT calculations, where it was shown that these complexes $[\text{PtMe}_3(\text{bpy})(\text{L}-\kappa\text{S}^4)]^+$ ($\text{L} = s^4\text{Ura}$, $s^2s^4\text{Ura}$) are about 5.8 (**4b**) and 3.3 kcal/mol (**5b**), respectively, more stable than the respective complexes, having thiouracil ligands bound through the C2=X groups ($\text{X} = \text{O}$, **4a**; **5**, **5a**). For $[\text{PtMe}_3(\text{bpy})(s^2\text{Ura}-\kappa\text{S}^2)][\text{BF}_4]$ (**3**) no preferred coordination mode could be assigned solely based on DFT calculations. Analysis of NMR spectra showed the κS^2 coordination. *In vitro* cytotoxic studies of complexes **3–5** on nine different cell lines (8505C, A253, FaDu, A431, A549, A2780, DLD-1, HCT-8, HT-29) revealed in most cases moderate activities. However, **3** and **5** showed significant activity towards A549 and A2780, respectively, possessing IC_{50} values comparable to those of cisplatin. Cell cycle perturbations and trypan blue exclusion test on cancer cell line A431 using $[\text{PtMe}_3(\text{bpy})(s^2s^4\text{Ura}-\kappa\text{S}^4)][\text{BF}_4]$ (**5**) showed induction of apoptotic cell death. Furthermore, the reaction of $[\text{PtMe}_3(\text{OAc}-\kappa^2\text{O},\text{O})(\text{Me}_2\text{CO})]$ (**6**) with 4-thiouracil yielded the dinuclear complex $[(\text{PtMe}_3)_2(\mu-s^4\text{Ura}-\eta)_2]$ (**7**), which has been characterized by microanalysis, NMR (^1H , ^{13}C , ^{195}Pt) and IR spectroscopy as well as ESI mass spectrometry. X-ray diffraction analysis of crystals yielded in an isolated case exhibited the presence of a hexanuclear thiouracilato platinum(IV) complex, possessing each three different kinds of methyl platinum(IV) moieties and 4-thiouracilato ligands. This exhibited the ability of 4-thiouracil platinum(IV) complexes to form multinuclear complexes.

© 2010 Elsevier B.V. All rights reserved.

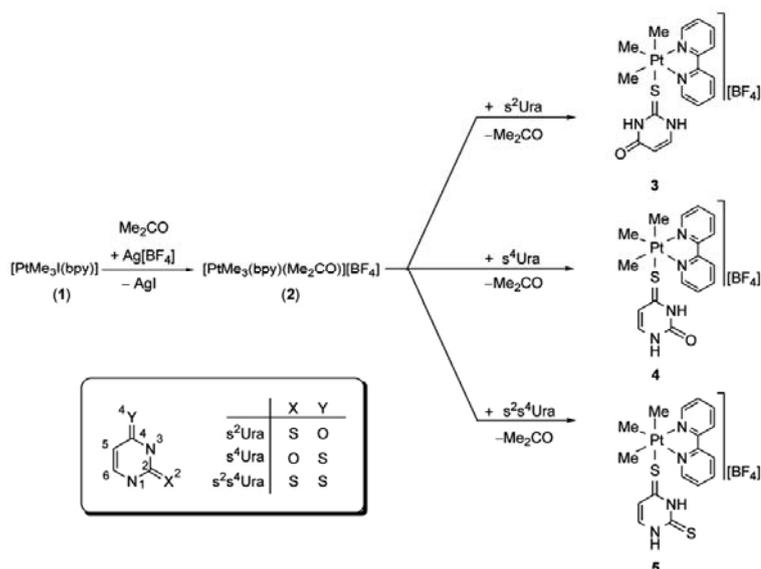
1. Introduction

Since the first isolation of 2-thiouracil by Carbon in 1965 and the findings that thiouracils are minor compounds of tRNA in *Escherichia coli* bacteria and mammalian tissues [1], there has been a growing interest in the study of thionucleobases, their biological activities and their coordination modes in metal complexes. Because of their similarity to the oxygen analogues, the biological activity of thionucleobases is mainly based on inhibitory properties. Thus, they act as antimetabolites and interfere with metabolic processes in multiple ways, including incorporation into DNA and RNA and suppression of protein and glycoprotein syntheses [2]. There is a wide field of potential applications for thiouracils and

their derivatives ranging from therapeutics [3] and cancerostatics [4] up to the use as radiotracers [5]. Metal complexes are also of great interest in bioinorganic chemistry. Gold(I) complexes with thioguanine and 2-thiouracil ligands showed antiarthritic and anti-tumor activities, comparable to the established drugs Auranofin and cisplatin, respectively [6].

Especially platinum complexes are in the focus of research since the discovery of the cancerostatic properties of cisplatin by Rosenberg [7]. Up to now thousands of platinum complexes have been tested, but only few entered clinical trials [8]. Platinum(IV) complexes have attracted significant attention due to their kinetic inertness and the resulting possibility of oral administration. Today it is believed that platinum(IV) cancerostatics are just the prodrugs, being reduced to platinum(II) species in the organism [9], although it has been shown that Pt(IV) complexes can interact with DNA without reduction leading to cancerostatic effects

* Corresponding author. Tel.: +49 345 5525620; fax: +49 345 55227028.
E-mail address: dirk.steinborn@chemie.uni-halle.de (D. Steinborn).



Scheme 1. Syntheses of the complexes $[PtMe_3(bpy)(L-\kappa S)](BF_4)$ ($L = s^2Ura$, **3**; s^4Ura , **4**; s^2s^4Ura , **5**).

[10,11]. From a coordination chemistry perspective, thionucleobases are interesting ligands because of their multiple donor sites and their various tautomeric forms. Thus, getting control over the coordination mode is still a challenge which can be achieved by a proper selection of the metal complex fragment and/or by blocking donor sites at the ligand by means of derivatization. Here we report the synthesis and characterization of platinum(IV) complexes with thiouracil ligands and the examination of their cytotoxic properties.

2. Results and discussion

2.1. Syntheses and NMR spectroscopic characterization of mononuclear thiouracil platinum(IV) complexes

The reaction of $[PtMe_3(bpy)]$ (**1**) with silver tetrafluoroborate in acetone led to the formation of $[PtMe_3(bpy)(Me_2CO)](BF_4)$ (**2**). Complex **2** was found to react with stoichiometric amounts of 2-thiouracil (s^2Ura), 4-thiouracil (s^4Ura) and 2,4-dithiouracil (s^2s^4Ura) yielding the ionic complexes $[PtMe_3(bpy)(L-\kappa S)](BF_4)$ ($L = s^2Ura$, **3**; s^4Ura , **4**; s^2s^4Ura , **5**) (Scheme 1). The compounds were isolated as yellow moderately airstable and hygroscopic substances in yields of 54–68%. Their identities were confirmed by microanalyses, 1H , ^{13}C and ^{195}Pt NMR spectroscopy as well as by IR spectroscopy. NMR spectroscopic measurements (see Table 1 for selected data) gave proof of the 1:1 ($PtMe_3 : L$) constitution of the complexes **3–5**. The 1H NMR spectra of **3–5** showed broad resonances in a range of 11.0–12.2 ppm for the N–H protons. Thus, the thiouracil ligands are present in their oxothione (**3**, **4**) and dithione (**5**) tautomeric form, respectively.

The comparison of the coordination induced shifts (CIS's) of the thiouracil ligands (see Table 1) showed oppositional trends for complex **3** compared to the complexes **4** and **5**, in particular for the signals of C5/H5 and C6/H6. While a downfield shift¹ for C5/H5 of $-5.1/-0.19$ ppm is observed in $[PtMe_3(bpy)(s^2Ura-\kappa S^2)](BF_4)$

(**3**), the appropriate signals in $[PtMe_3(bpy)(s^4Ura-\kappa S^4)](BF_4)$ (**4**) and $[PtMe_3(bpy)(s^2s^4Ura-\kappa S^2)](BF_4)$ (**5**) showed a highfield shift in the same order of magnitude ($+4.9...+5.6/+0.07...+0.10$ ppm). Furthermore, for the resonances of C6/H6 in complex **3** no remarkable coordination induced shifts ($-0.1/+0.06$ ppm) were found, whereas significant CIS's to lower field ($-6.4...-7.2/-0.26...-0.35$ ppm) could be observed for complexes **4** and **5**. This indicated a different coordination mode of s^2Ura in complex **3** (κS^2) than for s^4Ura and s^2s^4Ura in complexes **4** and **5** (κS^4).

The coupling constants $^1J_{Pt,C}$ of the methyl ligands *trans* to the thiouracil ligands can be regarded to be a measure for their *trans* influence [12]. The markedly higher $^1J_{Pt,C}$ coupling constant in complex **3** (673.7 Hz) compared with those in complexes **4** (651.5 Hz) and **5** (649.5 Hz) showed unambiguously the *trans* influence order $s^2Ura-\kappa S^2 < s^4Ura-\kappa S^4 \approx s^2s^4Ura-\kappa S^2$. Obviously, this is due to the two electronegative N atoms attached to the C2=S group in the $s^2Ura-\kappa S^2$ ligand. Furthermore, the very close values in complexes **4** and **5** (651.5/649.5 Hz) indicated, that the non-coordinated C2=O/C2=S group does not affect the *trans* influence significantly.

Table 1

Selected 1H and ^{13}C NMR spectroscopic data (δ in ppm, J in Hz) of complexes $[PtMe_3(bpy)(L-\kappa S)](BF_4)$ (**3–5**) in acetone- d_6 .

L	s^2Ura (3)	s^4Ura (4)	s^2s^4Ura (5)
δ_H ($^2J_{Pt,H}$)			
CH ₃ <i>trans</i> to L	0.69 (73.7)	0.67 (71.0)	0.67 (71.1)
CH ₃ <i>trans</i> to N	1.23 (68.1)	1.29 (68.5)	1.29 (68.5)
δ_C ($^1J_{Pt,C}$)			
CH ₃ <i>trans</i> to L	3.2 (673.7)	3.8 (651.5)	4.2 (649.5)
CH ₃ <i>trans</i> to N	-5.0 (667.0)	-5.3 (666.4)	-5.5 (664.5)
$\Delta\delta_H$ [$\Delta\delta_C^a$]			
C2 ^b	+2.4	+1.0	+1.3
C4	+1.0	+3.2	+4.7
C5/H5	-5.1/-0.19	+4.9/+0.10	+5.6/+0.07
C6/H6	-0.1/+0.06	-7.2/-0.35	-6.4/-0.26

^a Coordination induced shifts (CIS's). Downfield/highfield shifts upon coordination are referred as negative/positive values.

^b See numbering scheme in Scheme 1.

¹ Downfield/highfield shifts upon coordination are referred as negative/positive values.

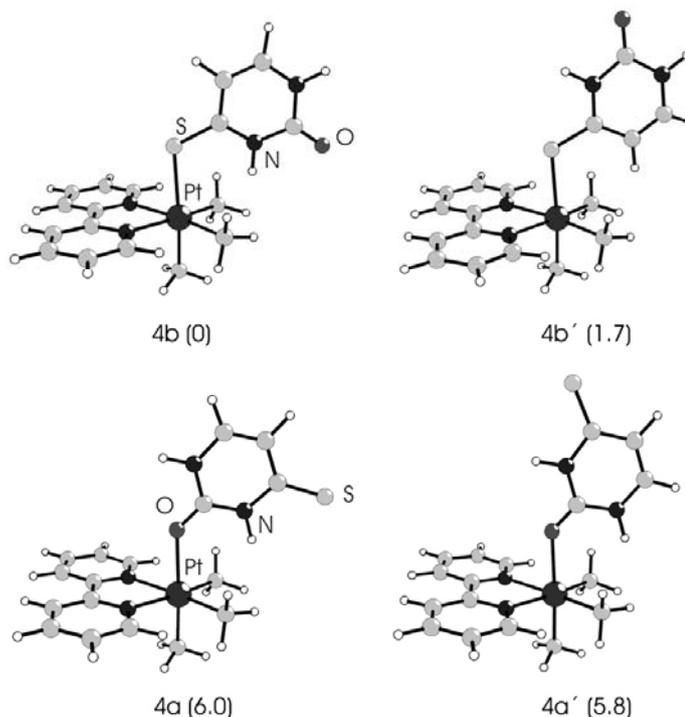


Fig. 1. Calculated equilibrium structures of the cationic complexes $[\text{PtMe}_3(\text{bpy})(\text{s}^4\text{Ura}-\kappa\text{S}^4)]^+$ (**4b**, **4b'**) and $[\text{PtMe}_3(\text{bpy})(\text{s}^2\text{s}^4\text{Ura}-\kappa\text{O}^2)]^+$ (**4a**, **4a'**). ΔG values are given in parentheses regarding to **4b** as the most stable complex.

Comparison to analogous $[\text{PtMe}_3(\text{bpy})(\text{L}-\kappa\text{S})][\text{BF}_4]$ complexes having S bound thioctyosine [13] and thiourea derivative ligands [14] ($\nu_{\text{Pt-C}}$: 642.1–658.0 Hz) exhibits a similar donor strength like s^4Ura and $\text{s}^2\text{s}^4\text{Ura}$.

2.2. Quantum chemical calculations

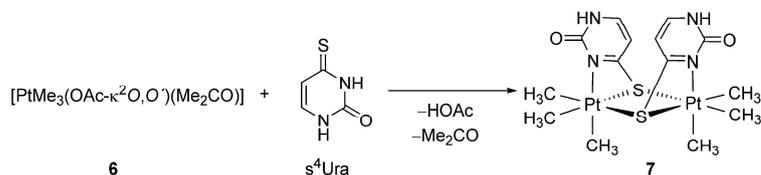
DFT calculations using the hybrid functional B3LYP and high-quality 6-311G(d,p) basis sets for all main group atoms as well as a pseudopotential considering relativistic effects and a double ζ basis set for Pt (see Section 4) were performed to get insight into the $\text{C}2=\text{X}$ versus $\text{C}4=\text{Y}$ (X, Y = S, O) coordination in complexes $[\text{PtMe}_3(\text{bpy})(\text{L})]^+$ (L = s^2Ura , **3a/b**, s^4Ura , **4a/b**; $\text{s}^2\text{s}^4\text{Ura}$, **5a/b**). In the following the platinum complexes with thiouracil ligands coordinated through $\text{C}2=\text{X}$ and $\text{C}4=\text{Y}$ groups are assigned as **3a–5a** and **3b–5b**, respectively. For each complex and coordination mode two equilibrium structures were found where the non-coordinated exocyclic heteroatom groups (C=O/C=S) are either pointing towards the equatorial PtC_2N_2 complex plane or away from it. The latter ones are marked with a dash, see Fig. 1 for an example. In all complexes the respective thiouracil ligand is (almost) perpendicularly arranged to the $[\text{PtC}_2\text{N}_2]$ complex plane (interplanar angles: 86.6–90.0°) and approximately bisecting the C–Pt–C angle of this plane.

The relative energies and free enthalpies of all calculated equilibrium structures are given in Table 2. Both of them go closely parallel and in the following only the free enthalpies are discussed. In type **4** and **5** complexes those having κS^4 coordinated ligands where the non-coordinated $\text{C}2=\text{X}$ groups point towards the

$[\text{PtC}_2\text{N}_2]$ plane (**4b**, **5b**) are the most stable complexes. The conformers where the non-coordinated $\text{C}2=\text{X}$ groups point away from the $[\text{PtC}_2\text{N}_2]$ plane (**4b'**, **5b'**) are slightly less stable by 1.7 and 2.1 kcal/mol, respectively. The coordination via the $\text{C}2=\text{O}$ (**4a/a'**) and $\text{C}2=\text{S}$ (**5a/a'**) group, respectively, results in complexes with higher ΔG values (5.8, **4a'**; 3.3 kcal/mol, **5a**). Contrary to that, the 2-thiouracil complexes (**3a/a'**, **3b/b'**) showed no significant differences of the free enthalpies ($\Delta G \leq 0.5$ kcal/mol). Obviously, the donor strength of the $\text{C}2=\text{S}$ group of s^2Ura is lowered by the two vicinal electron withdrawing nitrogen atoms to such an extent that it is comparable with the $\text{C}4=\text{O}$ group.

Table 2
Coordination modes of the ligands, relative energies E_{rel} and free enthalpies ΔG (in kcal/mol) of calculated complexes $[\text{PtMe}_3(\text{bpy})(\text{L})]^+$ with thiouracil ligands.

Complex	Donor group	E_{rel}	ΔG
<i>L = s²Ura</i>			
3a	C2=S (κS^2)	0	0
3a'	C2=S (κS^2)	0.5	0.5
3b	C4=O (κO^4)	0.5	0.4
3b'	C4=O (κO^4)	0.6	0.5
<i>L = s⁴Ura</i>			
4b	C4=S (κS^4)	0	0
4b'	C4=S (κS^4)	1.7	1.7
4a	C2=O (κO^2)	5.8	6.0
4a'	C2=O (κO^2)	5.5	5.8
<i>L = s²s⁴Ura</i>			
5b	C4=S (κS^4)	0	0
5b'	C4=S (κS^4)	1.4	2.1
5a	C2=S (κS^2)	2.6	3.3
5a'	C2=S (κS^2)	2.8	3.4



Scheme 2. Synthesis of the dinuclear complex $[(\text{PtMe}_3)_2(\mu\text{-s}^4\text{Ura-H})_2]$ (7).

2.3. Syntheses and spectroscopical characterization of di- and hexanuclear 4-thiouracilato complexes

Reaction of $[\text{PtMe}_3(\text{OAc-}\kappa^2\text{O,O}')(\text{Me}_2\text{CO})]$ (**6**) and 4-thiouracil (s^4Ura) led to the formation of the dinuclear complex $[(\text{PtMe}_3)_2(\mu\text{-s}^4\text{Ura-H})_2]$ (**7**) (Scheme 2). The complex was isolated as yellow, airstable powder in a yield of 70%. The identity of the complex was confirmed by microanalysis, IR spectroscopy, ^1H , ^{13}C and ^{195}Pt NMR spectroscopy and ESI mass spectrometry. Selected NMR spectroscopic data and the chemical induced shifts of $[(\text{PtMe}_3)_2(\mu\text{-s}^4\text{Ura-H})_2]$ (**7**) are arranged in Table 3. The relative intensities of the signals in the ^1H NMR spectrum gave proof of an 1:1 complex ($\text{PtMe}_3\text{:s}^4\text{Ura-H}$). Furthermore, only one N–H proton could be found, showing the presence of monodeprotonated thiouracilato ligands. One signal set each for C5/H5 and C6/H6 indicated an identical binding of the two $\text{s}^4\text{Ura-H}$ ligands. The most

remarkable CIS's were observed for H5 (+0.20 ppm) and H6 (−0.39 ppm), as well as for C6 (−7.1 ppm).

The methyl protons and carbon atoms of the PtMe_3 moiety showed three singlets flanked by platinum satellites. Interestingly, the two signals positioned closely together both in the ^1H (0.98/1.06 ppm) and ^{13}C NMR spectra (1.1/3.1 ppm) are not correlating with each other (Table 3). Thus, they must not be assigned to the two methyl groups in *trans* position to the $\mu\text{-S}$ atoms. As for other complexes of the type $[(\text{PtMe}_3)_2(\mu\text{-S-N})_2]$ (S–N = N,S heterocyclic ligand) [15], a definite assignment can not be made, even when the magnitudes of the $^1J_{\text{Pt,C}}$ coupling constants are taken into account.

High resolution ESI-MS experiments were performed using methanol solutions (Fig. 2). The full scan mass spectra of the negative ESI mass spectrum showed several peaks among them the peak for the deprotonated dinuclear complex $[(\text{PtMe}_3)_2(\mu\text{-s}^4\text{Ura-H})_2\text{-H}]^-$ at 733.0578 m/z (calcd.: 733.0558 m/z) showing an isotopic envelope in good agreement with the calculated one. Furthermore, other peaks could be identified as monodeprotonated fragments of tri-, tetra- and pentanuclear species $[(\text{PtMe}_3)_n(\mu\text{-s}^4\text{Ura-H})_n\text{-H}]^-$ ($n = 3\text{--}5$), whereas the peak of the tetranuclear complex is the most intensive one. ESI-MS experiments showed a skimmer voltage dependent ratio of the di- and tetranuclear species (1:1, 0.4:1, 0.2:1 at −4, −6, and −8 V, respectively). Furthermore, a peak at 972.0867 m/z was identified to be $[(\text{PtMe}_3)_3(\mu\text{-s}^4\text{Ura-H})_2\text{-2H}]^-$ whose intensity proved also to be dependent on this skimmer voltage. All these findings indicated that the higher aggregated species, in particular the tetranuclear one, were yielded from the dinuclear complex $[(\text{PtMe}_3)_2(\mu\text{-s}^4\text{Ura-H})_2\text{-H}]^-$ during the ionization process and/or by thermal decomposition during the ESI experiment. Further proof of the dinuclear nature of complex **7** was given by positive

Table 3
 ^1H and ^{13}C NMR spectroscopic data (δ in ppm, J in Hz) of $[(\text{PtMe}_3)_2(\mu\text{-s}^4\text{Ura-H})_2]$ (**7**) in acetone- D_6 .

	δ_{C} ($^1J_{\text{Pt,C}}$) ^a	δ_{H} ($^2J_{\text{Pt,H}}$) ^a	$\Delta\delta_{\text{C}}/\Delta\delta_{\text{H}}$ ^b
C5/H5	112.0	6.04	+0.9/+0.20
C6/H6	145.1	7.71	−7.1/−0.39
NH		10.82	
C2		150.8	−1.7
C4		191.1	+0.8
PtMe ₃	3.1 (663.0)	1.46 (75.5)	
	1.1 (684.2)	1.06 (75.9)	
	−11.1 (678.9)	0.98 (74.3)	

^a Correlated signals in ^1H – ^{13}C COSY NMR spectra are given in the same line.
^b Coordination induced shifts (CIS's). Downfield/highfield shifts upon coordination are referred as negative/positive values.

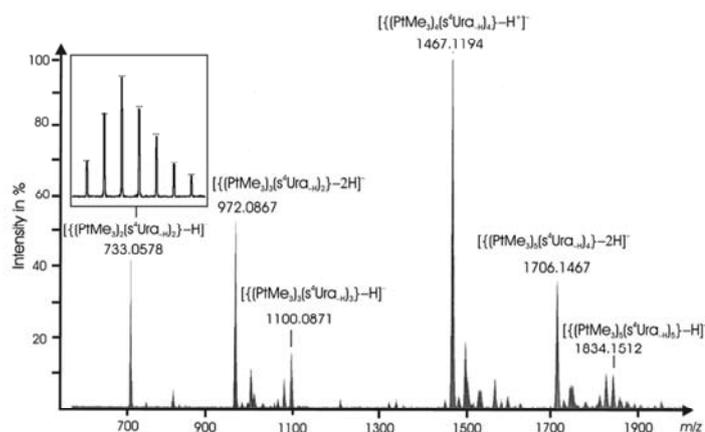


Fig. 2. Negative ESI mass spectrum of $[(\text{PtMe}_3)_2(\mu\text{-s}^4\text{Ura-H})_2]$ (**7**) and isotopic pattern of the anion $[(\text{PtMe}_3)_2(\mu\text{-s}^4\text{Ura-H})_2\text{-H}]^-$ at 733.0578 m/z showing the expected intensity due to the isotopic composition (calculated intensities by horizontal bars).

ESI-MS experiments, which showed no peaks of higher aggregated fragments than the sodium and potassium aggregates of the dinuclear species $[\{PtMe_3\}_2(\mu-s^4Ura_{-H})_2]+Na]^+$ (found/calcd.: 757.0510/757.0534 m/z) and $[\{PtMe_3\}_2(\mu-s^4Ura_{-H})_2]+K]^+$ (found/calcd.: 773.0253/773.0273 m/z).

In an isolated case yellow crystals of a decomposition product (**7a**·2 Me₂CO) were obtained in acetone-D₆ solutions, which were suitable for X-ray diffraction analysis. The compound crystallized in the monoclinic space group $P\bar{1}$. The molecular structure of **7a** is shown in Fig. 3, selected bond lengths and angles are given in Table 4. The hexanuclear complex exhibits a crystallographic imposed inversion center, thus containing three different platinum(IV) moieties. Two of them (Pt1, Pt2) build up a Pt₂(μ-S)₂ unit having [PtC₂S₂N] (Pt1) and [PtC₂S₂N] (Pt2) donor sets. Hence, one methyl ligand of Pt2 has been cleaved off. The third platinum center (Pt3) exhibits a [PtC₃N₂O] donor set which contains an aqua ligand as a result of hydrolysis. Furthermore, three different thiouracilato ligands are found, namely a twofold deprotonated s⁴Ura_{-2H} ligand (A) exhibiting a μ-1κN^{3a},3'κN^{1a},1:2κ²Sa coordination mode, and two monodeprotonated s⁴Ura_{-H} ligands (B, C) in a μ-2κN^{3b},1:2κ²Sb and μ-2κS^c,3κN^{1c} binding fashion.

In accordance with the high *trans* influence of methyl ligands the Pt–S bonds in the dinuclear Pt₂(μ-S)₂ fragment *trans* to the Me are remarkably longer (2.527(4)–2.603(4) Å) than the Pt2–Sa bond (2.360(4) Å) in *trans* position to the Sc atom. Deprotonation and coordination of the 4-thiouracilato ligands led to a significant elongation of the C–S bonds compared to that in 1-methyl-4-thio-

uracil (1.75 versus 1.669 Å) [16]. The Pt₂(μ-S)₂ ring is slightly hinged (torsional angle Pt1–Sa··Sb–Pt2: 174.8°). The S,N3 chelating binding mode of the thiouracilato ligands A and B gives rise to severe deviations from the ideal octahedral geometry for the platinum atoms Pt1 and Pt2 (Sa–Pt1–N3a 65.0(3)°, Sb–Pt2–N3b 64.7(3)°). Within the hexanuclear arrangement a strong twofold N–H···O hydrogen bond (N1b··Ob' 2.77(2) Å) is found. It is worth mentioning that the twofold N3–H···S' hydrogen bond of the Watson–Crick type in 1-methyl-4-thiouracil is much weaker (N3··S' 3.328 Å) [16]. Furthermore, the thiouracilato ligands A and B are arranged in a face-to-face (*cis*) conformation. The centroid–centroid distance of 3.5 Å and the displacement angle² of 20.0° indicated stabilization through π–π stacking [17]. All these values are very similar to the structures of dinuclear complexes $[(PtMe_3)_2(\mu-S-N)]$ (S–N = N,S heterocyclic ligand) having also central Pt₂(μ-S)₂ cores [15].

2.4. Cytotoxic investigations

The *in vitro* antitumoral activities of the uncoordinated thiouracils and the complexes $[PtMe_3(bpy)(L-\kappa S)](BF_4)$ (L = s²Ura, **3**; s⁴Ura, **4**; s²s⁴Ura, **5**) were tested on nine different cancer cell lines: human anaplastic thyroid cancer (8505C), head and neck tumor (A253 and FaDu), cervical cancer (A431), lung carcinoma (A549), ovarian cancer (A2780) and colon carcinoma (DLD-1, HCT-8 and HT-29). The free thionucleobases s²Ura, s⁴Ura and s²s⁴Ura exhibited no activity in the investigated range of concentrations (0.1–125 μM). Complexes **3–5** showed a dose-dependent antiproliferative effect towards all cell lines (Table 5). The highest activities, which are comparable to cisplatin, were observed for the complexes $[PtMe_3(bpy)(s^2Ura-\kappa S^2)](BF_4)$ (IC₅₀: 1.7 μM, **3**; 1.5 μM, cisplatin) and $[PtMe_3(bpy)(s^2s^4Ura-\kappa S^4)](BF_4)$ (IC₅₀: 1.8 μM, **5**; 0.6 μM, cisplatin) towards the lung carcinoma A549 and ovarian cancer cell line A2780, respectively. In all other cases the complexes exhibited only moderate cytotoxicities (IC₅₀: 8.1–42.1 μM) being two to thirty times less active than cisplatin. Within the complexes $[PtMe_3(bpy)(L-\kappa S)](BF_4)$, complex **5** (L = s²s⁴Ura; IC₅₀: 1.8–18.3 μM) proved to be more active than complexes **3** (L = s²Ura; IC₅₀: 1.7–36.5 μM) and **4** (L = s⁴Ura; IC₅₀: 10.2–42.1 μM). Comparison of the cytotoxicities of complex **5** with those of analogous complexes having thionucleobase ligands, $[PtMe_3(bpy)(L-\kappa S)](BF_4)$ (L = 2-thiocytosine, SCy; 1-methyl-2-thiocytosine 1-MeSCy) [13], and of the starting complex $[PtMe_3(bpy)]$ (**1**) [15] (Table 4) exhibited similar activities in most cases. Towards the cell lines A2780, DLD-1 and HT-29 complex **5** was up to four times more active than the respective thiocytosine platinum(IV) complexes and beyond that also more active than $[PtMe_3(bpy)]$ (**1**) towards the ovarian carcinoma cell line A2780.

To test whether the cell death induced by the most active complex $[PtMe_3(bpy)(s^2s^4Ura-\kappa S^4)](BF_4)$ (**5**), was mediated by apoptosis, cell cycle perturbations were analyzed on cervical cancer A431 cell line. The cells were treated with IC₉₀ concentration of **5** for 24 h (Fig. 4). When compared to control, the compound **5** caused no changes in G2/M and S phases but a decrease by about 35% in the number of cells in G1-phase with a concomitant increase in the number of apoptotic cells (SubG1-peak) was observed. Those results indicated that apoptosis caused by **5** on cervical cancer A431 cell line may be due to disturbances caused in G1-phase in the cell cycle. Furthermore, programmed cell death was confirmed by trypan blue exclusion test, in which floating cells of A431 showed the ability to exclude the blue dye indicating that **5** caused cell death by the induction of apoptosis (Fig. 5).

² The displacement, measured by the angle between the ring normal and the centroid–centroid vector, is a measure for the ring–ring overlap [17].

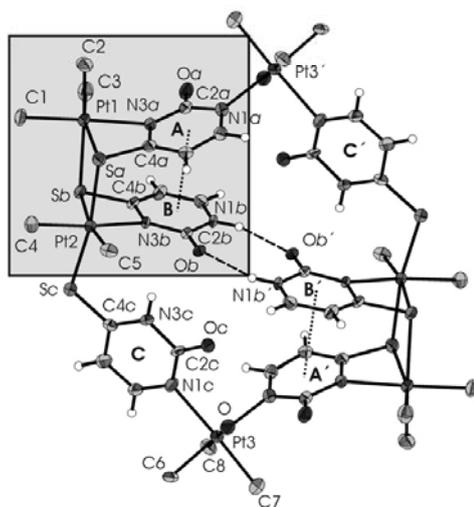


Fig. 3. Molecular structure of the hexamer **7a** in crystals of **7a**·2 Me₂CO. The gray shaded rectangular shows the preserved part of the starting complex **7**.

Table 4
Selected bond lengths (in Å) and angles (in °) of **7a**·2 Me₂CO.

Pt1–Sa	2.603(4)	Pt2–Sc	2.321(4)	C2c–Oc	1.23(2)
Pt1–Sb	2.527(4)	Pt2–N3b	2.18(1)	C4a–Sa	1.75(2)
Pt1–N3a	2.21(1)	Pt3–N1a'	2.18(1)	C4b–Sb	1.75(1)
Pt2–Sa	2.360(4)	C2a–Oa	1.26(2)	C4c–Sc	1.75(2)
Pt2–Sb	2.559(4)	C2b–Ob	1.22(2)		
Pt1–Sa–Pt2	93.8(1)	Sa–Pt1–N3a	65.0(3)	N1c–Pt3–C7	177.7(7)
Pt1–Sb–Pt2	96.8(1)	Sb–Pt2–N3b	64.7(3)	N1c–Pt3–N1d	92.9(5)
N3a–Pt1–C1	170.8(6)	N3b–Pt2–C4	168.6(6)		

Table 5

Results of the cytotoxicity assay on the nine tumor cell lines 8505C (anaplastic thyroid carcinoma), A253 and FaDu (head and neck tumor), A431 (cervical cancer), A549 (lung carcinoma), A2780 (ovarian carcinoma), DLD-1, HCT-8 and HT-29 (colon carcinoma) represented by the IC_{50} (μ M).^a

Cell line	3	4	5	[PtMe ₃ (bpy)(L)][BF ₄] ^b L = SCy/1-MeSCy	[PtMe ₃ (bpy)] ^c	Cisplatin
8505C	18.4 ± 1.7	19.0 ± 1.1	10.3 ± 0.1	9.45 ± 0.44/8.50 ± 0.34	11.6 ± 1.6	5.02 ± 0.23
A253	10.4 ± 0.1	10.3 ± 0.2	8.13 ± 0.12	8.50 ± 0.34/8.01 ± 0.44	7.38 ± 0.71	0.81 ± 0.02
FaDu	29.3 ± 0.5	38.2 ± 1.2	18.3 ± 1.7	22.0 ± 2.0/22.5 ± 2.0		1.21 ± 0.14
A431	16.9 ± 0.9	20.5 ± 0.8	13.6 ± 0.2	14.1 ± 0.6/13.7 ± 0.5		0.65 ± 0.04
A549	1.74 ± 0.17	10.2 ± 1.0	11.2 ± 0.5	9.56 ± 0.16/9.25 ± 0.14	8.22 ± 1.45	1.51 ± 0.02
A2780	10.8 ± 0.2	10.7 ± 0.2	1.83 ± 0.31	6.80 ± 0.26/6.10 ± 0.35	9.43 ± 0.97	0.55 ± 0.03
DLD-1	36.5 ± 1.4	42.1 ± 2.1	16.7 ± 0.6	31.4 ± 2.8/23.0 ± 1.7	18.4 ± 2.3	5.14 ± 0.12
HCT-8	13.8 ± 0.5	14.8 ± 0.6	8.67 ± 0.38	12.5 ± 0.3/11.7 ± 0.3		1.50 ± 0.23
HT-29	11.6 ± 0.3	12.4 ± 0.6	10.9 ± 0.5	26.9 ± 2.2/27.0 ± 1.7		0.60 ± 0.08

^a Mean values ± SD (standard deviation) from three experiments.

^b Data taken from literature [13].

^c Data taken from literature [15].

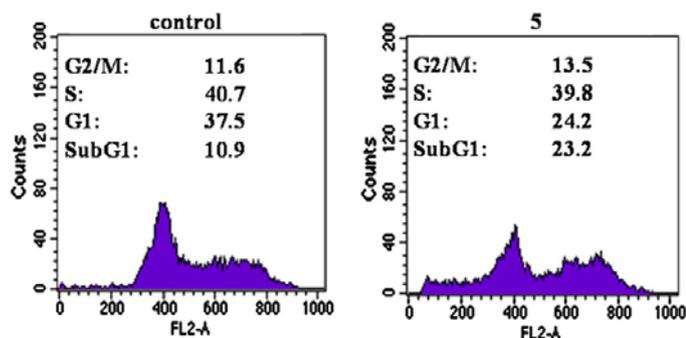


Fig. 4. Cell cycle analysis (DNA content (FL2-A) versus cell number (Counts)) of A431 cells untreated (control) and treated with the IC_{50} concentration of [PtMe₃(bpy)(s²s⁴Ura-κS⁴)] [BF₄] (5) for 24 h. A decrease by about 35% in number of cells in G1-phase and the concomitant increase in SubG1-phase indicates induction of apoptotic cell death.

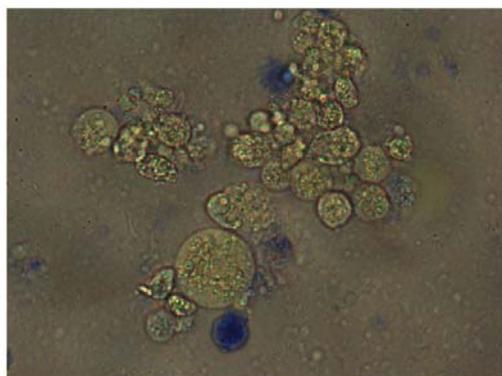


Fig. 5. Trypan blue exclusion test in the cell line A431 induced by [PtMe₃(bpy)-(s²s⁴Ura-κS⁴)] [BF₄] (5). Floated cells showed the ability to exclude the blue dye, indicating induction of apoptotic cell death.

3. Conclusion

Reactions of [PtMe₃(bpy)(Me₂CO)][BF₄] (2) with thiouracils led to the formation of mononuclear complexes of the type [PtMe₃(bpy)(L-κS)][BF₄] (L = s²Ura, 3; s⁴Ura, 4; s²s⁴Ura, 5). The thiouracil ligands were found to be in their oxothione (s²Ura, s⁴Ura) and dithione (s²s⁴Ura) tautomeric forms. This is in accordance with quantum chemical calculations and IR spectroscopic studies at

low temperature inert matrices which have also shown that these are the most stable tautomers [18,19]. The coordination of the s⁴Ura and s²s⁴Ura ligands in complexes 4 and 5 through the C4=S groups, established experimentally and by DFT calculations, can be understood in terms of the donor strength. These C4=S groups are stronger donors than the C2=X (X = O, S) groups which possess two adjacent electronegative N atoms. This is in accord with quantum chemical calculations of s²s⁴Ura where the HOMO was found to be a non-bonding (lone-pair) p-type molecular orbital located mainly at S4 [20]. Although in the case of complex 3 DFT calculations did not show a preferential coordination site of the s²Ura ligand, an isomerically pure complex 3 was isolated exhibiting a C2=S bound 2-thiouracil ligand.

The precursor complex [PtMe₃(bpy)(Me₂CO)][BF₄] (2) discussed so far has at its disposal only one substitution-labile ligand (acetone) thus allowing only monodentate coordination of the thiouracil ligands. In contrast to that, [PtMe₃(OAc-κ²O,O')(Me₂CO)] (6) has up to three substitution-labile ligands, namely one when the acetone ligand is cleaved off and the acetato ligand is still coordinated in a chelating binding fashion, two when the acetone ligand is cleaved off and the acetato ligand remains to be κ¹O coordinated or three in the case of complete cleavage of the acetato ligand [21]. The latter case was found to occur in the reaction with 4-thiouracil, forming under its deprotonation the dinuclear neutral complex [(PtMe₃)₂(μ-s⁴Ura-κ₄)₂] (7). Thus, this reaction proceeds fully analog to the formation of complexes [(PtMe₃)₂(μ-S-N)]₂ having N,S heterocyclic ligands [15]. The decomposition of the dinuclear complex 7 in acetone by traces of water into the hexanuclear complex 7a-2 Me₂CO gives proof for the versatile coordination modes of 4-thiouracil as well as for the formation of

oligonuclear complexes as it was also found in uracil platinum(II) complexes [22]. The way of formation of complex **7a-2** Me₂CO is unknown. Basically, the starting complex **7** remains to be intact in the dinuclear building block Pt1-(μ-S)₂-Pt2 having bound the two thiouracilato ligands A and B in **7a-2** Me₂CO (see the gray shadowed rectangular in Fig. 3). Thus, a deprotonation of the N1a-H group of complex **7** followed by a platination and a cleavage of the methyl ligand *trans* to Sa can be assumed to be intermediate steps. The cleavage of a methyl ligand from a PtMe₃ unit is quite common in reductive elimination reactions yielding a platinum(II) complex under formation of ethane [23]. However, Pt-CH₃ cleavage reactions without reduction of platinum(IV) are rarely known. Thus, a protolytic cleavage of a Pt-CH₃ bond activated by another methyl ligand in *trans* position is described [24]. Furthermore, apart from consecutive reductive elimination/oxidative addition reactions (with cleavage and reformation of Pt(IV)-CH₃ bonds) [25], the cleavage of Pt-CH₃ bonds in [(PtMe₃)₄] by halogens [26] and methyl ligand transfer reactions [27] are reported. It is worth to be mentioned that in complex **7a-2** Me₂CO the κN¹,κS⁴ coordination mode of the 4-thiouracilato ligand (Fig. 3, type C) is observed for the first time, which underlines on a further example the versatile binding patterns of thionucleobase ligands.

4. Experimental

4.1. General considerations

Syntheses were performed at room temperature under argon using standard Schlenk techniques. Acetone was dried over phosphorus pentoxide and diethyl ether over Na benzophenone. All solvents were distilled prior to use. NMR spectra were obtained with Varian UNITY 500 and Gemini 2000 spectrometers using solvent signals (¹H and ¹³C NMR spectroscopy) as internal references and Na₂[PtCl₆] (δ(¹⁹⁵Pt) = 0 ppm) as external reference. IR spectra were recorded on a Galaxy Mattson FT IR spectrometer, using KBr pellets. [PtMe₃(bpy)] [28] and [(PtMe₃)₄] [29] were prepared according to literature. All other chemicals were purchased from commercial sources. The positive and negative ion high resolution ESI mass spectra were obtained from a Bruker Apex III Fourier transform ion cyclotron resonance (FT-ICR) mass spectrometer (Bruker Daltonics, Billerica, USA) equipped with an Infinity™ cell, a 7.0 Tesla superconducting magnet (Bruker, Karlsruhe, Germany), an RF-only hexapole ion guide and an external electrospray ion source (Agilent, off axis spray, voltages (positive ions): endplate, -3.700 V; capillary, -4.200 V; capillary exit, +100 V; skimmer 1, +15.0 V; skimmer 2, +10.0 V; voltages (negative ions): endplate, 3.700 V; capillary, 4.200 V; capillary exit, -100 V; skimmer 1, -15.0 V; skimmer 2, -6.0 V). Nitrogen was used as drying gas at 150 °C. The sample solutions were introduced continuously via a syringe pump with a flow rate of 120 μl h⁻¹. The data were acquired with 512 k data points and zero filled to 2048 k by averaging 32 scans.

4.1.1. ¹H and ¹³C NMR data of thiouracils

²Ura: ¹H NMR (400 MHz, (CD₃)₂CO) δ 11.1 (s, br, 2H, N1H, N3H), 7.47 (d, 1H, ³J_{H,H} = 7.6 Hz, H6), 5.85 (d, 1H, ³J_{H,H} = 7.5 Hz, H5). ¹H NMR (400 MHz, (CD₃)₂SO) δ 12.3 (s, br, 2H, N1H, N3H), 7.38 (d, 1H, ³J_{H,H} = 7.5 Hz, H6), 5.80 (d, 1H, ³J_{H,H} = 7.5 Hz, H5). ¹³C NMR (100 MHz, (CD₃)₂CO) δ 142.1 (C6), 105.9 (C5). ¹³C NMR (100 MHz, (CD₃)₂SO) δ 175.8 (C2), 160.8 (C4), 141.8 (C6), 105.2 (C5). ⁴Ura: ¹H NMR (400 MHz, (CD₃)₂CO) δ 11.2 (s, br, NH), 10.5 (s, br, NH), 7.33 (d, 1H, ³J_{H,H} = 7.1 Hz, H6), 6.24 (d, 1H, ³J_{H,H} = 7.1 Hz, H5). ¹H NMR (400 MHz, (CD₃)₂SO) δ 12.4 (s, br, 1H, NH), 11.5 (s, br, 1H, NH), 7.32 (d, 1H, ³J_{H,H} = 7.1 Hz, H6), 6.16 (d, 2H, ³J_{H,H} = 7.1 Hz, H5). ¹³C NMR (100 MHz, (CD₃)₂CO) δ 138.0 (C6), 112.9 (C5). ¹³C

NMR (100 MHz, (CD₃)₂SO) δ 191.9 (C4), 149.1 (C2), 138.9 (C6), 112.2 (C5). ⁴Ura: ¹H NMR (400 MHz, (CD₃)₂CO) δ 7.33 (d, 1H, ³J_{H,H} = 7.2 Hz, H6), 6.56 (d, 1H, ³J_{H,H} = 7.2 Hz, H5). ¹H NMR (400 MHz, (CD₃)₂SO) δ 13.2 (s, br, 2H, N1H, N3H), 7.26 (d, 1H, ³J_{H,H} = 7.1 Hz, H6), 6.49 (d, 2H, ³J_{H,H} = 7.1 Hz, H5). ¹³C NMR (100 MHz, (CD₃)₂CO) δ 189.1 (C4), 174.3 (C2), 136.7 (C6), 117.7 (C5). ¹³C NMR (100 MHz, (CD₃)₂SO) δ 187.4 (C4), 172.6 (C2), 136.5 (C6), 116.9 (C5).

4.1.2. Syntheses of [PtMe₃(bpy)(L-κS)][BF₄] (**3-5**)

A suspension of [PtMe₃(bpy)] (70.0 mg; 0.14 mmol) in acetone (10 ml) and Ag[BF₄] (26.5 mg; 0.14 mmol) was stirred for 30 min in the absence of light. After removing silver iodide by filtration the respective thiouracil (0.14 mmol) was added to the stirred clear solution. After 2 h the volume of the solution was concentrated *in vacuo* to 1 ml and ether (3 ml) was added. The yellow solid was filtered and dried *in vacuo*.

[PtMe₃(bpy)(²Ura-κS²)] [BF₄] (**3**). Yield: 56 mg (68%). Anal. Calc. for C₁₇H₂₁BF₄N₄OSPt (611.11): C, 33.38; H, 3.46; N, 9.17. Found: C, 34.11; H, 3.91; N, 9.04%. ¹H NMR (400 MHz, (CD₃)₂CO) δ 11.34 (s, br, 2H, N1H, N3H), 8.96 (m, 2H, ³J_{Pt,H} = 18.8 Hz, H6/H6'), 8.74 (d, 2H, H3, H3'), 8.37 (m, 2H, H4/H4'), 7.95 (m, 2H, H5/H5'), 7.41 (d, 1H, ³J_{H,H} = 7.9 Hz, H6-_{TU}), 6.04 (d, 1H, ³J_{H,H} = 7.9 Hz, H5-_{TU}), 1.23 (s+d, 6H, ²J_{Pt,H} = 68.1 Hz, N_{trans}-PtCH₃), 0.69 (s+d, 3H, ²J_{Pt,H} = 73.7 Hz, S_{trans}-PtCH₃). ¹³C NMR (125 MHz, (CD₃)₂CO) δ 173.4 (C2-_{TU}), 159.5 (C4-_{TU}), 155.2 (C2/C2'), 148.0 (s+d, ³J_{Pt,C} = 15.4 Hz, C6/C6'), 142.2 (C6-_{TU}), 141.4 (C4/C4'), 129.0 (s+d, ⁴J_{Pt,C} = 13.4 Hz, C5/C5'), 111.0 (C5-_{TU}), 3.2 (s+d, ¹J_{Pt,C} = 673.7 Hz, S_{trans}-PtCH₃), -5.0 (s+d, ¹J_{Pt,C} = 667.0 Hz, N_{trans}-PtCH₃). ¹⁹⁵Pt NMR (107 MHz, (CD₃)₂CO) δ -2687.7. FT-IR (KBr, cm⁻¹) 2897 m, 1690 s, 1600 w, 1542 s, 1443 m, 1218 m, 1159 w, 1060 s, 1021 s, 766 s.

[PtMe₃(bpy)(⁴Ura-κS⁴)] [BF₄] (**4**). Yield: 45 mg (54%). Anal. Calc. for C₁₇H₂₁BF₄N₄OSPt (611.11): C, 33.38; H, 3.46; N, 9.17. Found: C, 34.36; H, 3.97; N, 8.71%. ¹H NMR (400 MHz, (CD₃)₂CO) δ 11.48 (s, br, 1H, NH), 11.04 (s, br, 1H, NH), 9.07 (m, 2H, ³J_{Pt,H} = 18.5 Hz, H6/H6'), 8.82 (d, 2H, H3/H3'), 8.42 (m, 2H, H4/H4'), 7.99 (m, 2H, H5/H5'), 7.68 (d, 1H, ³J_{H,H} = 7.1 Hz, H6-_{TU}), 6.14 (d, 1H, ³J_{H,H} = 7.1 Hz, H5-_{TU}), 1.29 (s+d, 6H, ²J_{Pt,H} = 68.5 Hz, N_{trans}-PtCH₃), 0.67 (s+d, 3H, ²J_{Pt,H} = 71.0 Hz, S_{trans}-PtCH₃). ¹³C NMR (500 MHz, (CD₃)₂CO) δ 188.1 (C4-_{TU}), 155.6 (C2/C2'), 148.1 (s+d, ³J_{Pt,C} = 14.8 Hz, C6/C6'), 147.6 (C2-_{TU}), 145.2 (C6-_{TU}), 141.5 (C4/C4'), 128.9 (s+d, ³J_{Pt,C} = 13.7 Hz, C5/C5'), 125.9 (s+d, ³J_{Pt,C} = 8.0 Hz, C3/C3'), 107.9 (C5-_{TU}), 3.8 (s+d, ¹J_{Pt,C} = 651.5 Hz, S_{trans}-PtCH₃), -5.3 (s+d, ¹J_{Pt,C} = 666.4 Hz, N_{trans}-PtCH₃). ¹⁹⁵Pt NMR (107 MHz, (CD₃)₂CO) δ -2719.3. FT-IR (KBr, cm⁻¹) 3116 w, 2952 w, 2898 m, 1735 s, 1601 s, 1471 w, 1444 m, 1229 w, 1124 s, 1058 s, 766 m.

[PtMe₃(bpy)(⁴Ura-κS⁴)] [BF₄] (**5**). Yield: 46 mg (55%). Anal. Calc. for C₁₇H₂₁BF₄N₄S₂Pt (627.09): C, 32.53; H, 3.38; N, 8.93. Found: C, 32.44; H, 3.33; N, 8.45%. ¹H NMR (400 MHz, ((CD₃)₂CO) δ 12.22 (s, br, 2H, NH), 9.05 (m, 2H, ³J_{Pt,H} = 18.3 Hz, H6/H6'), 8.80 (d, 2H, H3/H3'), 8.41 (m, 2H, H4/H4'), 7.98 (m, 2H, H5/H5'), 7.59 (d, 1H, ³J_{H,H} = 7.1 Hz, H6-_{2A-TU}), 6.49 (d, 1H, ³J_{H,H} = 7.1 Hz, H5-_{2A-TU}), 1.29 s+d, 6H, ²J_{Pt,H} = 68.5 Hz, N_{trans}-PtCH₃), 0.67 (s+d, 3H, ²J_{Pt,H} = 71.1 Hz, S_{trans}-PtCH₃). ¹³C NMR (500 MHz, (CD₃)₂CO) δ 184.4 (C4-_{2A-TU}), 173.0 (C2-_{2A-TU}), 155.5 (C2/C2'), 148.2 (C6/C6'), 143.1 (C6-_{2A-TU}), 141.6 (C4/C4'), 129.2 (s+d, ³J_{Pt,C} = 13.4 Hz, C5/C5'), 126.1 (C3/C3'), 112.8 (C5-_{2A-TU}), 4.2 (s+d, ¹J_{Pt,C} = 649.5 Hz, DTU_{trans}-PtCH₃), -5.5 (s+d, ¹J_{Pt,C} = 664.5 Hz, N_{trans}-PtCH₃). ¹⁹⁵Pt NMR (107 MHz, (CD₃)₂CO) δ -2726.4. FT-IR (KBr, cm⁻¹) 3217 w, 3106 w, 2957 w, 2897 m, 1603 s, 1548 s, 1490 w, 1473 w, 1445 m, 1227 m, 1116 s, 1077 s, 1028 s, 766 s.

4.1.3. Synthesis of [(PtMe₃)₂(μ-S⁴Ura-*H*)₂] (**7**)

A suspension of [(PtMe₃)₄] (50.0 mg, 0.04 mmol) and AgOAc (23.0 mg, 0.14 mmol) in acetone (10 ml) was stirred for 15 h in the absence of light. Silver iodide was removed by filtration and

the clear, colorless solution was added to 4-thiouracil (17.4 mg, 0.14 mmol). After stirring for 2 h the solution was filtered to remove undissolved material. The clear, yellow solution was concentrated in *vacuo* to 1 ml and ether (3 ml) was added. The precipitated product was isolated by filtration, washed with pentane (2 × 2 ml) and dried in *vacuo*. Yield: 36 mg (70%).

Anal. Calc. for $C_{14}H_{24}N_4S_2O_2Pt_2$ (734.06): C, 22.83, H, 3.29, N, 7.63. Found: C, 23.04; H, 3.54; N, 7.26%. 1H NMR (400 MHz, $(CD_3)_2CO$) δ 10.82 (s, br, 1H, N3H, N3'H), 7.71 (d, 2H, $^3J_{H,H} = 6.64$ Hz, H6/H6'), 6.04 (d, 2H, $^3J_{H,H} = 6.64$ Hz, H5/H5'), 1.46 (s+d, 6H, $^2J_{Pt,H} = 75.5$ Hz, PtCH₃), 1.06 (s+d, 6H, $^2J_{Pt,H} = 75.9$ Hz, PtCH₃), 0.98 (s+d, 6H, $^2J_{Pt,H} = 74.3$ Hz, PtCH₃). ^{13}C NMR (500 MHz, $(CD_3)_2CO$) δ 191.1 (C4/C4'), 150.8 (C2/C2'), 145.1 (C6/C6'), 112.0 (C5/C5'), 3.1 (s+d, $^1J_{Pt,C} = 663.0$ Hz, PtCH₃), 1.1 (s+d, $^1J_{Pt,C} = 684.2$ Hz, PtCH₃), -11.1 (s+d, $^1J_{Pt,C} = 678.9$ Hz, PtCH₃). ^{195}Pt NMR (107 MHz, $(CD_3)_2CO$) δ -2445.3. FT-IR (KBr, cm^{-1}) 3080 w, 2936 w, 2897 m, 2811 w, 1671 s, 1596 s, 1517 m, 1437 m, 1395 m, 1220 m, 1128 m, 1015 m, 783 m. ESI-MS (*m/z*, relative intensity) 1834.1512 (14) $\{[(PtMe_3)_5(s^4Ura_{-H})_5]-H\}^-$, 1706.1467 (37) $\{[(PtMe_3)_5(s^4Ura_{-H})_4]-2H\}^-$, 1467.1194 (100) $\{[(PtMe_3)_4(s^4Ura_{-H})_4]-H\}^-$, 1100.0871 (20) $\{[(PtMe_3)_3(s^4Ura_{-H})_3]-H\}^-$, 972.0867 (53) $\{[(PtMe_3)_3(s^4Ura_{-H})_2]-2H\}^-$, 733.0578 (42) $\{[(PtMe_3)_2(s^4Ura_{-H})_2]-H\}^-$.

4.2. X-ray crystallography

Single crystals of 7a·2 Me₂CO for X-ray diffraction measurements were obtained from an acetone-D₆ solution. Intensity data were collected on a STOE IPDS diffractometer with Mo K α radiation ($\lambda = 0.71073$ Å, graphite monochromator) at 220(2) K. A summary of the crystallographic data, the data collection parameters and the refinement parameters is given in Table 6. A numerical absorption correction was applied (T_{min}/T_{max} 0.14/0.34). The structure was solved by direct methods with SHELXS-97 [30] and refined using full matrix least square routines against F^2 with SHELXL-97 [30]. Non-hydrogen atoms were refined with anisotropic displacement parameters. Hydrogen atoms were positioned geometrically and refined with isotropic displacement parameters according to the "riding model". The solvent molecule acetone is disordered over

Table 6
Crystal data, data collection and refinement parameters of 7a·2 Me₂CO.

Formula	$C_{46}H_{76}N_{12}O_{10}Pt_6S_6$
FW	1160.04
Crystal system	triclinic
Space group	P1
<i>a</i> (Å)	10.590(1)
<i>b</i> (Å)	12.428(1)
<i>c</i> (Å)	13.614(1)
α (°)	75.40(1)
β (°)	74.91(1)
γ (°)	74.80(1)
<i>V</i> (Å ³)	1636.6(3)
<i>Z</i>	2
<i>D</i> _{calc} (g cm ⁻³)	2.354
<i>T</i> (K)	220(2)
μ (mm ⁻¹)	13.022
θ (°)	2.10–25.95
<i>F</i> (0 0 0)	1080
Index ranges	-12 ≤ <i>h</i> ≤ 12 -15 ≤ <i>k</i> ≤ 15 -16 ≤ <i>l</i> ≤ 16
Reflections collected	12166
Reflections observed [<i>i</i> > 2 σ (<i>i</i>)]	4269
Refins independent	5940 (<i>R</i> _{int} = 0.0709)
Data/restraints/parameters	5940/68/394
GO <i>F</i> (<i>F</i> ²)	0.978
<i>R</i> ₁ , <i>wR</i> ₂ [<i>I</i> > 2 σ]	0.0589/0.1404
<i>R</i> ₁ , <i>wR</i> ₂ (all data)	0.0806/0.1489
Largest difference in peak and hole (e Å ⁻³)	4.757 and -4.033 (near Pt)

two positions and was freely refined with occupation factors of 52 and 48%, respectively.

4.3. Computational details

DFT calculations of compounds were carried out by the GAUSSIAN03 program package [31] using the hybrid functional B3LYP [32]. The 6-311G(d,p) basis sets as implemented in GAUSSIAN03 were employed for main group elements. The valence shell of platinum has also been approximated by a split valence basis set; for its core orbitals an effective core potential in combination with consideration of relativistic effects has been used [33]. The appropriateness of the functional in combination with the basis sets and effective core potential used for reliable interpretation of structural and energetic aspects of related platinum complexes has been demonstrated [13,15,34].

4.4. In vitro cytotoxic studies

Stock solutions of investigated platinum complexes and reference compound cisplatin were made in dimethyl sulfoxide (DMSO) at concentration of 20 mM and diluted by nutrient medium to various working concentrations. Nutrient medium was RPMI-1640 (PAA Laboratories) supplemented with 10% fetal bovine serum (Biochrom AG) and penicillin/streptomycin (PAA Laboratories).

4.4.1. Cell cultures

The human tumor cell lines: human anaplastic thyroid cancer (8505C), head and neck tumor (A253 and FaDu), cervical cancer (A431), lung carcinoma (A549), ovarian cancer (A2780) and colon carcinoma (DLD-1, HCT-8 and HT-29) were cultivated in the Biozentrum, Martin-Luther University Halle-Wittenberg. All cells were maintained as monolayers in nutrient medium in a humidified atmosphere with 5% CO₂.

4.4.2. Cytotoxicity assay

The cytotoxic activity of the platinum compounds was measured by the sulforhodamine-B (SRB) assay [35]. In brief, exponentially growing cells were seeded into 96-well plates and 24 h later, after the cell adherence, nine different concentrations of investigated compounds were added to the wells. The final concentrations were in the range from 0.1 to 125 μ M. All experiments were done in triplicate. Nutrient medium with corresponding concentrations of compounds, but void of cells was used as blank. Five days after seeding the cells were fixed with 10% trichloroacetic acid and processed according to the published SRB assay protocol. Absorbance was measured at 570 nm using a 96-well plate reader (SpectraFluor Plus Tecan, Germany) and the percentages of surviving cells relative to untreated controls were determined. Concentration IC₅₀ was determined as the concentration of a drug that inhibited cell survival by 50%, compared with vehicle-treated control.

4.4.3. Trypan blue exclusion test

Apoptotic cell death was analyzed by trypan blue dye (Sigma-Aldrich, Germany) on A431 cell line. The cell culture flasks with 70–80% confluence were treated with IC₉₀ dose of [PtMe₃(bpy)(s³s⁴Ura-*k*S⁴)] [BF₄] (5) for 24 h. The supernatant medium with floating cells was collected after treatment and centrifuged to collect the dead and apoptotic cells. The cell pellet was resuspended in serum free media. Equal amounts of cell suspension and trypan blue were mixed and this was analyzed under a microscope. The cells which were viable excluded the dye and were colorless and the ones whose cell membrane was destroyed were turning into blue. If the proportion of colorless cells were more compared to

the ones that were colored then the death can be characterized as apoptotic.

4.4.4. Cell cycle analysis

Cell cycle was assessed by flow cytometry using a fluorescence-activated cell sorter (FACS) [36]. For this assay, 1×10^6 A431 cells, were seeded in 25 cm^2 cell culture flasks, with 10 ml of medium. After 24 h of incubation, $[\text{PtMe}_3(\text{bpy})(\text{s}^2\text{s}^4\text{Ura-}\kappa\text{S}^4)](\text{BF}_4)$ (5) was added at IC_{50} value. Following 24 h of incubation, cells were harvested by mild trypsinization, collected by centrifugation, washed with PBS and both adherent and floating cells were resuspended in 100 μl of PBS and fixed with 2 ml of 70% ethanol at 4°C for at least 1 h. The fixed samples are then centrifuged, the cell pellet is washed with 2 ml of staining buffer (PBS + 2% FCS + 0.01% NaN_3) and again centrifuged. The cell pellet is resuspended in 100 μl of RNase A (1 mg/ml) and incubated for 30 min at 37°C . At the end of incubation the samples are treated with propidium iodide (20 $\mu\text{g}/1 \text{ ml}$ of staining buffer) and allowed to stand in dark at least for 30 min before analysis. The fluorescence intensity was determined by a FacsCalibur (Becton Dickinson, Heidelberg, Germany). Each analysis was done using about 1×10^4 events.

Acknowledgement

Gifts of chemicals by Merck (Darmstadt) are gratefully acknowledged.

Appendix A. Supplementary material

CCDC 762861 contains the supplementary crystallographic data for this paper. These data can be obtained free of charge from The Cambridge Crystallographic Data Center via www.ccdc.cam.ac.uk/data_request/cif. Supplementary data associated with this article can be found, in the online version, at [doi:10.1016/j.ica.2010.03.079](https://doi.org/10.1016/j.ica.2010.03.079).

References

- [1] (a) J.A. Carbon, L. Hung, D.S. Jones, *Proc. Natl. Acad. Sci. U S A* 53 (1965) 979; (b) M.N. Lipsett, *J. Biol. Chem.* 240 (1965) 3975; (c) J. Carbon, H. David, M.H. Studier, *Science* 161 (1968) 1146; (d) D.H. Gauss, M. Sprinzl, *Nucleic Acids Res.* 12 (1984) r1; (e) Y. Yamada, M. Saneyoshi, S. Nishimura, H. Ishikura, *FEBS Lett.* 7 (1970) 207.
- [2] L.S. Goodman, A. Gilman (Eds.), *Pharmacological Basis of Therapeutics*, 5th ed., Macmillan, New York, 1975, p. 1248.
- [3] E.B. Astwood, *J. Am. Med. Assoc.* 122 (1943) 78.
- [4] (a) R.K. Ralph, R.E.F. Matthews, A.I. Matus, *Biochim. Biophys. Acta* 108 (1965) 53; (b) M. Bretner, T. Kulikowski, J.M. Dzik, M. Balinska, W. Rode, D. Shugar, *J. Med. Chem.* 36 (1993) 3611; (c) M. Bretner, M. Balinska, K. Krawiec, B. Kierdaszuk, D. Shugar, T. Kulikowski, *Nucleosides, Nucleotides Nucleic Acids* 14 (1995) 657.
- [5] (a) A. Napolitano, A. Palumbo, M. d'Ischia, G. Prota, *J. Med. Chem.* 39 (1996) 5192; (b) U. Márs, V. Tolmachev, A. Sundin, *Nucl. Med. Biol.* 27 (2000) 845.
- [6] (a) M.W. Whitehouse, P.D. Cookson, G. Siasios, E.R.T. Tiekink, *Met.-Based Drugs* 5 (1998) 245; (b) E.R.T. Tiekink, P.D. Cookson, B.M. Linahan, L.K. Webster, *Met.-Based Drugs* 1 (1994) 299; (c) L.K. Webster, S. Rainone, E. Horn, E.R.T. Tiekink, *Met.-Based Drugs* 3 (1996) 63.
- [7] B. Rosenberg, L. Van Camp, T. Krigas, *Nature* 205 (1965) 698.
- [8] M.A. Fuertes, C. Alonso, J.M. Pérez, *Chem. Rev.* 103 (2003) 645.
- [9] M.D. Hall, T.W. Hambley, *Coord. Chem. Rev.* 232 (2002) 49.
- [10] O. Nováková, O. Vrána, V.I. Kiseleva, V. Brabec, *Eur. J. Biochem.* 228 (1995) 616.
- [11] I.R. Kelland, B.A. Murrer, G. Abel, C.M. Giandomenico, P. Mistry, K.R. Harrap, *Cancer Res.* 52 (1992) 822.
- [12] (a) T.G. Appleton, H.C. Clark, L.E. Manzer, *Coord. Chem. Rev.* 10 (1973) 335; (b) C. Vetter, C. Wagner, J. Schmidt, D. Steinborn, *Inorg. Chim. Acta* 359 (2006) 4326.
- [13] C. Vetter, C. Wagner, G.N. Kaluderović, R. Paschke, D. Steinborn, *Inorg. Chim. Acta* 362 (2009) 189.
- [14] C. Vetter, unpublished results.
- [15] C. Vetter, G.N. Kaluderović, R. Paschke, S. Gómez-Ruiz, D. Steinborn, *Polyhedron* 28 (2009) 3699.
- [16] S.W. Hawkinson, *Acta Crystallogr., Sect. B* 31 (1975) 2153.
- [17] C. Janiak, *J. Chem. Soc., Dalton Trans.* (2000) 3885.
- [18] (a) H. Rostkowska, K. Szczepaniak, M.J. Nowak, J. Leszczynski, K. KuBulat, W.B. Person, *J. Am. Chem. Soc.* 112 (1990) 2147; (b) L. Lapinski, H. Rostkowska, M.J. Nowak, J.S. Kwiatkowski, J. Leszczyński, *Vib. Spectrosc.* 13 (1996) 23.
- [19] (a) A. Les, L. Adamowicz, *J. Am. Chem. Soc.* 112 (1990) 1504; (b) J. Leszczynski, K. Lammertsma, *J. Phys. Chem.* 95 (1991) 3128.
- [20] P. Aslanidis, P.J. Cox, A. Kaltzoglou, A.C. Tsipis, *Eur. J. Inorg. Chem.* (2006) 334.
- [21] C. Vetter, P. Pornsuriyasak, J. Schmidt, N.P. Rath, T. Rülffer, A.V. Demchenko, D. Steinborn, *Dalton Trans.*, in press.
- [22] (a) H. Rauter, E.C. Hillgeris, B. Lippert, *J. Chem. Soc. Chem. Commun.* (1992) 1385; (b) B. Lippert, *Inorg. Chem.* 20 (1981) 4326; (c) A. Schreiber, H. Rauter, M. Krumm, S. Menzer, E.C. Hillgeris, B. Lippert, *Met.-Based Drugs* 1 (1994) 241; (d) H. Rauter, I. Mutikainen, M. Blomberg, C.J.L. Lock, P. Amo-Ochoa, E. Freisinger, L. Randaccio, E. Zangrando, E. Chiarparin, B. Lippert, *Angew. Chem., Int. Ed.* 36 (1997) 1296.
- [23] (a) R. Lindner, C. Wagner, D. Steinborn, *J. Am. Chem. Soc.* 131 (2009) 8861; (b) K.I. Goldberg, J. Yan, E.M. Breitung, *J. Am. Chem. Soc.* 117 (1995) 6889; (c) U. Fekl, K.I. Goldberg, *J. Am. Chem. Soc.* 124 (2002) 6804.
- [24] (a) J.E. Hux, R.J. Puddephatt, *Inorg. Chim. Acta* 100 (1985) 1; (b) J.E. Hux, R.J. Puddephatt, *J. Organomet. Chem.* 437 (1992) 251.
- [25] P. Romero, M. Valderrama, R. Contreras, D. Boys, *J. Organomet. Chem.* 673 (2003) 102.
- [26] J.R. Hall, G.A. Swile, *Aust. J. Chem.* 24 (1971) 423.
- [27] M.S. Safa, M.C. Jennings, R.J. Puddephatt, *Chem. Commun.* (2009) 1487.
- [28] D.E. Clegg, J.R. Hall, G.A. Swile, *J. Organomet. Chem.* 38 (1972) 403.
- [29] (a) W.J. Pope, S.J. Peachey, *Proc. Chem. Soc.* 23 (1907) 86; (b) J.C. Baldwin, W.C. Kaska, *Inorg. Chem.* 14 (1975) 2020.
- [30] G.M. Sheldrick, *Acta Crystallogr., Sect. A: Found. Crystallogr.* 64 (2008) 112.
- [31] M.J. Frisch, G.W. Trucks, H.B. Schlegel, G.E. Scuseria, M.A. Robb, J.R. Cheeseman, J.A. Montgomery Jr., T. Vreven, K.N. Kudin, J.C. Burant, J.M. Millam, S.S. Iyengar, J. Tomasi, V. Barone, B. Mennucci, M. Cossi, G. Scalmani, N. Rega, G.A. Petersson, H. Nakatsuji, M. Hada, M. Ehara, K. Toyota, R. Fukuda, J. Hasegawa, M. Ishida, T. Nakajima, Y. Honda, O. Kitao, H. Nakai, M. Klene, X. Li, J.E. Knox, H.P. Hratchian, J.B. Cross, V. Bakken, C. Adamo, J. Jaramillo, R. Gomperts, R.E. Stratmann, O. Yazyev, A.J. Austin, R. Cammi, C. Pomelli, J.W. Ochterski, P.Y. Ayala, K. Morokuma, G.A. Voth, P. Salvador, J.J. Dannenberg, V.G. Zakrzewski, S. Dapprich, A.D. Daniels, M.C. Strain, O. Farkas, D.K. Malick, A.D. Rabuck, K. Raghavachari, J.B. Foresman, J.V. Ortiz, Q. Cui, A.G. Baboul, S. Clifford, J. Cioslowski, B.B. Stefanov, G. Liu, A. Liashenko, P. Piskorz, I. Komaromi, R.L. Martin, D.J. Fox, T. Keith, M.A. Al-Laham, C.Y. Peng, A. Nanayakkara, M. Challacombe, P.M.W. Gill, B. Johnson, W. Chen, M.W. Wong, C. Gonzalez, J.A. Pople, *Gaussian 03, Revision C.02*, Gaussian, Inc., Wallingford CT, 2004.
- [32] (a) A.D. Becke, *Phys. Rev. A* 38 (1988) 3098; (b) A.D. Becke, *J. Chem. Phys.* 98 (1993) 5648; (c) C. Lee, W. Yang, R.G. Parr, *Phys. Rev. B* 37 (1988) 785; (d) P.J. Stephens, F.J. Devlin, C.F. Chabalowski, M.J. Frisch, *J. Phys. Chem.* 98 (1994) 11623.
- [33] D. Andrae, U. Häußermann, M. Dolg, H. Stoll, H. Preuss, *Theor. Chim. Acta* 77 (1990) 123.
- [34] (a) K. Nordhoff, D. Steinborn, *Organometallics* 20 (2001) 1408; (b) T. Gosavi, C. Wagner, H. Schmidt, D. Steinborn, *J. Organomet. Chem.* 690 (2005) 3229; (c) M. Werner, T. Lis, C. Bruhn, R. Lindner, D. Steinborn, *Organometallics* 25 (2006) 5946; (d) D. Steinborn, S. Schwiager, *Chem. Eur. J.* 13 (2007) 9668.
- [35] P. Skehan, R. Storeng, D. Scudiero, A. Monks, J. McMahon, D. Vistica, J.T. Warren, H. Bokesch, S. Kenney, M.R. Boyd, *J. Natl. Cancer Inst.* 82 (1990) 1107.
- [36] A. Dietrich, T. Mueller, R. Paschke, B. Kalinowski, T. Behlendorf, F. Reipsch, A. Fruehauf, H.-J. Schmoll, C. Kloft, W. Voigt, *J. Med. Chem.* 51 (2008) 5413.

Synthesis and characterization of carbohydrate platinum(II) complexes with thioglycoside ligands

Cornelia Vetter ^a, P. Pornsuriyasak ^b, Jürgen Schmidt ^c, Martin Bette ^a, Nigam P. Rath ^b, Alexei V. Demchenko ^b, Dirk Steinborn ^{a*}

– Not yet submitted –

Abstract

The reaction of diacetylbis(benzylamine)platinum(II) (**1**) with thioglycosides of the type ch-SPT (PT = 4-(pyridine-2-yl)-thiazole-2-yl) yielded platinum(II) complexes of the composition [Pt(COMe)₂(ch-SPT)] (ch-SPT = OAc-SPT, **7**; OBz-SPT, **8**; OBn-SPT, **9**) in an equilibrium reaction. The formation of the complexes was unambiguously proofed by IR and NMR spectroscopy (¹H, ¹³C, ¹⁹⁵Pt) and high resolution ESI mass spectrometry. ¹H and ¹³C NMR spectra of **7–9** proved the chelating coordination mode due to the SPT-moiety. Isolation of the thioglycoside platinum(II) complexes by adding of diethyl ether failed and led to a shift of the equilibrium in favor of the educts. The analogous reaction of **1E** with ch-Sbpy ligands (bpy = 2,2'-bipyridine-6-yl) with formation of the complexes [Pt(COMe)₂(ch-Sbpy)] (ch-Sbpy = OAc-Sbpy, **10**; OBz-Sbpy, **11**) could be followed by an immediate change of color the reaction mixtures and also proved by high resolution ESI mass spectrometry. Unexpectedly, the respective NMR spectra for **10, 11** showed just the educts, indicating that the equilibrium lies almost completely on the educt side. Crystals of [Pt(COMe)₂(BnNH₂)₂] (**1**) and the uncoordinated OAc-SPT (**2**) could be yielded. The crystal structure of **1** proved the experimental found weak coordination of the benzylamine ligands by the uncommonly long Pt–N bond length of 2.164(2) Å.

Keywords: Platinum(II) carbohydrate complexes, Thioglycosides, Single-crystal X-ray diffraction analysis.

* Corresponding author: Tel. +345 5525620; fax: +345 5527028.
Email: dirk.steinborn@chemie.uni-halle.de (D. Steinborn)

1. Introduction

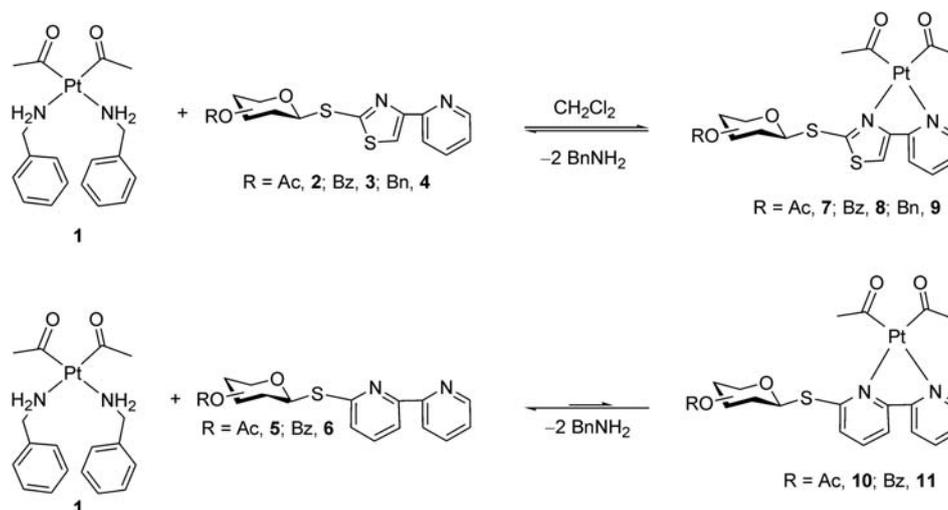
Thiofunctionalized carbohydrates received particular attention, since it was discovered that carbohydrates, containing a ring sulfur atom instead of oxygen, leads to temporary hyperglycemia [1] and sterility in rats [2]. Moreover it has been shown that this compounds possess cancerostatic [3] and enzyme inhibitory activities [4]. Also Thioglycosides (ch-SR), where the carbohydrate is linked *via* the glycosidic bond with a thioalcohol (HSR), as well as carbohydrates containing mercapto groups instead of hydroxyl groups have been proven to exhibit cytotoxic and antiinflammatory properties [5]. In bioinorganic chemistry metal complexes possessing bioactivity are of special interest. Platinum complexes and their application as cancerostatica were established with the discovery of cisplatin in 1965 by Rosenberg [6]. The antitumor effect of cisplatin is based on the intrastrand linkage of the Pt(NH₃)₂ unit mainly to two guanine nucleobases, which causes the inhibition of DNA and RNA replication and finally leads to apoptosis of the cell. To date thousands of platinum complexes, especially those containing platinum in the oxidation state +II, have been tested on their antiproliferative activity, however only few have entered clinical trails [7]. Thus, research for new platinum complexes with comparable or even increased activity and less toxic side effects than cisplatin is still going on. We are interested in the synthesis of platinum complexes with bioactive ligands [8]. Here we report about the reactions of platinum(II) complexes with thioglycosides of the types ch-SPT and ch-Sbpy (PT = 4-(pyridine-2-yl)-thiazole-2-yl; bpy = 2,2'-bipyridine-6-yl) starting from the diacetylbis(benzylamine) platinum(II) complex [Pt(COMe)₂(BnNH₂)₂], which contains exceedingly weakly coordinated benzylamine ligands [9].

2. Results and discussion

Syntheses and characterization of [Pt(COMe)₂(ch-SPT)] (ch-SPT = OAc-SPT, 7; OBz-SPT, 8; OBn-SPT, 9) and [Pt(COMe)₂(ch-Sbpy)] (ch-Sbpy = OAc-Sbpy, 10; OBz-Sbpy, 11)

The reaction of [Pt(COMe)₂(BnNH₂)₂] (**1**) with thioglycosides of the type ch-SPT (ch-SPT = OAc-SPT, **2**; OBz-SPT, **3**; OBn-SPT, **4**) in methylene chloride led to the formation of the complexes [Pt(COMe)₂(ch-SPT)] (ch-SPT = OAc-SPT, **7**; OBz-SPT, **8**; OBn-SPT, **9**) within seconds, according to Scheme 1. After adding of [Pt(COMe)₂(BnNH₂)₂] (**1**) to the solution of the thioglycosides in methylene chloride an immediately change of color occurred, from pale yellow/beige to intensive yellow (**7–9**). The complexes **7–9** are present in an equilibrium with the educts and are formed with a conversion grade up to 80%. Their formation could be

unambiguously verified by IR and ^1H , ^{13}C and ^{195}Pt NMR spectroscopy as well as by high resolution ESI-mass spectrometry. However, the complexes could not be isolated by addition of diethyl ether. Instead a shift of the equilibrium in favor of the educts could be observed. The ^1H and ^{13}C NMR spectroscopy clearly indicated the coordination due to the SPT moiety, by CIS (coordination induced shifts) of the protons and carbon atoms of the anomeric moiety up to 0.32 ppm (^1H) and 2.8 ppm (^{13}C). The pyranoside protons were shifted to a less extent (<0.1 ppm) and/or not at all, while the respective carbon atoms showed no coordination induced shifts. Due to the C_1 symmetry of the complexes two non-resolved broadened signals for the acetyl ligands were observed in the ^1H as well as in the ^{13}C NMR spectra.



Scheme 1.

High resolution ESI mass spectrometry measurements for complexes **7–9** in the reaction mixtures were performed in methanol solutions which showed in all cases the existence of the molecular cation $[\text{Pt}(\text{COMe})_2(\text{ch-SPT})_{+\text{H}}]^+$ (ch-SPT = OAc-SPT, **7**; OBz-SPT, **8**; OBn-SPT **9**) exhibiting an isotopic envelope characteristic for monocations containing one platinum atom [natural isotopic composition: ^{190}Pt (0.01%), ^{192}Pt (0.79%), ^{194}Pt (32.9%), ^{195}Pt (33.8%), ^{196}Pt (25.3%) and ^{198}Pt (7.2%)]. In Figure 1, the spectrum of $[\text{Pt}(\text{COMe})_2(\text{OAc-SPT})]$ (**7**) is shown as an example. The peak of the $[\text{Pt}(\text{COMe})_2(\text{OAc-SPT})_{+\text{Na}}]^+$ cation is found as the most intensive at 828.0863 m/z . Furthermore the peak of the protonated species $[\text{Pt}(\text{COMe})_2(\text{OAc-SPT})_{+\text{H}}]^+$ could be detected at 806.1028 m/z . The observed isotopic pattern of this molecular cation is in a very good agreement with the calculated values (Figure 1). Furthermore, other peaks could be assigned to the complex fragments $[\text{Pt}(\text{COMe})_2(\text{BnNH}_2)(\text{OAc-SPT})_{+\text{H}}]^+$ at 913.1780 m/z and $[\{\text{Pt}(\text{COMe})_2\}_2(\text{OAc-SPT})_{+\text{H}}]^+$ at 1087.1041 m/z . At least the peak at 1087.1041 m/z was formed due to the presence of free benzylamine.

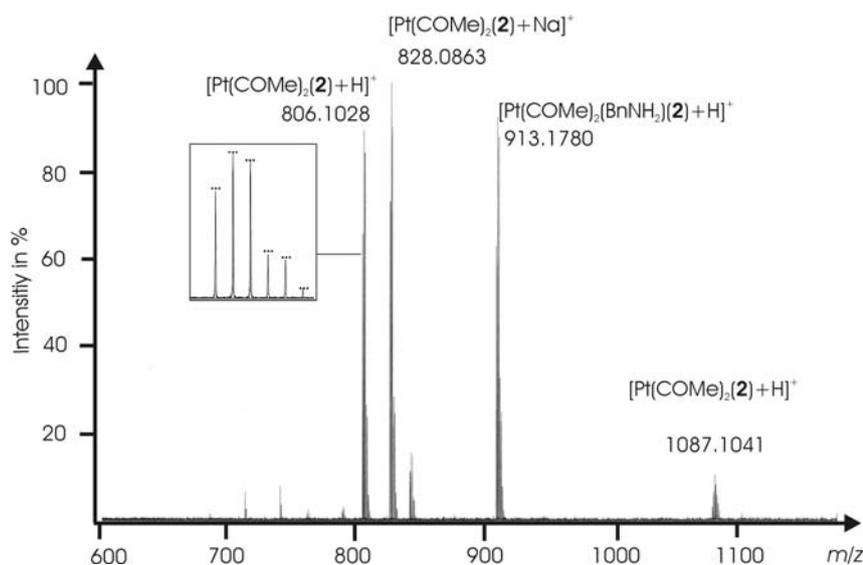


Figure 1. ESI-mass spectrum of $[\text{Pt}(\text{COMe})_2(\text{OAc-SPT})]$ (**7**) and isotopic pattern of the cation $[\text{Pt}(\text{COMe})_2(\mathbf{2})+\text{H}]^+$ at 806.1028 m/z showing the expected intensity due to the isotopic composition (calculated intensities by horizontal bars).

The analogous reactions of $[\text{Pt}(\text{COMe})_2(\text{BnNH}_2)_2]$ (**1**) with ch-Sbpy ligands (ch-Sbpy = OAc-Sbpy, **5**; OBz-Sbpy, **6**) proceeds, apparently, analogous to those reported for ch-SPT ligands (Scheme 1). An immediate change of color from beige to orange is observed after adding **1** to the solution of the ch-Sbpy ligands in methylene chloride. High resolution ESI mass spectrometry showed the formation of the complexes $[\text{Pt}(\text{COMe})_2(\text{ch-Sbpy})]$ (ch-Sbpy = OAc-Sbpy, **10**; OBz-Sbpy, **11**). The spectrum of $[\text{Pt}(\text{COMe})_2(\text{OAc-Sbpy})]$ (**10**) is shown in Figure 2 as an example. The most intensive peak is observed for $[\text{Pt}(\text{COMe})(\text{OAc-SPT})_{+\text{H}}]^+$ at 800.1428 m/z . The observed isotopic pattern of this molecular cation is in a very good agreement with the calculated values (Figure 2). Further peaks could be assigned to the species $[\text{OAc-Sbpy}_{+\text{H}}]^+$ at 519.1440 m/z , $[\text{Pt}(\text{COMe})_2(\text{BnNH}_2)(\text{OAc-Sbpy})_{+\text{H}}]^+$ at 907.2213 m/z and $[\{\text{Pt}(\text{COMe})_2\}_2(\text{OAc-Sbpy})_{+\text{H}}]^+$ at 1081.1447 m/z . In similarity to the spectrum of $[\text{Pt}(\text{COMe})_2(\text{OAc-SPT})]$ (**7**) at least the peak at 907.2213 m/z was formed due to the presence of free benzylamine. However, NMR spectra of the reaction mixture gave no evidence of complex formation, but showed just the presence of the educts. This is a clear difference to the ESI measurements and may be interpreted as an equilibrium reaction, which lies almost completely on the educt side.

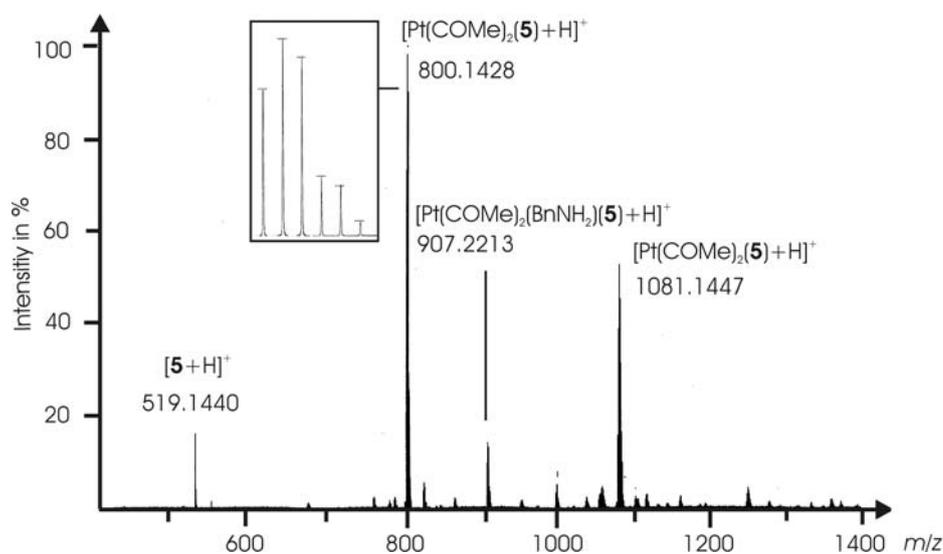


Figure 2. ESI-mass spectrum of $[\text{Pt}(\text{COMe})_2(\text{OAc-Sbpy})]$ (**10**) and isotopic pattern of the cation $[\text{Pt}(\text{COMe})_2(\mathbf{5})+\text{H}]^+$ at 800.1428 m/z showing the expected intensity due to the isotopic composition (calculated intensities by horizontal bars).

*X-ray diffraction analysis of $[\text{Pt}(\text{COMe})_2(\text{BnNH}_2)_2]$ (**1**)*

Crystals of $[\text{Pt}(\text{COMe})_2(\text{BnNH}_2)_2]$ (**1**) were obtained from the reaction mixture of OBz-SPT (**3**) and **1** in methylene chloride/ether (1:2) solution. The complex crystallized in the monoclinic space group $I2/a$. The molecular structure is shown in Figure 3. Selected bond lengths and angles are given in Table 1. Complex **1** exhibits crystallographic imposed C_2 symmetry. The platinum center is square-planar coordinated by two nitrogen and two carbon atoms. The ligands of the same type (benzylamine and acetyl ligands) are on the opposite side of the coordination plane (“*transoid*” conformation). While the mean plane of the benzylamine ligands are planar to the coordination plane in rough approximation (angle: 8.3°), the angle between the mean plane of the acetyl ligands and the coordination plane is 53.9° . The Pt–C bonds ($1.979(2)\text{ \AA}$) belong to the shortest ones described so far in literature (median: 2.003 \AA ; lowest/highest quartile: $1.981/2.016\text{ \AA}$, $n = 32$; n – number of observations) [10]. In contrast, the Pt–N bonds ($2.164(2)\text{ \AA}$) are remarkably longer compared to literature values (median: 2.041 \AA ; lowest/highest quartile: $2.027/2.058\text{ \AA}$, $n = 867$) [10]. Thus, it can be stated that the benzylamine ligands are extremely weakly coordinated. This is in accord with the high substitution lability of the benzylamine ligands in $[\text{Pt}(\text{COMe})_2(\text{BnNH}_2)_2]$ (**1**) [9].

The molecules in **1** are packed like a “staircase” in infinite columns (Figure 3). The interplanar distance between two benzylamine ligands of 3.7 \AA and the corresponding

displacement angle of 10.7°^\dagger indicate a weak stabilization through π - π stacking [11]. The strands are linked through N-H \cdots O (N \cdots O 2.926(3) Å) and C-H \cdots O (C \cdots O 3.328(3) Å) hydrogen bonds, where the oxygen atoms act as bifurcated hydrogen acceptor. Furthermore, a weak intramolecular N-H \cdots O hydrogen bond is found. The geometrical parameters are in the expected range [12,13] and given in Table 2.

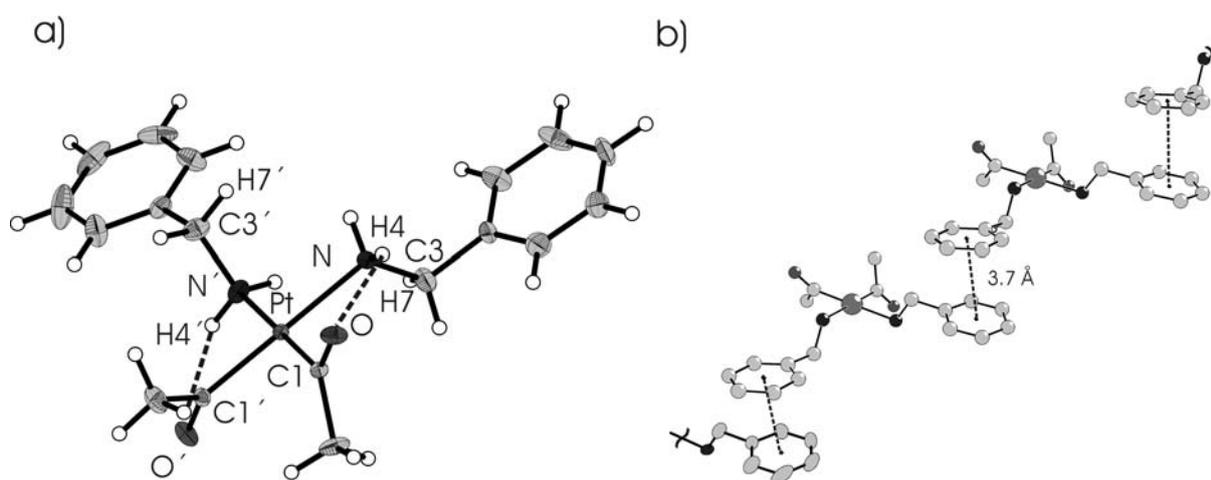


Figure 3. a) Molecular Structure of $[\text{Pt}(\text{COMe})_2(\text{BnNH}_2)_2]$ (**1**). The displacement ellipsoids are drawn at the 30% probability level. b) Solid state structure of $[\text{Pt}(\text{COMe})_2(\text{BnNH}_2)_2]$ (**1**) showing the packing of the cations by π - π stacking. H atoms are omitted for clarity.

Table 1. Selected bond lengths (in Å) and angles (in deg) of **1**.

Pt-C1	1.979(2)	C1-O	1.210(3)
Pt-N	2.164(2)	N-C3	1.459(4)
C1-Pt-C1'	91.8(1)	N-Pt-N'	92.7(1)
C1-Pt-N	87.8(1)	C1'-Pt-N	179.36(9)

[†] The displacement, measured by the angle between the ring normal and the centroid-centroid vector, is a measure for the ring-ring overlap [11].

Table 2. Characteristic parameters of the N–H⋯O and C–H⋯O hydrogen bonds (distances in Å, angles in deg) in **1**.

	D–H	H⋯A	D⋯A	D–H⋯A
N–H5⋯O	0.92	2.08	2.926(3)	153
C3–H7⋯O	0.99	2.38	3.328(3)	161
N–H4⋯O	0.92	2.55	3.095(3)	118

X-ray diffraction analysis of OAc-SPT (2)

In the reaction mixture of **1** and OAc-SPT (**2**) colorless crystals of **2** were obtained, which were suitable for X-ray diffraction analysis. The compound crystallizes in the space group $P2_12_12_1$. The molecular structure of the carbohydrate is shown in Figure 4. Selected bond length and angles are given in Table 3. The glucopyranoside ring is present in a distorted chair conformation in its 4C_1 form [14]. The oxygen atom O9 is disordered over two position with an occupation factor of 62 and 38%, respectively. The two pyridiyl rings of the bipyridine group are remarkably twisted (torsion angle N1–C13–C14–N2: -158.6°). As expected the nitrogen atoms are on opposite sites (“*transoid*” conformation) of the C13–C14 axis to yield the maximum spatial distance for the free electron pair of each nitrogen atom. The molecule exhibits an intramolecular C–H⋯O hydrogen bond (C15⋯O2 3.340(2) Å).

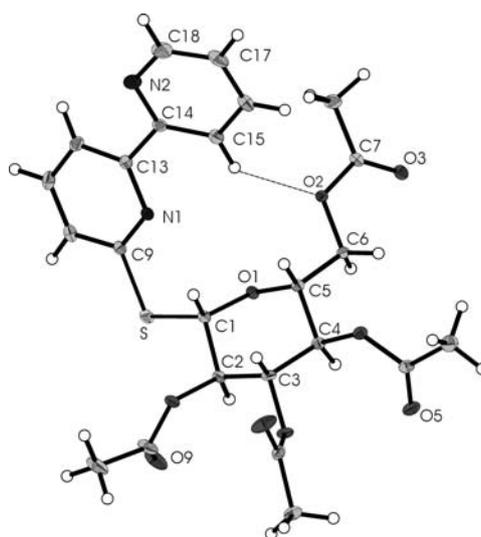
**Figure 4.** Molecular structure of OAc-SPT (**2**), showing the intramolecular C–H⋯O hydrogen bond (---). The displacement ellipsoids are drawn at the 30% probability level. Only the major occupied position of the disordered oxygen atom O9 is shown.

Table 3. Selected bond lengths (in Å) and angles (in deg) of **2**.

C1–S	1.799(2)	C1–C2	1.528(2)
C9–S	1.778(2)	C7–O3	1.206(2)
C1–O1	1.422(2)		
C1–S–C9	100.41(7)	O1–C1–S	108.8(1)
C1–O1–C5	111.5(1)	O2–C7–O3	123.8(1)
O1–C1–C2	107.6(1)		

The packing of OAc-SPT (**2**) is shown in Figure 5. The molecules are arranged in infinite zig-zag chains, which are stabilized through π – π interactions. The intermolecular distance of 3.6 Å and the displacement angle of 10.4° are in the expected range [11]. Additionally, two C–H \cdots O hydrogen bonds can be found within the chain (C3 \cdots O3' 3.327(2) Å; C5 \cdots O3' 3.424(2) Å) as well as one between the chains (C17 \cdots O5'' 3.359(2) Å) as attractive non-bonding interactions. The hydrogen bonds C17–H \cdots O5'' and C12–H \cdots O2 are most likely the reason for the twisting of the pyridyl ring N2, C14–C18. Geometrical parameters of all hydrogen bonds are arranged in Table 4.

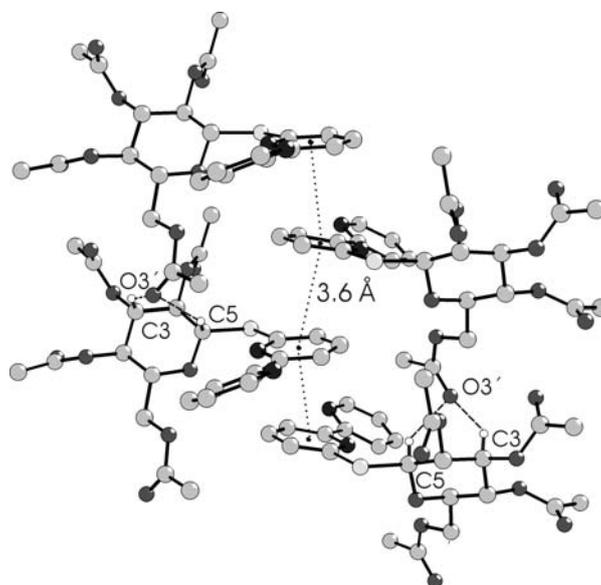


Figure 5. Solid state structure of OAc-SPT (**2**) showing the hydrogen bonding (---) and packing by π – π stacking (···). H atoms not involved in hydrogen bonding are omitted for clarity.

Table 4. Characteristic parameters of the C–H···O hydrogen bonds (distances in Å, angles in deg) in **2**.

	D–H	H···A	D···A	D–H···A
C3–H3···O3′	1.00	2.45	3.327(2)	145
C5–H5···O3′	1.00	2.55	3.424(2)	146
C15–H15···O2	0.95	2.53	3.340(2)	144
C17–H17···O5′′	0.95	2.44	3.359(2)	163

3. Conclusion

The synthesis of the complexes [Pt(COMe)₂(ch-SPT)] (ch-SPT = OAc-SPT, **7**; OBz-SPT, **8**; OBn-SPT, **9**) showed that [Pt(COMe)₂(BnNH₂)] (**1**) is a suitable starting complex for ligand substitution reactions. This could be further proved by X-ray diffraction analysis of [Pt(COMe)₂(BnNH₂)] (**1**), which showed an unusual long Pt–N bond which is in accord with the lability and easy cleavage of the benzylamine ligands. Surprisingly, the reactions are an equilibrium, which is shifted on the educt side by the addition of diethyl ether. For the reactions of **1** with ch-Sbpy (ch-Sbpy = OAc-Sbpy, **5**; OBz-Sbpy, **6**) contrary observations were made. While the ESI mass spectra proved the formation of the complexes [Pt(COMe)₂(ch-Sbpy)] (ch-Sbpy = OAc-Sbpy, **10**; OBz-Sbpy, **11**), the NMR spectra gave no indication of these complexes and showed just the presence of the educts, which indicated that the equilibrium lies almost completely on the side of the educts. This is a clear difference to analogous reactions with *N,N'*-donor ligands reported in literature, where the requisite complexes could be isolated in pure substance using this method [9]. Furthermore, the palladium complex [PdBr₂(ch-SPT)] showed a much greater stability, than the here reported complexes [15]. Further investigations for the syntheses and isolation of these complexes, by changing the solvent etc., have to be done, in particular of [Pt(COMe)₂(ch-Sbpy)] complexes **10** and **11**, to isolate the complexes in substance.

4. Experimental

4.1. General considerations

Syntheses were performed under Argon using standard Schlenk techniques. Methylene chloride and diethyl ether were dried over calcium chloride and Na benzophenone, respectively. All solvents were distilled prior to use. NMR spectra were obtained with Varian UNITY 500 and Gemini 2000 spectrometers using solvent signals (^1H and ^{13}C NMR spectroscopy) as internal references and $\text{Na}_2[\text{PtCl}_6]$ ($\delta(^{195}\text{Pt}) = 0$ ppm) as external reference. IR spectra were recorded on a Galaxy Mattson FT IR spectrometer, using KBr pellets. The positive ion high resolution ESI mass spectra were obtained from a Bruker Apex III Fourier transform ion cyclotron resonance (FT-ICR) mass spectrometer (Bruker Daltonics, Billerica, USA) equipped with an Infinity cell, a 7.0 Tesla superconducting magnet (Bruker), an RF-only hexapole ion guide and an external electron spray ion source (Agilent, off axis spray, voltages: endplate, -3.700V ; capillary, -4.200V ; capillary exit, 100V ; skimmer 1, 15.0 V ; skimmer 2, 6.0 V). Nitrogen was used as drying gas at 150°C . The sample solutions were introduced continuously via a syringe pump with a flow rate of $120\ \mu\text{l h}^{-1}$. The data were acquired with 512k data points and zero filled to 2048k by averaging 64 scans. Diacetylbis(benzylamine)platinum(II) (**1**) and the thioglycosides **2–6** were synthesized according to literature [9,15]

4.2. Syntheses of $[\text{Pt}(\text{COMe})_2(\text{ch})]$ ($\text{ch} = \text{OAc-SPT}$, **7**; OBz-SPT , **8**; OBn-SPT , **9**; OAc-Sbpy , **10**; OBz-Sbpy , **11**)

To a stirred solution of the 4-(pyridin-2-yl)thiazol-2-yl-thioglycoside and 2,2'-bipyridine-6-yl-thioglycoside (0.04 mmol), respectively, in methylene chloride (3 ml) solid diacetylbis(benzylamine)platinum(II) (20.0 mg, 0.04 mol) was added. An immediate change of color to orange/yellow, respectively, could be observed.

$[\text{Pt}(\text{COMe})_2(\text{OAc-SPT})]$ (**7**). Conversion grade: 80%. ^1H NMR (400 MHz, CD_2Cl_2): δ 8.44 (d, 1H, $^3J_{\text{Pt,H}} = 5.2$ Hz, $H_{6\text{SPT}}$), 8.14 (s, 1H, $H_{5'\text{SPT}}$), 7.99 (tr, 1H, $H_{4\text{SPT}}$), 7.92 (tr, 1H, $H_{3\text{SPT}}$), 7.36 (tr, 1H, $H_{5\text{SPT}}$), 5.31 (tr, 1H, $H_{3\text{ch}}$), 5.15 (m, 2H, $H_{2\text{ch}}/H_{4\text{ch}}$), 4.98 (d, 1H, $^3J_{\text{H,H}} = 10.1$ Hz, $H_{1\text{ch}}$), 4.26 (m, 2H, H_{6a} , H_{6b}), 3.93 (m, 1H, $H_{5\text{ch}}$), 2.33 (s+d, br, 3H, $\text{C}(\text{O})\text{CH}_3$), 2.20 (s+d, br, 3H, $\text{C}(\text{O})\text{CH}_3$), 2.19 (s, 3H, $\text{C}(\text{O})\text{CH}_{3\text{ch}}$), 2.10 (s, 3H, $\text{C}(\text{O})\text{CH}_{3\text{ch}}$), 2.03 (s, 3H, $\text{C}(\text{O})\text{CH}_{3\text{ch}}$), 2.03 (s, 3H, $\text{C}(\text{O})\text{CH}_{3\text{ch}}$), 2.00 (s, 3H, $\text{C}(\text{O})\text{CH}_{3\text{ch}}$). ^{13}C NMR (125 MHz, CD_2Cl_2): δ 170.6 ($\text{C}(\text{O})\text{CH}_3$), 170.1 ($\text{C}(\text{O})\text{CH}_3$), 169.9 ($\text{C}(\text{O})\text{CH}_3$), 169.7 ($\text{C}(\text{O})\text{CH}_3$), 151.0

Anhang

($C6_{SPT}$), 139.0 ($C4_{SPT}$), 125.8 ($C5_{SPT}$), 122.1 ($C3_{SPT}$), 121.8 ($C5'_{SPT}$). 84.3 ($C1_{ch}$), 76.8 ($C5_{ch}$), 73.4 ($C3_{ch}$), 69.4 ($C2_{ch}$), 68.3 ($C4_{ch}$), 62.1 ($C6_{ch}$), 45.6 ($C(O)CH_3$), 42.2 ($C(O)CH_3$), 21.0 ($C(O)CH_{3ch}$), 20.9 ($C(O)CH_{3ch}$), 20.7 ($2 \times C(O)CH_{3ch}$). ^{195}Pt -NMR (107 MHz, CDCl_3): δ -1274.7. IR (KBr) 1755 s, 1622 m, 1592 m, 1466 w, 1368 m, 1329 w, 1232 s, 1061 m, 911 w, 802 w cm^{-1} . HR-ESI-MS [$\text{Pt}(\text{COMe})_2(\mathbf{2})_{+H}$] $^+$ m/z (obsd./calc. %) 805.10088 (74/75), 806.10278 (100/100), 807.10434 (94/93), 808.10674 (30/33), 809.10618 (27/29), 810.10772 (7/8).

[$\text{Pt}(\text{COMe})_2(\text{OBz-SPT})$] (**8**). Conversion grade 65%. ^1H NMR (500 MHz, CD_2Cl_2): δ 8.33 (d, 1H, $^3J_{\text{H,H}} = 5.5$ Hz, $H6_{SPT}$), 7.96 (m, 3H, $H3_{SPT}$, $H4_{SPT}$, $H5'_{SPT}$), 7.44–7.22 (m, 21H, $\text{CH}_2\text{C}_6\text{H}_5$), 4.94–4.49 (m, 9H, $H1_{ch}$, $\text{CH}_2\text{C}_6\text{H}_5$), 3.87–3.69 (m, 5H, $H3_{ch}$, $H5_{ch}$, $H6a_{ch}$, $H6b_{ch}$), 3.66 (tr, 1H, $H2_{ch}$), 3.57 (m, 1H, $H5_{ch}$), 2.38 (s+d, br, 3H, $C(O)CH_3$), 2.24 (s+d, br, 3H, $C(O)CH_3$). ^{13}C NMR (50 MHz, CD_2Cl_2): 166.1 ($C(O)C_6H_5$), 170.1 ($C(O)C_6H_5$), 169.9 ($C(O)C_6H_5$), 169.7 ($C(O)C_6H_5$), 151.0 ($C6_{SPT}$), 139.0 ($C4_{SPT}$), 133.9–133.5 ($C(O)C_6H_5$), 130.4–128.5 ($C(O)C_6H_5$, $C5_{SPT}$), ($C3_{SPT}$), 123.3 ($C4_{Taz}$), 121.7 ($C5'_{SPT}$), 119.7 ($C3'_{SPT}$). 85.3 ($C1_{ch}$), 77.2 ($C5_{ch}$), 74.4 ($C3_{ch}$), 70.9 ($C2_{ch}$), 69.6 ($C4_{ch}$), 63.3 ($C6_{ch}$), 46.5 ($C(O)CH_3$), 44.1 ($C(O)CH_3$). ^{195}Pt NMR (107 MHz, CD_2Cl_2): δ -1276.3. IR (KBr) 1730 s, 1621 m, 1602 m, 1468 w, 1452 m, 1316 m, 1262 s, 1178 m, 1112 s, 1092 s, 1069 m, 1025 m, 803 w, 771 w, 709 s cm^{-1} . HR-ESI [$\text{Pt}(\text{COMe})_2(\mathbf{3})_{+H}$] $^+$ m/z (obsd./calc. %) 1053.16251 (64/64), 1054.16310 (100/99), 1055.16269 (99/100), 1056.16436(45/48), 1057.16354(30/33), 1058.16611 (12/13), 1059.16889 (5/5).

[$\text{Pt}(\text{COMe})_2(\text{OBn-SPT})$] (**9**). Conversion grade: 75%. ^1H NMR (400 MHz, CDCl_3): δ 8.49 (d, 1H, $H6_{SPT}$), 7.89 (m, 1H, $H4_{SPT}$), 7.74 (d, 1H, $H3_{SPT}$), 7.68 (s, 1H, $H5'_{SPT}$), 4.90–4.41 (m, 9H, $H1_{ch}$, $\text{CH}_2\text{C}_6\text{H}_6$), 3.75–3.61 (m, 5H, $H2_{ch}$, $H3_{ch}$, $H5_{ch}$, $H6a_{ch}$, $H6b_{ch}$), 3.53 (dd, 1H, $H4_{ch}$), 2.43 (s, br, 3H, $C(O)CH_3$), 2.29 (s, br, 3H, $C(O)CH_3$). ^{13}C NMR (125 MHz, CD_2Cl_2): δ . 151.1 ($C6_{SPT}$), 138.9 ($\text{CH}_2\text{C}_6\text{H}_5$), 138.7 ($\text{CH}_2\text{C}_6\text{H}_5$), 138.6 ($\text{CH}_2\text{C}_6\text{H}_5$), 138.5 ($\text{CH}_2\text{C}_6\text{H}_5$), 137.8 ($C4_{SPT}$), 128.9–128.9 ($\text{CH}_2\text{C}_6\text{H}_5$), 125.5 ($C5_{SPT}$), 121.7 ($C3_{SPT}$), 121.1 ($C5'_{SPT}$), 86.5 ($C3_{ch}$), 85.8 ($C1_{ch}$), 80.7 ($C2_{ch}$), 79.7 ($C5_{ch}$), 77.7 ($C4_{ch}$), 76.0 ($\text{CH}_2\text{C}_6\text{H}_5$), 75.4 ($\text{CH}_2\text{C}_6\text{H}_5$), 73.7 ($\text{CH}_2\text{C}_6\text{H}_5$), 69.0 ($C6_{ch}$), 45.9 ($C(O)CH_3$), 42.8 ($C(O)CH_3$). ^{195}Pt NMR (107 MHz, CD_2Cl_2): δ -1244.1. IR (KBr) 1730 s, 1621 m, 1602 m, 1468 w, 1452 m, 1316 m, 1262 s, 1178 m, 1112 s, 1092 s, 1069 m, 1025 m, 803 w, 771 w, 709 s cm^{-1} . HR-ESI [$\text{Pt}(\text{COMe})_2(\mathbf{4})_{+H}$] $^+$ m/z

Anhang

(obsd./calc. %) 997.24662 (64/65), 998.24799 (100/100), 999.24867 (100/100), 1000.25179 (47/47), 1001.25367 (32/32), 1002.25754 (12/13), 1003.25900 (4/5).

[Pt(COMe)₂(OAc-Sbpy)] (**10**). HR-ESI-MS [Pt(COMe)₂(**5**)_{+H}]⁺ *m/z* (obsd./calc. %) 799.14209 (75/74), 800.14280 (100/100), 801.14258 (92/90), 802.14664 (30/30), 803.14833 (26/25), 804.15137 (7/7).

[Pt(COMe)₂(OBz-Sbpy)] (**11**). HR-ESI-MS [Pt(COMe)₂(**6**)_{+H}]⁺ *m/z* (osvd./calc. %) 1047.20710 (62/64), 1048.20987 (100/100), 1049.21123 (99/98), 1050.21476 (44/44), 1051.21563 (29/29), 1052.21844 (11/12), 1053.21993 (4/4).

4.3. X-ray diffraction analysis

Single crystals of **1** and **2** suitable for X-ray diffraction measurements, were from methylene chloride/diethyl ether (1:2). Intensity data were collected on a STOE IPDS diffractometer (**1**) and on a Bruker Apex II Kappa diffractometer (**2**) with Mo- $K\alpha$ radiation ($\lambda = 0.71073 \text{ \AA}$, graphite monochromator) at 100(2) K. A summary of the crystallographic data, the data collection parameters and the refinement parameter is given in Table 5. Multiscan absorption corrections were applied (T_{\min}/T_{\max} 0.49/1.00, **1**; T_{\min}/T_{\max} 0.90/0.98, **2**). The structures were solved by direct methods with SHELXS-97 [16] and refined using full-matrix least-square routines against F^2 with SHELXL-97 [16]. Non-hydrogen atoms were refined with anisotropic displacement parameters. Hydrogen atoms were positioned geometrically and refined with isotropic displacement parameters according to the “riding model”. The oxygen atom O9 was found to be disordered and was refined freely with an occupation factor of 68 and 32%, respectively.

5. Acknowledgement

Gifts of Merck are gratefully acknowledged

Table 5. Crystal Data, data collection and refinement parameters of [Pt(COMe)₂(NH₂Bn)₂](**1**) and OAc-SPT (**2**).

	1	2
Empirical formula	C ₁₈ H ₂₄ N ₂ O ₂ Pt	C ₂₄ H ₂₆ N ₂ O ₉ S
Formula weight	495.48	518.53
Crystal system/space group	monoclinic/ <i>I</i> 2/ <i>a</i>	orthorhombic/ <i>P</i> 2 ₁ 2 ₁ 2 ₁
<i>Z</i>	4	4
<i>a</i> /Å	9.3628(2)	6.9807(7)
<i>b</i> /Å	20.0751(2)	16.605(2)
<i>c</i> /Å	9.6263(1)	21.739(2)
β /°	96.049(1)	
<i>V</i> /Å ³	1799.28(5)	2519.8(5)
ρ /g·cm ⁻³	1.829	1.367
μ (Mo-K α)/mm ⁻¹	7.809	0.183
<i>F</i> (000)	960	1088
Scan range/°	3.53 < θ < 28.28	3.06 < θ < 27.57
Reciprocal lattice segments	-11→12, -26→26,	-9→9, -21→21,
<i>h, k, l</i>	-12→12	-28→28
Reflections collected	22854	83292
Reflections independent	2236(<i>R</i> _{int} = 0.0277)	5803(<i>R</i> _{int} = 0.0544)
Data/restraints/parameters	2236/0/106	5803/0/339
Goodness-of-fit on <i>F</i> ²	1.065	1.032
<i>R</i> ₁ , <i>wR</i> ₂ [<i>I</i> > 2 σ (<i>I</i>)]	0.0153, 0.0380	0.0321, 0.0753
<i>R</i> ₁ , <i>wR</i> ₂ (all data)	0.0174, 0.0383	0.0368, 0.0776
Largest diff. peak and hole/e·Å ⁻³	1.213 and -0.679	0.235 and -0.238

References

- [1] a) D. J. Hoffman, R. L. Whistler, *Biochemistry* **1968**, 7, 4479. b) R. L. Whistler, W. C. Lake, *Biochem. J.* **1972**, 130, 919. c) B. Hellman, Å. Lernmark, J. Sehlin, I.-B. Täljedal, R. L. Whistler, *Biochem. Pharmacol.* **1973**, 22, 29.
- [2] J. R. Zysk, A. A. Bushway, R. L. Whistler, W. W. Carlton, *J. Reprod. Fertil.* **1975**, 45, 69.
- [3] a) J. H. Kim, S. H. Kim, E. W. Hahn, C. W. Song, *Science* **1978**, 200, 206. b) M. Bobek, R. L. Whistler, A. Bloch, *J. Med. Chem.* **1972**, 15, 168. c) M. Bobek, A. Bloch, R. Parthasarathy, R. L. Whistler, *J. Med. Chem.* **1975**, 18, 784.
- [4] a) H. Hashimoto, T. Fujimori, H. Yuasa, *J. Carbohydr. Chem.* **1990**, 9, 683. b) C.-H. Wong, Y. Ichikawa, T. Krach, C. G.-L. Narvor, D. P. Dumas, G. C. Look, *J. Am. Chem. Soc.* **1991**, 113, 8137. c) B. D. Johnston, B. M. Pinto, *J. Org. Chem.* **1998**, 63, 5797.
- [5] a) M. Takeuchi, M. Yoshikawa, R. Sasaki, H. Chiba, *Agric. Biol. Chem.* **1982**, 46, 2741. b) G. Guo, G. Li, D. Liu, Q.-J. Yang, Y. Liu, Y.-K. Jing, L.-X. Zhao, *Molecules* **2008**, 13, 1487. c) M. Singer, M. Lopez, L. F. Bornaghi, A. Innocenti, D. Vullo, C. T. Supuran, S.-A. Poulsen, *Bioorg. Med. Chem. Lett.* **2009**, 19, 2273. d) N. Khalifa, M. Ramla, A. E.-G. E. Amr, M. M. Abdulla, *Phosphorus, Sulfur, Silicon Relat. Elem.* **2008**, 183, 3046.
- [6] B. Rosenberg, L. Van Camp, T. Krigas, *Nature* **1965**, 205, 698.
- [7] M. A. Fuertes, C. Alonso, J. M. Pérez, *Chem. Rev.* **2003**, 103, 645.
- [8] a) C. Vetter, C. Wagner, J. Schmidt, D. Steinborn, *Inorg. Chim. Acta* **2006**, 359, 4326. b) C. Vetter, C. Wagner, G. N. Kaluderović, R. Paschke, D. Steinborn, *Inorg. Chim. Acta* **2009**, 362, 189. c) C. Vetter, G. N. Kaluderović, R. Paschke, S. Gómez-Ruiz, D. Steinborn, *Polyhedron* **2009**, 28, 3699. d) P. Pornsuriyasak, C. Vetter, S. Kaeothip, M. Kovermann, J. Balbach, D. Steinborn, A. V. Demchenko, *Chem. Commun.* **2009**, 6379.
- [9] a) T. Kluge, *diploma theses*, Martin-Luther-Universität Halle-Wittenberg, 2009. b) M. Bette, *diploma theses*, Martin-Luther-Universität Halle-Wittenberg, 2008.
- [10] Cambridge Structural Database (CSD), Version 5.30 2008, Cambridge University Chemical Laboratory, Cambridge (England).
- [11] C. Janiak, *J. Chem. Soc., Dalton Trans.* **2000**, 3885.
- [12] a) Y. Gu, T. Kar, S. Scheiner, *J. Am. Chem. Soc.* **1999**, 121, 9411.
- [13] a) T. Steiner, *New J. Chem.* **1998**, 1099. b) G. R. Desiraju, T. Steiner, *The Weak Hydrogen Bond*, Oxford University Press, Oxford, 1999. c) D. Braga, F. Grepioni, *Acc.*

Anhang

- Chem. Res.* **1997**, *30*, 81. d) D. Braga, F. Grepioni, K. Biradha, V. R. Pedireddi, G. R. Desiraju, *J. Am. Chem. Soc.* **1995**, *117*, 3156.
- [14] R. Bucourt, *Top. Stereochemistry* **1974**, *8*, 159.
- [15] P. Pornsuriyasak, N. P. Rath, A. V. Demchenko, *Chem. Commun.* **2008**, 5633.
- [16] G. M. Sheldrick, *Acta Crystallogr., Sect. A: Found. Crystallogr.* **2008**, *64*, 112.

Synthesis, characterization and reactivity of carbohydrate platinum(IV) complexes with thioglycoside ligands†

Cornelia Vetter,^a Papapida Pornsuriyasak,^b Jürgen Schmidt,^c Nigam P. Rath,^b Tobias Rüffer,^d Alexei V. Demchenko^{*b} and Dirk Steinborn^{*a}

Received 23rd December 2009, Accepted 16th April 2010

First published as an Advance Article on the web 1st June 2010

DOI: 10.1039/b927058b

Reactions of *fac*-[PtMe₃(4,4'-R₂bpy)(Me₂CO)][BF₄] (R = H, **1a**; ^tBu, **1b**) and *fac*-[PtMe₃-(OAc-κ²O,O')(Me₂CO)] (**2**), respectively, with thioglycosides containing thioethyl (ch-SEt) and thioimidate (ch-STaz, Taz = thiazoline-2-yl) anomeric groups led to the formation of the carbohydrate platinum(IV) complexes *fac*-[PtMe₃(4,4'-R₂bpy)(ch*)][BF₄] (ch* = ch-SEt, **8–14**; ch-STaz, **15–23**) and *fac*-[PtMe₃(OAc-κ²O,O')(ch*)] (ch* = ch-SEt, **24–28**; ch-STaz = **29–35**), respectively. NMR (¹H, ¹³C, ¹⁹⁵Pt) spectroscopic investigations and a single-crystal X-ray diffraction analysis of **19** (ch-STaz = 2-thiazolinyl 2,3,4,6-tetra-*O*-benzoyl-1-thio-β-D-galactopyranose) revealed the *S* coordination of the ch-SEt glycosides and the *N* coordination of the ch-STaz glycosides. Furthermore, X-ray structure analyses of the two decomposition products *fac*-[PtMe₃(bpy)(STazH-κS)][BF₄] (**21a**) and 1,6-anhydro-2,3,4-tri-*O*-benzoyl-β-D-glucopyranose (**23a**), where a cleavage of the anomeric C–S bond had occurred in both cases, gave rise to the assumption that this decomposition was mediated due to coordination of the thioglycosides to the high electrophilic platinum(IV) atom, in non-strictly dried solutions. Reactions of *fac*-[PtMe₃(Me₂CO)₃][BF₄] (**3**) with ch-SEt as well as with ch-SPT and ch-Sbpy thioglycosides (PT = 4-(pyridine-2-yl)-thiazole-2-yl; bpy = 2,2'-bipyridine-6-yl), having *N*,*S* and *N*,*N* heteroaryl anomeric groups, respectively, led to the formation of platinum(IV) complexes of the type *fac*-[PtMe₃(ch*)][BF₄] (ch* = ch-SEt, **36–40**, ch-SPT **42–44**, ch-Sbpy **45**, **46**). The thioglycosides were found to be coordinated in a tridentate κS,κ²O,O', κS,κN,κO and κS,κ²N,N' coordination mode, respectively. Analogous reactions with ch-STaz ligands succeeded for 2-thiazolinyl 2,3,4-tri-*O*-benzyl-6-*O*-(2,2'-bipyridine-6-yl)-1-thio-β-D-glucopyranoside (**5h**) resulting in *fac*-[PtMe₃(ch-STaz)][BF₄] (**41**, ch-STaz = **5h**), having a κ²N,N',N'' coordinated thioglycoside ligand.

1. Introduction

Carbohydrates are one of the most important classes of biomolecules. Attached to lipids, proteins and nucleobases they exert versatile functions in living organisms, ranging from immune defence and cell growth to inflammation and malignant transformations.^{1,2} Carbohydrate-based pharmaceuticals have been proven to be promising therapeutics for neurodegenerative diseases, because they can easily pass the blood brain barrier.³ Thiofunctionalized carbohydrates were proved

to possess significant bioactivity. It was found that 5-thio-β-D-glucopyranose, where the ring oxygen is replaced by sulfur, can cause temporary diabetes and sterility in rats.⁴ Moreover, this carbohydrate class, having a ring sulfur atom, exhibit cancerostatic properties⁵ and act as enzyme inhibitors.⁶ Up to now, it has also been shown that thioglycosides and carbohydrates with mercapto groups instead of hydroxyl groups are enzyme inhibitors and thereby possess antiproliferative and anti-inflammatory properties.⁷ Metal-coordination of carbohydrates also plays a significant role in biosyntheses, including metal transportation and storage or the regulation of metalloenzymes.^{8,9} Furthermore, metal-carbohydrate complexes have been investigated as potent radiopharmaca¹⁰ and cancerostatica, where platinum compounds are of considerable interest.¹¹ From a coordination chemistry perspective the syntheses of carbohydrate platinum(IV) complexes, particularly with non-functionalized carbohydrate ligands, represent a notable challenge, due to their weak donor ability and their propensity to act as reducing agents.¹² On the other hand, platinum(IV) complexes are kinetically inert due to the low-spin *d*⁶ electron configuration, so substitution reactions are not favored. However, numerous platinum(IV) complexes with neutral carbohydrate ligands have been synthesized using trimethylplatinum(IV) precursor complexes such as *fac*-[PtMe₃(Me₂CO)₃][BF₄]. Complexes of this type have proven especially useful in this respect because the high donor capability of the methyl ligands stabilizes

^aInstitut für Chemie – Anorganische Chemie, Martin-Luther-Universität Halle-Wittenberg, D-06120, Halle, Kurt-Mothes-Straße 2, Germany. E-mail: dirk.steinborn@chemie.uni-halle.de; Fax: +49345 5527028; Tel: +49345 5525620

^bDepartment of Chemistry and Biochemistry, University of Missouri-St. Louis, 63121, Missouri, One University Boulevard, USA. E-mail: demchenkoa@umsl.edu; Tel: +1314 5167995

^cLeibniz-Institut für Pflanzenbiochemie, D-06120, Halle, Weinberg 3, Germany

^dInstitut für Chemie – Technische Universität Chemnitz, D-09111, Chemnitz, Straße der Nationen 62, Germany

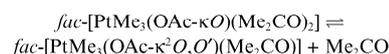
† Electronic supplementary information (ESI) available: Experimental data for *fac*-[PtMe₃I(4,4'-^tBu,bpy)]. Spectroscopic data for complexes **1–46**. Energies and Cartesian coordinates calculated for equilibrium structures **2** and **2'**. CCDC reference numbers 758897–758899. For ESI and crystallographic data in CIF or other electronic format see DOI: 10.1039/b927058b

the platinum(IV) oxidation state. Furthermore, the leaving ligands (acetone) are only weakly coordinated and their substitution is additionally facilitated by the high *trans* effect of the methyl ligands.¹³ Herein we present the synthesis, characterization and reactivity of various types of trimethylplatinum(IV) complexes with thioglycoside ligands.

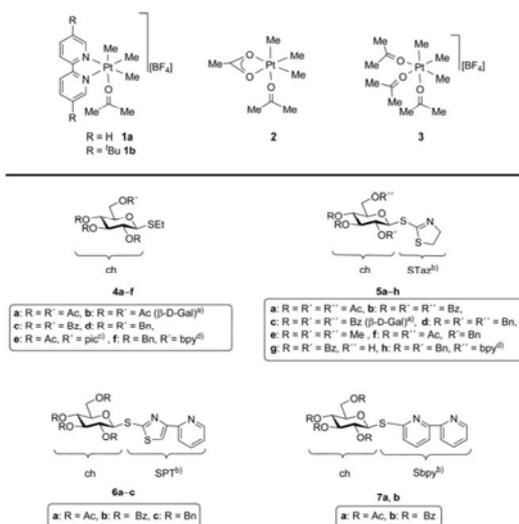
2. Results and discussion

2.1. Starting complexes and ligands

For the synthesis of trimethylplatinum(IV) complexes with thioglycoside ligands, starting complexes having up to three substitution-labile ligands were used. Complexes with one substitution-labile acetone ligand, *fac*-[PtMe₃(Me₂CO)(bpy)][BF₄] (**1a**) and *fac*-[PtMe₃(Me₂CO)(4,4'-*t*-Bu₂bpy)][BF₄] (**1b**; Scheme 1), were prepared by the reaction of *fac*-[PtMe₃(bpy)] and *fac*-[PtMe₃(4,4'-*t*-Bu₂bpy)], respectively, with Ag[BF₄].¹⁴ The reaction of the tetranuclear heterocubane complex *fac*-[(PtMe₃I)₄] with AgOAc resulted in the formation of *fac*-[PtMe₃(OAc)(Me₂CO)_{*n*}] (**2**). The acetato ligand can be bidentately or monodentately coordinated (OAc-κ²O, *n* = 1; OAc-κO, *n* = 2). DFT calculations showed that the free energy at 298 K of the reaction



amounts to be -44 kJ mol⁻¹ in the gas phase and -61 kJ mol⁻¹ in acetone. This gives proof that the acetato ligand is bidentately bound. Nevertheless, both complexes have at their disposal up to three substitution-labile coordination sites, namely one when the acetone ligand is cleaved off and the acetato ligand is still coordinated in a chelating binding fashion, two when the acetone



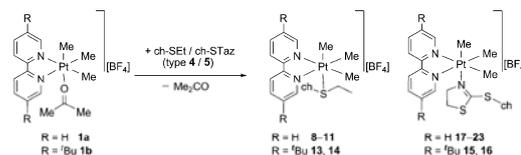
Scheme 1 Platinum(IV) precursor complexes and β-D-thioglycosides used as ligands. ^a β-D-Galactose: OR at C4 in axial position. ^b Abbreviations: ch-STaz: Taz = thiazoline-2-yl; ch-SPT: PT = 4-(pyridine-2-yl)-thiazole-2-yl; ch-Sbp: bpy = 2,2'-bipyridine-6-yl. ^c pic: 2-picolone-2-yl. ^d bpy₋₁₁: 2,2'-bipyridine-6-yl.

ligand is cleaved off and the acetato ligand remains to be κ'O coordinated or three in the case of complete cleavage of the acetato ligand.

The analogous reaction of *fac*-[(PtMe₃I)₄] with Ag[BF₄] led to *fac*-[PtMe₃(Me₂CO)₃][BF₄] (**3**; Scheme 1), which possesses three substitution-labile acetone ligands.¹³ It should be noted that all complexes described here were synthesized *in situ* and used directly for reactions with thioglycosides which are summarized in Scheme 1. Four different classes of thioglycosides have been investigated, namely those with SEt anomeric groups ch-SEt (**4a-f**) and those having *N,S* or *N,N* heterocyclic anomeric groups: ch-STaz (**5a-h**; Taz = thiazoline-2-yl), ch-SPT (**6a-c**; PT = 4-(pyridine-2-yl)-thiazole-2-yl) and ch-Sbp (**7a,b**; bpy = 2,2'-bipyridine-6-yl).

2.2. Cationic platinum(IV) complexes with monodentately coordinated thioglycoside ligands

Syntheses and X-ray diffraction analysis. Complexes **1a** and **1b** reacted in acetone with stoichiometric amounts of thioglycosides of type **4** and **5** (Scheme 1) yielding ionic complexes of the type *fac*-[PtMe₃(4,4'-R₂bpy)(ch-SEt-κS)][BF₄] (R = H: **8-11**; R = *t*-Bu: **13, 14**) and *fac*-[PtMe₃(4,4'-R₂bpy)(ch-STaz-κN)][BF₄] (R = H: **17-23**; R = *t*-Bu: **15, 16**), respectively (Scheme 2, Table 1). The complexes were isolated as moderately air-stable yellow and white powders, respectively, in yields of 45–94%. All complexes were characterized by ¹H, ¹³C and ¹⁹⁵Pt NMR spectroscopy as well as by IR spectroscopy, high resolution ESI mass spectrometry and in the case of **19** also by X-ray diffraction analysis.



Scheme 2 Syntheses of carbohydrate platinum(IV) complexes *fac*-[PtMe₃(4,4'-R₂bpy)(ch*)][BF₄] (ch* = ch-SEt, R = H: **8-11**, R = *t*-Bu: **13, 14**; ch-STaz, R = H: **17-23**, R = *t*-Bu: **15, 16**).

Small colorless needles of *fac*-[PtMe₃(bpy)(ch-STaz)][BF₄] (**19**; ch-STaz = **5c**) were formed in an acetone solution layered with tetrahydrofuran and diethyl ether. Complex **19** crystallized in the chiral space group *P*4₂,2. The asymmetric unit consists of two symmetry independent *fac*-[PtMe₃(bpy)(ch-STaz)]⁺ (ch-STaz = **5c**) cations, and two [BF₄]⁻ anions, wherein one exhibits a disorder. In Fig. 1, only one of the cations is illustrated, whereas the other one exhibits a similar structure. Selected bond lengths and angles are given in the figure caption. In complex **19** the platinum atom [PtC₃N₃] is octahedrally coordinated by three methyl ligands in *facial* arrangement, a bipyridine ligand and the thiazoline-2-yl ring, which is coordinated *via* the nitrogen atom. The angle between the thiazoline-2-yl ring and the equatorial [PtC₃N₃] plane is nearly perpendicular (86.5/89.8°[‡]). The Pt–N bond length (2.16(1)/2.17(2) Å) belongs to the longest bonds known for Pt(IV)–N(CH₂)=C complexes (median: 2.139 Å, lower/upper quartile:

[‡] The values of the two symmetry independent molecules are given separated by a slash.

Table 1 ^1H and ^{13}C NMR spectroscopic data (δ in ppm, J in Hz) of the methyl ligands and ^{195}Pt chemical shifts of the complexes *fac*-[PtMe₃(bpy)(ch*)][BF₄] (**8–12**; **17–23**) and *fac*-[PtMe₃(4,4'-tBu₂bpy)(ch*)][BF₄] (**13–16**)

Complex	ch*	δ_{H}		δ_{C}		$^1J_{\text{Pt,C}}$		$^2J_{\text{Pt,H}}$		δ_{Pt}
		<i>trans</i> ch*	<i>trans</i> N _{bpy}							
8	ch-SEt									
	4a	0.66	1.09	5.8	-5.0/-5.1	662.0	657.0./658.3	72.0	67.8	-2772
	4b	0.65	1.09/1.11	5.1	-5.1/-5.4	652.0	662.0/654.5	71.6	69.3/67.8	-2529
	4c	0.71	1.16	5.4	-4.5/-4.7	660.0	657.3/662.8	72.3	67.5	-2447
	4d	0.64	1.14/1.16	5.1	-5.1/-5.2	649.5	663.2/662.0	71.0	66.9/66.9	-2446
12	4e	0.68	1.18/1.19	5.2	-4.6/-4.7	648.4	662.2/661.5	71.1	67.4/67.4	-2469
13	4a	0.66	1.03/1.10	5.8	-5.2/-5.3	647.1	659.4/664.6	72.6	66.4/67.1	-2769
14	4c	0.59	1.04	5.8	-5.0/-5.2	658.3	655.8/662.0	72.2	68.2	-2435
15	ch-STaz									
	5c	0.53	1.13	-5.4	-3.3	678.2	675.7	71.4	68.1	-2716
	5g	0.32	0.83/1.02	-6.1	-3.2/-4.7	676.6	667.0/684.4	72.5	67.6/66.9	-2452
	5a	0.45	1.13/1.17	-5.5	-3.2/-4.2	673.1	677.0/677.8	72.2	68.5/67.2	-2730
	5b	0.38	0.93/1.08	-5.7	-3.6	672.4	676.2	72.2	67.2/67.2	-2683
	5e	0.39	0.93/1.08	-5.7	-3.6/-4.2	674.4	678.2/676.9	72.2	67.2/68.1	-2710
	5d	0.45	1.21/1.23	-5.7	-3.7/-4.0	674.3	679.4/679.3	72.2	67.2/68.1	-2695
	5f	0.42	1.18/1.19	-5.5	-4.0/-4.1	673.8	680.6/680.7	72.2	67.2/68.1	-2704
	5f	0.42	1.19	-5.6	-3.7/-4.1	677.5	679.4/679.8	72.2	68.1	-2444
	5g	0.37	0.93/1.06	-5.7	-3.6/-4.2	678.5	679.4/675.6	72.2	67.2/67.2	-2445

2.049/2.163 Å, $n = 36$; n – number of observations¹⁵), likely due to the high *trans* influence of the methyl ligands.^{13,16} The STaz ring exhibits a distorted half-chair conformation, while the pyranose ring assumes a distorted chair conformation.¹⁷ A complex hydrogen bond network of moderate to weak inter- and intramolecular hydrogen bonds of the types C–H...O, C–H...F and C–H...S, respectively, is found in crystals of **19**.

NMR spectroscopic characterization of the complexes 8–23. The ^1H and ^{13}C NMR spectra of complexes **8–23** showed unambiguously the coordination of the thioglycosides. Due to the coordination of the chiral carbohydrates to the platinum atom the complexes exhibited C_1 symmetry. Thus, a double signal set for the two halves of the bipyridine ligand, as along with the methyl ligands in *trans* position to the bipyridine ligand could be observed (Table 1). However, the chemical shifts of the methyl ligands were still very similar, leading to coincidence of signals for some compounds (Table 1). Coordination of the carbohydrates in complexes **8–23** led to a partial broadening of the signals of the carbohydrate protons and carbon atoms at room temperature, which has been proven to be characteristic for carbohydrate coordination also in other carbohydrate platinum(IV) complexes.¹³ A general shift of the resonances of the carbohydrate protons to higher field was observed for the complexes **8–23**. Furthermore, the shift differences of the signals for the two protons belonging to the CH₂ groups of the SEt and STaz moieties were significantly increased due to the coordination to the platinum atom. On the other hand, only marginal coordination-induced shifts (CIS \leq 1.6 ppm) for the resonances of the pyranose ring carbon atoms could be found.

In the case of complexes **8–11**, **13** and **14** the *S* coordination of the SEt group gave rise to upfield shifts of the CH₂ proton signals of the SEt group up to 0.32 ppm and of the H1 protons up to 0.11 ppm. Interestingly, the coordination-induced shifts both of the carbon atom resonances of the Et group and of the anomeric C atom resonances were small (\leq 1.0 ppm) with the exception of

complex **11**, where the carbon atom of the methylene group was shifted upfield by 1.9 ppm. For complex **12**, wherein thioglycoside **4e**, having an additional *N*-donor site (picoline-2-yl), was used, the coordination mode could not be unambiguously assigned. On the one hand, the picoline-2-yl resonances in the ^1H and ^{13}C NMR spectra are shifted downfield up to 0.2 and 2.4 ppm, respectively, which indicated an *N* coordination. Conversely, the broadening and increase of the shift differences for the signals of the CH₂ group of the SEt moiety in the ^1H NMR spectrum, as well as the $^1J_{\text{Pt,C}}$ coupling constant of the methyl ligand in *trans* position to the thioglycoside ligand of 648.4 Hz, indicated an *S* coordination.

In the case of complexes **15–23** the κN coordination of the STaz moiety has been proven unambiguously by the X-ray structure analysis of complex **19**. Comparison of ^1H and ^{13}C NMR data of complex **19** with those of the other complexes clearly demonstrated that the complexes **15–18** and **20–23** also possess bound κN coordinated ligands. Without the structural information on complex **19** it would be impossible to derive the coordination mode solely based on the NMR data. The signals for the NCH₂ and H1 protons showed the greatest CIS's (up to 0.98 ppm and 0.57 ppm, respectively). On the other hand, the carbon atom resonances of the SCH₂ groups were strongly shifted upfield (up to 3.4 ppm), whereas the carbon atom resonances of the NCH₂ groups were only marginally shifted (up to 0.4 ppm).

The ^1H and ^{13}C NMR signals of the methyl ligands *trans* to the thioglycoside ligands of type **4** were found in the range of 0.59–0.71 and 5.1–5.8 ppm, respectively. The requisite signals in complexes **15–23** with carbohydrate ligands of type **5** were found upfield shifted, with the shifts ranging from 0.32–0.53 ppm and -5.4 to -6.1 ppm, respectively. It had been shown, that the $^1J_{\text{Pt,C}}$ coupling constants in complexes of this type can be regarded to be a measure for the *trans* influence.¹⁶ The comparison of the $^1J_{\text{Pt,C}}$ couplings constants of the methyl ligands *trans* to the carbohydrate ligands in complexes **8–14** (647.1–662.0 Hz) with those in complexes **15–23** (672.4–678.5 Hz) indicated a higher *trans* influence of the thioglycosides with the SEt group than that of the respective

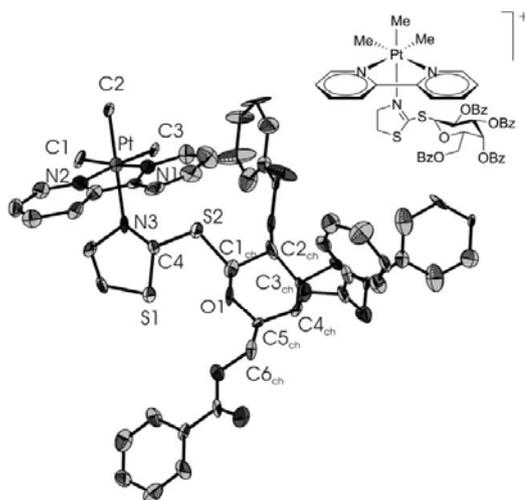


Fig. 1 Molecular structure of one of the two crystallographically independent cations of *fac*-[PtMe₃(bpy)(ch-STaz-κN)](BF₄) (19, ch-STaz = 5c). Hydrogen atoms are omitted for clarity. The ellipsoids are drawn at the 30% probability level. Selected bond lengths (in Å) and angles (in °): Pt–C1 2.14(2)/2.03(1), Pt–C2 1.98(1)/2.07(2), Pt–C3 2.02(2)/2.05(2), Pt–N3 2.16(1)/2.17(2), N3–C4 1.30(2)/1.33(2), C4–S2 1.73(2)/1.67(2), C1_{ch}–S2 1.85(2)/1.82(2), C1_{ch}–C2_{ch} 1.55(2)/1.64(2), C2_{ch}–C3_{ch} 1.51(2)/1.56(2), C3_{ch}–C4_{ch} 1.44(2)/1.54(2), C4_{ch}–C5_{ch} 1.43(2)/1.70(2), C5_{ch}–O1 1.41(2)/1.51(2), C1_{ch}–O1 1.42(2)/1.42(2), C1–Pt1–C2 88.8(6)/84.5(8), C2–Pt1–N3 179.5(6)/174.0(8), C3–Pt1–N2 175.3(6)/177.2(6), C4–S2–C1_{ch} 104.6(8)/101.8(9), C1_{ch}–O1–C5_{ch} 111(1)/117(1), O1–C1_{ch}–C2_{ch} 111(2)/111(2), C1_{ch}–C2_{ch}–C3_{ch} 104(1)/107(1), C2_{ch}–C3_{ch}–C4_{ch} 113(2)/117(2), C4_{ch}–C5_{ch}–O1 116(1)/104(1).^a The values of the two symmetry independent molecules are given separated by a slash.

STaz functionalized glycosides. Comparison with data given in the literature revealed that SEt carbohydrates in **8–14** possess a similar *trans* influence like in analogous platinum(IV) complexes having thionucleobase ligands *fac*-[PtMe₃(bpy)L](BF₄) (L = SCy, 1-MeSCy, s⁴Ura, s²s⁴Ura; ¹J_{Pt,C}: 642.1–651.5 Hz).¹⁸ The respective values in the complexes **15–23** were also found in accordance with those observed for trimethyl platinum(IV) complexes having *N*-bound ligands like 2-(methylthio)-2-thiazoline and pyrazole in *trans* position (¹J_{Pt,C}: 675.4, 682.3 Hz).¹⁹ ¹⁹⁵Pt chemical shifts for complexes **8–23** (Table 1) were found to be in the same range as for other trimethyl(bipyridine)platinum(IV) complexes.^{16,18} Between complexes **8–14** (–2435 to –2772 ppm) and **15–23** (–2444 to –2730 ppm) no distinct shift differences were found. Thus, differences in the donor strength of the carbohydrate ligands seems to be too small to be clearly reflected in the δ_{Pt} values.

On the decomposition of the carbohydrate platinum(IV) complexes. Under strictly dehydrated conditions solutions of the complexes **8–23** were stable over weeks. Within two to three months only a slow decomposition with formation of platinum black took place, as indicated by NMR spectroscopy. In contrast, solutions in acetone, which were not strictly dehydrated, were found to be less stable. Thus, a solution of *fac*-[PtMe₃(bpy)(ch-STaz-κN)](BF₄) (**21**, ch-STaz = **5c**) was found to decompose

with the formation of well-shaped crystals, which were suitable for X-ray diffraction analysis. The compound **21a** crystallized in the space group *P2₁/c*. The asymmetric unit consists of a *fac*-[PtMe₃(bpy)(STazH-κS)]⁺ cation and a disordered tetrafluoroborate anion. The molecular structure of the cation of **21a** is shown in Fig. 2. Selected bond lengths and angles are given in the figure caption. The primary donor set [PtC₃N₂S] of the octahedrally coordinated platinum atom is built up by three methyl ligands in *facial* arrangement, the bipyridine ligand and the thiazolidine-2-thione (STazH) ligand, which is coordinated *via* the exocyclic sulfur atom to the platinum atom. The five membered heterocycle possesses a distorted half chair conformation along the C12–C13 bond, based on the torsion angle concept.¹⁷ Compared to the C=S bond in the free ligand (1.671–1.680 Å²⁰) no significant coordination-induced lengthening can be observed. Thus, the C11–S bond (1.683(4) Å) in complex **21a** exhibits double bond character. In accordance with the high *trans* influence of the methyl ligands, the Pt1–S1 bond length (2.4818(9) Å) belongs to the longest ones known, as compared with thioketone platinum(IV) complexes (median: 2.372 Å, lower/upper quartile: 2.312/2.474 Å; *n* = 9,¹⁵). The interplanar angle between the STazH ligand and the equatorial [PtC₂N₂] plane is 75.7°. As shown in Fig. 3, cation–anion interactions in crystals of **21a** are related to hydrogen bond interactions of the type N3–H...F2 (N3...F2 2.854(4) Å). Furthermore, molecules of **21a** are packed like a “staircase” in infinite columns (Fig. 3). The distances between the bpy ligands (3.79/3.81 Å) together with the displacement angle of 26.2° and 25.1°, respectively, indicated a weak stabilization through π–π and/or σ–π (C–H...π) interactions.²¹

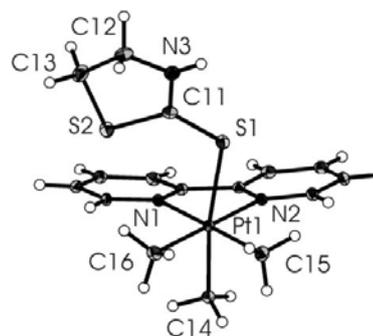


Fig. 2 Molecular structure of the cation of *fac*-[PtMe₃(bpy)(STazH-κS)](BF₄) (**21a**). The ellipsoids are drawn at the 30% probability level. Selected bond lengths (in Å) and angles (in °): Pt–C15 2.050(3), Pt–C16 2.048(3), Pt–C14 2.046(3), Pt–N1 2.155(2), Pt–N2 2.163(3), Pt–S1 2.4818(9), C11–S1 1.683(4), N1–Pt–N2 76.4(1), C15–Pt–C16 85.5(2), C14–Pt–N2 90.0(1), S1–Pt–C14 172.12(9), C15–Pt–N1 173.9(1), C11–S1–Pt 117.0(1).

Most likely, complex **21a** is a product of the hydrolysis of **21**, which was induced by traces of water in the reaction mixture, followed by an isomerization (Scheme 3(a)). The cleavage of the glycosidic bond in **21** gave proof for the platinum mediated activation of the glycosidic bond due to coordination to the

[‡] The displacement, measured by the angle between the ring normal and the centroid–centroid vector, is a measure for the ring–ring overlap.

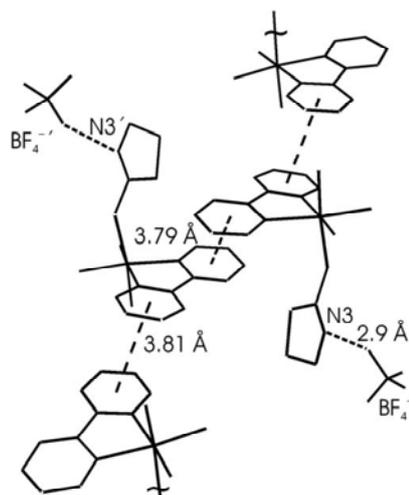
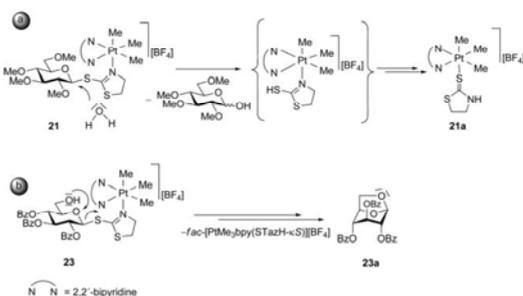


Fig. 3 Solid state structure of *fac*-[PtMe₃(bpy)(STazH-κS)][BF₄] (**21a**) showing the packing of the cations by π - π stacking (---) and the hydrogen bonds (···) between cations and anions. Hydrogen atoms are omitted for clarity. Only one of the two disordered positions of the fluorine atoms are shown.



Scheme 3 Possible mechanisms for the decomposition of **21** to **21a** (a) and **23** to **23a** (b).

electrophilic cationic Pt(IV) center. Another indication for this is the product of hydrolysis, obtained in the reaction of complex **1a** with 2-thiazolyl 2,3,4-tri-*O*-benzoyl-1-thio- β -D-glucopyranose (**5g**). Crystals of a decomposition product (1,6-anhydro-2,3,4-tri-*O*-benzoyl- β -D-glucopyranose, **23a**) were obtained from the acetone mother liquor. X-Ray diffraction analysis revealed that **23a** crystallizes in the space group *P1*. The unit cell consists of two symmetry independent, but structurally very similar, molecules. The molecular structure of one molecule is depicted in Fig. 4. Selected bond lengths and angles are given in the figure caption. The pyranose ring possesses a distorted chair conformation on O1 and C3, while the five membered ring exhibits an envelope conformation on O1.¹⁷ The anhydro moiety was most likely formed due to an intramolecular nucleophilic attack of the oxygen atom O6 belonging to the unprotected hydroxyl group at C6, whereas the glycosidic bond was activated by platinum coordination, as discussed above (Scheme 3(b)).

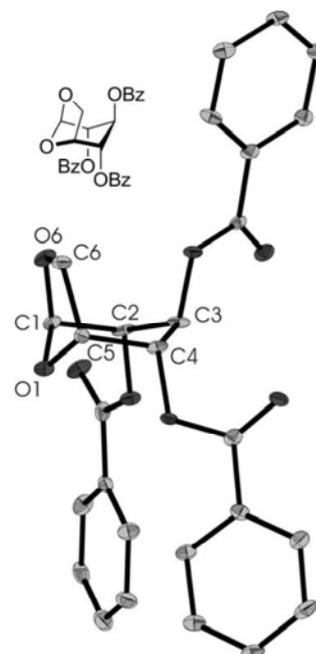
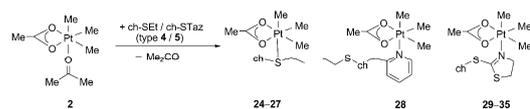


Fig. 4 Molecular structure of one of the two symmetry independent molecules of 1,6-anhydro-2,3,4-tri-*O*-benzoyl- β -D-glucopyranose (**23a**). Hydrogen atoms are omitted for clarity. Ellipsoids are drawn at the 30% probability level. Selected bond lengths (in Å) and angles (in °): O1–C5 1.425(5)/1.433(1), O1–C1 1.423(4)/1.417(5), O2–C1 1.417(4)/1.417(4), O2–C6 1.436(5)/1.439(4), C5–C6 1.533(5)/1.516(4), C1–C2 1.541(6)/1.507(7), C2–C3 1.513(6)/1.505(6), C3–C4 1.559(6)/1.554(6), C4–C5 1.523(6)/1.507(5), O1–C5–C6 102.2(3)/101.7(2), O2–C6–C5 103.5(3)/104.0(3), C1–O2–C6 107.1(3)/106.1(3), O1–C1–O2 106.1(3)/106.2(3), C1–O1–C5 102.2(3)/101.2(2), C2–C3–C4 113.4(4)/112.7(4), O1–C5–C4 108.7(3)/109.2(2), C5–C4–C3 111.7(3)/111.0(3), C3–C2–C1 112.2(3)/113.2(3), C2–C1–O1 109.3(3)/110.5(3). * The values of the two symmetry independent molecules are given separated by a slash.

2.3. Neutral platinum(IV) complexes with monodentately coordinated thioglycoside ligands

Synthesis and NMR spectroscopic characterization. The reaction of *fac*-[PtMe₃(OAc- κ^2 O,O')(Me₂CO)] (**2**) with carbohydrate ligands of type **4** and **5** (Scheme 1) led to the formation of the complexes *fac*-[PtMe₃(OAc- κ^2 O,O')(ch*)] (ch* = ch-SEt **24–28**; ch-STaz **29–35**) (Scheme 4, Table 2). The yellow, white and beige powders, respectively, are moderately air stable and were isolated in yields of 35–89%. The identities of the complexes **24–35** were confirmed by ¹H, ¹³C and ¹⁹⁵Pt NMR spectroscopy as well as by IR spectroscopy and high resolution ESI mass spectrometry.



Scheme 4 Syntheses of carbohydrate platinum(IV) complexes *fac*-[PtMe₃(OAc- κ^2 O,O')(ch*)] (ch* = ch-SEt, **24–28**; ch-STaz, **29–35**).

Table 2 Selected NMR and IR spectroscopic data (δ in ppm, J in Hz, ν in cm^{-1}) of the complexes *fac*-[PtMe₃(OAc- κ^2 O,O')(ch*)] (**24–35**)

Complex	ch*	δ_{H}^a	δ_{C}^a	$^2J_{\text{Pt,H}}^a$	δ_{Pt}	$\nu_{\text{sym. (CO}_2)}$	$\nu_{\text{asym. (CO}_2)}$	$\Delta\nu_{\text{CO}_2}$
	ch-SEt							
24	4a	1.08	-11.2	77.2	-2175	1411	1535	124
25	4b	1.07	-11.7	78.0	-2174	1411	1560	149
26	4c	1.10	-11.4	77.2	-2173	1409	1550	141
27	4d	0.96	-11.3	75.1	-2149	1404	1571	167
28	4e	1.15 ^b	-10.3	76.4	-2444	1402	1568	166
	ch-STaz							
29	5a	1.00	-11.7	77.8	-1910		1534	
30	5b	0.91 ^c	-11.1	77.2 ^c	-1921	1411		
31	5c	0.87	-11.3	73.0	-1918	1409	1535	126
32	5d	1.17	-11.3	74.4	-1907	1418	1552	134
33	5e	1.07	-11.4	75.6	-1904		1533	
34	5f	1.08	-11.3	76.4	-1911	1411		
35	5g	0.91	-11.5	76.4	-1916		1531	

^a Chemical shifts and coupling constants refer to the methyl ligands. ^b At $-80\text{ }^\circ\text{C}$: 0.98/0.92 ppm. ^c At $-50\text{ }^\circ\text{C}$: 0.72/0.78 ppm (74.4/70.4 Hz).

In the ^1H NMR spectra, the signals of the PtMe₃ protons exhibited broad mean signals at 0.87–1.17 ppm flanked by platinum satellites (singlet plus doublet). The requisite signals in the ^{13}C NMR spectra for **24–35** were found as broad mean singlets. The chemical shifts ($\delta_{\text{H}}/\delta_{\text{C}}$) and coupling constants ($^2J_{\text{Pt,H}}$) are assembled in Table 2. ^1H NMR measurements at $-50\text{ }^\circ\text{C}$ of the selected samples **28** and **30** showed that the expected split into three separate signals becomes apparent, although a broadening of the signals can be still observed. In the case of trimethylplatinum(IV) complexes with non-functionalized carbohydrate ligands at lower temperatures, three separated sharp signals were observed.¹⁵ As discussed in the previous section, some ^1H and ^{13}C NMR signals of the carbohydrate ligands in the complexes **24–35** are also broadened. In contrast to the previously discussed *fac*-[PtMe₃(4,4'-R₂bpy)(ch-SEt- κ S)] [BF₄] (**8–11**, **13**, **14**) complexes, only marginal CIS's up to 0.12 ppm could be observed for the signals of the CH₂ groups of the SEt moieties in the ^1H NMR spectra of the complexes **24–27**, having ch-SEt ligands. The chemical shifts for the signals of H1 of the carbohydrate backbones were shifted up to 0.10 ppm. The corresponding CIS's for the carbon atoms of the SEt groups and C1 resonances in the ^{13}C NMR spectra amount up to 1.3 ppm and 1.7 ppm, respectively. For complex **28**, where the ch-SEt ligand **4e** possesses at C6 an additional *N*-donor-site (picoline-2-yl), NOE experiments at $-80\text{ }^\circ\text{C}$ were performed to examine whether the nitrogen atom is involved in the coordination to platinum. Irradiation into the resonance for H6 of the picoline-2-yl group led to an increase of intensity for one signal of the PtMe₃ moiety, stating the spatial surrounding. Thus, a coordination of the nitrogen atom of picoline-2-yl to the platinum atom is likely. In accordance with this, signals of the picoline-2-yl groups were shifted downfield in ^1H and ^{13}C NMR spectra up to 0.24 and 2.1 ppm, respectively. Furthermore, the ^{195}Pt chemical shift of complex **28** was found to be about 270 ppm highfield shifted compared to those of complexes **24–27** ($-2444\text{ ppm versus }-2149\text{ to }-2175\text{ ppm}$, Table 2). However, a fast exchange between *N* and *S* coordination in solution could not be definitely ruled out, as indicated by the resonance downfield shift of 0.8 ppm for the CH₂ carbon atom signal of the SEt moiety.

The complexes with type 5 ligands *fac*-[PtMe₃(OAc- κ^2 O,O')(ch-STaz)] (**29–35**) showed remarkable upfield shifts for the signals of

H1 (0.34–0.50 ppm). The shift differences in ^1H NMR spectra of the two methylene proton resonances of the SCH₂ (up to 0.21 ppm) and NCH₂ (up to 0.30 ppm) were increased in complexes **24–28**. Furthermore, upfield shifts ranging from 2.5–3.2 ppm were observed in the ^{13}C NMR spectra for the signals of the carbon atoms of the SCH₂ groups (except **35**). This indicated an *N* coordination of the STaz groups, because the complexes *fac*-[PtMe₃(bpy)(ch-STaz- κ N)] [BF₄] (**15–23**), where this coordination mode could be unambiguously proved, showed analogous features. ^{195}Pt NMR chemical shifts of all these complexes between -1910 and -2444 ppm (Table 2) are in the expected range for trimethylplatinum(IV) complexes.^{13,16}

High resolution ESI mass spectrometry. High resolution ESI mass spectrometric measurements were performed for complexes **24–35**, which showed in all cases the existence of the molecular cation *fac*-[PtMe₃(ch*)]⁺-OAc (ch* = ch-SEt, **4a–4e**; ch-STaz; **5a–5g**), exhibiting an isotopic envelope characteristic for monocations containing one platinum atom [natural isotopic composition: ^{190}Pt (0.01%), ^{192}Pt (0.79%), ^{194}Pt (32.9%), ^{195}Pt (33.8%), ^{196}Pt (25.3%) and ^{198}Pt (7.2%)]. The observed isotopic patterns of the molecular cations were in very good agreement with the calculated values. In Fig. 5, the full scan mass spectrum and the expanded spectrum of *fac*-[PtMe₃(ch-SEt)]⁺ (complex **28** - OAc)⁺; ch-SEt = **4e**) is shown as an example. Furthermore, other peaks could be detected, which were assigned to be dinuclear complexes *fac*-[(PtMe₃)₂(OAc)(**4e**)]⁺ at 1124.3432 *m/z*, *fac*-[PtMe₃(**4e**)₂]⁺ at 1410.5450 *m/z* and *fac*-[(PtMe₃)₂(OAc)(**4e**)₂]⁺ at 1708.5787 *m/z*. According to the NMR spectra, in which the presence of such species can be clearly excluded, these species are formed during the ionization process and/or result from thermal decomposition during the ESI experiment.

IR spectroscopy. IR spectra were recorded to examine the coordination mode of the acetato ligand. The separation ($\Delta\nu_{\text{CO}_2}$) between the symmetric and asymmetric stretching band is a suitable tool to distinguish between the different coordination modes.²² Typical $\Delta\nu_{\text{CO}_2}$ values for a monodentate coordination are in general much higher (215–565 cm^{-1} ²²) than those observed in ionic acetates (164–171 cm^{-1} in MOAc, M = alkaline metal²²). On the other hand, a chelating coordination mode gives rise to $\Delta\nu_{\text{CO}_2}$

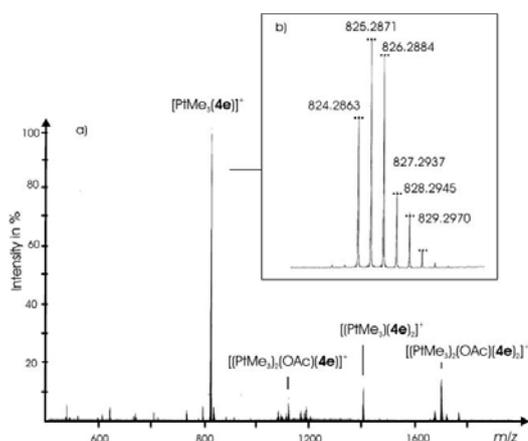


Fig. 5 (a) Positive ESI-mass spectrum of *fac*-[PtMe₃(ch-SEt)]⁺ (complex [28 - OAc]⁺; ch-SEt = 4e). (b) Isotopic pattern of the molecular ion *fac*-[PtMe₃(4e)]⁺ at 825.2871 *m/z* showing the expected intensity due to the isotopic composition given by horizontal bars.

values, which are similar or significantly lower (65–175 cm⁻¹)²² in comparison to those for ionic compounds. The stretching frequencies for the asymmetric and symmetric vibrational bands and the differences of those frequencies ($\Delta\nu_{\text{CO}_2}$) for the complexes 24–35 are given in Table 2. For the *fac*-[PtMe₃(OAc-κ²O,O')(ch-SEt)] complexes 24–28, $\Delta\nu_{\text{CO}_2}$ amounts to 124–167 cm⁻¹, indicating a chelating coordination mode of the acetato ligand. In the case of the *fac*-[PtMe₃(OAc-κ²O,O')(ch-STaz)] complexes 29–35, the assignment of the carboxyl stretching bands is often difficult because of the overlap with the absorption bands of the STaz moiety. Only for complexes 31 and 32 have both the symmetric and asymmetric vibrational bands been assigned unambiguously. The separation by 126 (31) and 134 cm⁻¹ (32), respectively, indicated a chelating coordination mode of the acetato ligand. As shown in Table 2, in the other complexes (29, 30, 33–35) the position

Table 3 ¹H and ¹³C NMR spectroscopic data (δ in ppm, *J* in Hz) of the methyl ligands and ¹⁹⁵Pt chemical shifts of the complexes *fac*-[PtMe₃(ch*)][BF₄] (36–46)

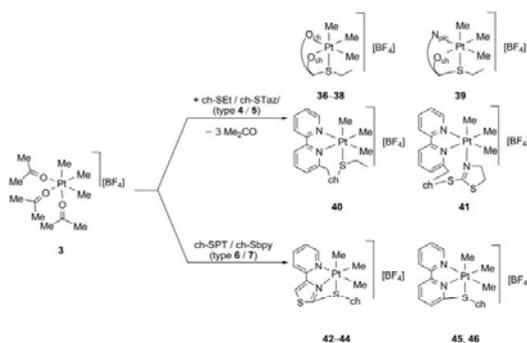
Complex	ch*	δ_{H}	δ_{C}	² <i>J</i> _{Pt,H}	δ_{Pt}
36	ch-SEt				
4a		1.28	-11.2	73.9	-2673
37	4c	1.26	-11.7	74.0 ^a	-2442
38	4d	1.18 ^a	-11.3	75.9	-2610
39	4e	1.06/1.12	-5.4/-8.6	69.8/72.8	-2068
40	4f	0.89/1.26/1.65	4.5/-1.3/-3.8	72.9/69.3/71.1	-2679
41	ch-STaz				
5h		0.81/1.31/1.75	0.2/-4.9/-8.1	73.0/71.4/70.5	-2377
42	ch-SPT				
6a		1.47	-5.8	br	-2154
43	6b	1.32	-5.9	br	-2158
44	6c	1.41	-5.7	br	-2151
45	ch-Sbpy				
7a		1.45 ^b	-3.4	70.5 ^b	-2123
46	7b	1.33	-3.5	br	-2120

^a At -50 °C: 0.94/1.07/1.33 ppm (76.9/80.6/79.3 Hz). ^b At -80 °C: 0.94/1.27/1.31 ppm (79.2/65.9/68.4 Hz).

of either ν_{asym} or ν_{sym} is in the same range as that observed in complexes 24–28, 31 and 32. Hence, the analogous coordination mode is likely.

2.4. Cationic platinum(IV) complexes with tridentately coordinated thioglycoside ligands

Syntheses and NMR spectroscopic investigations. Complex *fac*-[PtMe₃(Me₂CO)₃][BF₄] (3) reacted in anhydrous acetone with ligands of type 4 to give mononuclear complexes *fac*-[PtMe₃(ch-SEt)][BF₄] (36–40) in good yields of 62–87% (Scheme 5, Table 3), where the carbohydrate ligands could coordinate in a tridentate binding fashion. The colorless and beige powders are highly (36–38) and moderately (39, 40) air and moisture sensitive, respectively. All complexes were fully characterized by NMR (¹H, ¹³C, ¹⁹⁵Pt) spectroscopy, IR spectroscopy and high resolution mass spectroscopy.



Scheme 5 Syntheses of carbohydrate platinum(IV) complexes *fac*-[PtMe₃(ch*)][BF₄] (ch* = ch-SEt, 36–40; ch-STaz, 41; ch-SPT, 42–44; ch-Sbpy, 45, 46). N_{pic} = picoline-2-yl.

In the ¹H NMR spectra of 36–38 the methyl ligands possessed broad mean signals in a range of 1.18–1.28 ppm flanked by

platinum satellites. Chemical shifts and coupling constants are given in Table 3. Measurements at $-50\text{ }^{\circ}\text{C}$ using complex **38** as an example, showed the expected split into three separate, sharp signals, revealing the non-equivalence of the methyl ligands. For complexes **39** and **40** having protecting groups at C6 with additional *N*-donor sites (picoline-2-yl, bipyridine-6-yl), the ^1H NMR spectra showed two slightly broadened (**39**) and three separate sharp signals (**40**) for the methyl ligands, respectively, flanked by platinum satellites (Table 3). For the signals of the carbohydrate protons in the complexes **36–40**, a broadening of all signals was found for **36–38**. For complexes **39** and **40** only partial broadening was observed. The respective signals for the carbon atoms are partially broadened in all complexes **36–40**. Coordination-induced shifts ($\Delta\delta_{\text{H}}/\Delta\delta_{\text{C}}$) for the methylene group resonances of the SET moiety (0.16–0.52/0.5–3.2 ppm) and H1 (0.17–0.43/1.3–3.1 ppm) gave evidence that the sulfur atom is coordinated to the platinum atom. The two remaining coordination sites of the platinum atom in **36–38** are, most likely, occupied by any of the following: ring, ether or ester oxygen donor atoms of the carbohydrates. Thus, an $\kappa\text{S},\kappa^2\text{O},\text{O}'$ coordination mode of the carbohydrate ligands in complexes **36–38** can be assumed. In complexes **39** and **40**, the coordination of the picoline-2-yl and bipyridine-6-yl moiety could be clearly seen by a significant downfield shift of the appropriate signals in ^1H and ^{13}C NMR spectra up to 0.67 and 5.8 ppm, respectively. This corresponds to an $\kappa\text{S},\kappa\text{N},\kappa\text{O}$ (**39**) and $\kappa\text{S},\kappa^2\text{N},\text{N}'$ (**40**) coordination mode of the carbohydrate ligands.

Surprisingly, reactions of $\text{fac}[\text{PtMe}_3(\text{Me}_2\text{CO})_3][\text{BF}_4]$ (**3**) with ligands of type **5** led to no isolable products. After adding a solution of **3** in acetone to the thioglycoside, in contrast to the common reactions, white precipitates were formed. ^1H NMR spectra of the reaction mixtures showed a multitude of products in the carbohydrate area, including the α -hemiacetal. This indicated that a cleavage of the C1–S bonds had occurred in a similar fashion to the decomposition reactions shown in Scheme 3.

To succeed in the formation of $\text{fac}[\text{PtMe}_3(\text{ch-STaz})][\text{BF}_4]$ complexes, carbohydrate **5h** having a stabilizing bipyridine-6-yl moiety at C6 (as in **4f**) was selected. In the reaction of $\text{fac}[\text{PtMe}_3(\text{Me}_2\text{CO})_3][\text{BF}_4]$ (**3**) with **5h** the complex $\text{fac}[\text{PtMe}_3(\text{ch-STaz})][\text{BF}_4]$ (**41**; ch-STaz = **5h**) was isolated as a moderately air stable, yellow powder in a yield of 60%. ^1H and ^{13}C NMR spectra showed unambiguously the coordination of the bipyridine-6-yl moiety with chemical shift differences of the bipyridine resonances shifted downfield up to 0.92 ppm and 7.1 ppm, respectively. Furthermore, remarkable CIS's of the signals of H1 and C1, which amount to 0.23 (^1H NMR) and 4.9 ppm (^{13}C NMR), respectively, are observed. The identity of **41** was also confirmed by high resolution mass spectrometry (Fig. 6). The isotopic pattern of the molecular cation is in a very good agreement with the calculated values.

Obviously, carbohydrates possessing chelating donor groups are the key to yield stable $\text{fac}[\text{PtMe}_3(\text{ch}^*)][\text{BF}_4]$ complexes. Therefore, the carbohydrate classes ch-SPT (type **6**, Scheme 1) and ch-Sbpy (type **7**, Scheme 1), having a chelating group in the aglycone moiety, were included in the subsequent investigations. Reactions of $\text{fac}[\text{PtMe}_3(\text{Me}_2\text{CO})_3][\text{BF}_4]$ (**3**) with ligands of type **6** and **7** led to the formation of complexes **42–46**, which were isolated as yellow and beige powders, respectively, in yields of 54–75% (Scheme 5). These complexes are stable in anhydrous acetone solutions over a few weeks, without any evidence of decomposition. In chloroform, however, decomposition was observed within 4 days, which might

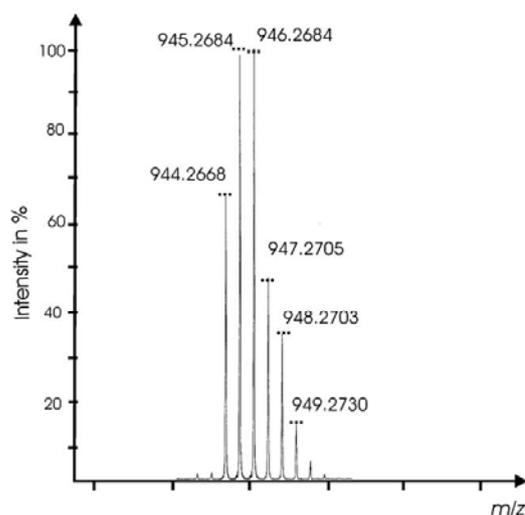


Fig. 6 Isotopic pattern of the cation $\text{fac}[\text{PtMe}_3(\mathbf{5h})]^+$ of complex **41** at 945.2684 m/z , showing the expected intensity due to the isotopic composition given by horizontal bars.

be caused by the presence of traces of hydrochloric acid. The identities of the complexes were confirmed by ^1H , ^{13}C and ^{195}Pt NMR spectroscopy, IR spectroscopy and high resolution ESI mass spectrometry.

The methyl ligands gave broad mean signals in the ^1H NMR spectra at 1.32–1.47 ppm, flanked by platinum satellites (Table 3). ^1H NMR experiments performed at $-80\text{ }^{\circ}\text{C}$ with complex **45** as an example showed the expected split into three separate signals due to the non-equivalence of the methyl ligands. The SPT and Sbpy moieties were unambiguously found to be coordinated to the platinum atom. This was verified by remarkable downfield shifts of the related signals of the protons and carbon atoms up to 1.0 ppm (^1H NMR) and 5.1 ppm (^{13}C NMR). The carbohydrate proton resonances are shifted up to 0.41 ppm and are partially broadened, whereas the ^{13}C NMR spectra of compounds **45** and **46** only showed a significant shift of 2.4 (**45**) and 2.9 (**46**) ppm for the signals of C1. Also, a broadening of the resonances of C1 and C2 (**42–46**) and C4 (**44**) can be observed. This indicates that the exocyclic sulfur of the SPT and Sbpy moieties might be the third donor atom coordinated to the platinum atom.

The ESI mass spectra for complexes **42–46** showed the presence of a mononuclear cation $\text{fac}[\text{PtMe}_3(\text{ch}^*)]^+$ ($\text{ch}^* = \text{ch-SPT}$, **42–44**; ch-Sbpy , **45**, **46**) containing one platinum atom. The full scan mass spectrum of **43**, depicted in Fig. 7, shows no other platinum-containing cations. The isotopic pattern of the $\text{fac}[\text{PtMe}_3(\text{ch-SPT})]^+$ ($\text{ch-SPT} = \mathbf{6b}$) cation at 1012.1890 m/z is in very good agreement with the calculated values.

3. Conclusion

Platinum(IV) complexes with thioglycoside ligands of the types $\text{fac}[\text{PtMe}_3(4,4'\text{-R}_2\text{bpy})(\text{ch}^*)][\text{BF}_4]$ ($\text{ch}^* = \text{ch-SET}$, **8–14**; ch-STaz , **15–23**), $\text{fac}[\text{PtMe}_3(\text{OAc-}\kappa^2\text{O},\text{O}')(\text{ch}^*)]$ ($\text{ch}^* = \text{ch-SET}$, **24–28**; ch-STaz , **29–35**) and $\text{fac}[\text{PtMe}_3(\text{ch}^*)][\text{BF}_4]$ ($\text{ch}^* = \text{ch-SET}$, **36–40**;

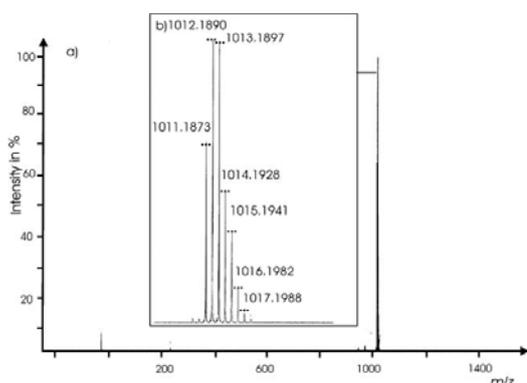


Fig. 7 (a) Positive ESI-mass spectrum of the cation $\text{fac}[\text{PtMe}_3(\mathbf{6b})]^+$ of complex **43**. (b) Isotopic pattern of the molecular ion $\text{fac}[\text{PtMe}_3(\mathbf{6b})]^+$ at 1012.1890 m/z showing the expected intensity due to the isotopic composition given by horizontal bars.

ch-STaz, **41**; ch-SPT, **42–44**; ch-Sbpy, **45, 46**), with the thioglycosides coordinated in a mono- (**8–35**) and tridentate (**36–46**) binding fashion have been synthesized. Despite the kinetic inertness of platinum(IV) complexes due to their low spin d^8 electron configuration, it could be shown that in trimethylplatinum(IV) complexes weakly coordinating ligands like acetone could be smoothly substituted by thioglycosides. These ligand exchange reactions are further supported by the high *trans* effect of the methyl ligands. Furthermore, platinum mediated decomposition of thioglycosides in complexes **21** and **23** involving the cleavage of the C–S glycosidic bonds, yielded the corresponding products **21a** and **23a** (Scheme 3). This result is in accordance with common glycosylation procedures, wherein the glycosidic bond of the glycosyl donor is activated in the first step by adding an electrophilic promoter, such as MeOTf or NIS/TfOH.²

As expected from the coordination chemistry perspective, complexes of platinum(IV) in which the thioglycoside ligands have three coordination sites at their disposal (*i.e.* using $\text{fac}[\text{PtMe}_3(\text{Me}_2\text{CO})_3][\text{BF}_4]$ (**3**) as starting complex) proved to be more air and moisture sensitive than the cationic complexes with bipyridine and the neutral complexes with acetato ligands. Thus, complexes with thioglycoside ligands having only the SET group as strong donor site could be prepared and characterized (**36–38**), whereas it was not possible with complexes having only the STaz group as the strongest donor site. In the latter cases, a partial cleavage of the glycosidic bonds instead of the anticipated complex formation took place. These cleavage reactions are promoted by the STaz coordination to Pt, as discussed before being a further example for the cleavage of glycosidic bonds by electrophilic promoters.² However, it can't be strictly ruled out that these reactions are also influenced by traces of water and/or $\text{Ag}[\text{BF}_4]$ (present in the reaction mixtures despite using strictly anaerobic conditions and from the *in situ* synthesis of complex **3**, respectively).^{23,24} Analogous platinum-mediated reactions, such as cleavage and formation of isopropylidene protecting groups and Schiff bases, were frequently observed in carbohydrate trimethylplatinum(IV) complexes, with non-functionalized carbohydrate ligands.^{12,13} In full accord with

these findings, we succeeded to get stable complexes of the type $\text{fac}[\text{PtMe}_3(\text{ch-STaz})][\text{BF}_4]$ with a derivative having additional strong donor sites in form of a 2,2'-bipyridine-6-yl protecting group at C6 of the carbohydrate moiety (**41**).

For the first time the investigations presented in this study give a deeper insight into the coordination chemistry of thioglycosides to platinum(IV) being a coordination center in a relatively high oxidation number. It has been shown that these ligands can be coordinated not only monodentately through a relatively strong donor site (κS or κN) but also *facial* tridentately using donor sets consisting of one stronger and two weaker donor sites ($\kappa\text{S}, \kappa^2\text{O}, \text{O}'$; O = oxygen atom from the carbohydrate backbone), two stronger and one weaker donor sites ($\kappa\text{S}, \kappa\text{N}, \kappa\text{O}$) or three stronger donor sites ($\kappa\text{S}, \kappa^2\text{N}, \text{N}'$ or $\kappa^3\text{N}, \text{N}', \text{N}''$). Furthermore, coordination of thioglycosides to the highly electrophilic platinum center may give rise to platinum-assisted cleavage of glycosidic C–S bonds, which creates a basis to a deeper understanding of stereocontrolled chemical glycosylations, mediated by metal coordination.¹⁴

4. Experimental

4.1. General considerations

General considerations. Syntheses were performed, in general, under strictly dehydrated conditions in an argon atmosphere using standard Schlenk techniques. As precipitates, the carbohydrate platinum complexes are stable for a few hours (2–4 h) even in open air, whereas a strictly anhydrous environment was required for handling their solutions in acetone. Acetone and pentane were dried over phosphorus pentoxide followed by 4 Å molecular sieves and LiAlH_4 , respectively. Diethyl ether was dried over *N*-benzophenone. All solvents were distilled prior to use. NMR spectra were obtained with Varian UNITY 500, Gemini 2000 and Bruker 800 spectrometers using solvent signals (^1H and ^{13}C NMR spectroscopy) as internal references and $\text{Na}_2[\text{PtCl}_6]$ ($\delta(^{195}\text{Pt}) = 0$ ppm) as external reference. IR spectra were recorded on a Galaxy Mattson FT IR spectrometer, using KBr pellets. The positive ion high resolution ESI mass spectra were obtained from a Bruker Apex III Fourier transform ion cyclotron resonance (FT-ICR) mass spectrometer (Bruker Daltonics, Billerica, USA) equipped with an Infinity cell, a 7.0 Tesla superconducting magnet (Bruker), a RF-only hexapole ion guide and an external electron spray ion source (Agilent, off axis spray, voltages: endplate, –3.700 V; capillary, –4.200 V; capillary exit, 100 V; skimmer 1, 15.0 V; skimmer 2, 6.0 V). Nitrogen was used as drying gas at 150 °C. The sample solutions were introduced continuously *via* a syringe pump with a flow rate of 120 $\mu\text{l h}^{-1}$. The data were acquired with 512 k data points and zero filled to 2048 k by averaging 64 scans. $\text{fac}\text{-}[\text{PtMe}_3\text{I}]_d$ ^{14,25} and $\text{fac}\text{-}[\text{PtMe}_3\text{I}(\text{bpy})]_d$ ²⁰ were prepared according to literature methods. All other materials were purchased from commercial sources. Synthesis of $\text{fac}\text{-}[\text{PtMe}_3\text{I}(4,4'\text{-Bu}_2\text{bpy})]$ and its analytical data as well as the NMR and IR spectroscopic data of the carbohydrate platinum complexes **1–46** are available as ESI.† Selected spectroscopic data of complexes **1–46** are given in Table 1–3.

General method for the synthesis of the complexes $\text{fac}\text{-}[\text{PtMe}_3(4,4'\text{-R}_2\text{bpy})(\text{ch}^*)][\text{BF}_4]$ ($\text{ch}^* = \text{ch-SEt}$, R = H: **8–12**; R = ^tBu: **13, 14**; ch-STaz, R = H: **17–23**, R = ^tBu: **15, 16**). A suspension of $\text{fac}\text{-}[\text{PtMe}_3\text{I}(\text{bpy})]$ (70.0 mg, 0.14 mmol) or $\text{fac}\text{-}[\text{PtMe}_3\text{I}(4,4'\text{-Bu}_2\text{bpy})]$ (88.9 mg, 0.14 mmol) and $\text{Ag}[\text{BF}_4]$ (26.5 mg, 0.14 mmol) in acetone (10 ml) was stirred for 30 min

under the absence of light. Precipitated AgI was removed by filtration and the clear, colorless solution of *fac*-[PtMe₃(Me₂CO)(4,4'-R₂bpy)][BF₄] (R = H, **1a**; R = ^tBu, **1b**) was added to the respective β-D-thiopyranoside (0.14 mmol). After 5 h the volume of the solution was reduced *in vacuo* to 3 ml and pentane (10 ml) was added. The precipitated solid was filtered, washed with pentane (2 × 2 ml) and dried *in vacuo*.

fac-[PtMe₃(bpy)(*ch*-SEt)][BF₄] (**8**, *ch*-SEt = **4a**). (88 mg, 72%); *m/z* (ESI) 788.2192 ([PtMe₃(bpy)(**4a**)]⁺. C₂₉H₄₁N₂O₃PtS requires 788.2181).

fac-[PtMe₃(bpy)(*ch*-SEt)][BF₄] (**9**, *ch*-SEt = **4b**). (115 mg, 73%); *m/z* (ESI) 788.2193 ([PtMe₃(bpy)(**4b**)]⁺. C₂₉H₄₁N₂O₃PtS requires 788.2181).

fac-[PtMe₃(bpy)(*ch*-SEt)][BF₄] (**10**, *ch*-SEt = **4c**). (102 mg, 65%); *m/z* (ESI) 1036.2805 ([PtMe₃(bpy)(**4c**)]⁺. C₄₉H₄₉N₂O₃PtS requires 1036.2807).

fac-[PtMe₃(bpy)(*ch*-SEt)][BF₄] (**11**, *ch*-SEt = **4d**). (107 mg, 78%); *m/z* (ESI) 980.3623 ([PtMe₃(bpy)(**4d**)]⁺. C₄₈H₄₉N₂O₃PtS requires 980.3636).

fac-[PtMe₃(bpy)(*ch*-SEt)][BF₄] (**12**, *ch*-SEt = **4e**). (90 mg, 68%); *m/z* (ESI) 981.3586 ([PtMe₃(bpy)(**4e**)]⁺. C₄₈H₅₆N₃O₃PtS requires 981.3588).

fac-[PtMe₃(4,4'-^tBu₂bpy)(*ch*-SEt)][BF₄] (**13**, *ch*-SEt = **4a**). (82 mg, 65%); *m/z* (ESI) 900.3437 ([PtMe₃(4,4'-^tBu₂bpy)(**4a**)]⁺. C₃₇H₅₇N₂O₃PtS requires 900.3432).

fac-[PtMe₃(4,4'-^tBu₂bpy)(*ch*-SEt)][BF₄] (**14**, *ch*-SEt = **4c**). (72 mg, 54%); *m/z* (ESI) 1148.4030 ([PtMe₃(4,4'-^tBu₂bpy)(**6c**)]⁺. C₃₇H₅₇N₂O₃PtS requires 1148.4058).

fac-[PtMe₃(4,4'-^tBu₂bpy)(*ch*-STaz)][BF₄] (**15**, *ch*-STaz = **5c**). (82 mg, 45%); *m/z* (ESI) 1205.3743 ([PtMe₃(**5c**)(4,4'-^tBu₂bpy)]⁺. C₃₈H₆₄N₃O₃PtS₂ requires 1205.3732).

fac-[PtMe₃(4,4'-^tBu₂bpy)(*ch*-STaz)][BF₄] (**16**, *ch*-STaz = **5g**). (108 mg, 76%); *m/z* (ESI) 1101.3480 ([PtMe₃(4,4'-^tBu₂bpy)(**5g**)]⁺. C₃₈H₆₄N₃O₃PtS₂ requires 1101.3470).

fac-[PtMe₃(bpy)(*ch*-STaz)][BF₄] (**17**, *ch*-STaz = **5a**). (130 mg, 85%); *m/z* (ESI) 845.1841 ([PtMe₃(bpy)(**5a**)]⁺. C₃₀H₄₀N₃O₃PtS₂ requires 845.1854).

fac-[PtMe₃(bpy)(*ch*-STaz)][BF₄] (**18**, *ch*-STaz = **5b**). (76 mg, 64%); *m/z* (ESI) 1093.2478 ([PtMe₃(bpy)(**5b**)]⁺. C₃₀H₄₈N₃O₃PtS₂ requires 1083.2480).

fac-[PtMe₃(bpy)(*ch*-STaz)][BF₄] (**19**, *ch*-STaz = **5c**). (115 mg, 73%); *m/z* (ESI) 1093.2479 ([PtMe₃(bpy)(**5c**)]⁺. C₃₀H₄₈N₃O₃PtS₂ requires 1093.2480).

fac-[PtMe₃(bpy)(*ch*-STaz)][BF₄] (**20**, *ch*-STaz = **5d**). (72 mg, 72%); *m/z* (ESI) 1037.3305 ([PtMe₃(bpy)(**5d**)]⁺. C₃₀H₄₈N₃O₃PtS₂ requires 1037.3309).

fac-[PtMe₃(bpy)(*ch*-STaz)][BF₄] (**21**, *ch*-STaz = **5e**). (91 mg, 83%); *m/z* (ESI) 733.2074 ([PtMe₃(bpy)(**5e**)]⁺. C₂₆H₄₀N₃O₃PtS₂ requires 733.2057).

fac-[PtMe₃(bpy)(*ch*-STaz)][BF₄] (**22**, *ch*-STaz = **5f**). (112 mg, 94%); *m/z* (ESI-MS) 893.2203 ([PtMe₃(bpy)(**5f**)]⁺. C₃₅H₄₄N₃O₃PtS₂ requires 893.2218).

fac-[PtMe₃(bpy)(*ch*-STaz)][BF₄] (**23**, *ch*-STaz = **5g**). (91 mg, 83%); *m/z* (ESI) 989.2243 (ESI) ([PtMe₃(bpy)(**5g**)]⁺. C₄₅H₄₄N₃O₃PtS₂ requires 989.2218).

General method for the synthesis of the complexes [PtMe₃(OAc-κ²O,O')(ch*)][BF₄] (ch* = *ch*-SEt, **24–28; *ch*-STaz, **29–35**). A suspension of *fac*-[PtMe₃I₂] (50.0 mg, 0.04 mmol) and AgOAc**

(23.0 mg, 0.14 mmol) in acetone (10 ml) was stirred for 12 h under the absence of light. Precipitated AgI was removed by filtration and the clear, colorless solution of *fac*-[PtMe₃(OAc-κ²O,O')(Me₂CO)] (**2**) was directly added to the respective β-D-thiopyranoside (0.14 mmol). After 5 h the volume of the solution was reduced *in vacuo* to 3 ml and pentane (6 ml) was added. The precipitated solid was filtered, washed with pentane (2 × 2 ml) and dried *in vacuo*.

fac-[PtMe₃(OAc-κ²O,O')(*ch*-SEt)] (**24**, *ch*-SEt = **4a**). (55 mg, 57%); *m/z* (ESI) 632.1498 ([PtMe₃(OAc-κ²O,O')(**4a**)]⁺ -OAc. C₃₀H₄₀N₃O₃PtS₂ requires 632.1493).

fac-[PtMe₃(OAc-κ²O,O')(*ch*-SEt)] (**25**, *ch*-SEt = **4b**). (62 mg, 70%); *m/z* (ESI) 632.1498 [PtMe₃(OAc-κ²O,O')(**4b**)]⁺ -OAc. C₃₀H₄₀N₃O₃PtS₂ requires 632.1493).

fac-[PtMe₃(OAc-κ²O,O')(*ch*-SEt)] (**26**, *ch*-SEt = **4c**). (64 mg, 54%); *m/z* (ESI) 880.2108 ([PtMe₃(OAc-κ²O,O')(**4c**)]⁺ -OAc. C₃₀H₄₀N₃O₃PtS₂ requires 880.2119).

fac-[PtMe₃(OAc-κ²O,O')(*ch*-SEt)] (**27**, *ch*-SEt = **4d**). (64 mg, 54%); *m/z* (ESI) 824.2939 ([PtMe₃(OAc-κ²O,O')(**4d**)]⁺ -OAc. C₃₉H₄₉O₃PtS requires 824.2948).

fac-[PtMe₃(OAc-κ²O,O')(*ch*-SEt)] (**28**, *ch*-SEt = **4e**). (75 mg, 58%); *m/z* (ESI) 825.2871 ([PtMe₃(OAc-κ²O,O')(**4e**)]⁺ -OAc. C₃₈H₄₈N₃O₃PtS requires 825.2901).

fac-[PtMe₃(OAc-κ²O,O')(*ch*-STaz)] (**29**, *ch*-STaz = **5a**). (93 mg, 89%); *m/z* (ESI) 689.1172 ([PtMe₃(OAc-κ²O,O')(**5a**)]⁺ -OAc. C₂₀H₃₂N₃O₃PtS₂ requires 689.1166).

fac-[PtMe₃(OAc-κ²O,O')(*ch*-STaz)] (**30**, *ch*-STaz = **5b**). (120 mg, 86%); *m/z* (ESI) 937.1753 ([PtMe₃(OAc-κ²O,O')(**5b**)]⁺ -OAc. C₄₀H₄₀N₃O₃PtS₂ requires 937.1792).

fac-[PtMe₃(OAc-κ²O,O')(*ch*-STaz)] (**31**, *ch*-STaz = **5c**). (86 mg, 68%); *m/z* (ESI) 937.1789 ([PtMe₃(OAc-κ²O,O')(**4e**)]⁺ -OAc. C₁₆H₃₂N₃O₃PtS₂ requires 937.1792).

fac-[PtMe₃(OAc-κ²O,O')(*ch*-STaz)] (**32**, *ch*-STaz = **5d**). (102 mg, 80%); *m/z* (ESI) 881.2630 ([PtMe₃(OAc-κ²O,O')(**5d**)]⁺ -OAc. C₄₀H₄₈N₃O₃PtS₂ requires 881.2622).

fac-[PtMe₃(OAc-κ²O,O')(*ch*-STaz)] (**33**, *ch*-STaz = **5e**). (30 mg, 35%); *m/z* (ESI) 577.1368 [PtMe₃(OAc-κ²O,O')(**5e**)]⁺ -OAc. C₁₆H₃₂N₃O₃PtS₂ requires 577.1370).

fac-[PtMe₃(OAc-κ²O,O')(*ch*-STaz)] (**34**, *ch*-STaz = **5f**). (67 mg, 60%); *m/z* (ESI) 737.1525 ([PtMe₃(OAc-κ²O,O')(**5f**)]⁺ -OAc. C₂₅H₃₆N₃O₃PtS₂ requires 737.1530).

fac-[PtMe₃(OAc-κ²O,O')(*ch*-STaz)] (**35**, *ch*-STaz = **5g**). (44 mg, 35%); *m/z* (ESI) 833.1553 ([PtMe₃(OAc-κ²O,O')(**5g**)]⁺ -OAc. C₃₃H₃₆N₃O₃PtS₂ requires 833.1530).

General method for the synthesis of the complexes [PtMe₃(ch*)][BF₄] (ch* = *ch*-SEt, **36–40; *ch*-STaz, **41**, *ch*-SPT, **42–44**, *ch*-Sbpy, **45**, **46**). A suspension of *fac*-[PtMe₃I₂] (70.0 mg, 0.04 mmol) and Ag[BF₄] (26.5 mg, 0.14 mmol) in acetone (10 ml) was stirred for 30 min under the absence of light. Precipitated AgI was removed by filtration and the clear, colorless solution of *fac*-[PtMe₃(Me₂CO)]₂[BF₄] (**3**) was directly added to the respective β-D-thiopyranoside (0.14 mmol). After 5 h the volume of the solution was reduced *in vacuo* to 3 ml and pentane (10 ml) was added. The precipitated solid was filtered, washed with pentane (2 × 2 ml) and dried *in vacuo*.**

fac-[PtMe₃(*ch*-SEt)][BF₄] (**36**, *ch*-SEt = **4a**). (42 mg, 87%); *m/z* (ESI) 632.1492 [PtMe₃(**4a**)]⁺. C₁₅H₃₃O₃PtS requires 632.1493).

fac-[PtMe₃(*ch*-SEt)][BF₄] (**37**, *ch*-SEt = **4c**). (40 mg, 62%); *m/z* (ESI) 880.2115 ([PtMe₃(**4c**)]⁺. C₃₅H₄₁O₃PtS requires 880.2119).

Table 4 Crystal data, data collection and refinement parameters of *fac*-[PtMe₃(bpy)(ch-STaz-κN)][BF₄] (**19**, ch-STaz = **5c**), *fac*-[PtMe₃(bpy)(STazH-κS)][BF₄] (**21a**) and 1,6-anhydro-2,3,4-tri-*O*-benzoyl-β-D-glucopyranose (**23a**)

	19	21a	23a
Formula	C ₃₀ H ₄₈ BF ₄ N ₃ O ₉ PtS ₂	C ₁₆ H ₂₂ BF ₄ N ₃ PtS ₂	C ₂₇ H ₂₂ O ₈
FW	1180.94	602.39	474.45
Crystal system	Tetragonal	Monoclinic	Triclinic
Space group	<i>P</i> 4 ₁ 2 ₁ 2	<i>P</i> 2 ₁ / <i>c</i>	<i>P</i> 1
<i>a</i> /Å	22.1611(9)	13.2216(5)	9.6936(8)
<i>b</i> /Å	22.1611(9)	12.6149(5)	11.011(1)
<i>c</i> /Å	43.735(2)	12.8474(5)	11.449(1)
α /°			66.414(4)
β /°		115.776(2)	89.999(4)
γ /°			89.894(4)
<i>V</i> /Å ³	21479(2)	1929.6(1)	1119.9(2)
<i>Z</i>	16	4	2
<i>D</i> _{calc} /g cm ⁻³	1.461	2.074	1.407
<i>T</i> /K	100(2)	100(2)	100(2)
μ /mm ⁻¹	6.194	7.532	0.104
θ /°	4.47–61.49	1.71–36.00	1.94–26.44
<i>F</i> (000)	9472	1160	496
Index ranges	–23 ≤ <i>h</i> ≤ 20 –25 ≤ <i>k</i> ≤ 25 –49 ≤ <i>l</i> ≤ 47	–21 ≤ <i>h</i> ≤ 21 –19 ≤ <i>k</i> ≤ 20 –21 ≤ <i>l</i> ≤ 21	–11 ≤ <i>h</i> ≤ 12 –13 ≤ <i>k</i> ≤ 13 –14 ≤ <i>l</i> ≤ 14
Reflns collected	66857	56461	28835
Reflns obs [<i>I</i> > 2σ(<i>I</i>)]	4582	7098	6186
Reflns independent	16385 (<i>R</i> _{int} = 0.1328)	9070 (<i>R</i> _{int} = 0.0643)	8089 (<i>R</i> _{int} = 0.0699)
Data/restraints/parameters	16385/1332/1103	9070/1/257	8089/3/604
GOF(<i>F</i> ²)	0.617	1.034	1.003
<i>R</i> ₁ , <i>wR</i> ₂ (<i>I</i> > 2σ)	0.0481/0.0785	0.0347/0.0757	0.0602/0.1447
<i>R</i> ₁ , <i>wR</i> ₂ (all data)	0.1755/0.0966	0.0529/0.0828	0.0810/0.1593
Largest diff. peak and hole/e Å ⁻³	1.009 and –0.519	1.958 and –1.058	0.358 and –0.350
Flack parameter	–0.044(9)		0.4(10)

fac-[PtMe₃(ch-SEt)][BF₄] (**38**, ch-SEt = **4d**). (53 mg, 70%); *m/z* (ESI) 824.2948 ([PtMe₃(**4d**)]⁺. C₃₀H₄₀O₉PtS requires 824.2948).

fac-[PtMe₃(ch-SEt)][BF₄] (**39**, ch-SEt = **4e**). (92 mg, 72%); *m/z* (ESI) 825.2903 ([PtMe₃(**4e**)]⁺. C₃₈H₄₈NO₉PtS requires 825.2901).

fac-[PtMe₃(ch-SEt)][BF₄] (**40**, ch-SEt = **4f**). (118 mg, 85%); *m/z* (ESI) 888.2940 ([PtMe₃(**4f**)]⁺. C₄₃H₄₈N₃O₉PtS₂ requires 888.3010).

fac-[PtMe₃(ch-STaz)][BF₄] (**41**, ch-STaz = **5b**). (87 mg, 60%); *m/z* (ESI) 945.2684 ([PtMe₃(**5b**)]⁺. C₄₃H₄₈N₃O₉PtS₂ requires 945.2683).

fac-[PtMe₃(ch-SPT)][BF₄] (**42**, ch-SPT = **6a**). (77 mg, 65%); *m/z* (ESI) 764.1262 ([PtMe₃(**6a**)]⁺. C₂₅H₃₃N₂O₉PtS₂ requires 764.1275).

fac-[PtMe₃(ch-SPT)][BF₄] (**43**, ch-SPT = **6b**). (83 mg, 54%); *m/z* (ESI) 1012.1890 ([PtMe₃(**6b**)]⁺. C₄₅H₄₁N₂O₉PtS₂ requires 1012.1901).

fac-[PtMe₃(ch-SPT)][BF₄] (**44**, ch-SPT = **6c**). (98 mg, 67%); *m/z* (ESI) 956.2702 ([PtMe₃(**6c**)]⁺. C₄₅H₄₉N₂O₉PtS₂ requires 956.2731).

fac-[PtMe₃(ch-Sbpy)][BF₄] (**45**, ch-Sbpy = **7a**). (89 mg, 75%); *m/z* (ESI) 758.1679 ([PtMe₃(**7a**)]⁺. C₂₇H₃₅N₂O₉PtS requires 758.1711).

fac-[PtMe₃(ch-Sbpy)][BF₄] (**46**, ch-Sbpy = **7b**). (101 mg, 66%); *m/z* (ESI) 1006.2331 ([PtMe₃(**7b**)]⁺. C₄₇H₄₃N₂O₉PtS requires 1006.2337).

4.2. X-Ray crystallography†

Single crystals of *fac*-[PtMe₃(bpy)(ch-STaz-κN)][BF₄] (ch-STaz = **5c**, **19**), *fac*-[PtMe₃(bpy)(STazH-κS)][BF₄] (**21a**) and 1,6-anhydro-2,3,4-tri-*O*-benzoyl-glucopyranose (**23a**) for X-ray diffraction measurements were obtained from acetone/ether/THF (1 : 1 : 1)

(**19**) and acetone/ether/pentane solutions (1 : 1 : 1) (**21a**, **23a**), respectively. Intensity data were collected on a Oxford Gemini S diffractometer with Cu-Kα radiation ($\lambda = 1.54184$ Å, graphite monochromator) at 100(2) K (**19**) and on a Bruker Apex II Kappa diffractometer with Mo-Kα radiation ($\lambda = 0.71073$ Å, graphite monochromator) at 100(2) K (**21a**, **23a**). A summary of the crystallographic data, the data collection parameters and the refinement parameters is given in Table 4. Numerical (**21a**) and multiscan (**23a**) absorption corrections were applied (*T*_{min}/*T*_{max} 0.18/0.55, **21a**; *T*_{min}/*T*_{max} 0.97/0.98, **23a**). The structures were solved by direct methods with SHELXS-97²⁶ and refined using full matrix least square routines against *F*² with SHELXL-97.²⁶ Non-hydrogen atoms were refined with anisotropic displacement parameters. The hydrogen atom attached to nitrogen in **21a** was found in the difference Fourier map and refined freely. All other hydrogen atoms were positioned geometrically and refined with isotropic displacement parameters according to the “riding model”. Although measured at 100 K with Cu-Kα radiation the small sized needle-like crystals (0.3 × 0.03 × 0.03 mm) of complex **19** showed only a weak reflectivity resulting in a limited quality of the structure solution. The required fixing of disordered groups (phenyl rings and [BF₄][−] anions) for the refinement of **19**, led to the comparatively high number of restraints. The fluorine atom F4 of the tetrafluoroborate anion in complex **21a** was found to be disordered over two equally occupied positions.

4.3. Computational details

DFT calculations of compounds were carried out by the Gaussian 03 program package²⁷ using the hybrid functional B3LYP.²⁸ The

6-311G(d,p) basis sets as implemented in Gaussian 03 were employed for main group atoms. The valence shell of platinum has been approximated by a split valence basis set too; for its core orbitals an effective core potential in combination with consideration of relativistic effects has been used.²⁹ The appropriateness of the functional in combination with the basis sets and effective core potential used for reliable interpretation of structural and energetic aspects of related platinum complexes has been demonstrated.³⁰ All systems were fully optimized without any symmetry restrictions. The resulting geometries were characterized as equilibrium structures by the analysis of the force constants of normal vibrations. Solvent effects were considered according to the polarized continuum model as implemented in Gaussian 03.³¹

Acknowledgements

Financial support from the National Science Foundation (award CHE-0547566 to AVD), the National Institute of General Medical Sciences (award GM077170 to AVD), and gifts of chemicals by Merck (Darmstadt) is gratefully acknowledged. Special thanks to Prof. J. Balbach and Dipl.-Phys. M. Kovermann (Martin-Luther-Universität Halle-Wittenberg) for the NMR spectroscopic measurements on the 800 MHz spectrometer.

References

- 1 R. A. Dwek, *Chem. Rev.*, 1996, **96**, 683.
- 2 T. Lindhorst, *Essentials of Carbohydrate Chemistry*, Wiley-VCH, Weinheim, 2nd edn, 2003, 175 pp.
- 3 T. Storr, M. Merkel, G. X. Song-Zhao, L. E. Scott, D. E. Green, M. L. Bowen, K. H. Thompson, B. O. Patrick, H. J. Schugar and C. Orvig, *J. Am. Chem. Soc.*, 2007, **129**, 7453.
- 4 (a) D. J. Hoffman and R. L. Whistler, *Biochemistry*, 1968, **7**, 4479; (b) R. L. Whistler and W. C. Lake, *Biochem. J.*, 1972, **130**, 919; (c) B. Hellman, Å. Lernmark, J. Sehlin, I.-B. Täljedal and R. L. Whistler, *Biochem. Pharmacol.*, 1973, **22**, 29; (d) J. R. Zysk, A. A. Bushway, R. L. Whistler and W. W. Carlton, *J. Reprod. Fertil.*, 1975, **45**, 69.
- 5 (a) J. H. Kim, S. H. Kim, E. W. Hahn and C. W. Song, *Science*, 1978, **200**, 206.
- 6 (a) H. Hashimoto, T. Fujimori and H. Yuasa, *J. Carbohydr. Chem.*, 1990, **9**, 683; (b) C.-H. Wong, Y. Ichikawa, T. Krach, C. Gautheron-Le Narvor, D. P. Dumas and G. C. Look, *J. Am. Chem. Soc.*, 1991, **113**, 8137; (c) B. D. Johnston and B. M. Pinto, *J. Org. Chem.*, 1998, **63**, 5797.
- 7 (a) M. Takeuchi, M. Yoshikawa, R. Sasaki and H. Chiba, *Agric. Biol. Chem.*, 1982, **46**, 2741; (b) G. Guo, G. Li, D. Liu, Q.-J. Yang, Y. Liu, Y.-K. Jing and L.-X. Zhao, *Molecules*, 2008, **13**, 1487; (c) M. Singer, M. Lopez, L. F. Bornaghi, A. Innocenti, D. Vullo, C. T. Supuran and S.-A. Poulsen, *Bioorg. Med. Chem. Lett.*, 2009, **19**, 2273; (d) N. M. Khalifa, M. M. Ramla, A. E.-G. E. Amr and M. M. Abdulla, *Phosphorus, Sulfur Silicon Relat. Elem.*, 2008, **183**, 3046.
- 8 S. Yano, *Coord. Chem. Rev.*, 1988, **92**, 113.
- 9 D. M. Whitfield, S. Stojkovski and B. Sarkar, *Coord. Chem. Rev.*, 1993, **122**, 171.
- 10 (a) J. Petrig, R. Schibli, C. Dumas, R. Alberto and P. A. Schubiger, *Chem.-Eur. J.*, 2001, **7**, 1868; (b) D. J. Yang, C.-G. Kim, N. R. Schechter, A. Azhdarinia, D.-F. Yu, C.-S. Oh, J. L. Bryant, J.-I. Won, E. E. Kim and D. A. Podoloff, *Radiology*, 2003, **226**, 465; (c) T. Storr, Y. Sugai, C. A. Barta, Y. Mikata, M. J. Adam, S. Yano and C. Orvig, *Inorg. Chem.*, 2005, **44**, 2698; (d) T. Storr, C. L. Fisher, Y. Mikata, S. Yano, M. J. Adam and C. Orvig, *Dalton Trans.*, 2005, 654.
- 11 Y. Mikata, Y. Shinohara, K. Yoneda, Y. Nakamura, I. Brudzińska, T. Tanase, T. Kitayama, R. Takagi, T. Okamoto, I. Kinoshita, M. Doe, C. Orvig and S. Yano, *Bioorg. Med. Chem. Lett.*, 2001, **11**, 3045.
- 12 D. Steinborn and H. Junicke, *Chem. Rev.*, 2000, **100**, 4283.
- 13 (a) H. Junicke, C. Bruhn, D. Ströhl, R. Kluge and D. Steinborn, *Inorg. Chem.*, 1998, **37**, 4603; (b) D. Steinborn, H. Junicke and C. Bruhn, *Angew. Chem., Int. Ed. Engl.*, 1997, **36**, 2686; (c) H. Junicke, C. Bruhn, R. Kluge, A. S. Serianni and D. Steinborn, *J. Am. Chem. Soc.*, 1999, **121**, 6232; (d) H. Junicke, R. Kluge and D. Steinborn, *J. Inorg. Biochem.*, 2000, **81**, 43.
- 14 P. Pornsuriyasak, C. Vetter, S. Kaeothip, M. Kovermann, J. Balbach, D. Steinborn and A. V. Demchenko, *Chem. Commun.*, 2009, 6379.
- 15 Cambridge Structural Database (CSD) Version 5.30 2008, University Chemical Laboratory, Cambridge (England).
- 16 (a) T. G. Appleton, H. C. Clark and L. E. Manzer, *Coord. Chem. Rev.*, 1973, **10**, 335; (b) C. Vetter, C. Wagner, J. Schmidt and D. Steinborn, *Inorg. Chim. Acta*, 2006, **359**, 4326.
- 17 R. Bucourt, *Top. Stereochem.*, 1974, **8**, 159.
- 18 (a) C. Vetter, C. Wagner, G. N. Kaluderović, R. Paschke and D. Steinborn, *Inorg. Chim. Acta*, 2009, **362**, 189; (b) C. Vetter, G. N. Kaluderović, R. Paschke and D. Steinborn, *Inorg. Chim. Acta*, 2010, DOI: 10.1016/j.ica.2010.03.079.
- 19 (a) C. Vetter, diploma thesis, Martin-Luther-Universität Halle-Wittenberg, Halle 2005; (b) R. Lindner, G. N. Kaluderović, R. Paschke, C. Wagner and D. Steinborn, *Polyhedron*, 2008, **27**, 914.
- 20 (a) E. S. Raper, R. E. Oughtred and I. W. Nowell, *Inorg. Chim. Acta*, 1983, **77**, L89; (b) H. T. Flakus, A. Miro and P. G. Jones, *Spectrochim. Acta, Part A*, 2002, **58**, 225; (c) R. S. Corrêa, S. A. Santana, R. Salloum, R. M. Silva and A. C. Doriguetto, *Acta Crystallogr., Sect. C: Cryst. Struct. Commun.*, 2006, **62**, o115.
- 21 C. Janiak, *J. Chem. Soc., Dalton Trans.*, 2000, 3885.
- 22 (a) G. B. Deacon and R. J. Phillips, *Coord. Chem. Rev.*, 1980, **33**, 227; (b) L. C. Francesconi, D. R. Corbin, A. W. Clauss, D. N. Hendrickson and G. D. Stucky, *Inorg. Chem.*, 1981, **20**, 2059; (c) M. Gasgnier and A. Petit, *J. Mater. Sci.*, 1994, **29**, 6479.
- 23 S. Kaeothip, P. Pornsuriyasak and A. V. Demchenko, *Tetrahedron Lett.*, 2008, **49**, 1542.
- 24 A. V. Demchenko, P. Pornsuriyasak, C. De Meo and N. N. Malysheva, *Angew. Chem., Int. Ed.*, 2004, **43**, 3069.
- 25 J. C. Baldwin and W. C. Kaska, *Inorg. Chem.*, 1975, **14**, 2020.
- 26 G. M. Sheldrick, *Acta Crystallogr., Sect. A: Found. Crystallogr.*, 2008, **64**, 112.
- 27 M. J. Frisch, G. W. Trucks, H. B. Schlegel, G. E. Scuseria, M. A. Robb, J. R. Cheeseman, J. A. Montgomery, Jr., T. Vreven, K. N. Kudin, J. C. Burant, J. M. Millam, S. S. Iyengar, J. Tomasi, V. Barone, B. Mennucci, M. Cossi, G. Scalmani, N. Rega, G. A. Petersson, H. Nakatsuji, M. Hada, M. Ehara, K. Toyota, R. Fukuda, J. Hasegawa, M. Ishida, T. Nakajima, Y. Honda, O. Kitao, H. Nakai, M. Klene, X. Li, J. E. Knox, H. P. Hratchian, J. B. Cross, V. Bakken, C. Adamo, J. Jaramillo, R. Gomperts, R. E. Stratmann, O. Yazyev, A. J. Austin, R. Cammi, C. Pomelli, J. Ochterski, P. Y. Ayala, K. Morokuma, G. A. Voth, P. Salvador, J. J. Dannenberg, V. G. Zakrzewski, S. Dapprich, A. D. Daniels, M. C. Strain, O. Farkas, D. K. Malick, A. D. Rabuck, K. Raghavachari, J. B. Foresman, J. V. Ortiz, Q. Cui, A. G. Baboul, S. Clifford, J. Cioslowski, B. B. Stefanov, G. Liu, A. Liashenko, P. Piskorz, I. Komaromi, R. L. Martin, D. J. Fox, T. Keith, M. A. Al-Laham, C. Y. Peng, A. Nanayakkara, M. Challacombe, P. M. W. Gill, B. G. Johnson, W. Chen, M. W. Wong, C. Gonzalez and J. A. Pople, *GAUSSIAN 03 (Revision B.04)*, Gaussian, Inc., Wallingford, CT, 2004.
- 28 (a) A. D. Becke, *Phys. Rev. A: At., Mol., Opt. Phys.*, 1988, **38**, 3098; (b) A. D. Becke, *J. Chem. Phys.*, 1993, **98**, 5648; (c) C. Lee, W. Yang and R. G. Parr, *Phys. Rev. B: Condens. Matter Phys.*, 1988, **37**, 785; (d) P. J. Stephens, F. J. Devlin, C. F. Chabalowski and M. J. Frisch, *J. Phys. Chem.*, 1994, **98**, 11623.
- 29 (a) D. Andrae, U. Häußermann, M. Dolg, H. Stoll and H. Preuss, *Theor. Chim. Acta*, 1990, **77**, 123; (b) See <http://bse.pnl.gov/bse/portal>.
- 30 (a) K. Nordhoff and D. Steinborn, *Organometallics*, 2001, **20**, 1408; (b) T. Gosavi, C. Wagner, H. Schmidt and D. Steinborn, *J. Organomet. Chem.*, 2005, **690**, 3229; (c) M. Werner, T. Lis, C. Bruhn, R. Lindner and D. Steinborn, *Organometallics*, 2006, **25**, 5946; (d) D. Steinborn and S. Schwiager, *Chem.-Eur. J.*, 2007, **13**, 9668; (e) S. Schwiager, R. Herzog, C. Wagner and D. Steinborn, *J. Organomet. Chem.*, 2009, **694**, 3548; (f) R. Lindner, C. Wagner and D. Steinborn, *J. Am. Chem. Soc.*, 2009, **131**, 8861.
- 31 (a) E. Cancès, B. Mennucci and J. Tomasi, *J. Chem. Phys.*, 1997, **107**, 3032; (b) M. Cossi, V. Barone, B. Mennucci and J. Tomasi, *Chem. Phys. Lett.*, 1998, **286**, 253; (c) B. Mennucci and J. Tomasi, *J. Chem. Phys.*, 1997, **106**, 5151.

Coordination chemistry approach to the long-standing challenge of stereocontrolled chemical glycosylation†

Papapida Pornsuriyasak,^a Cornelia Vetter,^b Sophon Kaothip,^a Michael Kovermann,^{cd} Jochen Balbach,^{cd} Dirk Steinborn^{*b} and Alexei V. Demchenko^{*a}

Received (in College Park, MD, USA) 25th February 2009, Accepted 8th September 2009

First published as an Advance Article on the web 24th September 2009

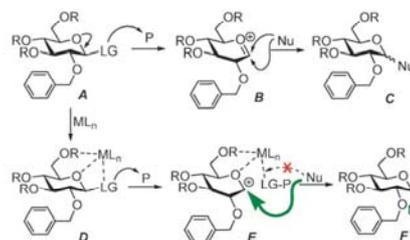
DOI: 10.1039/b903942b

This study clearly demonstrates that a multi-dentate metal coordination to the leaving group, along with O-5 and/or a protecting group at O-6, has a strong effect on the stereo-selectivity of chemical glycosylation.

Although complete information about the functions of natural complex carbohydrates is yet to emerge, some aspects of their involvement in many biological phenomena are already known.^{1,2} Further improvement in this field would be significantly facilitated if we could rely on detailed knowledge of the structure, conformation and properties of the carbohydrate molecules involved. Therefore, the development of effective methods for assembling simple carbohydrates into more elaborate networks (oligosaccharides and conjugates thereof) has become critical for the field of glycosciences.^{3–5}

Since the *O*-glycosylation reaction leads to the formation of a new chirality (anomeric) center, particular care has to be taken with regards to stereocontrol, which is particularly important when the synthesis of challenging 1,2-*cis*-glycosides is undertaken.^{6,7} A generic reaction pathway for glycosyl donors with a non-participating 2-*O*-benzyl substituent (A) is depicted in Scheme 1. Promoter (P) mediated departure of the anomeric leaving group (LG) results in formation of the oxocarbenium ion B. In uncontrolled glycosylation, nucleophilic attack of the glycosyl acceptor (Nu) can then take place from either the top or the bottom face of the flattened ring, often leading to anomeric mixtures C (Scheme 1).⁸

The central hypothesis at the base of this study is whether metal coordination (ML_n), in particular multi-dentate coordination to the leaving group along with the O-5 and/or remote position(s) (intermediate D), has an effect on the stereo-selectivity of glycosylation. We assumed that even upon promoter-assisted LG “departure”, such a complex would sterically hinder the top face of the key intermediate E



Scheme 1 Direct vs. coordination-mediated glycosylations.

(for sugars of the D-series). As a result, the nucleophilic attack of the glycosyl acceptor would be primarily directed from the opposite side, resulting in an α -D-linked (1,2-*cis* for D-gluco) product F. We began investigating this concept by using conventional thioglycoside **1a**⁹ and trimethylplatinum(IV) complexes thereof.^{10,11} Typical MeOTf-promoted glycosidation¹² of **1a** with glycosyl acceptor **3** provided no stereoselectivity for the formation of disaccharide **4** (entry 1.1, Table 1). Although

Table 1 Investigation of per-benzylated *S*-ethyl and *S*-thiazolinyl glycosides as glycosyl donors and ligands

Entry	Donor	Promoter	Time	Yield (%)	α/β
1.1	1a	MeOTf	10 min	92	1.0/1
1.2	1b–d	MeOTf, NIS/TfOH, or DMTST	48 h	0	—
1.3	2a	Cu(OTf) ₂	1 h	95	1.5/1
1.4	2b	Cu(OTf) ₂	20 h	62	2.4/1
1.5	2c	Cu(OTf) ₂	15 h	88	2.5/1
1.6	2d	Cu(OTf) ₂	16 h	79	2.3/1

^a Department of Chemistry and Biochemistry, University of Missouri—St. Louis, One University Boulevard, St. Louis, Missouri 63121, USA. E-mail: demchenko@umsl.edu

^b Institut für Chemie-Anorganische Chemie, Martin-Luther-Universität Halle-Wittenberg, D-06120 Halle, Kurt-Mothes Straße 2, Germany. E-mail: dirk.steinborn@chemie.uni-halle.de

^c Institut für Physik, Fachgruppe Biophysik, Martin-Luther-Universität Halle-Wittenberg, D-06099 Halle (Saale), Germany

^d Mitteldeutsches Zentrum für Struktur und Dynamik der Proteine (MZP), Martin-Luther-Universität Halle-Wittenberg, D-06099 Halle (Saale), Germany

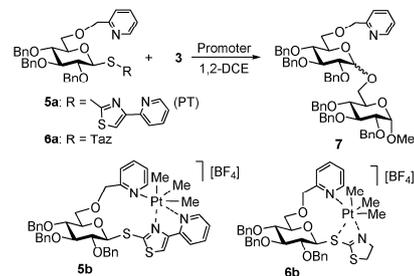
† Electronic supplementary information (ESI) available: Extended experimental data, experimental procedures for the synthesis of new compounds, and their ¹H and ¹³C NMR spectra. See DOI: 10.1039/b903942b.

a variety of factors, such as the effect of the reaction solvent, can dramatically increase the stereoselectivity,^{13–15} herein, we chose 1,2-dichloroethane (1,2-DCE), which has a minimal solvation effect on the reactants and intermediates. The synthesis of various platinum(IV) complexes **1b–d**, all of which are coordinated to the platinum atom *via* the anomeric sulfur, was successfully achieved (see the ESI†). Unfortunately, all of our attempts to glycosidate such complexes under conventional conditions for thioglycoside activation¹⁶ have failed (entry 1.2). No glycosylation took place and only partial hydrolysis of glycosyl donor and methylation of glycosyl acceptor **3** (with MeOTf) were observed as major side reactions.

It is possible that coordination of platinum to the anomeric sulfur prevents its subsequent interaction with electrophilic promoters. In this context, glycosyl donors with multiple reactive centers on the leaving group, such as glycosyl thioimidates,¹⁷ would help to address this concern. Arguably, even upon complexation, these compounds would allow for activation *via* the non-engaged center. Theoretically, either direct coordination of a metal to the anomeric sulfur or remote coordination to the nitrogen should improve the thioimidoyl leaving group ability.^{18,19} The discovery of the temporary deactivation concept, however, implies that some complexes of non-ionizing nature may have an opposite, deactivating, effect on the thioimidoyl leaving group ability.^{20,21} It has been demonstrated that trimethylplatinum complexes coordinate to carbohydrates and to *N,S*-heterocycles like thiazoline-2-thione without being reduced.^{10,11,22} Therefore, investigation of *S*-thiazolinyl (STaz) derivative **2a**^{23,24} was of particular interest. Encouragingly, glycosidation of complexes **2b–d** in the presence of Cu(OTf)₂ provided a notable improvement in stereoselectivity (entries 1.4–1.6) in comparison to that achieved in the glycosidation of the uncomplexed glycosyl donor **2a** (entry 1.3). In compounds **2b–d** the carbohydrate ligands were found to coordinate to the platinum atom *via* the nitrogen atom of the STaz group and additionally for compound **2b** through the oxygen atoms of glucopyranose (see the ESI†).

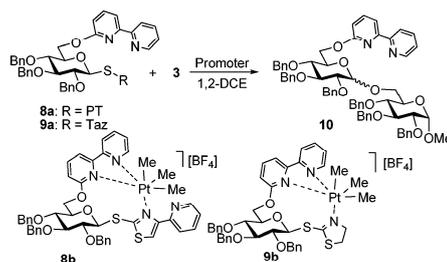
Weakly coordinating donor sites in neutral carbohydrates afford complexes that are often unstable in the presence of stronger donor sites. Therefore, these results could not serve as a reliable proof of the concept of coordination-assisted improvement in stereoselectivity. These glycosylations could partially proceed *via* the complex destruction that would result in the complete leaving group departure as occurs in direct glycosylations. Hence, we assumed that targeted enhanced coordination of the carbohydrate ligands can be achieved by introducing stronger *N*-Lewis-basic substituents. To execute this approach, we obtained 6-*O*-picolyl derivatives of 4-(pyridin-2-yl)thiazol-2-yl thioglycosides (SPT)²¹ and STaz glycosides, **5a** and **6a**, respectively. Direct glycosidation of these glycosyl donors proceeded with poor stereoselectivity (entries 2.1 and 2.2, Table 2), whereas glycosidation of the corresponding complexes **5b** and **6b** under essentially the same activation conditions gave improved (2–2.5 fold) stereoselectivity (entries 2.3 and 2.4). This result is a clear indication that improved stereoselectivity can be achieved by applying specifically designed ligands capable of stronger coordination.

Table 2 Investigation of 6-*O*-picolylated *S*-pyridylthiazolyl and *S*-thiazolinyl glycosides as glycosyl donors and ligands



Entry	Donor	Promoter	Time/h	Yield (%)	α/β
2.1	5a	AgOTf	22	66	1.1/1
2.2	6a	Cu(OTf) ₂	16	83	2.0/1
2.3	5b	AgOTf	20	58	2.1/1
2.4	6b	Cu(OTf) ₂	24	62	5.2/1

Table 3 Investigation of 6-*O*-bipyridine-substituted *S*-ethyl and *S*-thiazolinyl glycosides as glycosyl donors and ligands



Entry	Donor	Promoter	Time/h	Yield (%)	α/β
3.1	8a	AgOTf	14	82	1.5/1
3.2	9a	Cu(OTf) ₂	48	73	1.7/1
3.3	8b	AgOTf	16	67	2.2/1
3.4	9b	Cu(OTf) ₂	24	65	9.4/1

In order to pursue this concept further, we obtained glycosyl donors **8a** and **9a** bearing a bipyridine protecting group at C-6. The results of this study are highlighted in Table 3. While the improvement in the case of the SPT glycosyl donor was unremarkable, a 5-fold improvement with the complexed glycosyl donor **9b** is significant. Thus, while glycosidation of **9a** showed only a slight preference for the α -anomer (1.7/1, entry 3.2), the glycosidation of its complexed counterpart **9b** allowed a 9.4/1 α/β -anomeric ratio of disaccharide **10** (entry 3.4). The coordination sites in the complex **9b** (three nitrogen atoms as shown in Table 3) were unambiguously proven (see the ESI†).

Similarly, a 3–3.5 fold improvement was achieved in the glycosylation of common secondary glycosyl acceptors **11** and **12** with the complexed STaz glycosyl donor **9b**. The results of this study are highlighted in Table 4, and are available in more detail as a part of the ESI†.

Table 4 Investigation of secondary glycosyl acceptors **11** and **12**

Entry	Donor	Acceptor	Product	Yield (%)	α/β
4.1	9a	11	13	53	2.2/1
4.2	9a	12	14	61	2.0/1
4.3	9b	11	13	50	7.2/1
4.4	9b	12	14	48	6.0/1

It should be noted that although significant improvements of the chemical glycosylation have already emerged,⁸ examples of highly stereocontrolled glycosylations are still rare. To date, very little is known about the effect of metal coordination on the reactivity and stereoselectivity of carbohydrates in glycosylations. We expect that the studies presented herein will ultimately evolve into a well-rounded and versatile metal-assisted methodology for the synthesis of a broad range of complex glycostructures.

AVD thanks the National Science Foundation (CHE-0547566) and American Heart Association (0855743G), and DS thanks the Deutsche Forschungsgemeinschaft for financial support of this work. We also thank Dr R. Kluge (Martin-Luther-Universität Halle-Wittenberg) and Dr J. Schmidt (Leibniz-Institut für Pflanzenbiochemie) for ESI-MS determinations.

Notes and references

- 1 *Essentials of Glycobiology*, ed. A. Varki, R. Cummings, J. Esko, H. Freeze, G. Hart and J. Marth, Cold Spring Harbor Laboratory Press, Cold Spring Harbor, N. Y., 1999.
- 2 C. R. Bertozzi and L. L. Kiessling, *Science*, 2001, **291**, 2357–2364.
- 3 A. V. Demchenko, *Lett. Org. Chem.*, 2005, **2**, 580–589.
- 4 P. H. Seeberger and D. B. Werz, *Nature*, 2007, **446**, 1046–1051.
- 5 J. T. Smoot and A. V. Demchenko, *Adv. Carbohydr. Chem. Biochem.*, 2009, **62**, 161–250.
- 6 A. V. Demchenko, *Synlett*, 2003, 1225–1240.
- 7 A. V. Demchenko, *Curr. Org. Chem.*, 2003, **7**, 35–79.
- 8 *Handbook of Chemical Glycosylation: Advances in Stereoselectivity and Therapeutic Relevance*, ed. A. V. Demchenko, Wiley-VCH, Weinheim, 2008.
- 9 F. Andersson, P. Fugedi, P. J. Garegg and M. Nashed, *Tetrahedron Lett.*, 1986, **27**, 3919–3922.
- 10 H. Junicke, C. Bruhn, R. Kluge, A. S. Serianni and D. Steinborn, *J. Am. Chem. Soc.*, 1999, **121**, 6232–6241.
- 11 D. Steinborn and H. Junicke, *Chem. Rev.*, 2000, **100**, 4283–4317.
- 12 H. Lönn, *J. Carbohydr. Chem.*, 1987, **6**, 301–306.
- 13 R. Eby and C. Schuerch, *Carbohydr. Res.*, 1974, **34**, 79–90, and references therein.
- 14 G. Wulff and G. Rohle, *Angew. Chem., Int. Ed. Engl.*, 1974, **13**, 157–170.
- 15 A. Demchenko, T. Stauch and G. J. Boons, *Synlett*, 1997, 818–820.
- 16 P. J. Garegg, *Adv. Carbohydr. Chem. Biochem.*, 1997, **52**, 179–205.
- 17 P. Pornsuriyasak, M. N. Kamat and A. V. Demchenko, *ACS Symp. Ser.*, 2007, **960**, 165–189.
- 18 M. N. Kamat, N. P. Rath and A. V. Demchenko, *J. Org. Chem.*, 2007, **72**, 6938–6946.
- 19 S. Kaethip, P. Pornsuriyasak, N. P. Rath and A. V. Demchenko, *Org. Lett.*, 2009, **11**, 799–802.
- 20 P. Pornsuriyasak, U. B. Gangadharmath, N. P. Rath and A. V. Demchenko, *Org. Lett.*, 2004, **6**, 4515–4518.
- 21 P. Pornsuriyasak, N. P. Rath and A. V. Demchenko, *Chem. Commun.*, 2008, 5633–5635.
- 22 C. Vetter, C. Wagner, J. Schmidt and D. Steinborn, *Inorg. Chim. Acta*, 2006, **359**, 4326–4334.
- 23 A. V. Demchenko, P. Pornsuriyasak, C. De Meo and N. N. Malysheva, *Angew. Chem., Int. Ed.*, 2004, **43**, 3069–3072.
- 24 P. Pornsuriyasak and A. V. Demchenko, *Chem.–Eur. J.*, 2006, **12**, 6630–6646.

Structural and Computational Studies of 1-Methyl-2-thiocytosine and its Coordination Mode in a Dinuclear Platinum(IV) Complex [(PtMe₃)₂(μ-1-MeSCy-1κN³,1:2κ²S)₂][BF₄]₂

Cornelia Vetter^a, Christoph Wagner^a, Ralph Kluge^b, and Dirk Steinborn^a

^a Institut für Chemie – Anorganische Chemie, Martin-Luther-Universität Halle-Wittenberg, Kurt-Mothes-Straße 2, 06120 Halle, Germany

^b Institut für Chemie – Organische Chemie, Martin-Luther-Universität Halle-Wittenberg, Kurt-Mothes-Straße 2, 06120 Halle, Germany

Reprint requests to Prof. D. Steinborn. Tel.: +345 5525620. Fax: +345 5527028.

E-mail: dirk.steinborn@chemie.uni-halle.de

Z. Naturforsch. **2010**, *65b*, 578 – 586; received January 20, 2010

X-Ray diffraction analysis of 1-methyl-2-thiocytosine (1-MeSCy, **1**) revealed that its crystals contain two structurally very similar independent molecules (A, B). These molecules are connected through a complex network of hydrogen bonds. Centrosymmetric di- and tetrameric units AA' and BAA'B', respectively, are formed through N–H...N hydrogen bonds (N4a...N3a' 3.019(4) Å, AA'; N4a...N3b 2.988(4) Å, BAA'B'), and the tetrameric units are connected through N–H...S hydrogen bonds. The arrangement of A and B molecules found in crystals of **1** was confirmed by DFT calculations up to tetrameric BAA'B' units, yielding similar equilibrium structures, and the energies of the N–H...N hydrogen bonds between A and A' and A and B were calculated to be about 10 kcal mol⁻¹. Reaction of 1-MeSCy (**1**) with [PtMe₃(Me₂CO)₃][BF₄] (**2**) led to the formation of the ionic dinuclear complex [(PtMe₃)₂(μ-1-MeSCy-1κN³,1:2κ²S)₂][BF₄]₂ (**3**) which was fully characterized by NMR (¹H, ¹³C, ¹⁹⁵Pt) and IR spectroscopy, ESI mass spectrometry and microanalysis. A single-crystal X-ray diffraction analysis of **3** confirmed the dinuclear structure of the complex. The complex cation consists of a central [Pt₂(μ-S)₂] core having bound the 1-methyl-2-thiocytosine ligands in a 1κN³,1:2κ²S coordination mode in a face-to-face arrangement, the thionucleobase ligands being present as the amino-thione tautomer.

Key words: Thionucleobases, Platinum Complexes, Hydrogen Bonding, Single-crystal X-Ray Diffraction Analysis, DFT Calculations

Introduction

Thionucleobases and thionucleosides can be found in many biological processes. 2-Thiouracil has been found in t-RNA of *E. coli* bacteria [1]. Furthermore, the nucleosides of 4-thiouracil and 2-thiocytosine are present in t-RNA of several sources [2–5]. Further insight into the function of these compounds can be achieved by investigations of model compounds. The most simple models for these nucleosides are the derivatives methylated at the position next to the carbohydrate moiety. They should exist in the same tautomeric form as the requisite nucleosides. Depending on the solvent, thionucleobases can exist as many different tautomers. For 2-thiocytosine, in particular, it has been found that in aqueous solution and polycrys-

talline films the thione-amino tautomer is the predominant species [6–9]. In accordance with these observations the thione-amino form is present in crystals of 2-thiocytosine [10]. Methylation of a nucleobase limits the number of possible tautomers and may severely influence the resulting hydrogen bonding pattern. Metal coordination of thionucleobases is also of particular interest [11], especially because the coordination behavior of thionucleobases has not been studied as extensively as that of the naturally occurring oxygen analogs. It has been shown that metal thionucleobase complexes exhibit interesting bioactive properties [12]. Here we report the crystal structure of 1-methyl-2-thiocytosine (**1**) as well as the synthesis and the crystal structure of its ionic, dinuclear platinum(IV) complex [(PtMe₃)₂(μ-1-MeSCy-1κN³,1:2κ²S)₂][BF₄]₂ (**3**).

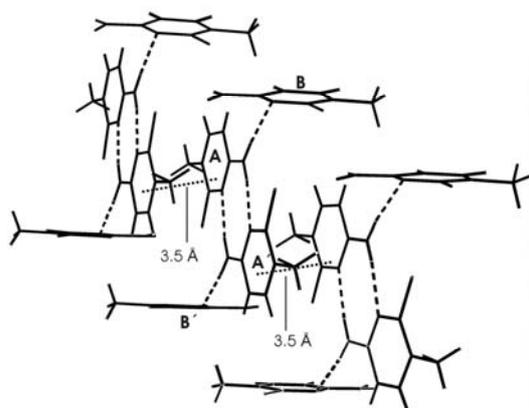


Fig. 2. Packing of molecules A and B and π - π stacking (...) between A and A' molecules in crystals of **1**.

distances proved to be 3.467 Å (lower/upper quartile: 3.408/3.551 Å, for 1873 observations) [17].

In crystals of **1** the dimeric units AA' and the monomeric units B are packed in infinite strands like a "staircase", as shown in Fig. 2. Within the AA' strands an interplanar ring distance of 3.5 Å and a displacement angle of 17.5° between pairs of pyrimidine rings of A indicate a stabilization through π - π stacking and/or C-H- π stacking [19]. Though a relatively short interplanar distance of 3.0 Å between the molecules in the B strands was found, a displacement angle of 59.9° of the B molecules suggests the absence of significant stabilization through π - π /C-H- π interactions.

Quantum-chemical calculations

To gain insight into the strength of the hydrogen bonds that are found in crystals of 1-methyl-2-thiocytosine (**1**), DFT calculations (using the B3LYP hybrid functional and 6-31++G(d,p) basis sets) of the monomeric 1-MeSCy **1m**, the doubly N4-H...N3' hydrogen-bonded dimer **1d** and the tetramer **1t**, having two further monomers attached to **1d** through N4-H...N3' hydrogen bonds, were performed. The equilibrium structures are shown in Fig. 3, selected structural parameters are given in Table 2. As Table 2 reveals, the involvement of **1m** in a hydrogen-bonded system gives rise to only small structural changes.

Dimer **1d** and tetramer **1t** can be regarded as models for the dimer AA' and the tetramer BAA'B' found in the solid-state structure of **1**. As shown in Table 2, there is good agreement of the calculated (**1t**) and the experimental structure (**1**). The most obvious differ-

Table 2. Calculated parameters (distances in Å, angles in deg) of the monomeric 1-MeSCy (**1m**), the twofold hydrogen-bridged dimer of the type AA' (**1d**) and the tetrameric unit of the type BAA'B' (**1t**). For comparison, the corresponding experimentally measured values in crystals of **1** are given.

	1m	1d	1t	1
C2-N1	1.420	1.411	1.402/1.410 ^a	1.381(3)/1.390(3) ^a
C2-S	1.678	1.689	1.702/1.686	1.702(3)/1.692(3)
C2-N3	1.357	1.351	1.350/1.356	1.344(3)/1.343(3)
C4-N3	1.323	1.341	1.345/1.332	1.343(3)/1.334(3)
C4-N4	1.361	1.338	1.339/1.358	1.327(3)/1.338(4)
N1-C2-N3	117.5	118.0	118.8/118.0	119.7(2)/119.4(2)
C2-N3-C4	121.6	122.4	121.3/121.7	120.9(2)/120.4(2)
N4...N3'		2.948	3.063/3.161 ^b	3.019(4)/2.988(4) ^b
N4-H		1.032	1.027/1.015	0.87/0.87
H...N3'		1.916	2.038/2.200	2.16/2.14
N4-H...N3'		179.4	175.3/157.3	174/165

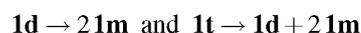
^a The first value refers to molecules A and the second value to molecules B; ^b the first value refers to hydrogen bonds in the dimers AA' and the second value to the hydrogen bonding within units AB.

ence is that the dimeric units AA' in **1d** and **1t** were calculated to be (nearly perfectly) planar (greatest deviation from the mean plane: 0.003 Å for N4a/N4a'), whereas in **1** the two halves of the dimer are shifted parallel by 0.36 Å (see Fig. 1). Furthermore, in the tetramer **1t** the interplanar angle between the central dimeric unit (AA') and its attached monomers (B/B') is found to be 36.9°, whereas in the solid-state structure of **1** the B/B' units are nearly perpendicular to the dimeric unit AA' (86.4(8)°). A tetrameric structure **1t'**, obtained by a restricted optimization such that the interplanar angle between the AA' unit and the B/B' molecules found in the experimental structure (86.4°) is obtained, proved to be only 6.2 kcal mol⁻¹ higher in energy than the equilibrium structure **1t**. As found in the experimental structure of **1**, the free electron pair of N3b in the calculated structure **1t** is not pointing directly towards the central H atom. However, the calculated angle between the N4a-H vector and the mean plane of the pyrimidine ring (22.8°) is remarkably smaller than in crystals of **1** (34.9°). This can be accounted for by further hydrogen bonds (N-H...S) and also π - π stackings in crystals of **1** that were not taken into consideration in the calculations.

The strength of intermolecular hydrogen bonds, ΔH_{hb} , is defined as the enthalpy of the reaction



when all components are in their equilibrium conformations. The energies for the reactions



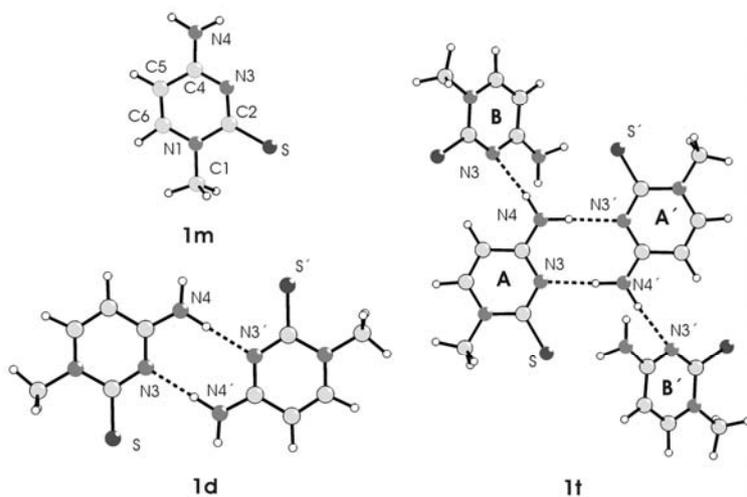
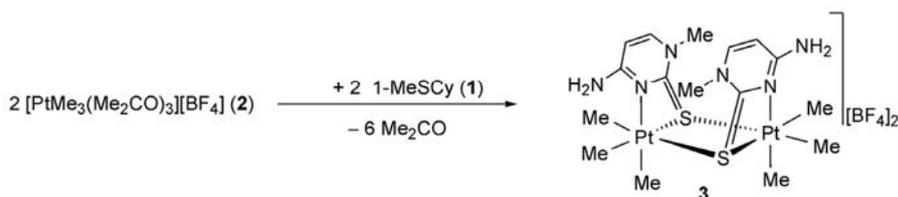


Fig. 3. Calculated equilibrium structures of the monomeric 1-MeSCy (**1m**), the twofold hydrogen-bonded dimer of the type AA' (**1d**) and the tetrameric unit of the type BAA'B' (**1t**).



Scheme 1.

were found to be endothermic by 20.2 and 21.7 kcal mol⁻¹, respectively. Considering basis BSSE set superposition errors [20], values of 19.4 and 19.6 kcal mol⁻¹, respectively, were obtained. Thus, both types of the N4–H···N3' hydrogen bonds, namely those building up the dimers and tetramers, are of approximately the same strength (about 10 kcal mol⁻¹ per hydrogen bond). Thus, these hydrogen bonds are stronger than those in gaseous water dimers (5.0 kcal mol⁻¹) [20,21] which are benchmarks for hydrogen bonds. Classifying hydrogen bonds with respect to their energies [22] (weak < 4, moderate 4–15, strong 14–40 kcal mol⁻¹) they have to be regarded as moderate.

Synthesis and spectroscopic characterization of $[(\text{PtMe}_3)_2(\mu\text{-1-MeSCy-1}\kappa\text{N}^3,1:2\kappa^2\text{S})_2][\text{BF}_4]_2$ (**3**)

$[\text{PtMe}_3(\text{Me}_2\text{CO})_3][\text{BF}_4]$ (**2**) [23] was reacted with 1-methylthiocytosine (**1**) in acetone solution to yield $[(\text{PtMe}_3)_2(\mu\text{-1-MeSCy-1}\kappa\text{N}^3,1:2\kappa^2\text{S})_2][\text{BF}_4]_2$ (**3**) (Scheme 1). The slightly air- and moisture-sensitive complex was isolated in 56% yield. By contrast, the analogous reaction with 2-thiocytosine led to the formation of several products. Complex **3** was

Table 3. ¹H and ¹³C NMR data (δ in ppm, J in Hz) of 1-MeSCy (**1**) and $[(\text{PtMe}_3)_2(\mu\text{-1-MeSCy-1}\kappa\text{N}^3,1:2\kappa^2\text{S})_2]$ (**3**) in CD₃OD.

	1		3	
	δ_{H}	$\delta_{\text{C}}^{\text{b}}$	$\delta_{\text{H}} (^2J_{\text{Pt,H}})$	δ_{C}
H5/C5 ^a	6.09	97.0	6.53	101.8
H6/C6	7.73	146.8	7.98	147.8
N1–CH ₃	3.72	43.3	3.64	40.7
C2		180.6		184.4
C4		160.5		160.4
PtMe ₃			1.22(75.5) ^c	-7.3

^a Numbering scheme according to Fig. 1a; ^b due to insufficient solubility of 1-MeSCy (**1**) the chemical shifts of **1** in [D₆]DMSO are given; ^c at -50 °C: 1.189/1.194 ppm (74.7/81.5).

fully characterized by ¹H, ¹³C and ¹⁹⁵Pt-NMR spectroscopy, as well as by ESI-MS spectrometry, IR spectroscopy, and X-ray diffraction analysis. Table 3 shows the ¹H and ¹³C-NMR data of $[(\text{PtMe}_3)_2(\mu\text{-1-MeSCy-1}\kappa\text{N}^3,1:2\kappa^2\text{S})_2][\text{BF}_4]_2$ (**3**). A remarkably downfield shift for the signals of H5 and the respective carbon atom C5 by 0.44 and 4.8 ppm, respectively, is observed. Moreover, the doublet of H5 exhibits platinum satellites (⁴J_{Pt,H} = 11.6 Hz) indicating the involvement of N3 in platinum coordination [24]. The signals of H6/C6 are also shifted to lower field but to a lesser extent (0.25/1.0 ppm), and no platinum satellites

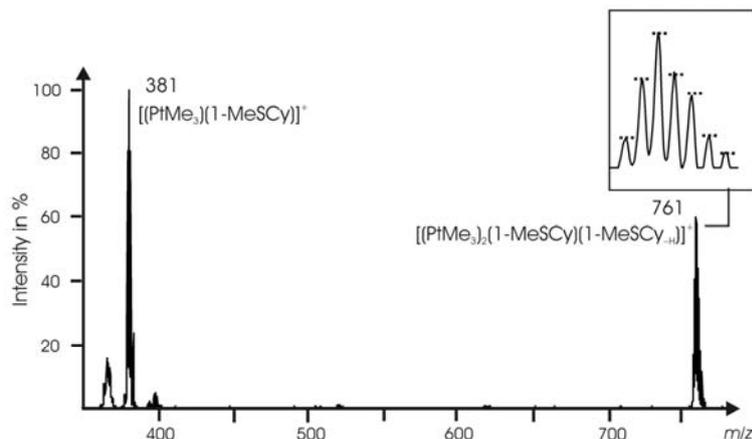


Fig. 4. Full scan mass spectrum of $[(\text{PtMe}_3)_2(\mu\text{-1-MeSCy-1}\kappa\text{N}^3,1:2\kappa^2\text{S}_2)][\text{BF}_4]_2$ (**3**). Inset: isotopic pattern of the molecular ion $[\text{PtMe}_3(\text{1-MeSCy})(\text{1-MeSCy-H})]^+$ at $m/z = 761$ showing the expected intensities due to the isotopic composition in horizontal bars.

are found. The shift of the signal for C2 by 3.8 ppm to lower field indicates the sulfur coordination to the platinum(IV) atom. Thus, from the NMR experiments a $\kappa\text{N}^3, \kappa\text{S}$ coordination could be derived, as definitely established by X-ray diffraction measurement (see below). For the protons of the three methyl ligands at room temperature only one sharp signal flanked by platinum satellites is found, whereas at $-50\text{ }^\circ\text{C}$ a splitting into at least two singlets, flanked by platinum satellites, becomes apparent (Table 3).

ESI-MS measurements using acetone solutions have confirmed the presence of a dinuclear cation $[(\text{PtMe}_3)_2(\text{1-MeSCy})(\text{1-MeSCy-H})]^+$ at $m/z = 761$ (Fig. 4). The isotopic pattern has been found to be characteristic for a monocation containing two platinum atoms [natural isotopic composition: ^{190}Pt (0.01%), ^{192}Pt (0.79%), ^{194}Pt (32.9%), ^{195}Pt (33.8%), ^{196}Pt (25.3%) and ^{198}Pt (7.2%)] in good agreement with calculated data. Furthermore, at $m/z = 381$ the monocation $[\text{PtMe}_3(\text{1-MeSCy})]^+$ has been found. Collision-induced dissociation (CID) experiments have shown that this peak is also formed by fragmentation of the isolated parent ion $[(\text{PtMe}_3)_2(\text{1-MeSCy})(\text{1-MeSCy-H})]^+$.

Crystal structure of $[(\text{PtMe}_3)_2(\mu\text{-1-MeSCy-1}\kappa\text{N}^3,1:2\kappa^2\text{S}_2)][\text{BF}_4]_2$ ($3 \cdot 1.5 \text{ C}_6\text{H}_6$)

Colorless crystals of $3 \cdot 1.5 \text{ C}_6\text{H}_6$ were obtained from acetone solutions layered with benzene and ether. The complex crystallizes as the racemate in the space group $P2_1/c$. The crystals consist of the dinuclear cation $[(\text{PtMe}_3)_2(\mu\text{-1-MeSCy-1}\kappa\text{N}^3,1:2\kappa^2\text{S}_2)]^{2+}$, two $[\text{BF}_4]^-$ anions and one and a half benzene solvate molecules. The molecular structure of the cation of

Table 4. Selected bond lengths and angles of $[(\text{PtMe}_3)_2(\mu\text{-1-MeSCy-1}\kappa\text{N}^3,1:2\kappa^2\text{S}_2)]$ ($3 \cdot 1.5 \text{ C}_6\text{H}_6$) (distances in Å, angles in deg).

Pt1–C1	2.057(6)	Pt1–S1	2.551(2)	Pt2–S1	2.525(2)
Pt1–C3	2.055(8)	Pt1–S2	2.501(2)	Pt2–S2	2.542(2)
Pt2–C4	2.062(8)	Pt1–N4	2.257(5)	S1–C7	1.737(7)
Pt2–C5	2.047(6)	Pt2–N1	2.243(5)	S2–C12	1.726(7)
C1–Pt1–C2	87.7(4)	S1–C7–N1	114.2(5)	S2–Pt1–N4	66.0(1)
C3–Pt1–N4	166.7(3)	C4–Pt2–C5	87.7(3)	Pt1–S1–Pt2	92.56(6)
S1–Pt2–N1	65.4(1)	C6–Pt2–N1	166.8(3)	Pt1–S2–Pt2	93.34(6)

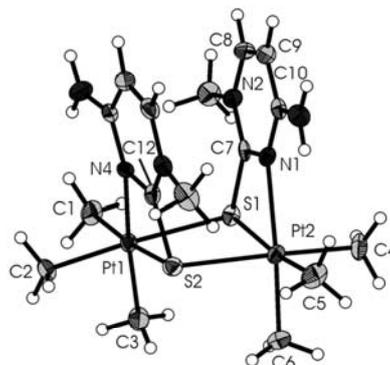


Fig. 5. Molecular structure of the cation of one enantiomer in crystals of $[(\text{PtMe}_3)_2(\mu\text{-1-MeSCy-1}\kappa\text{N}^3,1:2\kappa^2\text{S}_2)][\text{BF}_4]_2$ ($3 \cdot 1.5 \text{ C}_6\text{H}_6$). The displacement ellipsoids are drawn at the 30% probability level.

one enantiomer is shown in Fig. 5. Selected bond lengths and angles are given in Table 4. The primary donor sets of the octahedrally coordinated platinum atoms $[\text{PtC}_3\text{NS}_2]$ are built up of three methyl ligands in *facial* arrangement and two $\mu\text{-1-methyl-2-thiocytosine-1}\kappa\text{N}^3,1:2\kappa^2\text{S}$ ligands. The central $[\text{Pt}_2(\mu\text{-S})_2]$ core is slightly hinged ($\text{Pt1-S1}\cdots\text{S2-Pt2}$: 168.2°). The two 1-methyl-2-thiocytosine ligands are arranged

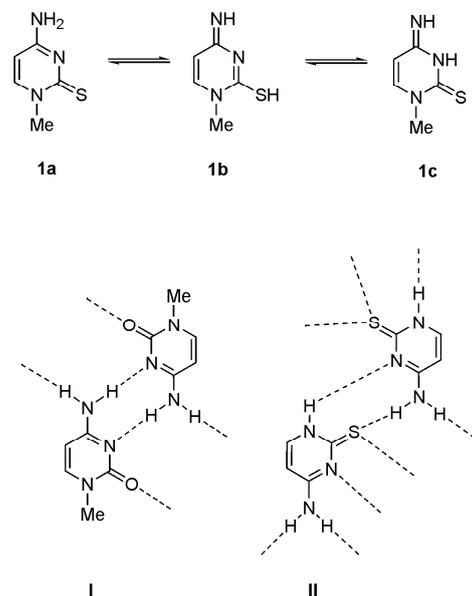
face-to-face, with the dinuclear molecule exhibiting C_2 symmetry in rough approximation. The distance between the heterocyclic ligands (3.4 Å) as well as the angle between the centroid-centroid vector and the ring normal (10.4°) indicate stabilization through π - π stacking [19]. The chelating coordination of the 1-methyl-2-thiocytosine ligands leads to the formation of strained four-membered rings (S2–Pt1–N4 66.0(1)°; S1–Pt2–N1 65.4(1)°), giving rise to greater deviations from the ideal octahedral coordination of the platinum atom. Moreover, the coordination of the sulfur atom to the platinum atom leads to a slight elongation of the S1–C7 and S2–C12 bonds (1.737(7)/1.726(7) Å) compared to the respective bond lengths in **1** (1.702(3)/1.692(3) Å). In accordance with the high *trans* influence of the methyl ligands [25] the bridging Pt–S bonds (2.501(2)–2.551(2) Å) are rather long (median: 2.490 Å, lower/upper quartile: 2.477/2.513 Å, for 41 observations [17]) but comparable to those in other dinuclear sulfur-bridged platinum(IV) complexes with *trans* methyl ligands (2.465(2)–2.551(1) Å) [26].

Inspection of the packing motif in crystals of **3** · 1.5 C₆H₆ reveals π - π interactions between the heterocyclic ring N1, N2, C7–C10 and one benzene ring (centroid-centroid distance: 3.6 Å; angle between the centroid-centroid vectors and the ring normals: 23.4°). Furthermore, there are cation-anion interactions formed through N–H...F and C–H...F hydrogen bonds, involving the fluorine atoms of the [BF₄][–] anions.

Conclusions

The possible tautomers of 1-methyl-2-thiocytosine, namely the thione-amino form (**1a**) as the most stable tautomer both in the gas and aqueous phase, the imino-thiol tautomer (**1b**) and the imino-thione tautomer (**1c**) are shown in Scheme 2 [8]. In the present investigations it has been demonstrated that the tautomer **1a** is also present in crystals of **1**. The same holds for the molecular structures of thiocytidine [27] and 2-thiocytosine [10], as shown by previous X-ray diffraction analyses.

The hydrogen bonding pattern in crystals of 1-MeSCy (**1**) was found to be very similar to that in 1-methylcytosine crystals (1-MeCy, see Formula **I** in Scheme 2) [13,14]. The oxygen analog also forms centrosymmetric dimers through two identical N4–H...N3' hydrogen bonds. These dimeric units are



Scheme 2.

connected through N4–H...O hydrogen bonds forming ribbons. In crystals of the non-methylated 2-thiocytosine a more complex hydrogen bonding pattern was observed (see Formula **II** in Scheme 2), which is completely different from that in 1-MeSCy (**1**). The central unit is also a dimer, but the two halves are linked unsymmetrically through N1–H...N3' and N4'–H...S hydrogen bonds. Further weaker N–H...N and N–H...S hydrogen bonds are connecting the dimers yielding ribbons [10].

Apart from the [PtMe₃(bpy)(1-MeSCy- κ S)][BF₄] complex reported by us [12], the new compound [(PtMe₃)₂(μ -1-MeSCy-1 κ N³,1:2 κ S²)₂][BF₄]₂ (**3**) is the first transition metal complex containing 1-methyl-2-thiocytosine ligands. By contrast, a large number of transition metal complexes with the oxygen analog 1-methylcytosine (1-MeCy) are known [28]. In its platinum(II) complexes predominantly N3 coordination is observed [29], and frequently an additional coordination of N4 of the monodeprotonated 1-methylcytosinato ligands to another Pt or Pd center gives rise to the formation of complexes having bridging μ -1-MeCy-1 κ N³,2 κ N⁴ ligands [30]. On the other hand, a chelating coordination through N3 and O (1-MeCy- κ N³, κ O ligands) in 1-methylcytosine metal complexes analogous to that in complex **3** is rare [31].

The heterocyclic rings in **3** have been found to be in a face-to-face arrangement, as in the neutral dinuclear complexes of the type [(PtMe₃)₂(μ -S[–]N-

$1\kappa N,1:2\kappa^2 S)_2]$ [26], with the geometrical parameters (Pt–S and C–S bond lengths, Pt1–S1...S2–Pt2 dihedral angle, π – π stacking) in the same order of magnitude. Thus, the synthesis of $[(PtMe_3)_2(\mu-1-MeSCy-1\kappa N^3,1:2\kappa^2 S)_2][BF_4]_2$ (**3**) has provided another example of the versatile coordination modes of thionucleobase models.

Experimental Section

General considerations

The synthesis of $[(PtMe_3)_2(\mu-1-MeSCy-1\kappa N^3,1:2\kappa^2 S)_2][BF_4]_2$ (**3**) was performed under argon using standard Schlenk techniques. Acetone was dried over phosphorus pentoxide. Benzene and diethyl ether were dried over Na benzophenone. All solvents were distilled prior to use. NMR spectra were obtained with Varian UNITY 500 and Gemini 2000 spectrometers using solvent signals (1H and ^{13}C -NMR spectroscopy) as internal references and $Na_2[PtCl_6]$ ($\delta(^{195}Pt) = 0$ ppm) as external reference. IR spectra were recorded on a Galaxy Mattson FT IR spectrometer, using KBr pellets. Microanalyses were performed by the University of Halle microanalytical laboratory using a CHNS-932 (LECO) instrument. The ESI mass spectrum was obtained on a Finnigan LCQ spectrometer (Thermo Electron Corp.) using a 10^{-5} M solution of the complex in acetone under the following conditions: flow 8 $\mu L/min$, positive ion polarity mode, ESI spray voltage 4.1 kV; capillary temperature 200 °C; capillary voltage 34 V; tube lens offset 10 V; sheath gas N_2 ; damping gas He. The CID experiments were carried out in the mass analyzer region with use of He as the collision gas and by applying a resonance excitation RF voltage (varying from 0 to 5 V, peak-to-peak). The masses, charge states and isotopic envelopes of the parent and fragment ions (CID) were established by applying the zoom-scan mode (high resolution < 0.2, 10 a. m. u. width). 1-Methyl-2-thiocytosine (**1**) [32] and $[(PtMe_3I)_4]$ [33] were prepared according to the literature. All other chemicals were purchased from commercial sources.

Spectroscopic characterization of 1-methyl-2-thiocytosine (**1**) and synthesis of $[(PtMe_3)_2(\mu-1-MeSCy-1\kappa N^3,1:2\kappa^2 S)_2][BF_4]_2$ (**3**)

1-Methyl-2-thiocytosine (**1**)

Yield: 1.2 g (70 %). – 1H -NMR (400 MHz, CD_3OD): $\delta = 7.73$ (d, $^3J_{H,H} = 7.3$ Hz, 1H, H6), 6.09 (d, $^3J_{H,H} = 7.3$ Hz, 1H, H5), 3.72 (s, 3H, NCH_3). – 1H -NMR (400 MHz, $[D_6]DMSO$): $\delta = 7.81$ (d, $^3J_{H,H} = 7.3$ Hz, 1H, H6), 7.48 (s, br, 1H, NH_2), 7.41 (s, br, 1H, NH_2), 5.98 (d, $^3J_{H,H} = 7.3$ Hz, 1H, H5), 3.59 (s, 3H, NCH_3). – ^{13}C -NMR (100 MHz, $[D_6]DMSO$): $\delta = 180.6$ (C2), 160.5 (C4), 146.8 (C6), 97.0

Table 5. Crystal data, data collection and refinement parameters of 1-MeSCy (**1**) and $[(PtMe_3)_2(\mu-1-MeSCy-1\kappa N^3,1:2\kappa^2 S)_2][BF_4]_2$ (**3** · 1.5 C_6H_6).

	1	3 · 1.5 C_6H_6
Empirical formula	$C_5H_7N_3S$	$C_{25}H_{41}B_2F_8N_6Pt_2S_2$
Formula weight	141.20	1053.56
Crystal system/	monoclinic	monoclinic
Space group	$P2_1/n$	$P2_1/c$
Z	8	4
a, Å	5.9919(8)	10.2340(5)
b, Å	19.343(3)	35.854(2)
c, Å	11.293(7)	9.9832(5)
β , deg	99.14(1)	107.701(6)
V, Å ³	1292.3(8)	3489.7(3)
ρ , g cm ⁻³	1.44	2.01
$\mu(MoK\alpha)$, mm ⁻¹	0.4	8.2
F(000), e	592	2012
Scan range, deg	$2.11 \leq \theta \leq 25.03$	$2.09 \leq \theta \leq 26.02$
Reciprocal lattice segment hkl	$\pm 7, +23, -8 \rightarrow 13$	$\pm 12, \pm 44, -11 \rightarrow 12$
Refl. collected	2473	18975
Refl. independent / R_{int}	2252 / 0.0580	6517 / 0.0675
Data / parameters	2252 / 220	6517 / 413
R_1/wR_2 [$I \geq 2\sigma(I)$]	0.0407 / 0.0943	0.0338 / 0.0670
R_1/wR_2 (all data)	0.0602 / 0.1080	0.0581 / 0.0732
Goodness-of-fit on F^2	1.094	0.934
Largest diff. peak / hole, eÅ ⁻³	0.20 / -0.18	1.09 / -0.78

(C5), 43.3 (C1). – $C_5H_7N_3S$ (141.04): calcd. C 42.54, H 5.00, N 29.79; found C 42.55, H 5.29, N 29.31.

$[(PtMe_3)_2(\mu-1-MeSCy-1\kappa N^3,1:2\kappa^2 S)_2][BF_4]_2$ (**3**)

A suspension of $[(PtMe_3I)_4]$ (50.0 mg, 0.04 mmol) and $Ag[BF_4]$ (27.0 mg, 0.14 mmol) in acetone (10 mL) was stirred for 30 min in the absence of light. Silver iodide was removed by filtration, and the clear, colorless filtrate was added directly to 1-methyl-2-thiocytosine (19.3 mg, 0.14 mol). After stirring for 2 h the volume was reduced *in vacuo* to 1 mL, and ether (3 mL) was added. The colorless precipitate was isolated, washed with pentane (2×2 mL) and dried *in vacuo*. Yield: 72 mg (56 %). IR (KBr): $\nu = 3454$ m, 3352 m, 3111 w, 2961 w, 2899 m, 1792 w, 1650 s, 1537 m, 1506 s, 1400 m, 1368 m, 1215 m, 1081 s, 821 w cm^{-1} . – 1H -NMR (500 MHz, CD_3OD , r.t.): $\delta = 7.98$ (d, $^3J_{H,H} = 7.5$ Hz, 2H, $H6/H6'$), 6.53 (d, $^3J_{H,H} = 7.5$ Hz, $^4J_{Pt,H} = 11.6$ Hz, 2H, $H5/H5'$), 3.64 (s, 6H, NCH_3 , NCH_3'), 1.22 (s+d, $^2J_{Pt,H} = 75.5$ Hz, 18H, $Pt(CH_3)_3$). – 1H -NMR (500 MHz, CD_3OD , -50 °C): $\delta = 8.05$ (d, $^3J_{H,H} = 7.5$ Hz, 2H, $H6/H6'$), 6.53 (d, $^3J_{H,H} = 7.5$ Hz, 2H, $H5/H5'$), 3.63 (s, 6H, NCH_3 , NCH_3'), 1.194 (s+d, $^2J_{Pt,H} = 81.5$ Hz, 6H, $PtCH_3$), 1.189 (s+d, $^2J_{Pt,H} = 74.7$ Hz, 6H, $PtCH_3$). – ^{13}C -NMR (125 MHz, CD_3OD): $\delta = 184.4$ (C2), 160.4 (C4), 147.8 (C6), 101.8 (C5), 40.7 (NCH_3), -7.3 (s+d, br, $Pt(CH_3)_3$). – ^{195}Pt -NMR (107 MHz, CD_3OD): $\delta = -2318.4$. – MS ((+)-ESI): m/z (%) = 761 (62) $[(PtMe_3)_2(1-MeSCy)(1-MeSCy-H)]^+$,

381 (100) [(PtMe₃)(1-MeSCy)]⁺ · C₁₆H₃₄B₂F₈N₆S₂Pt₂ (938.16): calcd. C 20.47, H 3.65, N 8.96; found C 20.13, H 4.13, N 8.74.

X-Ray crystallography

Single crystals of **1** and **3** · 1.5 C₆H₆, suitable for X-ray diffraction measurements, were obtained by recrystallization from ethanol (**1**) and acetone/benzene (**3** · 1.5 C₆H₆). Intensity data were collected on a STADI (**1**) and a Stoe IPDS diffractometer (**3** · 1.5 C₆H₆) with MoK_α radiation (λ = 0.71073 Å, graphite monochromator) at 293(2) K (**1**) and 220(2) K (**3** · 1.5 C₆H₆). A summary of the crystallographic data, the data collection parameters and the refinement parameters is given in Table 5. A numerical absorption correction was applied for **3** · 1.5 C₆H₆ (T_{min}/T_{max} = 0.24 / 0.58). The structures were solved by Direct Methods with SHELXS-97 [34] and refined using full-matrix least-squares routines against F² with SHELXL-97 [34]. Non-hydrogen atoms were refined with anisotropic displacement parameters. Hydrogen atoms in 1-MeSCy (**1**) were found in the difference Fourier map and refined freely, whereas the hydrogen atoms in **3** · 1.5 C₆H₆ were positioned geometrically and refined with isotropic displacement parameters according to the "riding model".

CCDC 761534 and CCDC 761535 contain the supplementary crystallographic data for compounds **1** and **3** · 1.5

C₆H₆. These data can be obtained free of charge via www.ccdc.cam.ac.uk/data_request/cif.

Quantum-chemical calculations

All DFT calculations were carried out by the GAUSSIAN03 program package [35] using the hybrid functional B3LYP [36] and the basis sets 6-31++G(d,p) as implemented in the GAUSSIAN program. All systems were fully optimized. For the monomeric molecule no symmetry restrictions were applied, whereas the dimeric and tetrameric molecules were calculated in C_i symmetry. The resulting geometries were characterized as equilibrium structures by the analysis of the force constants of the normal vibrations. Basis set superposition errors (BSSE) were estimated with counterpoise-type calculations [37].

Supplementary Information

Tables of Cartesian coordinates of atom positions calculated for the equilibrium structures of the monomer **1m**, the hydrogen-bonded dimer **1d** and tetramer **1t** (available online only).

Acknowledgement

Gifts of chemicals by Merck (Darmstadt) are gratefully acknowledged.

- [1] J. A. Carbon, L. Hung, D. S. Jones, *Proc. Natl. Acad. Sci. U. S. A.* **1965**, *53*, 979.
- [2] M. N. Lipsett, *J. Biol. Chem.* **1965**, *240*, 3975.
- [3] J. Carbon, H. David, M. H. Studier, *Science* **1968**, *161*, 1146.
- [4] D. H. Gauss, M. Sprinzl, *Nucleic Acids Res.* **1983**, *11*, r1.
- [5] Y. Yamada, M. Saneyoshi, S. Nishimura, H. Ishikura *FEBS Lett.* **1970**, *7*, 207.
- [6] J. G. Contreras, J. B. Alderete, *J. Phys. Org. Chem.* **1995**, *8*, 395.
- [7] Y. Podolyan, L. Gorb, A. Blue, J. Leszczynski, *J. Mol. Struct. (Theochem.)* **2001**, *549*, 101.
- [8] P. Ü. Cıvcır, *J. Phys. Org. Chem.* **2001**, *14*, 171.
- [9] H. Rostkowska, M. J. Nowak, L. Lapinski, M. Bretner, T. Kulikowski, A. Lés, L. Adamowicz, *Spectrochim. Acta Part A* **1993**, *49*, 551.
- [10] S. Furberg, L. H. Jensen, *Acta Crystallogr.* **1970**, *B26*, 1260.
- [11] a) B. T. Khan, S. M. Zakeeruddin, *Trans. Met. Chem.* **1991**, *16*, 119; b) B. T. Khan, T. K. Annapoorna, S. Shamsuddin, K. Najmuddin, *Polyhedron* **1992**, *11*, 2109; c) J. Jolley, W. I. Cross, R. G. Pritchard, C. A. McAuliffe, K. B. Nolan, *Inorg. Chim. Acta* **2001**, *315*, 36; d) T. E. Chávez-Gil, E. Meléndez, *Inorg. Chim. Acta* **2004**, *357*, 1092; e) E. Meléndez, M. Marrero, C. Rivera, E. Hernandez, A. Segal, *Inorg. Chim. Acta* **2000**, *298*, 178; f) J. D. E. T. Wilton-Ely, M. Wang, D. M. Benoit, D. A. Tocher, *Eur. J. Inorg. Chem.* **2006**, 3068; g) C.-L. Ma, Y. Shi, Q.-F. Zhang, Q. Jiang, *Polyhedron* **2005**, *24*, 1109.
- [12] a) C. Vetter, C. Wagner, G. N. Kaluđerović, R. Paschke, D. Steinborn, *Inorg. Chim. Acta* **2009**, *362*, 189; b) M. W. Whitehouse, P. D. Cookson, G. Siasios, E. R. T. Tiekink, *Met.-Based Drugs* **1998**, *5*, 245; c) E. R. T. Tiekink, P. D. Cookson, B. M. Linahan, L. K. Webster, *Met.-Based Drugs* **1994**, *1*, 299; d) L. K. Webster, S. Rainone, E. Horn, E. R. T. Tiekink, *Met.-Based Drugs* **1996**, *3*, 63.
- [13] F. S. Mathews, A. Rich, *Nature* **1964**, *201*, 179.
- [14] M. Rossi, T. J. Kistenmacher, *Acta Crystallogr.* **1977**, *B33*, 3962.
- [15] S. C. Nyburg, C. H. Faerman, L. Prasad, *Acta Crystallogr.* **1987**, *B43*, 106.
- [16] S. C. Nyburg, C. H. Faerman, *Acta Crystallogr.* **1985**, *B41*, 274.
- [17] Cambridge Structural Database (CSD) Version 5.30 2008, University Chemical Laboratory, Cambridge (England).

- [18] G. A. Jeffrey, W. Saenger, *Hydrogen Bonding in Biological Structures*, Springer Verlag, Berlin, 1994, pp. 132.
- [19] C. Janiak, *J. Chem. Soc., Dalton Trans.* **2000**, 3885.
- [20] W. Koch, M. C. Holthausen, *A Chemist's Guide to Density Functional Theory*, Wiley-VCH, Weinheim **2000**, p. 213.
- [21] M. W. Feyereisen, D. Feller, D. A. Dixon, *J. Phys. Chem.* **1996**, *100*, 2993.
- [22] a) J. Emsley, *Chem. Soc. Rev.* **1980**, *9*, 91; b) G. A. Jeffrey, *An Introduction to Hydrogen Bonding*, Oxford University Press, Oxford, 1997.
- [23] H. Junicke, C. Bruhn, D. Ströhl, R. Kluge, D. Steinborn, *Inorg. Chem.* **1998**, *37*, 4603.
- [24] F. Pichierri, D. Holthenrich, E. Zangrando, B. Lippert, L. Randaccio, *J. Biol. Inorg. Chem.* **1996**, *1*, 439.
- [25] a) T. G. Appleton, H. C. Clark, L. E. Manzer, *Coord. Chem. Rev.* **1973**, *10*, 335; b) C. Vetter, C. Wagner, J. Schmidt, D. Steinborn, *Inorg. Chim. Acta* **2006**, *359*, 4326.
- [26] C. Vetter, G. N. Kaluderović, R. Paschke, S. Gómez-Ruiz, D. Steinborn, *Polyhedron* **2009**, *28*, 3699.
- [27] G. H.-Y. Lin, M. Sundaralingam, S. K. Arora, *J. Am. Chem. Soc.* **1971**, *93*, 1235.
- [28] B. Lippert, *Coord. Chem. Rev.* **2000**, *200–202*, 487.
- [29] a) W.-Z. Shen, G. Trötscher-Kaus, B. Lippert, *Dalton Trans.* **2009**, 8203; b) K. Butsch, S. Elmas, N. S. Gupta, R. Gust, F. Heinrich, A. Klein, Y. v. Mering, M. Neugebauer, I. Ott, M. Schäfer, H. Scherer, T. Schurr, *Organometallics* **2009**, *28*, 3906; c) B. Longato, D. Montagner, E. Zangrando, *Dalton Trans.* **2009**, 2400; d) P. J. Sanz Miguel, P. Lax, B. Lippert, *J. Inorg. Biochem.* **2006**, *100*, 980.
- [30] a) G. Kampf, P. J. Sanz Miguel, M. M. Cerdà, M. Willermann, B. Lippert, A. Schneider, *Chem. Eur. J.* **2008**, *14*, 6882; b) G. Kampf, M. Willermann, E. Zangrando, L. Randaccio, B. Lippert, *Chem. Commun.* **2001**, 747; c) F. Pichierri, E. Chiarparin, E. Zangrando, L. Randaccio, D. Holthenrich, B. Lippert, *Inorg. Chim. Acta* **1997**, *264*, 109; d) T. Wienkoetter, M. Sabat, G. Fusch, B. Lippert, *Inorg. Chem.* **1995**, *34*, 1022.
- [31] a) T. F. Mastropietro, D. Armentano, N. Marino, G. De Munno, J. Anastassopoulou, T. Theophanides, *Cryst. Growth Des.* **2007**, *7*, 609; b) G. Valle, R. Ettore, V. Peruzzo, *Acta Crystallogr.* **1996**, *C52*, 626.
- [32] D. J. Brown, B. T. England, *J. Chem. Soc. C* **1971**, 2507.
- [33] a) W. J. Pope, S. J. Peachey, *Proc. Chem. Soc.* **1907**, *23*, 86; b) J. C. Baldwin, W. C. Kaska, *Inorg. Chem.* **1975**, *14*, 2020.
- [34] G. M. Sheldrick, SHELXS/L-97, Programs for Crystal Structure Determination, University of Göttingen, Göttingen (Germany) **1997**. See also: G. M. Sheldrick, *Acta Crystallogr.* **1990**, *A46*, 467; *ibid.* **2008**, *A64*, 112.
- [35] M. J. Frisch, G. W. Trucks, H. B. Schlegel, G. E. Scuseria, M. A. Robb, J. R. Cheeseman, J. A. Montgomery, Jr., T. Vreven, K. N. Kudin, J. C. Burant, J. M. Millam, S. S. Iyengar, J. Tomasi, V. Barone, B. Menonucci, M. Cossi, G. Scalmani, N. Rega, G. A. Petersson, H. Nakatsuji, M. Hada, M. Ehara, K. Toyota, R. Fukuda, J. Hasegawa, M. Ishida, T. Nakajima, Y. Honda, O. Kitao, H. Nakai, M. Klene, X. Li, J. E. Knox, H. P. Hratchian, J. B. Cross, V. Bakken, C. Adamo, J. Jaramillo, R. Gomperts, R. E. Stratmann, O. Yazyev, A. J. Austin, R. Cammi, C. Pomelli, J. W. Ochterski, P. Y. Ayala, K. Morokuma, G. A. Voth, P. Salvador, J. J. Dannenberg, V. G. Zakrzewski, S. Dapprich, A. D. Daniels, M. C. Strain, O. Farkas, D. K. Malick, A. D. Rabuck, K. Raghavachari, J. B. Foresman, J. V. Ortiz, Q. Cui, A. G. Baboul, S. Clifford, J. Cioslowski, B. B. Stefanov, G. Liu, A. Liashenko, P. Piskorz, I. Komaromi, R. L. Martin, D. J. Fox, T. Keith, M. A. Al-Laham, C. Y. Peng, A. Nanayakkara, M. Challacombe, P. M. W. Gill, B. Johnson, W. Chen, M. W. Wong, C. Gonzalez, J. A. Pople, GAUSSIAN 03 (revision C.02), Gaussian, Inc., Wallingford, CT (USA) **2004**.
- [36] a) A. D. Becke, *Phys. Rev. A* **1988**, *38*, 3098; b) A. D. Becke, *J. Chem. Phys.* **1993**, *98*, 5648; c) C. Lee, W. Yang, R. G. Parr, *Phys. Rev. B* **1988**, *37*, 785; d) P. J. Stephens, F. J. Devlin, C. F. Chabalowski, M. J. Frisch, *J. Phys. Chem.* **1994**, *98*, 11623.
- [37] S. F. Boys, F. Bernardi, *Mol. Phys.* **1970**, *19*, 553.

metal-organic compounds

Acta Crystallographica Section E

Structure Reports

Online

ISSN 1600-5368

(Acetato- κ O)(2,2'-bipyridine- κ^2 N,N')-trimethylplatinum(IV) monohydrate

Cornelia Vetter, Christoph Wagner and Dirk Steinborn*

Anorganische Chemie, Institut für Chemie, Martin-Luther-Universität, Kurt-Mothes-Strasse 2, Halle-Wittenberg, D-06120 Halle, Germany
Correspondence e-mail: dirk.steinborn@chemie.uni-halle.de

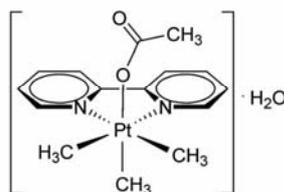
Received 25 January 2010; accepted 8 February 2010

Key indicators: single-crystal X-ray study; $T = 293$ K; mean $\sigma(\text{C}-\text{C}) = 0.019$ Å; R factor = 0.040; wR factor = 0.119; data-to-parameter ratio = 14.7.

In the title hydrate, $[\text{Pt}(\text{CH}_3)_3(\text{CH}_3\text{COO})(\text{C}_{10}\text{H}_8\text{N}_2)] \cdot \text{H}_2\text{O}$, the Pt^{IV} atom exhibits a distorted octahedral coordination geometry built up by three methyl ligands in a facial arrangement, a bipyridine ligand and a monodentately bound acetate ligand. In the crystal structure, intermolecular $\text{O}-\text{H} \cdots \text{O}$ hydrogen bonds are observed between the water molecule and the platinum complex, which link the molecules into chains along the c axis.

Related literature

For ligand-substitution reactions of platinum complexes, see: Vetter *et al.* (2006); Clegg *et al.* (1972); Lindner *et al.* (2008); Steinborn & Junicke (2000). For a description of the Cambridge Structural Database, see: Allen (2002).



Experimental

Crystal data

$[\text{Pt}(\text{CH}_3)_3(\text{C}_2\text{H}_5\text{O}_2)(\text{C}_{10}\text{H}_8\text{N}_2)] \cdot \text{H}_2\text{O}$
 $M_r = 473.44$
 Monoclinic, $P2_1/c$
 $a = 10.972$ (3) Å
 $b = 13.455$ (3) Å
 $c = 13.768$ (3) Å
 $\beta = 125.05$ (3)°
 $V = 1663.9$ (8) Å³
 $Z = 4$
 Mo $K\alpha$ radiation
 $\mu = 8.44$ mm⁻¹
 $T = 293$ K
 $0.48 \times 0.34 \times 0.24$ mm

Data collection

Stoe STADI-IV diffractometer
 Absorption correction: ψ scan
 (*X-RED32*; Stoe & Cie, 1996)
 $T_{\text{min}} = 0.031$, $T_{\text{max}} = 0.089$
 4494 measured reflections

2931 independent reflections
 2455 reflections with $I > 2\sigma(I)$
 $R_{\text{int}} = 0.031$
 2 standard reflections every 60 min
 intensity decay: random, $\pm 5\%$

Refinement

$R[F^2 > 2\sigma(F^2)] = 0.040$
 $wR(F^2) = 0.119$
 $S = 1.06$
 2931 reflections
 199 parameters
 2 restraints

H atoms treated by a mixture of independent and constrained refinement
 $\Delta\rho_{\text{max}} = 1.61$ e Å⁻³
 $\Delta\rho_{\text{min}} = -1.79$ e Å⁻³

Table 1

Selected geometric parameters (Å, °).

C1—Pt1	2.036 (10)	N2—Pt1	2.152 (7)
C2—Pt1	2.041 (11)	O1—Pt1	2.168 (6)
C3—Pt1	2.032 (9)		
N1—Pt1	2.161 (7)		
C1—Pt1—C2	85.1 (5)	C2—Pt1—N1	98.2 (4)
C1—Pt1—N2	99.9 (4)	N2—Pt1—N1	76.7 (3)
C2—Pt1—N2	174.8 (5)	C3—Pt1—O1	176.2 (4)
C1—Pt1—N1	176.5 (4)		

Table 2

Hydrogen-bond geometry (Å, °).

$D-H \cdots A$	$D-H$	$H \cdots A$	$D \cdots A$	$D-H \cdots A$
O3—H22 \cdots O1	0.88 (11)	1.96 (11)	2.836 (12)	172 (15)
O3—H21 \cdots O2 ⁱ	0.85 (9)	1.96 (10)	2.810 (14)	177 (11)

Symmetry code: (i) $x, -y + \frac{1}{2}, z + \frac{1}{2}$.

Data collection: *STADI4* (Stoe & Cie, 1996); cell refinement: *STADI4*; data reduction: *STADI4*; program(s) used to solve structure: *SHELXS97* (Sheldrick, 2008); program(s) used to refine structure: *SHELXL97* (Sheldrick, 2008); molecular graphics: *DIAMOND* (Brandenburg, 2001); software used to prepare material for publication: *SHELXL97*.

Supplementary data and figures for this paper are available from the IUCr electronic archives (Reference: TK2621).

References

- Allen, F. H. (2002). *Acta Cryst.* **B58**, 380–388.
 Brandenburg, K. (2001). *DIAMOND*. Crystal Impact GbR, Bonn, Germany.
 Clegg, D. E., Hall, J. R. & Swile, G. A. (1972). *J. Organomet. Chem.* **38**, 403–420.
 Lindner, R., Kaluerović, G. N., Paschke, R., Wagner, C. & Steinborn, D. (2008). *Polyhedron*, **27**, 914–922.
 Sheldrick, G. M. (2008). *Acta Cryst.* **A64**, 112–122.
 Steinborn, D. & Junicke, H. (2000). *Chem. Rev.* **100**, 4283–4317.
 Stoe & Cie (1996). *STADI4* and *X-RED32*. Stoe & Cie GmbH, Darmstadt, Germany.
 Vetter, C., Wagner, C., Schmidt, J. & Steinborn, D. (2006). *Inorg. Chim. Acta*, **359**, 4326–4334.

Acta Cryst. (2010). E66, m286 [doi:10.1107/S160053681000499X]

(Acetato- κO)(2,2'-bipyridine- $\kappa^2 N, N'$)trimethylplatinum(IV) monohydrate

C. Vetter, C. Wagner and D. Steinborn

Comment

Due to the low-spin d^6 electron configuration of platinum(IV), ligand substitution reactions of their complexes may be hampered. Starting from complexes having a PtMe_3 unit (Vetter *et al.*, 2006; Clegg *et al.*, 1972; Lindner *et al.*, 2008), substitution reactions were found to proceed smoothly even with weak donors (Steinborn & Junicke, 2000) because the leaving ligand is additionally activated by the high *trans* effect exerted by the methyl ligand.

The asymmetric unit of the title hydrate comprises a neutral platinum complex, $[\text{PtMe}_3(\text{OAc-}\kappa O)(\text{bpy})]$, and a water molecule. The primary coordination sphere of the platinum atom is built up by three methyl ligands in *facial* binding fashion, a bipyridine ligand and a monodentately bound acetato ligand. As expected for Pt(IV) complexes, an octahedral coordination geometry was found, which is distorted due to the restricted bite of the 2,2'-bipyridine ligand [N1—Pt1—N2 76.7 (3) $^\circ$]; the other angles between *cis* arranged ligands are between 85.1 (5) and 99.9 (4) $^\circ$. Due to the high *trans* influence of the methyl ligands the Pt1—O1 bond was found to be relatively long (2.168 (6) Å) compared to those of other carboxylato platinum(IV) [median: 2.013, lower/upper quartile: 2.001/2.044 Å, 496 observations taken from the CSD, version 5.30 (Allen, 2002)]. In the crystal structure quite strong intermolecular O—H \cdots O hydrogen bonds were found in which the water molecules act as hydrogen donors and the oxygen atoms of acetato ligand as hydrogen acceptors (Table 1). Due to these hydrogen bonds the molecules are linked in infinite chains along the *c* axis.

Experimental

Under anaerobic conditions $[(\text{PtMe}_3\text{I})_4]$ (50 mg, 0.03 mmol) and AgOAc (23 mg, 0.14 mmol) were stirred in acetone (10 ml) for 15 h in the absence of light. The precipitated AgI was filtered off and the solvent was reduced *in vacuo* to 3 ml. Then *n*-pentane was added and the white precipitate was collected by filtration, washed with *n*-pentane (2×1 ml) and recrystallized from chloroform.

Refinement

The water-H atoms were found in a difference map and refined with each O—H distance restrained to 0.85 (1) Å. All other H atoms were positioned geometrically and allowed to ride on the respective parent atoms with C—H = 0.93–0.96 Å [$U_{\text{iso}}(\text{H}) = 1.2 U_{\text{eq}}(\text{C})$]. The maximum and minimum residual electron density peaks of 1.61 and -1.79 e Å $^{-3}$, respectively, were located 1.19 Å and 1.21 Å from the Pt1 atom.

supplementary materials

Figures

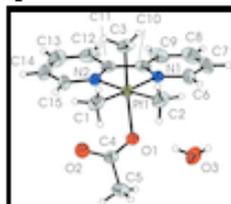


Fig. 1. Structure of the asymmetric unit of the title hydrate $[\text{PtMe}_3(\text{OAc-}\kappa\text{O})(\text{bpy})] \cdot \text{H}_2\text{O}$. Displacement ellipsoids are drawn at the 30% probability level and the H atoms are shown as small spheres of arbitrary radii.

(Acetato- κO)(2,2'-bipyridine- $\kappa^2\text{N},\text{N}'$)trimethylplatinum(IV) monohydrate

Crystal data

$[\text{Pt}(\text{CH}_3)_3(\text{C}_2\text{H}_3\text{O}_2)(\text{C}_{10}\text{H}_8\text{N}_2)] \cdot \text{H}_2\text{O}$

$M_r = 473.44$

Monoclinic, $P2_1/c$

Hall symbol: $-P\ 2_1/c$

$a = 10.972(3)\ \text{\AA}$

$b = 13.455(3)\ \text{\AA}$

$c = 13.768(3)\ \text{\AA}$

$\beta = 125.05(3)^\circ$

$V = 1663.9(8)\ \text{\AA}^3$

$Z = 4$

$F(000) = 912$

$D_x = 1.890\ \text{Mg m}^{-3}$

Mo $K\alpha$ radiation, $\lambda = 0.71073\ \text{\AA}$

Cell parameters from 26 reflections

$\theta = 15.1\text{--}25.2^\circ$

$\mu = 8.44\ \text{mm}^{-1}$

$T = 293\ \text{K}$

Block, orange

$0.48 \times 0.34 \times 0.24\ \text{mm}$

Data collection

Stoe STADI-IV
diffractometer

Radiation source: fine-focus sealed tube
graphite

$\omega/2\theta$ scans

Absorption correction: ψ scan
(X-RED32; Stoe & Cie, 1996)

$T_{\text{min}} = 0.031$, $T_{\text{max}} = 0.089$

4494 measured reflections

2931 independent reflections

2455 reflections with $I > 2\sigma(I)$

$R_{\text{int}} = 0.031$

$\theta_{\text{min}} = 25.0^\circ$, $\theta_{\text{max}} = 2.3^\circ$

$h = -13 \rightarrow 13$

$k = -16 \rightarrow 0$

$l = -13 \rightarrow 16$

2 standard reflections every 60 min

intensity decay: random, $\pm 5\%$

Refinement

Refinement on F^2

Least-squares matrix: full

$R[F^2 > 2\sigma(F^2)] = 0.040$

$wR(F^2) = 0.119$

Secondary atom site location: difference Fourier map

Hydrogen site location: inferred from neighbouring sites

H atoms treated by a mixture of independent and constrained refinement

$w = 1/[\sigma^2(F_o^2) + (0.0676P)^2 + 4.3682P]$

where $P = (F_o^2 + 2F_c^2)/3$

sup-2

$S = 1.06$	$(\Delta/\sigma)_{\max} = 0.001$
2931 reflections	$\Delta\rho_{\max} = 1.61 \text{ e \AA}^{-3}$
199 parameters	$\Delta\rho_{\min} = -1.79 \text{ e \AA}^{-3}$
2 restraints	Extinction correction: SHELXL (Sheldrick, 2008), $F_c^* = kFc[1 + 0.001xFe^2\lambda^3/\sin(2\theta)]^{-1/4}$
0 constraints	Extinction coefficient: 0.0018 (3)
Primary atom site location: structure-invariant direct methods	

Special details

Geometry. All esds (except the esd in the dihedral angle between two l.s. planes) are estimated using the full covariance matrix. The cell esds are taken into account individually in the estimation of esds in distances, angles and torsion angles; correlations between esds in cell parameters are only used when they are defined by crystal symmetry. An approximate (isotropic) treatment of cell esds is used for estimating esds involving l.s. planes.

Refinement. Refinement of F^2 against ALL reflections. The weighted R -factor wR and goodness of fit S are based on F^2 , conventional R -factors R are based on F , with F set to zero for negative F^2 . The threshold expression of $F^2 > \sigma(F^2)$ is used only for calculating R -factors(gt) etc. and is not relevant to the choice of reflections for refinement. R -factors based on F^2 are statistically about twice as large as those based on F , and R -factors based on ALL data will be even larger.

Fractional atomic coordinates and isotropic or equivalent isotropic displacement parameters (\AA^2)

	x	y	z	$U_{\text{iso}}^*/U_{\text{eq}}$
C1	-0.0620 (12)	0.7592 (8)	0.1850 (9)	0.072 (3)
H1	-0.0535	0.7673	0.1198	0.087*
H3	-0.1629	0.7714	0.1584	0.087*
H2	-0.0345	0.6926	0.2150	0.087*
C2	-0.0048 (12)	0.7967 (10)	0.4045 (11)	0.081 (3)
H6	0.0412	0.8284	0.4804	0.097*
H5	0.0170	0.7269	0.4158	0.097*
H4	-0.1106	0.8063	0.3591	0.097*
C3	-0.0935 (11)	0.9574 (8)	0.2409 (10)	0.069 (3)
H9	-0.0603	1.0175	0.2869	0.083*
H8	-0.1760	0.9304	0.2387	0.083*
H7	-0.1241	0.9718	0.1616	0.083*
C4	0.3091 (10)	0.7018 (7)	0.3608 (9)	0.058 (2)
C5	0.4295 (13)	0.6271 (9)	0.4412 (12)	0.081 (4)
H11	0.4636	0.5950	0.3986	0.098*
H10	0.3899	0.5782	0.4667	0.098*
H12	0.5113	0.6608	0.5091	0.098*
C6	0.2491 (12)	0.9787 (10)	0.5540 (9)	0.077 (3)
H13	0.2051	0.9358	0.5784	0.093*
C7	0.3426 (14)	1.0548 (11)	0.6304 (10)	0.092 (4)
H14	0.3583	1.0638	0.7038	0.110*
C8	0.4096 (15)	1.1153 (11)	0.5953 (15)	0.098 (5)
H15	0.4738	1.1652	0.6454	0.117*
C9	0.3823 (12)	1.1025 (9)	0.4859 (13)	0.085 (4)

Anhang

supplementary materials

H16	0.4276	1.1437	0.4611	0.102*
C10	0.2869 (9)	1.0279 (7)	0.4123 (9)	0.058 (2)
C11	0.2542 (10)	1.0116 (7)	0.2937 (9)	0.057 (2)
C12	0.3080 (12)	1.0709 (9)	0.2434 (14)	0.085 (4)
H17	0.3648	1.1271	0.2829	0.102*
C13	0.2752 (16)	1.0446 (13)	0.1327 (15)	0.098 (5)
H18	0.3103	1.0832	0.0975	0.117*
C14	0.1935 (17)	0.9642 (12)	0.0776 (12)	0.091 (4)
H19	0.1719	0.9459	0.0041	0.109*
C15	0.1410 (13)	0.9078 (9)	0.1301 (9)	0.069 (3)
H20	0.0846	0.8514	0.0911	0.083*
N1	0.2221 (8)	0.9665 (5)	0.4471 (6)	0.0486 (16)
N2	0.1687 (8)	0.9318 (6)	0.2344 (6)	0.0525 (17)
O1	0.2551 (7)	0.7497 (5)	0.4062 (6)	0.0615 (17)
O2	0.2727 (10)	0.7105 (7)	0.2563 (8)	0.089 (2)
O3	0.4338 (10)	0.7587 (8)	0.6577 (9)	0.088 (3)
H21	0.382 (12)	0.767 (9)	0.685 (10)	0.07 (4)*
H22	0.379 (15)	0.763 (12)	0.580 (10)	0.12 (6)*
Pt1	0.07572 (3)	0.85719 (3)	0.31606 (3)	0.04758 (19)

Atomic displacement parameters (\AA^2)

	U^{11}	U^{22}	U^{33}	U^{12}	U^{13}	U^{23}
C1	0.077 (7)	0.052 (6)	0.069 (7)	-0.020 (5)	0.031 (6)	0.003 (5)
C2	0.070 (6)	0.095 (9)	0.094 (8)	0.007 (6)	0.057 (6)	0.031 (7)
C3	0.057 (5)	0.067 (7)	0.075 (7)	0.015 (5)	0.033 (5)	0.015 (5)
C4	0.058 (5)	0.050 (5)	0.066 (6)	0.001 (4)	0.036 (5)	0.008 (5)
C5	0.071 (7)	0.076 (8)	0.100 (9)	0.017 (6)	0.050 (7)	0.004 (6)
C6	0.075 (7)	0.102 (9)	0.054 (6)	0.018 (6)	0.036 (5)	-0.005 (6)
C7	0.079 (8)	0.108 (11)	0.054 (6)	0.023 (8)	0.018 (6)	-0.027 (7)
C8	0.069 (8)	0.082 (9)	0.107 (12)	-0.003 (6)	0.030 (8)	-0.035 (8)
C9	0.055 (6)	0.068 (7)	0.103 (10)	-0.002 (5)	0.029 (6)	-0.020 (7)
C10	0.043 (4)	0.049 (5)	0.073 (6)	0.009 (4)	0.027 (4)	-0.003 (4)
C11	0.055 (5)	0.055 (6)	0.072 (6)	0.018 (4)	0.042 (5)	0.017 (5)
C12	0.066 (6)	0.070 (7)	0.134 (12)	0.007 (6)	0.067 (7)	0.031 (8)
C13	0.095 (9)	0.120 (13)	0.116 (12)	0.016 (8)	0.083 (9)	0.047 (10)
C14	0.106 (9)	0.121 (12)	0.079 (8)	0.039 (9)	0.072 (8)	0.037 (8)
C15	0.088 (7)	0.078 (7)	0.058 (6)	0.014 (6)	0.051 (6)	0.003 (5)
N1	0.048 (4)	0.051 (4)	0.048 (4)	0.009 (3)	0.029 (3)	0.006 (3)
N2	0.056 (4)	0.058 (4)	0.052 (4)	0.008 (4)	0.036 (3)	0.009 (4)
O1	0.063 (4)	0.062 (4)	0.055 (4)	0.014 (3)	0.032 (3)	0.006 (3)
O2	0.108 (6)	0.095 (6)	0.084 (6)	0.025 (5)	0.067 (5)	0.014 (5)
O3	0.070 (5)	0.118 (8)	0.068 (5)	-0.001 (5)	0.035 (5)	0.014 (5)
Pt1	0.0491 (2)	0.0487 (3)	0.0473 (3)	0.00074 (14)	0.02902 (18)	0.00514 (14)

Geometric parameters (\AA , $^\circ$)

C1—Pt1	2.036 (10)	C7—H14	0.9300
C1—H1	0.9600	C8—C9	1.37 (2)

sup-4

supplementary materials

C1—H3	0.9600	C8—H15	0.9300
C1—H2	0.9600	C9—C10	1.382 (15)
C2—Pt1	2.041 (11)	C9—H16	0.9300
C2—H6	0.9600	C10—N1	1.345 (13)
C2—H5	0.9600	C10—C11	1.474 (15)
C2—H4	0.9600	C11—N2	1.349 (13)
C3—Pt1	2.032 (9)	C11—C12	1.391 (15)
C3—H9	0.9600	C12—C13	1.40 (2)
C3—H8	0.9600	C12—H17	0.9300
C3—H7	0.9600	C13—C14	1.33 (2)
C4—O2	1.258 (13)	C13—H18	0.9300
C4—O1	1.259 (12)	C14—C15	1.381 (17)
C4—C5	1.518 (14)	C14—H19	0.9300
C5—H11	0.9600	C15—N2	1.326 (12)
C5—H10	0.9600	C15—H20	0.9300
C5—H12	0.9600	N1—Pt1	2.161 (7)
C6—N1	1.335 (13)	N2—Pt1	2.152 (7)
C6—C7	1.403 (18)	O1—Pt1	2.168 (6)
C6—H13	0.9300	O3—H21	0.85 (9)
C7—C8	1.36 (2)	O3—H22	0.88 (11)
Pt1—C1—H1	109.5	N1—C10—C11	117.4 (8)
Pt1—C1—H3	109.5	C9—C10—C11	121.4 (11)
H1—C1—H3	109.5	N2—C11—C12	120.2 (11)
Pt1—C1—H2	109.5	N2—C11—C10	115.6 (8)
H1—C1—H2	109.5	C12—C11—C10	124.2 (11)
H3—C1—H2	109.5	C11—C12—C13	118.7 (13)
Pt1—C2—H6	109.5	C11—C12—H17	120.6
Pt1—C2—H5	109.5	C13—C12—H17	120.6
H6—C2—H5	109.5	C14—C13—C12	119.7 (12)
Pt1—C2—H4	109.5	C14—C13—H18	120.2
H6—C2—H4	109.5	C12—C13—H18	120.2
H5—C2—H4	109.5	C13—C14—C15	119.7 (13)
Pt1—C3—H9	109.5	C13—C14—H19	120.1
Pt1—C3—H8	109.5	C15—C14—H19	120.1
H9—C3—H8	109.5	N2—C15—C14	121.9 (12)
Pt1—C3—H7	109.5	N2—C15—H20	119.1
H9—C3—H7	109.5	C14—C15—H20	119.1
H8—C3—H7	109.5	C6—N1—C10	119.3 (9)
O2—C4—O1	126.2 (9)	C6—N1—Pt1	126.3 (8)
O2—C4—C5	117.9 (10)	C10—N1—Pt1	114.4 (6)
O1—C4—C5	116.0 (10)	C15—N2—C11	119.8 (9)
C4—C5—H11	109.5	C15—N2—Pt1	124.8 (8)
C4—C5—H10	109.5	C11—N2—Pt1	115.4 (6)
H11—C5—H10	109.5	C4—O1—Pt1	126.0 (6)
C4—C5—H12	109.5	H21—O3—H22	112 (10)
H11—C5—H12	109.5	C3—Pt1—C1	89.0 (5)
H10—C5—H12	109.5	C3—Pt1—C2	89.2 (5)
N1—C6—C7	121.4 (13)	C1—Pt1—C2	85.1 (5)
N1—C6—H13	119.3	C3—Pt1—N2	89.6 (4)

supplementary materials

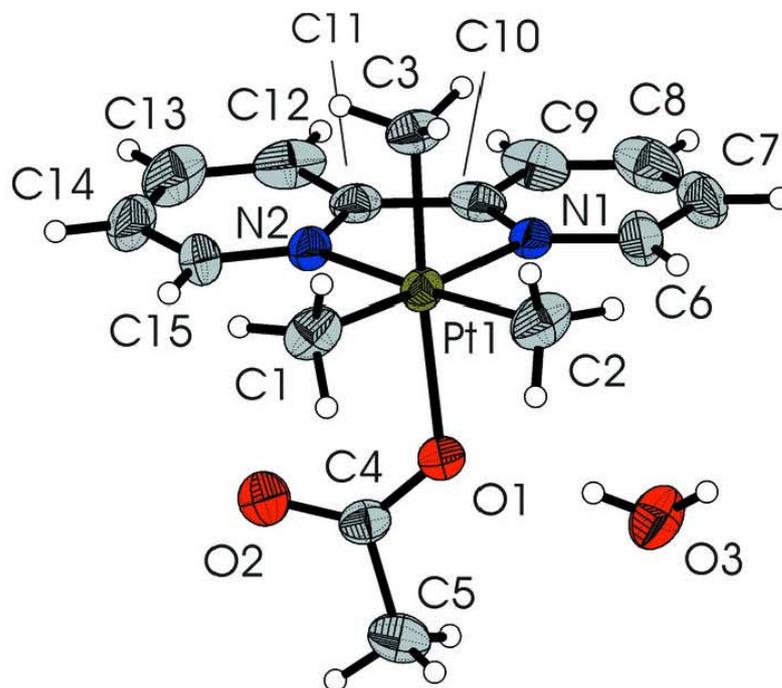
C7—C6—H13	119.3	C1—Pt1—N2	99.9 (4)
C8—C7—C6	118.8 (13)	C2—Pt1—N2	174.8 (5)
C8—C7—H14	120.6	C3—Pt1—N1	89.8 (4)
C6—C7—H14	120.6	C1—Pt1—N1	176.5 (4)
C7—C8—C9	119.7 (13)	C2—Pt1—N1	98.2 (4)
C7—C8—H15	120.1	N2—Pt1—N1	76.7 (3)
C9—C8—H15	120.1	C3—Pt1—O1	176.2 (4)
C8—C9—C10	119.6 (14)	C1—Pt1—O1	92.5 (4)
C8—C9—H16	120.2	C2—Pt1—O1	87.4 (4)
C10—C9—H16	120.2	N2—Pt1—O1	93.6 (3)
N1—C10—C9	121.2 (11)	N1—Pt1—O1	88.9 (3)
N1—C6—C7—C8	-1.9 (18)	C12—C11—N2—Pt1	-173.8 (7)
C6—C7—C8—C9	2(2)	C10—C11—N2—Pt1	7.6 (9)
C7—C8—C9—C10	-0.1 (19)	O2—C4—O1—Pt1	3.0 (15)
C8—C9—C10—N1	-1.1 (16)	C5—C4—O1—Pt1	-177.2 (7)
C8—C9—C10—C11	179.9 (10)	C15—N2—Pt1—C3	-92.8 (8)
N1—C10—C11—N2	-4.0 (12)	C11—N2—Pt1—C3	83.5 (7)
C9—C10—C11—N2	175.0 (9)	C15—N2—Pt1—C1	-3.8 (9)
N1—C10—C11—C12	177.5 (9)	C11—N2—Pt1—C1	172.4 (6)
C9—C10—C11—C12	-3.5 (14)	C15—N2—Pt1—N1	177.3 (8)
N2—C11—C12—C13	-1.7 (15)	C11—N2—Pt1—N1	-6.4 (6)
C10—C11—C12—C13	176.7 (10)	C15—N2—Pt1—O1	89.3 (8)
C11—C12—C13—C14	0.2 (19)	C11—N2—Pt1—O1	-94.5 (6)
C12—C13—C14—C15	0(2)	C6—N1—Pt1—C3	93.0 (9)
C13—C14—C15—N2	0.5 (18)	C10—N1—Pt1—C3	85.4 (7)
C7—C6—N1—C10	0.7 (15)	C6—N1—Pt1—C2	3.8 (9)
C7—C6—N1—Pt1	-177.7 (8)	C10—N1—Pt1—C2	-174.6 (6)
C9—C10—N1—C6	0.8 (13)	C6—N1—Pt1—N2	-177.4 (8)
C11—C10—N1—C6	179.8 (8)	C10—N1—Pt1—N2	4.2 (6)
C9—C10—N1—Pt1	179.3 (7)	C6—N1—Pt1—O1	-83.4 (8)
C11—C10—N1—Pt1	-1.7 (10)	C10—N1—Pt1—O1	98.2 (6)
C14—C15—N2—C11	-2.0 (15)	C4—O1—Pt1—C1	53.9 (8)
C14—C15—N2—Pt1	174.0 (8)	C4—O1—Pt1—C2	138.9 (9)
C12—C11—N2—C15	2.6 (13)	C4—O1—Pt1—N2	-46.2 (8)
C10—C11—N2—C15	-176.0 (8)	C4—O1—Pt1—N1	-122.8 (8)

Hydrogen-bond geometry (Å, °)

<i>D</i> —H... <i>A</i>	<i>D</i> —H	H... <i>A</i>	<i>D</i> ... <i>A</i>	<i>D</i> —H... <i>A</i>
O3—H22...O1	0.88 (11)	1.96 (11)	2.836 (12)	172 (15)
O3—H21...O2 ¹	0.85 (9)	1.96 (10)	2.810 (14)	177 (11)

Symmetry codes: (i) *x*, -*y*+3/2, *z*+1/2.

Fig. 1



DANKSAGUNG

Meinem sehr verehrten Lehrer, Herrn Prof. Dr. Steinborn, danke ich an dieser Stelle für die Überlassung des überaus interessanten und ergiebigen Themas, dessen freier Gestaltung, die Anfertigung von quantenchemischen Rechnungen und für die zahlreichen Anregungen, Hinweise und Diskussionen bei der Anfertigung der Arbeit. Darüber hinaus möchte ich mich auch für die Ermöglichung der Forschungsaufenthalte bedanken.

Herrn Dr. T. Ruffer, Herrn Dr. C. Wagner, Herrn Dr. S. Gomez-Ruiz, Herrn Dipl. Chem. M. Bette und Herrn Prof. Dr. K. Merzweiler danke ich für die mühevollen Anfertigung der Röntgeneinkristallstrukturanalysen und die Hilfe bei der Auswertung der Daten.

Bei Herrn Dr. D. Ströhl, Frau R. Flächsenhaar, Y. Schiller, Herrn Dipl. Phys. M. Kovermann und Herrn Prof. Dr. J. Balbach möchte ich mich für die Anfertigung der NMR-Spektren bedanken.

Herrn Dr. Schmidt danke ich für die Diskussionen und Hilfe bei der Auswertung von NMR-Spektren.

Herrn Dr. J. Schmidt sowie Herrn Dr. R. Kluge danke ich für die Aufnahme der zahlreichen ESI-Massenspektren.

Herrn Dr. G. N. Kaluđerović und Herrn Dr. R. Pascke danke ich für die Durchführungen der *In vitro* Studien zur Untersuchung der Cytotoxizitäten sowie für zahlreiche Diskussionen und Hilfe bei der Auswertung der Daten. Besonderer Dank gilt Herrn Dr. G. N. Kaluđerović ebenso für die Anfertigung quantenchemischer Rechnungen.

Frau R. Herzog danke ich ganz herzlich für die Unterstützung bei präparativen Arbeiten.

Herrn Prof. A. V. Demchenko danke ich für die Einladung zu Forschungsaufenthalten an der University of Missouri, St. Louis.

Weiterhin möchte ich mich für das sehr angenehme Arbeitsklima und die interessanten Diskussionen und Gespräche bei den Mitgliedern der Arbeitsgruppe um Prof. Steinborn bedanken. Außerdem danke ich allen Angehörigen des Institutes, die zum Gelingen dieser Arbeit beigetragen haben.

Des Weiteren möchte ich mich besonders bei meinen Eltern, meiner Familie, meinem Freund und meinen Freunden bedanken, die mir stets Rückhalt und Unterstützung geboten haben. Ohne sie wäre die Anfertigung dieser Arbeit nicht möglich gewesen.

LEBENS LAUF

Persönliche Daten

Name: Cornelia Vetter
Geburtsdatum: 03.12.1981
Geburtsort: Lutherstadt Wittenberg
Staatsangehörigkeit: deutsch
Familienstand: ledig
Wohnort: 06112 Halle, Conradstraße 3

1988–1992 Grundschole Gräfenhainichen
1992–2000 Paul-Gerhardt-Gymnasium Gräfenhainichen, Abschluss: Abitur
2000–2005 Studium der Chemie an der Martin-Luther-Universität Halle-
Wittenberg, Abschluss: Dipl.-Chem. (sehr gut)
2005–2009 Doktorandin an der Martin-Luther-Universität Halle-
Wittenberg
seit 2010 Post-Doc am Max-Planck-Institut, Forschungsstelle für
Enzymologie der Proteinfaltung

EIDESSTATTLICHE ERKLÄRUNG

Hiermit erkläre ich an Eides statt, dass ich die vorliegende Arbeit selbstständig und nur unter Verwendung der angegebenen Quellen und Hilfsmittel angefertigt habe.

Diese Arbeit wurde bisher an keiner anderen Universität oder Hochschule vorgelegt.

Halle (Saale), den 28.01.2010